An Isotopic Study of Ground-Water Flow Near Cerro Negro, New Mexico

by
Page Pegram

Submitted in Partial Fulfillment of the
Requirements for the Degree of Master of
Science in Hydrology

New Mexico Institute of Mining and Technology
Socorro, New Mexico
December, 1995

Abstract

Carbon-14 dating of ground water can be used to determine the flow rate of ground water along a flow path. This study uses the computer program NETPATH to analyze net geochemical mass-balance reactions and radiocarbon ages along a flow path that intersects the Cerro Negro volcanic intrusion. The NETPATH chemical mass balance indicates that cation exchange between Ca^{+} and Na^{+} forces the dissolution of calcite and precipitation of dolomite and gypsum. The radiocarbon dating feature of NETPATH indicates that ground-water samples near Cerro Negro are greater than 38,000 years old. The model-predicted $\delta^{13}C$ composition of the final water is compared to the measured $\delta^{13}C$ to test the accuracy of the model. Radiocarbon ages are also calculated using a simple dissolution model in which it is assumed that the only carbon source is the dissolution of carbonate minerals. The ages predicted by the simple dissolution model are virtually identical to those calculated by the NETPATH model, implying that, for aquifers with few sources of carbon, a simple "back of the envelope" calculation can nearly match the corrected radiocarbon ages of a more elaborate model. Flow rates based on the NETPATH radiocarbon ages are calculated to be between 8.47×10^{-8} m/s and 3.49×10^{-9} m/s.

Table of Contents

List of Figures

List of Tables

Introduction

Purpose

Concern over past waste-disposal practices at United States Department of Energy (DOE) work sites and research labs has led the DOE to support large scale scientific research projects that seek to provide the scientific foundations to resolve their mid- to long-term waste and cleanup problems. Support for these projects comes from the Subsurface Science Program. The Deep Microbiology Subprogram is one of several focal points of the Subsurface Science Program. This subprogram provides funding for basic research on microbes in subsoils and ground water, with the goal of providing a foundation of knowledge that will contribute to better bioremediation techniques. Ultimately the goal is to reduce environmental risks and to use cost-effective strategies to clean up DOE sites (DOE, 1994)

Goals of Cerro Negro study

The Cerro Negro Microbial Origins Project is part of the Deep Microbiology Subprogram of the DOE's Subsurface Science Program. This subprogram, in particular, focuses on the ecology and the origins of microbes in deep sediments and aquifers, with an emphasis on survival and long distance transport over thousands of years. The primary objective of the Cerro Negro study is to investigate the origins of microorganisms in deep subsurface environments and to evaluate the potential roles of in situ survival and bacterial transport. This objective is addressed through a scientific drilling effort at Cerro Negro, a volcanic intrusion near Seboyeta, New Mexico.

Cerro Negro is a volcanic neck that intruded older sedimentary rocks approximately 3.39 million years ago. The heat associated with the volcanic intrusion would probably have sterilized the surrounding rocks. The main purpose of research at Cerro Negro is to determine if the previously sterilized rocks are still sterile or if microorganisms have re-established themselves in the last 3.39 million years. If microorganisms are found in the sterilized zone this is good evidence that they have been transported into the area with the ground water.

Specific Goals of Isotope study

The specific goal of this study is to use isotopic methods to determine ground-water flow rates near Cerro Negro in order to better constrain microbial transport rates

and the possibility of microbial re-colonization by transport with the ground water. This goal will be accomplished through geochemical modeling and radiocarbon dating of water samples along a flow path near Cerro Negro. The radiocarbon ages will allow an accurate estimation of the ground-water flow rates in the area. This information, along with estimates of vertical flow rates, can later be integrated with water level information into a computer model that simulates the three-dimensional ground-water flow in the area.

Regional Hydrogeology

Geologic Setting

Cerro Negro is located in the southeast corner of the San Juan Basin (Figure 1), a structural depression covering approximately 77,000 km^2 of northwest New Mexico and southwest Colorado (Stone et al, 1983). The San Juan Basin lies within the Colorado Plateau physiographic province (Figure 2), a large, relatively flat and geologically undeformed upland region south and east of the Rocky Mountains. Cerro Negro is one of the volcanic necks of the late Cenozoic age Mount Taylor volcanic field, which lies in a transition zone that separates the Colorado Plateau and the Rio Grande Rift. This study will focus on the Cretaceous sedimentary rocks through which Cerro Negro intruded, but descriptions of all geologic units of the San Juan Basin will be given.

Stratigraphy

The San Juan Basin contains rocks ranging in age from Cambrian to Tertiary, but principally Permian through Tertiary. Figure 3 (from Molenaar, 1977) shows a stratigraphic cross section of these units. The stratigraphy is dominated by layer-cake sedimentary strata of alternating sandstones, limestones and shales. Sedimentary rocks of Jurassic and Cretaceous age crop out around the basin rim and over a broad area in the southern and western parts of the basin. Tertiary sedimentary rocks cover most of the central basin and Quaternary deposits are restricted mainly to major valleys.

The Jurassic sedimentary strata were deposited in various desert environments (dune fields, playas, saline lakes, and wet alluvial aprons). Alluvial and fluvial deposition continued into Early Cretaceous time. During the Cretaceous Period a large inland sea covered much of the western United States and Canada. The shoreline of this shallow inland sea shifted back and forth across the area that is now the San Juan Basin. The Cretaceous sequence of sandstones, shales, and limestones represents alternating periods of sea transgression and regression (Stone et al., 1983). The following are stratigraphic descriptions of each unit and are taken from Stone et al. (1983) unless otherwise noted.

Pre Permian

The oldest Paleozoic deposits, of Cambrian, Devonian, and Mississippian ages, are present only in the extreme north and northwest parts of the San Juan Basin (Armstrong and Mamet, 1977), and are not well known because of their great depth.

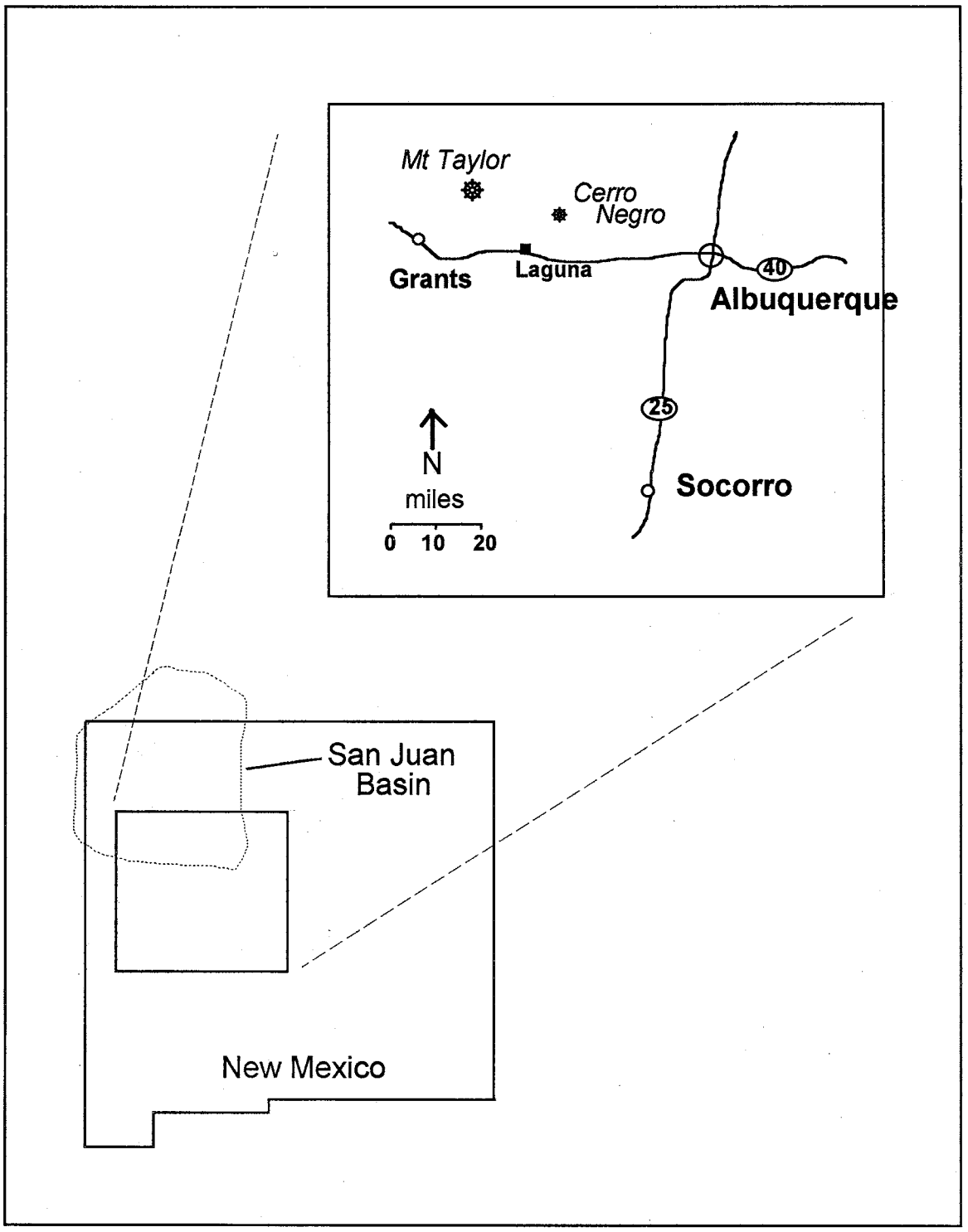

Figure 1: Location map of Cerro Negro and San Juan Structural Basin

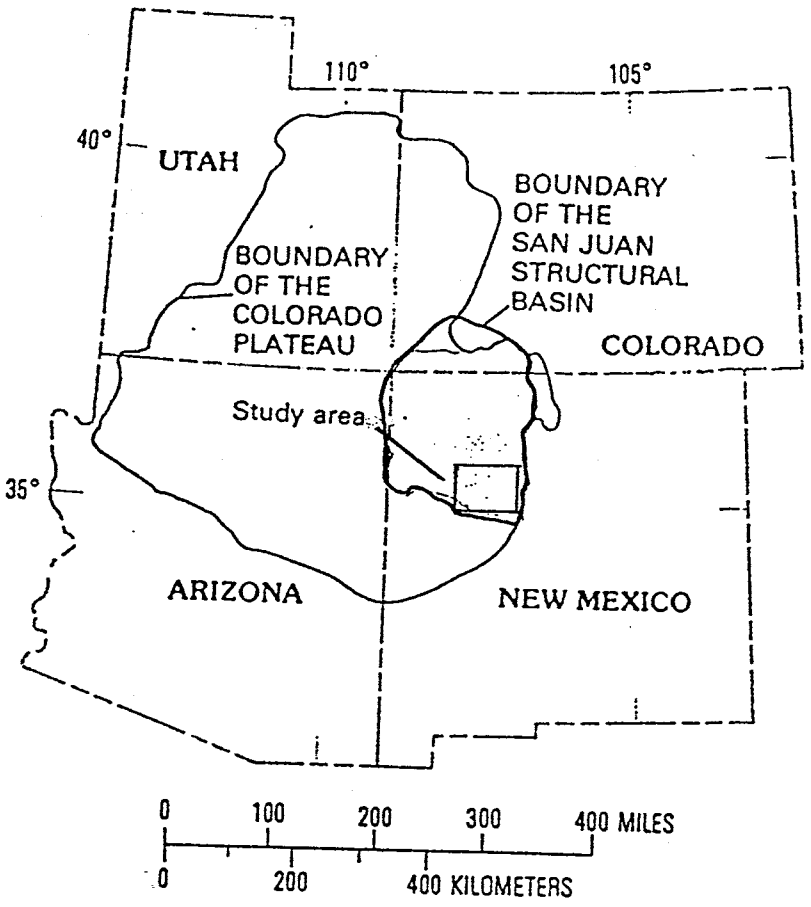

Figure 2: Location of the San Juan structural basin, Colorado Plateau, and study area. (from Craigg et al., 1990)

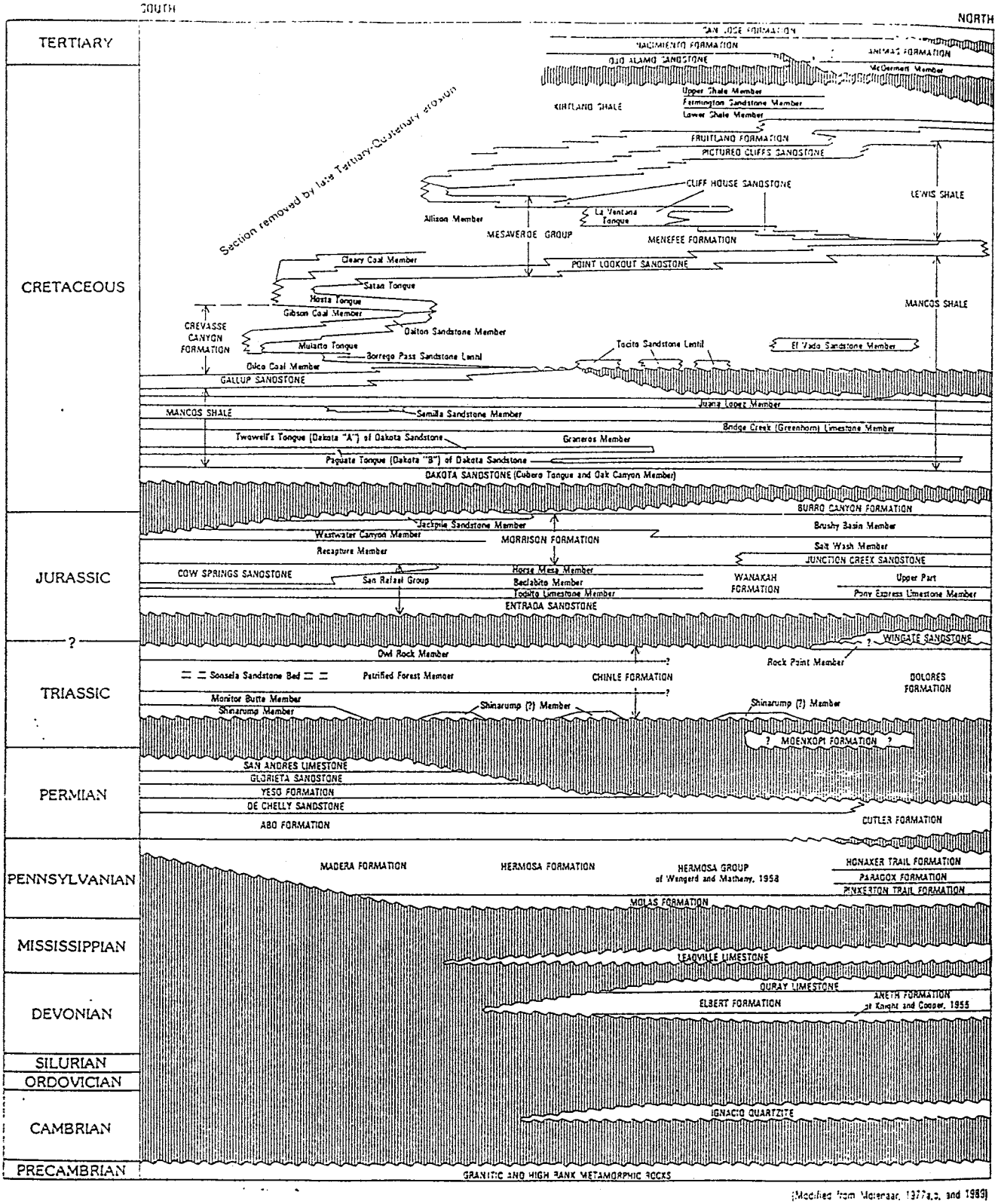

Figure 3: Time and rock stratigraphic framework and nomenclature for San Juan Basin. (from Craigg et al., 1990)

Permian

Permian rocks in the San Juan Basin include limestone, sandstone, siltstone and gypsum of the Yeso Formation, Glorieta Sandstone, and San Andres Limestone. The marine evaporites of the Yeso Formation are largely untested but are unlikely to be a good source of water. The Glorieta Sandstone and San Andres Limestone intertongue and behave as a single unit hydraulically. This unit is not a significant aquifer throughout the San Juan Basin, but it is important to note that in the Grants-Bluewater area in the southwest part of the basin carbonate dissolution has created significant permeability. The Glorieta-San Andres aquifer is the principal source of water for the communities along Intestate 40 between Grants and Gallup. The city of Grants derives its water from this aquifer.

Triassic

The Triassic Chinle Formation is composed of mudstone, sandstone, and limestone. Occasional sandstone beds in this formation are minor aquifers of local importance, but are not significant on a basin-wide scale.

Jurassic

Jurassic rocks in the San Juan Basin include the Entrada Sandstone, Todilto Limestone, Summerville Formation, Cow Springs-Bluff Sandstone, and the Morrison Formation. Many stock wells, and a few public-supply and industrial wells in the southern part of the basin obtain water from sandstone units of Jurassic age.

The Entrada Sandstone is composed of sandstones and siltstones and forms distinctive red cliffs along the southern basin margin. Transmissivity in the Entrada is moderate (5 to 10×10^{-4} m^2/s) but water quality is generally not suitable for drinking.

The Todilto Formation consists of gypsum overlying limestone. The Summerville Formation consists of alternating beds of mudstone and sandstone. Neither of these units yields significant amounts of water to wells and both are considered aquitards.

The Cow Springs and Bluff Sandstone formations are treated together because they are closely related stratigraphically and probably behave as a single unit. The units intertongue and consist of fine to medium grained arkosic sandstones. Although this unit is fairly thick and continuous, its transmissivity is low (approximately 5×10^{-5} m^2/s) (Jobin, 1962) and it is considered an aquitard.

The Morrison Formation is the uppermost Jurassic unit present in the San Juan Basin and is a major source of both uranium and water in the southern part of the basin. The Morrison is a sequence of non-marine sandstone, mudstone, and limestone consisting

of four members (in ascending order): the Salt Wash Sandstone Member, the Recapture Shale Member, the Westwater Canyon Member, and the Brushy Basin Shale Member. The Westwater Canyon Member, in particular, yields significant amounts of water and is the major aquifer along the southern margin of the basin.

Cretaceous

The Dakota Sandstone is the lowermost Cretaceous unit in the San Juan Basin and consists of a sequence of sandstones, mudstones, and coal. The Dakota intertongues extensively with the overlying Mancos Shale. Four local subdivisions of the Dakota are recognized: the Twowells, Paguate, and Cubero Sandstone Tongues, and the Oak Canyon Member. Some stock and domestic wells produce water from the Dakota, but many wells that produce from the Dakota are also completed in overlying or underlying rocks.

The Mancos Shale intertongues with the Dakota Sandstone below, as well as with the Gallup Sandstone and Mesaverde Group above. Below the main body, the Mancos Shale is subdivided into the Clay Mesa Shale and the Whitewater Arroyo Shale, in ascending order. The main body of the Mancos is a gray, friable shale with sparse beds of yellowish-gray, friable sandstone (Moench and Schlee, 1963). The Mancos Shale is considered a confining layer.

The Mesaverde Group consists of five units (in ascending order): the Gallup Sandstone, the Crevasse Canyon Formation, Point Lookout Sandstone, Menefee Formation, and Cliff House Sandstone. The Mancos Shale intertongues with all but the Menefee Formation and the Cliff House Sandstone.

The Gallup Sandstone is the lowest unit in the Mesaverde Group. It is a fine-grained sandstone and forms prominent cliffs. The highest transmissivity ($4x10^{-4}$ m^2/s) for this unit occurs in the southwest part of the basin near the town of Gallup (Stone et al., 1983) Many wells and springs in the southern and western sides of the basin produce water from this unit. The city of Gallup is the principal user of water from the Gallup Sandstone.

The Crevasse Canyon Formation consists of three members: the Dilco Coal Member, the Dalton Sandstone Member, and the Gibson Coal Member. The Mulatto Tongue of the Mancos Shale lies between the Dilco Coal and Dalton Members. The main aquifer in this group is the Dalton Sandstone Member, a fine to medium-grained sandstone. Scattered wells and springs in the Crevasse Canyon Formation produce water for stock and domestic use.

The Point Lookout Sandstone is a fine to medium grained sandstone with a transmissivity of approximately $2x10^{-4}$ m^2/s (Stone et al., 1983).The Point Lookout is

divided into the Upper Part and the Hosta Tongue, with the Satan Tongue of the Mancos Shale in between. Though a few stock and domestic wells tap the Point Lookout Sandstone this unit is not widely used as a source of water.

The Menefee Formation consists of interbedded claystone, carbonaceous siltstone, and shale, coal, and sandstone. Because of its widespread distribution at the surface and the thickness of its sandstone members, the Menefee Formation is a common source of water for stock and domestic uses.

The Cliffhouse Sandstone is the uppermost unit in the Mesaverde Group. Several stock and domestic wells produce water from this sandstone near outcrops in the central part of the basin. Transmissivity data are limited for the Cliffhouse Sandstone but one test indicated a transmissivity of 6.5×10^{-5} m^2/s.

Structure

The San Juan Basin is a Laramide (Late Cretaceous to Early Tertiary) structural depression lying on the eastern edge of the Colorado Plateau. The basin is primarily a thick sequence of sedimentary rocks ranging in age from Cambrian through Tertiary. These sedimentary rock layers dip from the basin margins toward the structural center of the basin. Older sedimentary rocks crop out around the basin margins and are successively overlain by younger rocks toward the center. (Figure 4)

Structures of the San Juan Basin and adjacent uplifts developed principally during the Laramide Orogeny (Late Cretaceous to Early Tertiary). By this time the shallow inland sea had retreated and the formation of the basin was accelerating. Vertical uplift of the plateau as a whole, as well as faulting, fracturing, and igneous activity took place in Late Cenozoic time (Woodward and Callendar, 1977).

The structure of the San Juan Basin is described by Woodward and Callendar (1977). The basin is bounded by monoclinal folds on the north, northeast, and west and by faults on the east and southeast. Refer to Figure 5 for the structural elements of the San Juan Basin.

The north, northeast, and northwest boundaries of the basin are excellent examples of monoclines. To the west the Defiance monocline separates the Defiance uplift from the Gallup Basin. The Hogback Monocline forms a sharp boundary between the Central Basin and the Four Corners Platform to the northeast and the San Juan Uplift to the north. The Hogback Monocline also forms the northeast boundary, separating the Central Basin from the Chama Embayment and the Brazos Uplift.

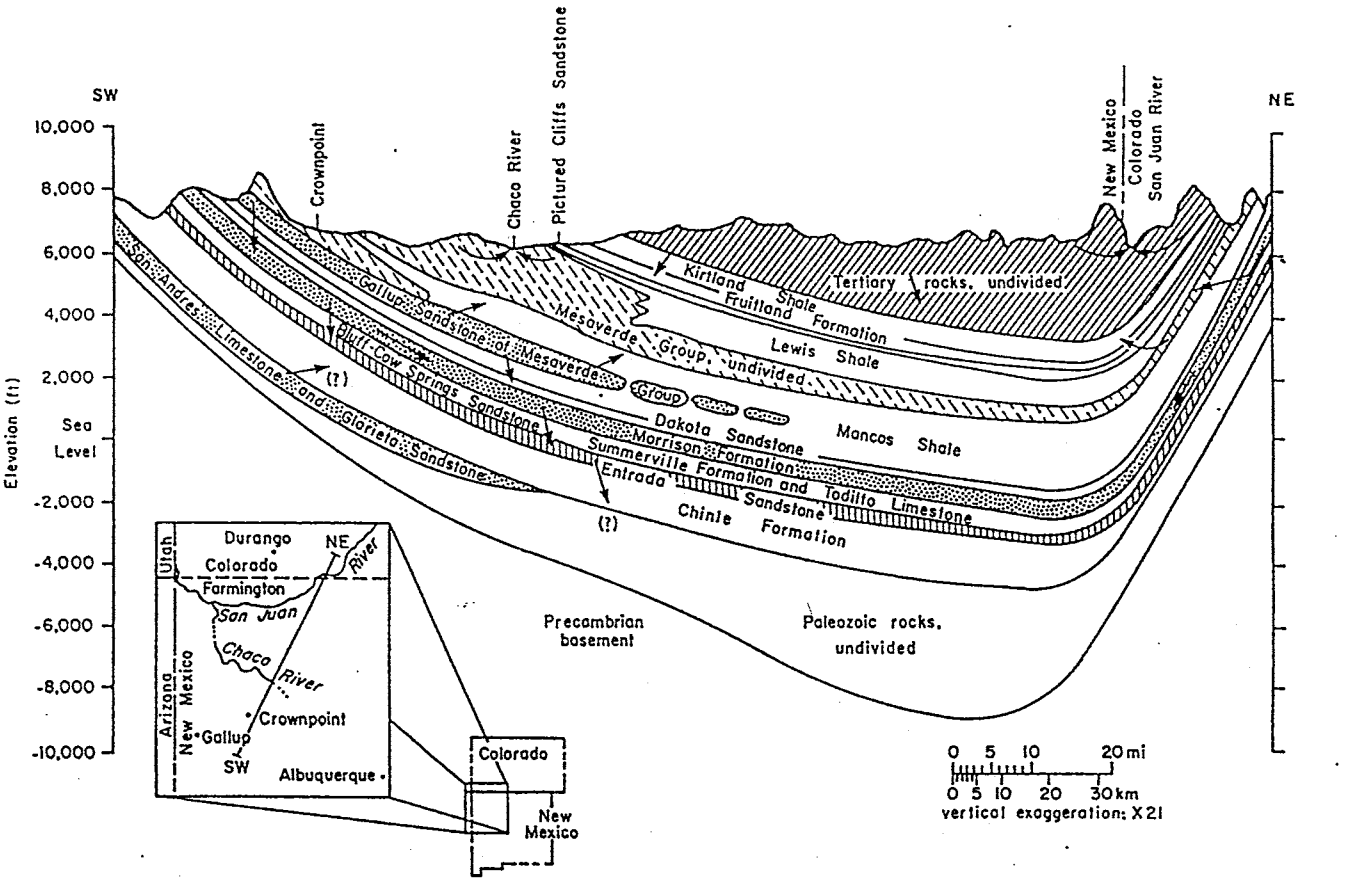

Figure 4: Generalized cross-section of San Juan Basin, showing major aquifers (stippled), confining beds (blank), and direction of ground-water flow (arrows) (from Stone et al., 1983).

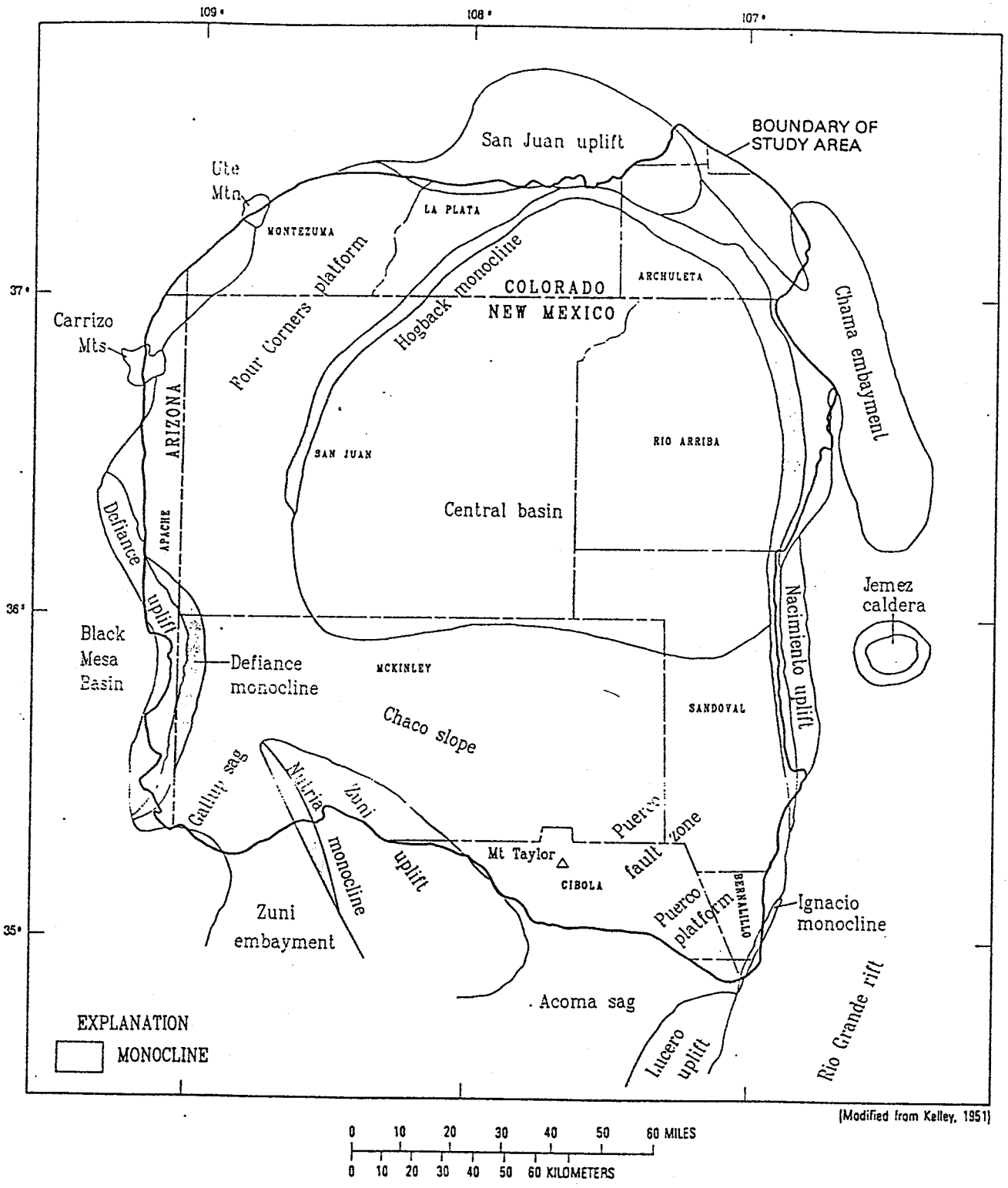

Figure 5: Structural elements of the San Juan basin and adjacent areas (from Craigg et al., 1990).

The Nacimiento Uplift, the up-thrown block of a high-angle reverse fault, bounds the basin on the east. Farther south the Nacimiento Uplift blends into the Rio Puerco Fault Zone. The Rio Puerco Fault Zone consists of northwest-trending folds, monoclinal folds, and northeast-trending en-echelon normal faults.

The southern margin of the San Juan basin is defined by the Acoma Basin and the Zuni Uplift. The Acoma Basin is a broad, north-plunging syncline with a moderately steeply dipping west limb and a gently dipping east limb. The west limb of the Acoma Basin is adjacent to the Zuni uplift, a doubly plunging anticlinorium trending northwest.

Hydrology

Aquifer properties

Sandstone aquifers prevail in the San Juan Basin. Table 1 summarizes the geologic and hydrologic characteristics of sixteen major aquifers identified by Stone et al. (1983) in the basin. Their divisions are based on geologic framework, which ultimately controls the occurrence, movement, and quality of ground water.

Regional flow regime

In general, ground water in the San Juan Basin moves toward the basin center from recharge areas along the southern, northeastern, and western basin margins. Topography also plays an important role in local flow regimes, with ground water flowing from topographically high outcrop areas toward lower outcrop areas (Stone et al., 1983) Recharge occurs mainly on the flanks of the mountains that surround the basin: the Zuni, Chuska, and Cebolleta Mountains to the south and west, and the San Juan Mountains to the north. The main discharge areas for the basin are streams and rivers: the San Juan River in the northwest and the Rio Salado, Rio Puerco, and Rio San Jose in the southeast (Stone et al., 1983). Risser and Lyford (1983) also suggest the Rio Puerco Fault Zone as a discharge area in the southeast.

Vertical movement of ground water between aquifers is part of the regional flow system in the San Juan Basin but is difficult to determine using the available data. Differences in the potentiometric surface between aquifers drive this vertical movement. Ward et al. (1982) report that in all places in the Laguna Pueblo area where data are available, potentiometric levels in Permian rocks are higher than those in overlying units, leading to possible upward leakage where the overlying units are thin or fractured. Stone et al. (1983) indicate that leakage rates through shale beds are very low, except in areas where fractures and faults are present. Craigg (1980) reports that many springs in the

southeast San Juan Basin are associated with northeast-trending faults and dikes, or with volcanic necks. These leakage avenues may also exist under the Cebolleta Mountains because of volcanic activity at Mt. Taylor.

Table 1: Summary of Geologic and Hydrologic Characteristics of Major Aquifers in the San Juan Basin (from Stone et al., 1983)

	Brief Description	Thickness (m)	Depth (m)	Transmissivity (m^2/d)	Specific Conductance (umhos/cm)
Valley Fill (Quaternary	unconsolidated fluvial, colluvial, eolian deposits	generally <30	at surface	$<1.1x10^{-3}$ to $<1.6x10^{-2}$	<1000->7000
Chuska Sandstone (Eocene/Oligocene)	eolian sandstone, lacustrine mudstone	213-549	at surface	unknown	<500
San Jose Formation (Eocene)	alluvial sandstone, mudstone	<61-823	at surface	two tests give $4.3x10^{-5}$ and $1.3x10^{-4}$	320-3000 (2000 average)
Nacimiento/Animas Formations (Paleocene)	alluvial and fluvial sandstone and mudstone	127-6800	0-811	no data, but up to $1.1x10^{-4}$ expected for coarser sandstones	<2000
Ojo Alamo Sandstone (Paleocene)	alluvial sandstone, minor mudstone	22-95	0-806	$5.4x10^{-5}$ to $2.7x10^{-4}$ within 25 mi. of outcrop	<1000 near outcrop; >9000 at depth
Kirtland Shale-Fruitland Formation (Cretaceous)	fluvial sandstone, mudstone: coal measures	<30-610	0-914	$<1.1x10^{-5}$	>5000
Pictured Cliffs Sandstone (Cretaceous)	marine sandstone	8-86	0-1258	$1.1x10^{-9}$ to $3.2x10^{-6}$	>2000 even near outcrop; <41000 at basin center
Cliff House Sandstone (Cretaceous)	marine sandstone	6-75	0-1875	$<1.1x10^{-5}$ to $<6.5x10^{-5}$	2000 near outcrop; >30000 at depth
Menefee Formation (Cretaceous)	coal measures	122-305	0-1909	$<5.4x10^{-5}$	<3000 south of Chaco River; no data north
Point Lookout Sandstone (Cretaceous)	marine sandstone	12-126	0-1951	$2.2x10^{-6}$ (north of Crownpoint): $2.2x10^{-6}$ or less elsewhere	>1500 (59000 in basin center)
Crevasse Canyon Formation (Cretaceous)	coal measures, marine sandstone	128-213	0-975	probably $<5.4x10^{-5}$	<2000 near outcrop; greater elsewhere
Gallup Sandstone (Cretaceous)	marine sandstone	28-213	0-1311	up to $4.3x10^{-4}$ in southwest: $1.1x10^{-4}$ or less in northeast	<1000 near outcrop; 4000 at northeast limit
Dakota Sandstone (Cretaceous)	marine sandstone, coal measures	61-107	0-2591	variable: up to $1.1x10^{-4}$ locally	<2000 near outcrop; >10000 at depth
Morrison Formation (Jurassic)	alluvial and fluvial sandstone, mudstone	128-274	0-2713	up to $5.4x10^{-4}$ in south: decreases northward	<1000 in south and west; >10000 at depth
Bluff-Cow Springs Sandstones (including Summerville Formation) (Jurassic)	eolian sandstone	18-61	0-2743	probably $<5.4x10^{-5}$	<2000 near outcrop; greater at depth
Entrada Sandstone	eolian sandstone	40-226	0-2838	$<5.4x10^{-5}$ near outcrop: > $1.1x10^{-4}$ at depth	<1500 near outcrop; >10000 at depth

Cerro Negro Site Description

Local Geology

Stratigraphy

The stratigraphic units that crop out in the vicinity of Cerro Negro are shown in cross-section in Figure 6. These are the units that are most important to the Cerro Negro project. They range from the Jurassic Morrison Formation to the Cretaceous Point Lookout Sandstone. Table 2 summarizes the geologic and hydrologic characteristics of these units near Cerro Negro.

Structure

Sedimentary rocks in the Cerro Negro area dip gently to the north-northwest, into the San Juan Basin. Structure contours on the base of the Dakota Sandstone show a regional dip in this area of about 2% (Schlee and Moench, 1963). Although deformation of strata in the area is minor, three general periods of deformation are recognized. The earliest occurred in the Jurassic, prior to deposition of the Dakota Sandstone. These Jurassic structural features include a regional northward homoclinal dip, two sets of broad, low-amplitude folds, hundreds of sandstone pipes and intraformational faulting. The two later deformational events probably spanned most of the Tertiary and possibly extended into Holocene time. These two events, early Cenozoic folding followed by late Cenozoic fracturing and uplift, probably overlapped in time (Moench and Schlee, 1967).

Faults in the Cerro Negro region are widely spaced and of small displacement. Schlee and Moench (1963) indicate several north to northeast trending normal faults north of Cerro Negro, although there is very little noticeable displacement along these faults.

Fractures and joints are present in significant numbers in the area. The geologic staff of SOHIO measured numerous joints in the Two Wells Sandstone during their geologic investigation. The majority of the joints had a northeast or northwest orientation (Hydro-Engineering, 1981). The SOHIO staff also interpreted several weak lineaments from aerial photographs of the area. Moench and Schlee (1967) describe at least six joint sets which are present throughout the sedimentary strata in the region. They appear to form a major joint system that developed in response to late Cenozoic tectonic activity.

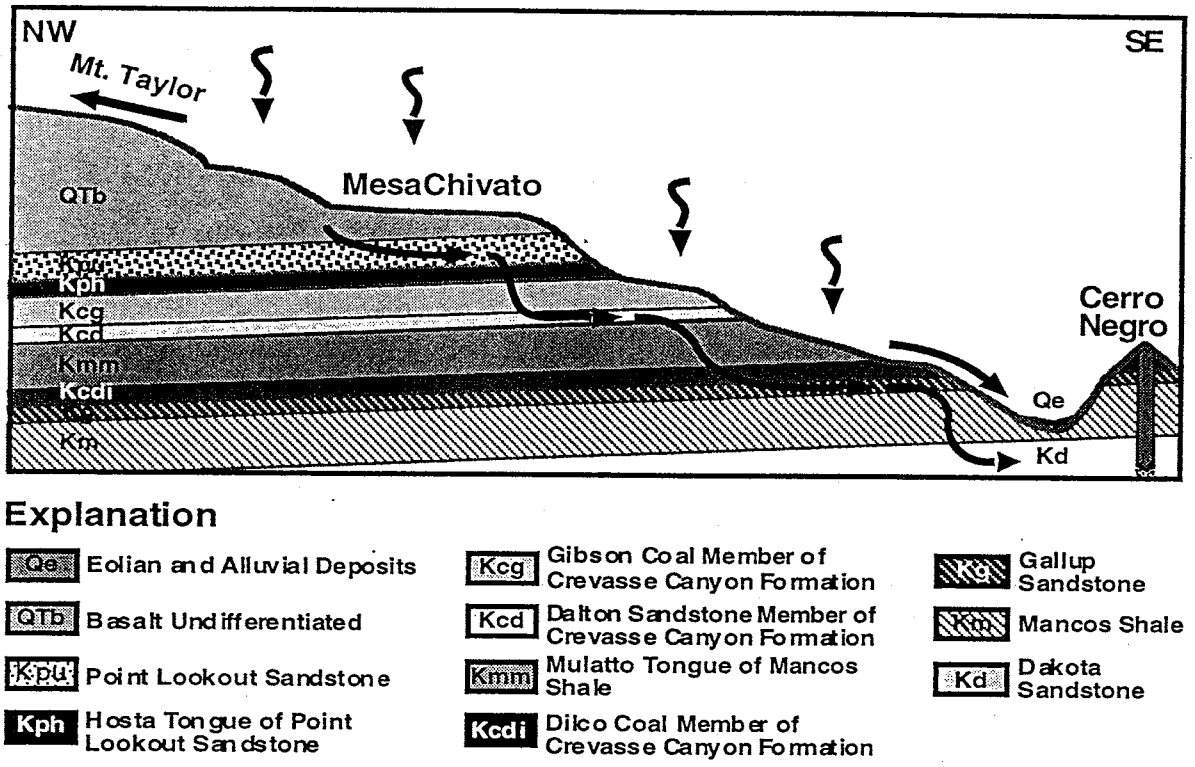

Figure 6: Generalized cross-section from Mesa Chivato to Cerro Negro showing flow direction.

Table 2: Summary of geologic and hydrologic characteristics of important geologic units near Cerro Negro. Data are taken from (1) Craigg (1980), (2) Cheryl D. Gullett, Pacific Northwest Laboratories, personal communication, 1995, (3) R. Bruce Hallett, Golder Federal Services, personal communication, 1995, (4) Moench and Schlee (1963), (5) Stone et al. (1983), (6)Hallett (1994), (7) Azimi-Zonooz and Duffy (1993), (8) Domenico and Schwartz (1990), (9) Freeze and Cherry (1979).

Formation	Age	Depositional Environment	Grain Size	Porosity (%)	Permeability (m^2)	Major Mineral Constituents
Basalts	Quaternary	flow from Mt. Taylor volcanic field[1]	aphanitic[1]			olivine, plagioclase feldspar[4]
Point Lookout Sandstone	Cretaceous	coastal marine[5]	fine-medium[5]	18.2-21.3[1]	8 to 87x10^{-18} (horiz.) 7 to 53x10^{-18} (vert.)[1]	quartz, feldspar, chert, clay matrix[1]
Satan Tongue of Mancos	Cretaceous	marine, transgressive[3]	very fine-fine[1]	0-10[8]	10^{-20}-10^{-16} (9)	-
Hosta Tongue of Point Lookout	Cretaceous	coastal marine[5]	fine-medium[4]	5-30[8]	10^{-17}-10^{-13} (9)	-
Gibson Coal Member of Crevasse Canyon	Cretaceous	-	-	-	-	-
Dalton Sandstone Member of Crevasse Canyon	Cretaceous	-	very fine-medium[5]	5-30[8]	10^{-17}-10^{-13} (9)	-
Mulatto Tongue of Mancos	-	-	-	0-10[8]	10^{-20}-10^{-16} (9)	-
Dilco Coal Member of Crevasse Canyon Formation	-	-	-	-	-	-
Gallup Sandstone	Cretaceous	regressive shoreline[1]	fine-medium[1]	5-30[8]	10^{-17}-10^{-13} (9)	quartz, feldspar, quartz cement, pyrite, hematite limonite[6]
Mancos Shale (main body)	Cretaceous	marine, near edge of continental shelf[3]	silt-clay[3]	12.25[2]	8x10^{-20} (2)	gypsum, calcite, dolomite, lignite[7]
Two Wells Sandstone of Dakota	Cretaceous	offshore, shallow-water marine shelf[3]	fine -very fine sand[3]	14.57[2]	5x10^{-20} (2)	quartz, calcite cement[3] chlorite matrix, K-spar, pyrite, mica, limonite[8]
Whitewater Arroyo Shale of Mancos	Cretaceous	low energy, shallow water marine shelf[3]	clay- fine sand[3]	9.32[2]	4x10^{-20} (2)	calcite cement[3]
Paguate Sandstone of Mancos	Cretaceous	open-marine shelf to nearshore marine[3]	clay-very fine sand[3]	8.45[2]	4x10^{-20} (2)	quartz, calcite cement, glauconite trace[3]
Clay Mesa Shale of Dakota	Cretaceous	open-marine shelf to shallower nearshore[3]	silt-very fine sand[3]	0-10[8]	10^{-20}-10^{-16} (9)	calcite cement[3]
Cubero Sandstone of Dakota	Cretaceous	deep to shallow nearshore[3]	medium sand[3]	14.97[2]	5x10^{-20} (2)	quartz, calcite cement[3]
Oak Canyon Member of Dakota	Cretaceous	terrestrial and marine[3]	clay-fine sand[3]	12.59[2]	9x10^{-20} (2)	quartz, kaolinite[3]
Morrison Formation	Jurassic	terrestrial, braided stream[3]	clay-medium sand[3]	-	-	-

Cerro Negro Intrusion

Cerro Negro is a dike-like volcanic neck, one of the Rio Puerco necks, that lies in the Mount Taylor volcanic field. The Mount Taylor volcanic field is part of a broad belt of late Cenozoic volcanism that marks the transition between the Rio Grande Rift and the Colorado Plateau.

Cerro Negro consists of two plugs, three non-continuous dikes, and minor pyroclastic deposits that erupted through a Mesozoic sequence of sedimentary strata. These igneous features are oriented in a N5E trend and are situated on the edge of a cliff formed of Gallup Sandstone. The northern peak is the larger of the two plugs and it reaches an elevation of 2201 m, with an irregular basal diameter of approximately 38 m. The smaller plug is about 122 m south of the larger plug and reaches an elevation of 2147 m, with a basal diameter of 30 m. Both plugs are composed of homogeneous, non-vesicular olivine basalt (Hallet, 1994).

Activity of the Mount Taylor volcanic field spans approximately three million years (4.5-1.5 Ma). A sample collected from the southern plug of Cerro Negro yielded a $^{40}Ar/^{39}Ar$ age of 3.39 ± 0.02 Ma (Hallet, 1994).

Local Hydrology

Wells - Location and access

Ground water is the main source of water for domestic, irrigation and livestock use in the vicinity of Cerro Negro. Therefore, there are several wells available as sampling points. Table 3 summarizes basic information on the wells that were sampled for this study. Most of the wells are located on the Cebolleta Land Grant and were accessed with permission from the land grant officials. The Elkins and Presbyterian wells are located on private land, and we obtained permission to sample these from Kin Elkins of Cubero, NM. The Bibo, Seboyeta, and Moquino wells are municipal water supply wells for the corresponding towns. The Elkins, Presbyterian, and Bibo#2 wells are small domestic wells, and the rest are monitor wells (discussed below) or livestock wells

Table 3: Basic information on wells that were sampled for isotope study. Notes: bgs-below ground surface, amsl-above mean sea level, NA-not available. UTM (Universal Transverse Mercator) locations measured by GPS and corrected to base station in Albuquerque, NM, except for those marked with *, which were estimated from topographic maps. Water level measurements marked with # were not given enough time to equilibrate.

Well Name	UTM Coordinates		Ground Surface Elevation	Depth to Water	Water Level Elevation	Tot Depth of Well	Screened Interval	Screened Unit
	easting (m)	northing (m)	(m amsl)	(m bgs)	(m amsl)	(m)	(m bgs)	
Elkins	275625*	3895975*	2361.3	27.2	2334.1	36.0	NA	Volcanic Conglomerate, possibly upper Pt Lookout SS
Presbyterian	275725*	3895975*	2328.7	NA	NA	NA	NA	" "
Seboyeta	282401	3898401	1969.0	NA	NA	243.8	207.3-231.6	Cubero and top of Morrison
Bibo	281429	3895320	1938.5	NA	NA	137.2	61.0-73.2, 126.5-137.2	Two Wells and Paguate SS
Moquino	284088	3894708	1891.9	61.0	1830.9	167.6	118.9-167.6	Westwater SS of Morrison Fm
CNV-W2	285438	3897475	1937.0	<68.9#	>1868.1#	37.3	39.0-44.8	Two Wells SS
CNV-W3	285438	3897475	1937.0	67.8	1869.2	198.7	54.3-60.7	Cubero SS
CNV-W5	285438	3897475	1937.0	<70.2#	>1866.8#	164.0	46.9-50.0	Paguate SS
MW-65	286500*	3896750*	1912.7	45.9	1866.7	78.6	65.7-78.5	Two Wells SS
MW-64	286500*	3896415*	1895.8	29.9	1865.9	57.4	45.2-57.4	Two Wells SS
MW-60	286650*	3896575*	1902.0	37.5	1864.5	65.0	51.8-64.0	Two Wells SS
MW-68	286875*	3896975*	1933.1	67.6	1865.5	101.5	88.3-100.5	Two Wells SS
L-Bar	288339	3896638	1875.7	NA	NA	159.1	NA	Morrison Fm
Bibo#2	282602	3896998	1932.1	49.8	1882.4	64.6	NA	Two Wells SS?

L-Bar Tailings Pond -History and monitoring

This study has benefited from data collected at a nearby uranium mill tailings pond. The L-Bar mill tailings pond is located approximately 3 km southeast of Cerro Negro. These tailings resulted from a sulfuric-acid leach processing of uranium ore at the L-Bar uranium mine, which was operated by SOHIO-Western Mining Company. SOHIO ceased operations at L-Bar in 1982. The tailings accumulated from 1976 to 1982 and were piled to a height of 5 m. The pond was constructed on top of the Mancos Shale and was lined with clay. Sodium chloride rock salt was added to the clay in the bottom of the tailings pond during construction. The tailings are characterized by low pH, high concentrations of soluble salts, a high moisture content, and interstitial fluids of high ionic strength. Toxic and radioactive elements exist in the tailings in high concentrations, but with irregular distribution (Longmire and Brookins, 1982).

Water levels and water chemistry have been monitored since 1975 in monitor wells located around the tailings pond. To date, over 100 monitor wells have been installed. The majority of these wells are completed in the Two Wells Sandstone, with a few completed in the lower, Paguate Sandstone. These wells are sampled twice a year and are analyzed for pH, temperature, conductivity, chloride, sulfate, nitrate, bicarbonate, as well as heavy metals and radionuclides. Leachate draining directly from the pond is also analyzed. The results of the monitoring program are published in semi-annual reports prepared by Hydro-Engineering (1981-1987) and Intera, Inc. (1988-present). These data have been especially useful in determining the local direction of ground-water flow and as a tracer test to determine the vertical hydraulic conductivity of the Mancos Shale.

Horizontal ground-water flow pattern

The monitor wells at the L-Bar tailings pond can be used to determine the local horizontal and vertical flow patterns. Figure 7 shows the locations of monitor wells at the site. Figure 8 shows selected monitor wells that are completed in the Two Wells Sandstone, along with water level contours . The contours indicate a horizontal direction of flow that is toward the northwest and southwest. However, when regional water level data is added , it appears that the ambient regional flow direction is toward the east and southeast(Figure 9). The water table near the tailings pond is elevated, probably a result of mounding of the water table directly beneath the tailings pond. Figure 7 also shows the 100 mg/L concentration contour line for chloride (approximate background level). High chloride concentrations are considered an indication of leakage from the tailings pond through its rock salt liner. Thus, chloride is used as a tracer to establish infiltration

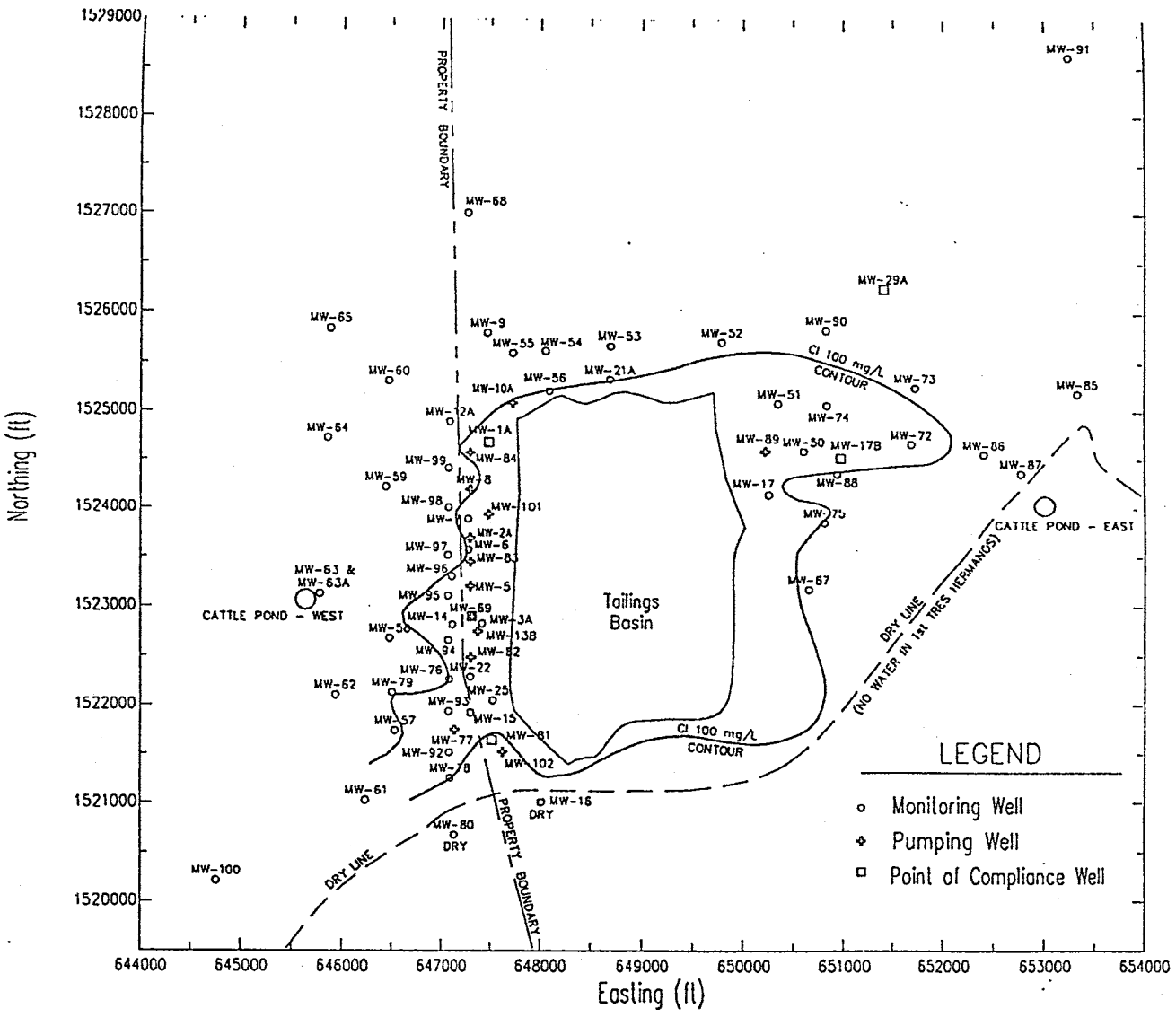

Figure 7: L-Bar uranium tailings site: monitor well locations (from Intera, Inc., 1993).

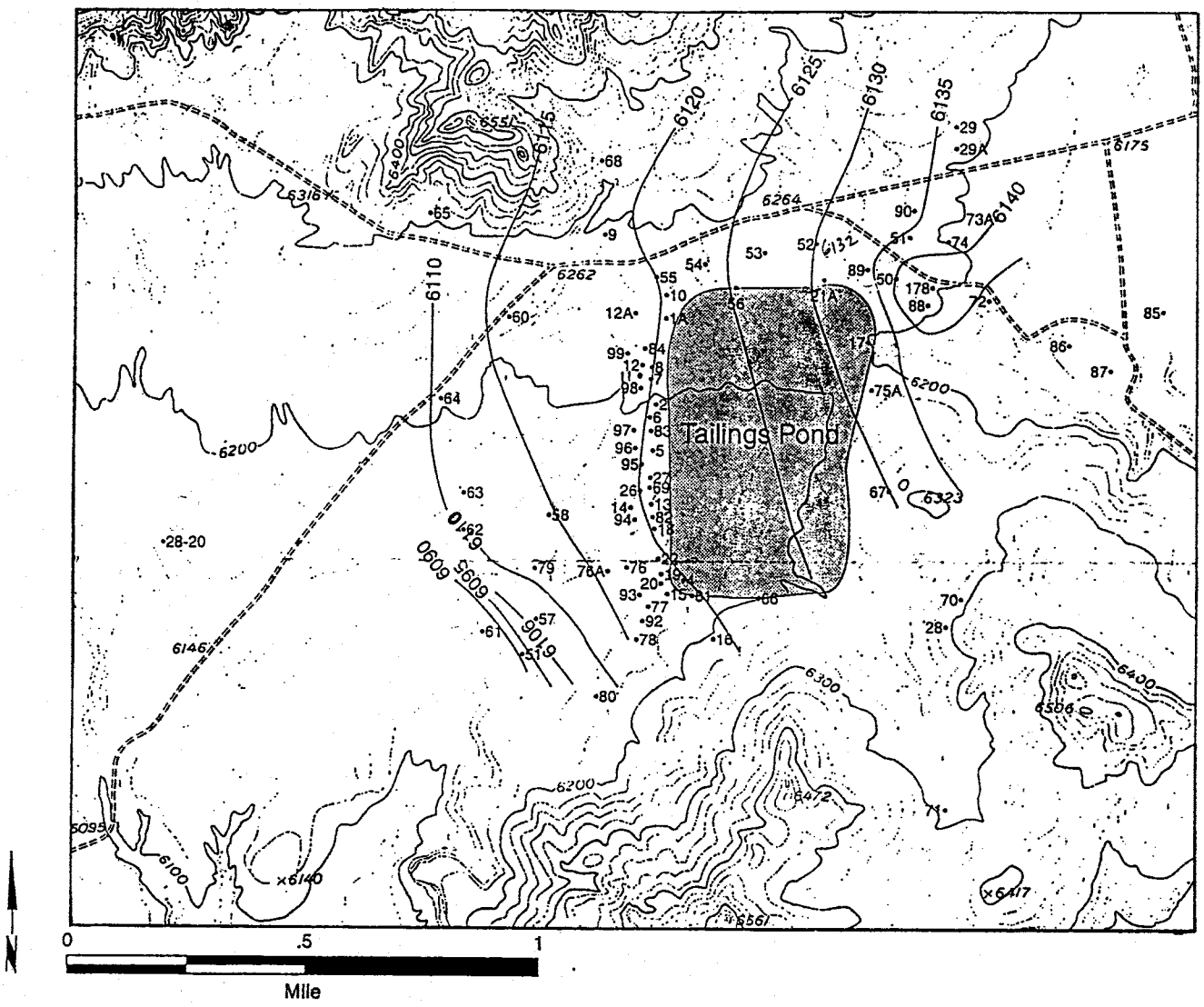

Figure 8. Water level contour map for the Two Wells Sandstone near the L-Bar tailings pond. Water level elevations are in feet above mean sea level.

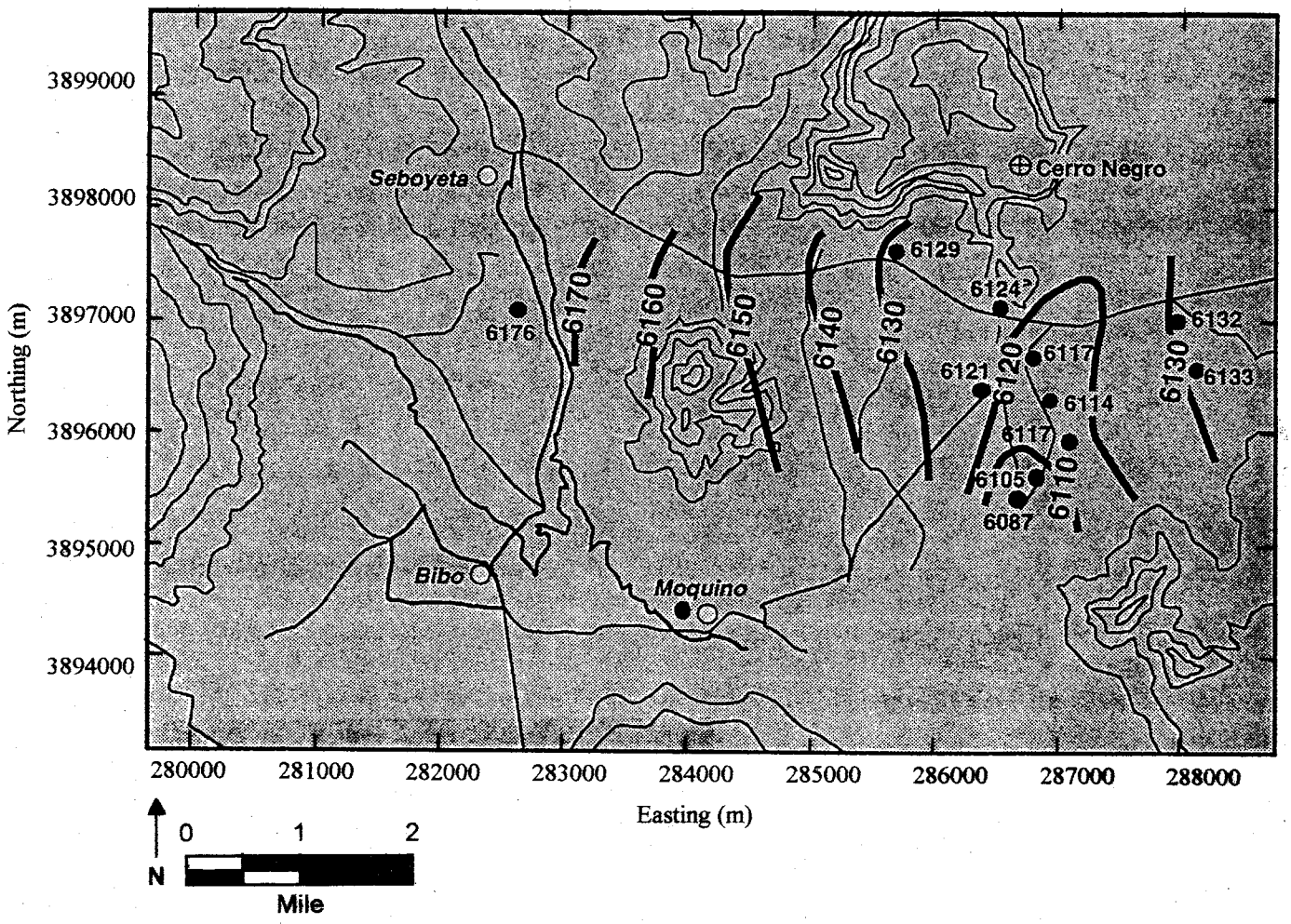

Figure 9: Regional water level map for the Two Wells Sandstone. Water level elevations are in feet above mean sea level. Easting and northing are based on 1000-meter Universal Transverse Mercator coordinate system.

and migration of contamination from the tailings pond. The chloride concentration contour in Figure 7 indicates that there has been leakage through the Mancos Shale and away from the pond.

Vertical flow gradients

Vetical flow gradients can also be determined from water level measurements in wells surrounding the tailings pond. Figure 10 shows water levels in three wells completed in different units near the L-Bar tailings pond (the Cerro Negro vertical well, CNV, was sampled at three isolated intervals, as disscussed in the following section on sampling strategy). Monitor well 60 is completed in the Two Wells Sandstone and is approximately 300 m from MW-11, which is completed in the Paguate Sandstone. The vertical gradient between these two units is downward, because the water level elevation in the upper unit (Two Wells) is higher than the water level elevation in the lower unit (Paguate).

Water levels were measured at isolated intervals in the CNV well and are indicated in Figure 10. However, the measurements in the Two Wells and Paguate aquifers in this well were taken after the water was allowed to equilibrate for only 24 hours. The water level shown in Figure 10 for the Cubero Sandstone was measured six months later, after complete equilibration, and had increased by nearly 85 m, from greater than 150 m below ground surface to 67.8 m below ground surface. This indicates that the measurements from the Two Wells and Paguate aquifers may not be accurate, and are probably much higher. Assuming these water levels are actually higher than indicated in Figure 10, the vertical gradient is downward.

Method of estimating vertical conductivity

The chloride concentration data from the tailings pond can be used to calculate the approximate vertical conductivity of the Mancos Shale by two different methods. The first is to determine the time it took for the chloride pulse to travel the distance from the tailings pond to the top of the Two Wells Sandstone layer. Dividing these two numbers will give a vertical seepage velocity. The vertical hydraulic conductivity can then be calculated by Darcy's Law.

Monitor well 1A (MW-1A) is located at the northwest corner of the tailings pond and is used for this first calculation. Figure 11 shows the necessary information . Drilling logs indicate that the Mancos Shale is 39.6 m (130 ft) thick in MW-1A. The high concentration chloride pulse reached MW-1A in the fall of 1979, or three years after tailings were first ponded. This gives a vertical seepage velocity (V_z) of 4.19×10^{-7} m/s

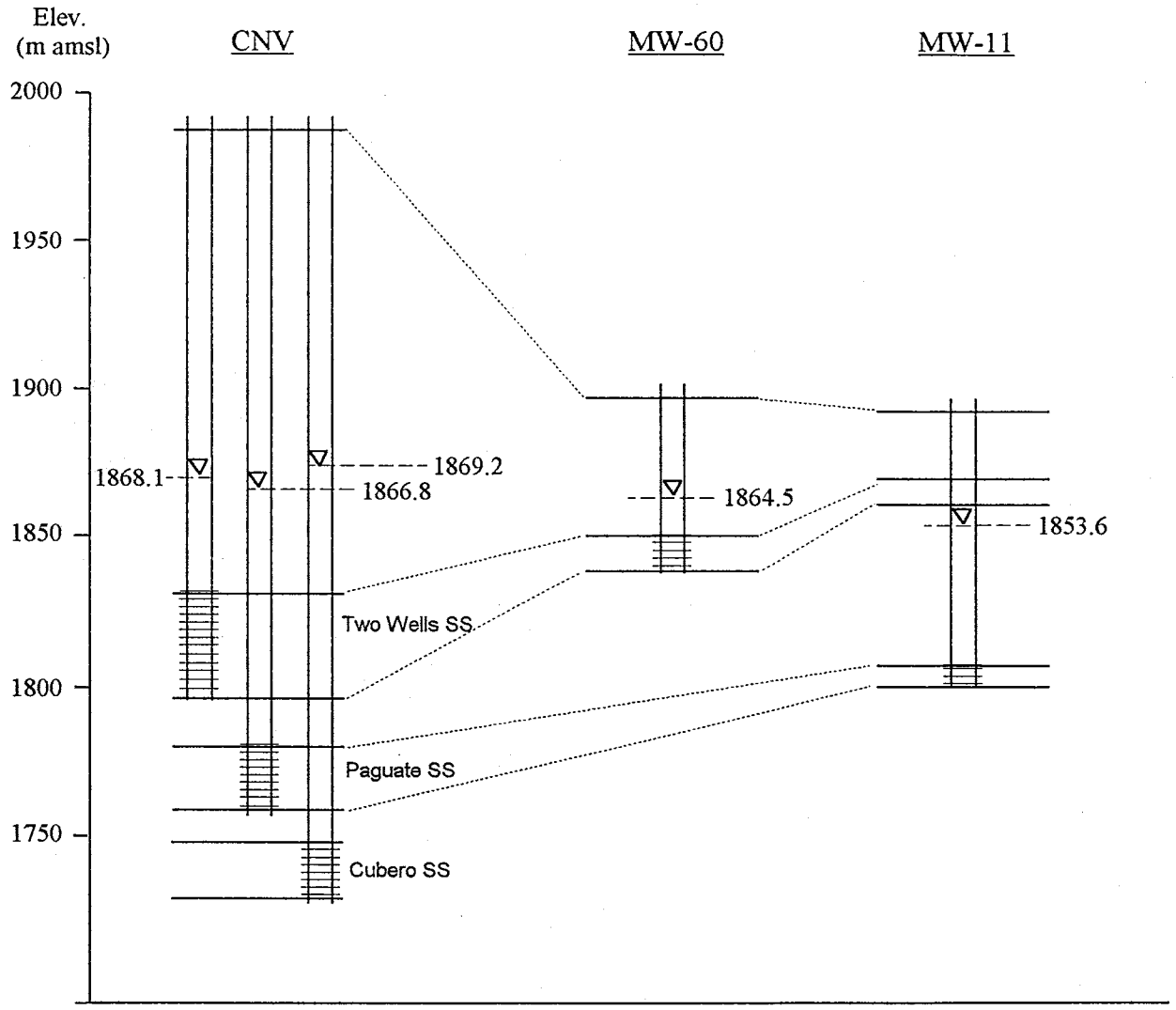

Figure 10: Water level measurements in the Two Wells, Cubero, and Paguate aquifers.

MW-1A	
Date	Cl^- (mg/L)
4-09-76	77
7-07-76	41
10-06-76	71
1-20-77	41
4-12-77	77
7-13-77	57
10-19-77	47
4-06-78	103
7-12-78	57
10-20-78	--
2-21-79	100
9-10-79	1180
3-25-80	1200
6-05-80	1400
8-19-80	1450
10-10-80	1200
11-25-80	756
1-21-81	290

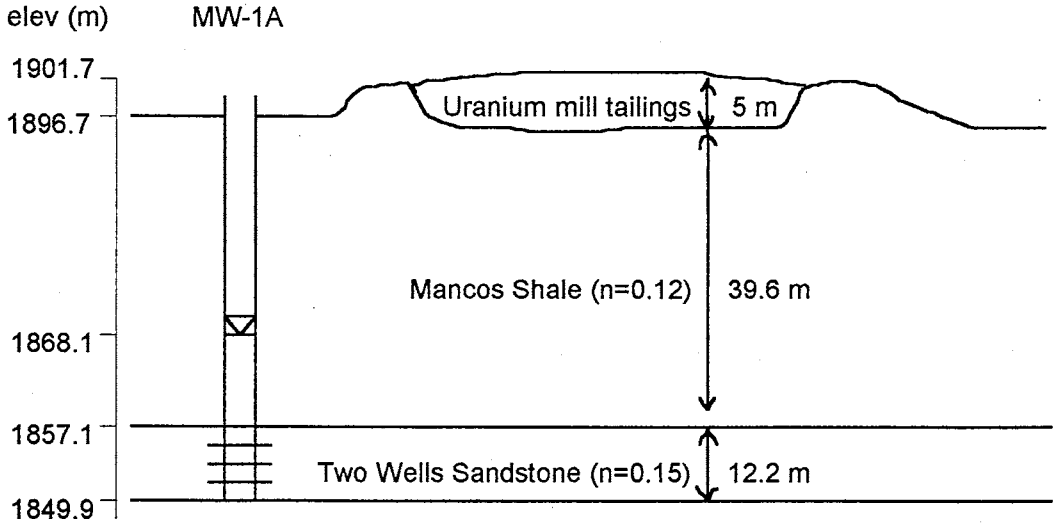

Figure 11: Chloride concentration and well data for MW-1A, necessary for estimating vertical conductivity.

(13.2 m/yr). At the same time, the water level in MW-1A was 1868.1 m (6129 ft). The ground surface elevation of MW-1A is 1896.7 m (6229.9 ft). Since the tailings were ponded to a depth of about 5 m (15 ft), the water level elevation in the pond can be approximated as 1901.7 m (6237.9 ft). The vertical gradient (J_Z)is given by

$$J_z = \frac{\Delta h}{\Delta z}$$

where Δh is the difference in water level elevation between the pond and the Two Wells Sandstone and Δz is the thickness of the Mancos Shale. This gives a vertical gradient of 0.85. The vertical hydraulic conductivity (K_Z) can be determined from Darcy's Law as follows:

$$K_z = \frac{V_z n}{J_z}$$

where n is the porosity. Using a porosity of 0.12 (the porosity of the Mancos Shale - Table 2), this equation gives a vertical conductivity of 5.90×10^{-8} m/s (1.86 m/yr). Ward et al. (1982) reported a vertical conductivity of 1.62×10^{-8} m/s (0.51 m/yr) using a similar method.

The second method is a mass balance approach. The approximate volume of contaminated aquifer (m^3) at a particular time is divided by the cross-sectional area of the tailings pond (m^2). The resulting length term is divided by the length of time since tailings disposal to give a vertical seepage velocity. Again, vertical conductivity can be calculated by Darcy's Law.

Figure 12 shows the chloride concentrations at monitor wells around the tailings pond in the fall of 1980, four years since tailings disposal began. The background concentration level for chloride is around 100 mg/L (Hydro-Engineering, 1981) The contour line in Figure 12 represents the approximate 100 mg/L chloride boundary, taken to represent the area of contamination around the pond, or approximately 9.39×10^5 m^2. The average thickness of the Two Wells Sandstone below the tailings pond is 12.2 m, with a porosity of 0.15, and the average thickness of the Mancos Shale is 44.2 m with a porosity of 0.12. The volume of contaminated water in the aquifer is then 6.70×10^6 m^3. The area of the pond itself is approximately 7.36×10^5 m^2. Dividing the volume of contamination by the area of the pond gives 9.10 m. Dividing this by the time since disposal began, 4 yr, gives a seepage velocity of 7.23×10^{-8} m/s (2.28 m/yr). Darcy's Law

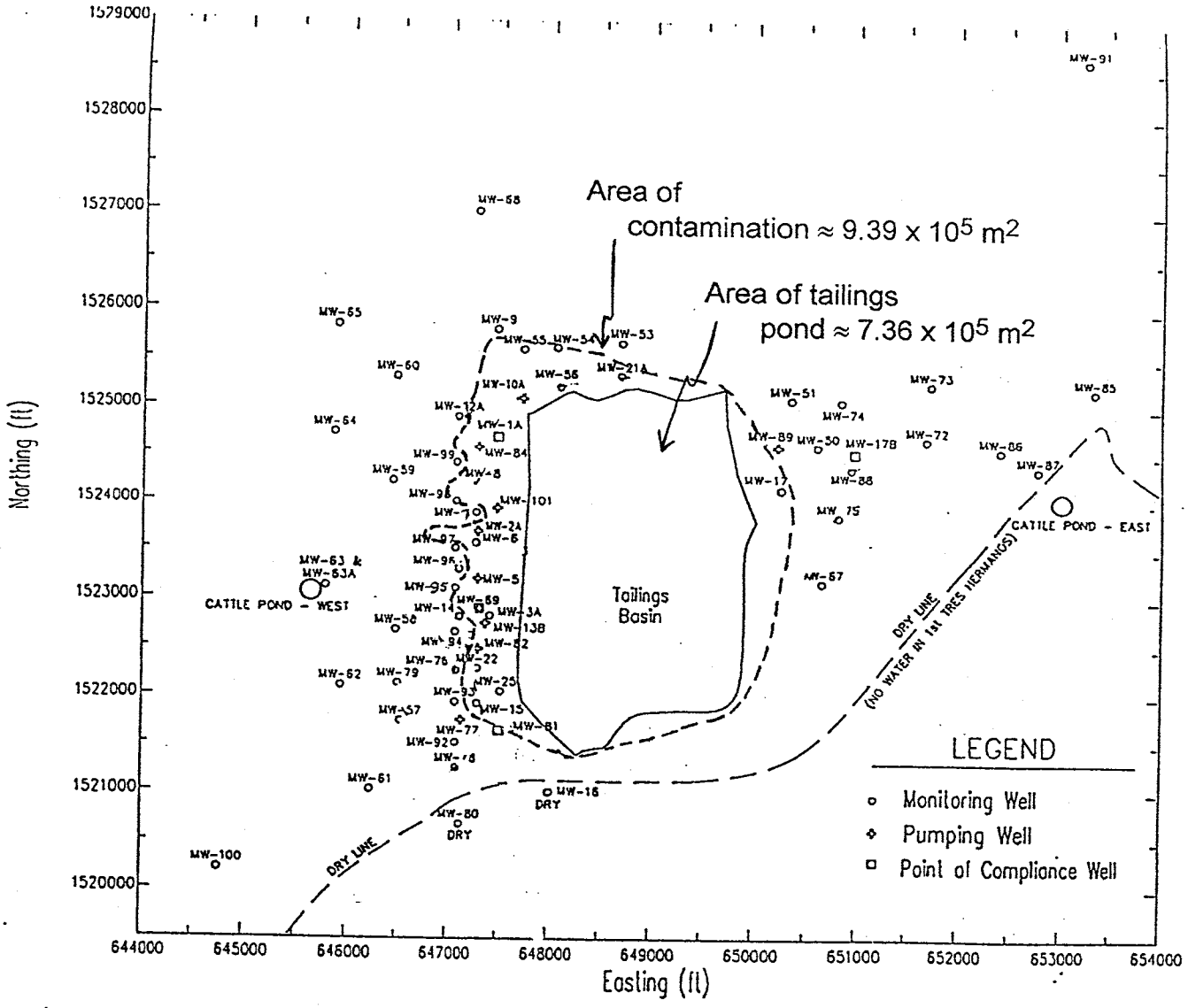

Figure 12: Map of L-Bar tailings pond. Dashed line represents approximate 100 mg/L chloride concentration contour in the fall of 1980.

can now be applied, assuming the same porosity and vertical gradient as above, to give a vertical hydraulic conductivity of 1.01×10^{-8} m/s (0.32 m/yr).

Borehole Drilling

Goals of drilling

Drilling at Cerro Negro took place in the summer and fall of 1994. The objective was to drill two boreholes - a vertical borehole well beyond the thermal aureole and an angled borehole extending from the unheated rock, through the aureole, to the Cerro Negro intrusion itself.

Locations of boreholes

The vertical borehole was located approximately 1200 m southwest of the main Cerro Negro plug on a flat expanse of alluvium-covered Mancos Shale. The angled borehole was located on the talus-covered flanks of the intrusion, approximately 450 m southwest of the main plug (Figure 13) Core samples were taken from the original vertical borehole, but that hole was plugged and a second vertical borehole was drilled for geophysical logging and completion as a water supply well. Problems with maintaining the drilling angle in the first angled borehole forced the drillers to abandon that hole and start again a few meters to the east. In all, four boreholes were drilled, with samples coded CNV, CNV-R, CNA, CNA-R.

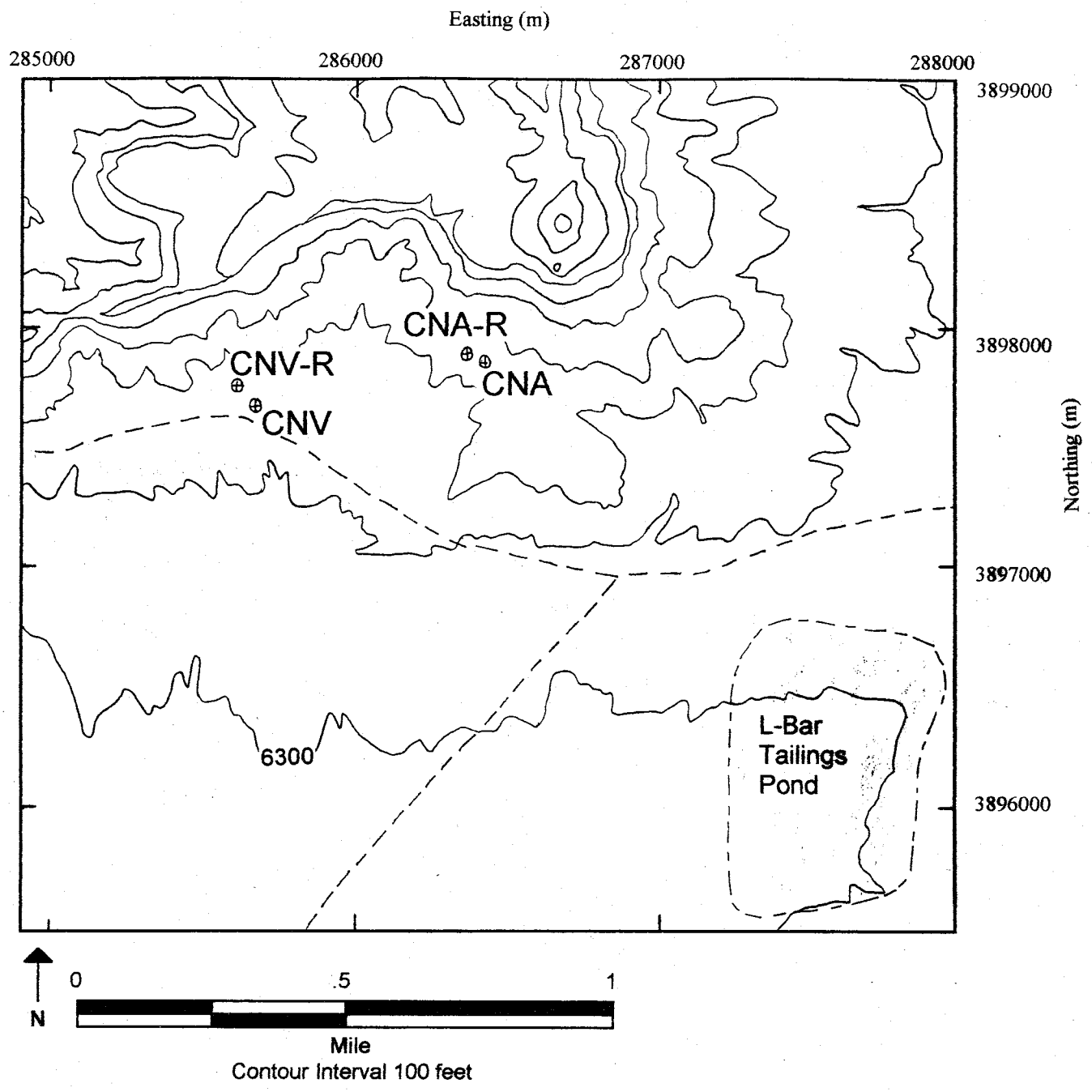

Figure 13: Map of Cerro Negro borehole locations. Easting and northing are based on 1000-meter Universal Transverse Mercator coordinate system.

Drilling methods

Tonto, Inc., of Salt Lake City, Utah, was contracted to perform the drilling at Cerro Negro. All boreholes were drilled with a rotary drill rig, using mud, air, or nitrogen as the drilling fluid, a diamond bit for coring and a tri-cone bit for advancing the borehole without coring.. Because of its potential to contaminate microbiology core samples, drilling mud was only used when necessary to advance the borehole. During core sampling, nitrogen was preferred as the drilling fluid so as not to introduce oxygen into the samples. However, problems arose during directional drilling of the angled borehole. The angle of drilling tended to dip when air and nitrogen were used, so drilling mud was used during non-critical core sampling.

Sampling strategy

Continuous core was obtained from both the first vertical borehole and the angled borehole. These cores were in 1.5 m sections and were geologically logged and saved in core boxes for geologic information or later sampling for non time dependent mineralogical or geochemical properties. A total of seventy six microbiological samples were collected from the cores. Twenty one samples were collected from the first Cerro Negro vertical borehole (CNV), forty six from the Cerro Negro angled borehole (CNAR), and nine from the Cerro Negro vertical repeat (CNVR) , or second vertical borehole. These were immediately processed on-site, under aseptic conditions, for distribution and microbiological analysis by principal investigators

Water samples were obtained at four depths in the first vertical borehole, representative of three different geologic units (Figure 14). These were taken using a down-hole packer system and pump. Pristine samples were obtained by pumping the formation until key indicator parameters (e.g., dissolved oxygen) were stable. Because of the difficulty of emplacing the packer system and pump it was not possible to obtain water samples from the angled borehole. Water level elevation measurements were taken in the vertical borehole after the water was allowed to equilibrate for approximately 24 hours.

Scope of sampling - other research and people involved

The Cerro Negro project is a collaborative effort among many geoscientists and microbiologists. Table 4 lists the principal investigators involved in the project along with their various contributions and specific analyses.

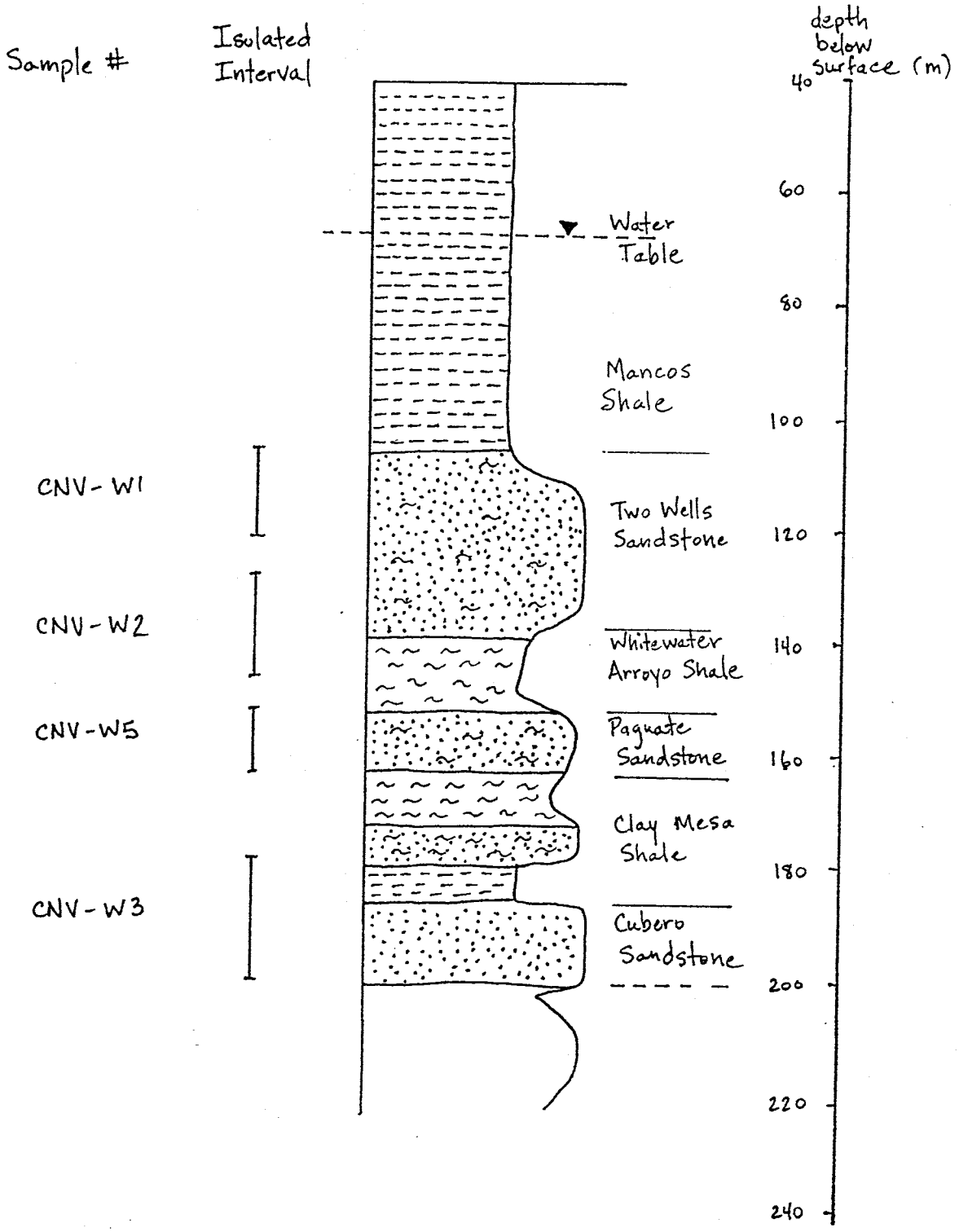

Figure 14: Water sample locations for Cerro Negro vertical borehole (CNV).

Table 4: Investigator Scientific Contributions

Microbiology

Investigator	Institution	Analysis	Contribution
D. Balkwill	Florida State University	culturable aerobes; preservation of aerobic cultures; 16S rRNA gene sequencing	characterization of in situ community; identification of cultures for molecular clocks; determination of phylogeny of organisms
D. Boone	Oregon Graduate Institute	culturable anaerobes; preservation of anaerobic cultures	characterization of in situ community; identification of cultures for molecular clocks; information about systematics of novel organisms
D. Caldwill	University of Saskatchewan	enrichment and preservation of microbial communities	starvation-survival in subsurface bacteria; community interactions
W. Chesbro	University of New Hampshire	culturable aerobes; role of Tween and elevated CO2 on growth; starvation characteristics of pure cultures	physiological adaptations; survival mechanisms
F. Colwell	Idaho National Engineering Laboratory	community-level substrate use patterns; enrichments for S and Fe lithotropes	characterization of subsurface community; identification of potential in situ nutrient sources
M. Fletcher	University of Maryland	bacterial attachment and transport through core material	factors controlling transport of bacteria
L. Forney	Michigan State University	effect of nutrient limitations on genetic rearrangement in subsurface bacteria	rates of genetic change of subsurface bacteria; evolution
J. Fredrickson, F. Brockman, T. Stevens	Pacific Northwest Laboratory	aerobic and anaerobic activities, enrichments and MPNs for selected aerobes and anaerobes	in situ activities and nutrient requirements; organism characteristic of depositional environment
R. Griffiths	Oregon State University	aerobic metabolic and enzymatic activities; influence of salt	in situ activities; survival mechanisms, adaptations
W. Holben	Agouron Institute	molecular analysis of whole community DNA based on %G+C fractionation	comparison of surface and subsurface communities

T. Kieft, P. Amy	New Mexico Tech, University of Nevada-Las Vegas	total microscopic counts, endogenous respiration; aerobic respiration of 14C-labeled organic compounds	in situ metabolic activities; endogenous nutrient sources; physiological adaptations
A. Matin, T. Schmidt	Stanford University, Michigan State University	starvation gene expression and role in survival of subsurface bacteria	genetic/physiologic mechanisms responsible for long-term survival
R. Miller	Oklahoma State University	presence of bacterial viruses; recA gene in subsurface bacteria	adaptation/evolution in subsurface bacteria; distinguishing ancient vs. modern organisms
S. Nierzwicki-Bauer	Rensselaer Polytechnic Institute	characterization of community using phylogenetic group-specific 16S rRNA-directed oligo probes	phylogenetic characterization of subsurface community; ID of bacteria for molecular clock analyses
T. Phelps	Oak Ridge National Laboratory	anaerobic activities; enrichments and MPN's of select anaerobes	in situ activities; nutrient requirements; nutrient sources
F. Roberto	Idaho National Engineering Laboratory	phylogenetic characterization of whole-community DNA; Fe lithotrophs	phylogenetic characterization of ancient rock/sediments
D. White, D. Ringelberg	University of Tennessee	lipid analysis for total biomass; community structure; nutritional status	characterization of in situ community; surface vs. subsurface comparisons

Geosciences

J. McKinley	Pacific Northwest Laboratory	pore-water chemical analysis; whole sediment analyses for C, N, P, S, and Fe	in situ activities and sources of nutrients; chemical conditions influencing survival
E. Murphy	Pacific Northwest Laboratory	analysis of vadose zone recharge rates; ground-water sampling for microorganisms and geochemical dating	hydrogeological and geochemical analysis for evaluating microbial transport
B. Bjornstad, P. Long, C. Murray	Pacific Northwest Laboratory	geologic logging; stratigraphic interpretation, mesoscopic petrographic relationships	geologic framework for samples; geologic history; environment of deposition
F. Phillips	New Mexico Tech	regional hydrology/14C dating of ground water	hydrologeologic flow regime, rate of ground-water flow
T.C. Onstott	Princeton University	geochemical analyses of fluids and gases in inclusions; C, O, and S stable isotopes, Ar/Ar dating	temperature/salinity and biomineralization history
S. Rawson, C. Gullett	Pacific Northwest Laboratory	sediment physical properties (i.e., porosity); petrography	constraints on transport; paleoenvironmental conditions

K. Wohletz	Los Alamos National Laboratory	thermal modeling of intrusion	temperature field as a function of time in sediments around the intrusion
J. Clayton	U.S. Geological Survey	organic carbon characterization	source of organic carbon, organic carbon diagenesis

Details on Analysis of Cerro Negro Samples

Geological Analyses

Physical Properties (Rawson, Gullett, Bjornstad)

- Permeability
- Porosity
- Pore throat size distribution
- Fracture Analysis
- Petrography (relict microbial textures, diagenetic history, mineral paragenesis)
- Moisture
- Sedimentary structures
- Paleontology
- Color

Chemical Analysis of Porewater/Ground Water (McKinley/Murphy)

- Cations/anions
- pH, Eh
- Redox species; DO, Fe(II)/Fe(III), S species
- DOC, organic acids, DIC, carbonate
- TOC
- Tritium analyses
- Dissolved gases: methane, hydrogen
- S species
- Total P, organic P
- Total N
- Carbonate C

Chemical Analyses of core (McKinley)

- Cations/anions
- pH, Eh
- Redox species (bulk): Fe(II)/Fe(III)
- organic acids, carbonate
- TOC
- S species
- Total P, organic P
- Total N
- Carbonate C
- Extractable forms of Fe: HCL Fe(II)/Fe)III), OHamine-HCL, DCB

Isotopic Analyses of Ground Water/Pore Water

- $\delta^{18}O$, δD, $\delta^{13}C$ of ground water and pore water samples (Murphy/McKinley)
- ^{14}C dating of ground water samples (Phillips)
- ^{18}O and $\delta^{34}S$ of sulfate from ground water and pore water samples (McKinley)

- D and $\delta^{13}C$ of dissolved methane and hydrogen in ground-water samples if present (Grossman)
- Noble gas concentrations of ground-water samples (Onstott)

Isotopic Analyses of Minerals (Onstott)

- ^{18}O and $\delta^{13}C$ of carbonate in shale and sandstone including concretions
- ^{34}S of pyrite
- ^{34}S of organics
- ^{13}C of organic matter in shales
- $^{40}Ar/^{39}Ar$ dating of illite/smectite clays

Compositional Analyses of minerals

- Fluid inclusions in authigenic minerals (Onstott)
- Fission track analyses of apatites in sandstones (Onstott)
- Clay mineralogy of shales (Rawson)
- Compositional analyses of carbonates and sulfides including concretions (Onstott)
- Organic maturity of shales (Clayton, USGS)
- Magnetic susceptibility determinations (Onstott, USGS)

Microbiological Analyses

Culturable Microorganisms

- Aerobes: marine salts/freshwater; dilute/high nutrients, sporeformers, microaerophiles, thermophiles, hydrogeotrophs, Fe oxidizers S oxydizers (Balkwill, Colwell, Kieft, Fredrickson, Phelps)
- Anaerobes: fermentors, denitrifiers, Fe/Mn reducers, SRB, methanogens, acetogens, thermophiles, hydrogenotrophs, sporeformers (Stevens, Phelps, Boone, Gredrickson)
- Phylogenetic analysis of cultures, 16S sequencing and use of specific probes (Balkwill, Nierzwicki-Bauer)

Direct Measures of Biomass and Community Structure

- PLFA, lipid biomarkers, dipicolinic acid (White/Ringelberg)
- Direct microscopic counts (Kieft, Nierzwicki-Bauer)
- Phylogenetic probe analysis (Nierzwicki-Bauer)
- Community fingerprint: G+C fractionation of community DNA
- 16S rRNA PCR of directly extracted DNA (Roberto)

Activity Measurements

- Metabolically active cells (Nierzwicki-Bauer)
- ^{3}H-glucose uptake, ^{14}C-glucose mineralization (Griffiths, Kieft, Phelps)
- Photophatase activity (Griffiths)
- $^{35}SO_4^{2-}$ reduction (Fredrickson)
- ^{3}H-acetate incorporation into lipids (Phelps/Pfiffner)
- Mineralizable organic C (Colwell)

- Endogenous respiration (Kieft)

Derivative Microbial Cultures

- Pure cultures for phylogeny, molecular clocks analysis
- Na requirements for pure cultures (indicative of marine origins)
- Confirmation of spore-formers

Methods

Background

Flow Path Analysis

This study uses flow path analysis to quantitatively evaluate chemical and isotopic changes in water samples taken from different parts of an aquifer. A flow path is the path that a particular "packet" of water takes in its flow through an aquifer. A flow path is presumed to be perpendicular to the lines of equal hydraulic potential as depicted on a potentiometric surface map (Domenico and Schwartz, 1990). As water flows through an aquifer along its flow path, the water interacts with the rock matrix and undergoes chemical reactions that may be both quantifiable and predictable. These are known as evolutionary waters (Plummer, 1991). In ground-water systems, hydrologic and hydrogeologic intuition are commonly required in selecting truly evolutionary waters. Using chemical analyses of water samples at a starting and ending point along a flow path, as well as mineral phases through which the water flows, one can determine the net geochemical mass-balance reactions that occur along the flow path.

Carbon-14 Dating of Ground Water

Carbon-14 is a radioactive isotope of carbon which has proven useful in dating ground water. Carbon-14 has a half life of 5730 years (Godwin, 1962). It is formed continuously in the upper atmosphere by the action of cosmic-ray-produced thermal neutrons on ^{14}N (Libby, 1955), is oxidized to CO_2, and mixes rapidly with atmospheric CO_2. Any material that comes in contact with atmospheric CO_2, such as plants or water, will contain carbon-14 in equilibrium with that of the atmosphere. Carbon-14 activity measurements are reported as percent modern ^{14}C (pmc). Thus, the ^{14}C activity remains constant, at the atmospheric ^{14}C activity, so long as the material is in equilibrium with atmospheric CO_2. When the material is cut off from the atmospheric CO_2 reservoir, ^{14}C begins to decrease by radioactive decay and the amount of ^{14}C in a sample will be a function of the time since cutoff.

Carbon-14 in ground water comes mainly from dissolution of CO_2 gas in the vadose zone. If there are no further sources of carbon after the ground water loses contact with the soil gas, the age of the water can be determined from the decay equation:

$$time = -\frac{1}{\lambda_{14}} \ln \frac{A}{A_0}$$

where λ_{14} is the decay constant for ^{14}C of

$$\lambda = \frac{\ln 2}{5730}$$

and A is the measured activity of ^{14}C in a water sample and A_0 is the initial ^{14}C activity of the water.

The main problem in applying this method is that some aquifer minerals contain carbon. Dissolution of carbonate minerals provides a source of carbon to the ground water. Dissolution of CO_2 derived from organic material can also be a source of carbon. These sources of dissolved carbon contain no ^{14}C because of their age, and they dilute the ^{14}C signal that the water has from the original soil gas interaction. Thus, the observed ^{14}C activity may reflect an input of "dead" carbon in addition to radioactive decay, and the water sample will appear falsely old.

Often, the most important process affecting ^{14}C activity is the dissolution of calcite, as described above. However there can be several sources and sinks of carbon that may affect the ^{14}C activity of ground water. Mook (1980), Reardon and Fritz (1978), and Wigley et al. (1978) list the following processes that can affect the ^{14}C activity of water:

1. The congruent dissolution of carbonate minerals, which adds "dead" carbon, or carbon without ^{14}C activity to the ground water. Overall, this process lowers the ^{14}C activity measured for the sample.
2. The incongruent dissolution of carbonate or other Ca containing minerals accompanied by the precipitation of calcite. This process will remove ^{14}C as calcite precipitates and, if dolomite is the mineral dissolving, add dead carbon through congruent dissolution as described above. This process could occur in the saturated zone if calcite rapidly dissolves to equilibrium, then subsequently precipitates as dolomite slowly dissolves.
3. The addition of dead carbon from other sources such as the oxidation of old organic matter, sulfate reduction, and methanogenesis. These processes lower the ^{14}C activity of the sample.
4. Possible carbon isotopic exchange with carbonate minerals, which could lower the ^{14}C activity. This process is generally considered to have a negligible effect at normal ground water temperatures.

To obtain a valid water age it is necessary to understand which of the above processes may be affecting the observed ^{14}C activity. All ^{14}C effects that are a result of anything other than radioactive decay can be removed and the corrected initial activity can be used to calculate the true age.

Several methods are available for correcting the initial ^{14}C activity for dead carbon dilution. Traditionally, these adjustment models are applied to a single water analysis from the ground-water system and are suitable for considering inorganic reactions. Some of the better-known inorganic adjustment models are those of Vogel (1967, 1970), Tamers (1967, 1975), Pearson and White (1967), Mook (1972, 1976), Fontes and Garnier (1979), and Eichinger (1983).

The approach of Vogel (1967, 1970) is empirical and simply assumes A_0 has a value of 85±5 pmc. Measurements of dissolved carbon in 100 modern ground water samples from northwest Europe suggested that this value was in fact representative of soil water and shallow ground water in temperate climates.

The model of Tamers (1967,1970) uses the stoichiometry of carbonate solution reactions to calculate an A_0 based on the solution pH.

Pearson and White (1967) use $\delta^{13}C$ as a measure of the extent of carbonate reactions. This method relies on a $\delta^{13}C$ mass balance rather than the carbonate stoichiometry as a basis for ^{14}C dilution corrections.

The Mook (1972, 1976) model considers a system that is initially open to soil CO_2 and that all carbonate minerals, gas, and aqueous species are both in chemical and isotopic equilibrium with the soil CO_2 gas. Isotopic re-equilibration then occurs below the water table.

Fontes and Garnier (1979) also consider a two-stage evolution of recharge waters, which accounts for dissolution and isotopic exchange of carbonate minerals with CO_2 in the unsaturated zone as well as isotopic exchange with carbonate rocks in the saturated zone.

Eichinger (1983) developed an isotope-exchange/mass balance model accounting for equilibrium isotopic exchange for introduction of soil CO_2 into the water and equilibrium exchange between dissolved inorganic carbon and the carbonate rock.

All of these approaches are useful but they do not account for many of the processes affecting the ^{14}C activity of ground water. A more comprehensive approach is that of Wigley et al. (1978) which presents Rayleigh distillation and isotope mass balance models to predict isotopic evolution in carbonate mineral-water systems where both dissolution (incoming carbon) and precipitation (outgoing carbon with isotopic

fractionation) reactions occur. Wigley et al. (1978) proposed that geochemical mass-balance models could be constructed for evolutionary waters to adjust the initial ^{14}C values for reactions occurring along the flow path. With the mass balance modeling approach, a separate adjustment model is constructed for each pair of initial and final waters along a flow path.

Tritium

Tritium is a radioactive isotope of hydrogen (half-life of 12.4 years) that has also proven useful in dating ground water. Tritium (^{3}H) is measured in tritium units (TU) , with 1 TU corresponding to one atom of ^{3}H in 10^{18} atoms of ^{1}H (Fontes, 1980). Tritium is produced naturally in the upper atmosphere by cosmic ray spallation of ^{14}N. This free tritium collides with O_2 to form tritiated water (HTO), which then enters the water cycle (Harteck, 1954).

However, tritium generated by thermonuclear testing in the atmosphere between about 1952 and 1963 has swamped the natural production of tritium. Bomb testing caused an increase of tritium concentration in rainfall from a natural mean level of about 10 TU to over 2000 TU. Tritium levels declined once weapons testing stopped in 1963, but present-day levels remain above natural background (IAEA, 1983). Although the uncertainties and complexities of atmospheric loading of tritium make it difficult to work with tritium in such a quantitative way as ^{14}C, the bomb tritium pulse can be used as a natural tracer to determine recharge rates (eg., Daniels et al., 1991 and Solomon et al., 1992). The main application, though, is to differentiate pre-1952 water from younger water. The logic is that, assuming pre-1952 water has an original tritium concentration of 10 to 15 TU, the concentration today, considering over forty years of decay, would be less than 0.6 TU, or less than the detection limit for many analysis techniques. Thus, any detectable tritium in a sample implies that the water contains some component of more recent or post-1952 water (Fontes, 1980).

Stable Isotopes

The natural variation of the stable isotope ratios of hydrogen and oxygen in precipitation can be used as a tracer of the origin of ground water. Oxygen-18 is a stable isotope of oxygen, and the ratio of ^{18}O to the more abundant ^{16}O is a useful measurement in determining the origin of a water sample. Likewise, the ratio of hydrogen isotopes, ^{2}H (deuterium) to ^{1}H, can be used as a tracer. Both ratios are measured with respect to Standard Mean Ocean Water (SMOW) and are expressed as a per mil (‰) deviation from SMOW ($\delta^{18}O$ and δD).

Oxygen-18 and deuterium ratios are conservative in ground water, and ground water "remembers" the isotopic composition of its origin over long periods. The isotopic composition of ground water is often found to match the mean composition of precipitation over the recharge area. The main controls on $\delta^{18}O$ and δD of precipitation are temperature, elevation, and humidity. The most common processes affecting the isotope ratios of subsurface waters are evaporation (especially in arid climates), rock interactions and methanogenesis.

When the $\delta^{18}O$ and δD content of rain water from sampling sites around the world are plotted together, they lie along a straight line, known as the meteoric water line (Craig, 1961). The equation for this line is approximately $\delta D = 8\delta^{18}O + 10‰$. The meteoric water line provides an important key to the interpretation of deuterium and oxygen-18 data. Water with an isotopic composition falling on the meteoric water line is assumed to have originated from the atmosphere and to be unaffected by isotopic processes. Deviations from the meteoric water line indicate, in an often distinctive way, other isotopic processes. The most common deviation from the meteoric water line for ground water samples in arid zones is a shift to the right. Water samples plotting to the right of the meteoric water line have often undergone evaporation in the unsaturated zone, resulting in enrichment of heavy isotopes relative to precipitation (Fontes, 1981).

Temperature also plays a role in deviations from the meteoric water line. Decreasing temperature of formation leads to decreasing $\delta^{18}O$ and δD in precipitation (Dansgaard, 1964). This phenomenon has been very useful in the study of paleoclimates.

NETPATH

This study uses the computer program NETPATH (Plummer et al., 1994) to analyze net geochemical mass-balance reactions along a flow path. NETPATH uses geochemical mass balance modeling to aid in defining hypothetical geochemical reactions that can account for the observed variation in chemical, mineralogical, and isotopic compositions of ground water during its evolution between a starting composition and a final composition. This study also utilizes the radiocarbon dating feature of NETPATH, in which carbon mass balance is combined with Rayleigh distillation equations for all incoming carbon sources and all fractionating outgoing carbon phases, to adjust the initial ^{14}C activity for the modeled geochemical reactions and determine an corrected ^{14}C age.

Chemical Mass Balance

NETPATH starts with a database generated by the aqueous speciation program WATEQF (Plummer et al., 1976). WATEQF uses thermodynamic data to calculate the species distribution and mineral saturation index for each water sample. NETPATH then interprets net geochemical mass balance reactions between an initial and final water along a hydrologic flow path. The inverse geochemical modeling approach of NETPATH is discussed by Plummer and Back (1980), Parkhurst et al. (1982), Plummer et al. (1983), Plummer (1984), Plummer et al. (1990). This approach is based on the idea that, if the change in water composition between arbitrary starting and ending points in a ground-water system can be attributed only to effects of reactions, the net chemical reactions accounting for the change can be quantified by means of mass balance relations and thermodynamic and stoichiometric constraints. This is an inverse modeling approach because it predicts the possible chemical pathways that can explain beginning and ending observations. Mass balance calculations can only unambiguously demonstrate that certain reactions *cannot* occur in a system. Proof of reaction is never positive with this approach, but through a process of elimination there often remains a single reaction model that is consistent with the observed chemical and isotopic data.

In most ground water applications of mass balance modeling it is assumed that water originating in the recharge area of an aquifer evolves by reaction with the host rock as it moves down gradient in the system. Knowing the composition of an initial and final water along the flow path, and having selected a plausible set of reactants and products, a mass balance can be made on the change in total molality of each constituent along the reaction path. Plummer and Back (1980) describe the mass balance as n equations, one for each constituent, similar to

$$\sum_{j=1}^{\varphi} \alpha_j \beta_{c,j} = \Delta m_c \Big|_{c=1,n}$$

where φ is the total number of minerals and gases (reactants and products) in the mass balance reaction, n is the minimum number of constituents necessary to define the composition of the chosen minerals and gases, α_j is the stoichiometric (reaction) coefficient of the j^{th} mineral or gas in the mass balance reaction in moles per kg water (positive for reactants and negative for products), $\beta_{c,j}$ is the stoichiometric coefficient of the c^{th} constituent in the j^{th} mineral or gas, and Δm_c is the change in moles per kg water of the c^{th} constituent in the aqueous phase along the reaction path. When the values of Δ

m_c are known the net mass balance can be obtained by simultaneous solution of the n equations.

NETPATH refers to a net geochemical mass balance as a model. A model is defined as the masses (per kg water) of a set of plausible minerals and gases that must enter or leave the initial solution in order to exactly define a set of selected elemental and isotopic constraints observed in a final (evolutionary) water. A constraint is typically a chemical element, and is included in the model to constrain the masses of selected phases that can enter or leave the aqueous solution. Measured chemical compositions of initial and final waters are usually used as constraints. A phase is any mineral or gas that can enter or leave the aqueous solution along the evolutionary path. Only phases that are known to occur in the system should be included. Thus, detailed knowledge of the minerals present in the aquifer rocks will greatly improve the modeling results.

Carbon-14

The NETPATH model (Plummer et al., 1991, 1994) generalizes the approach of Wigley et al., (1978) for ^{14}C dating in hydrochemical systems where chemical and isotopic data have been measured. As mentioned previously, Wigley et al. (1978) proposed that geochemical mass-balance models could be constructed for evolutionary waters to adjust the initial ^{14}C values for reactions occurring along the flow path. NETPATH uses this calculated mass transfer (based on the NETPATH model chosen to be most consistent with the data and geochemical reasoning) to adjust the ^{14}C composition at the final well for chemical reaction but not radioactive decay, denoted A_{nd}. NETPATH computes A_{nd} using the defined value of A_0, defined ^{14}C isotopic content of carbon sources, defined ^{14}C fractionation factors, and the computed carbon mass transfer. Radiocarbon dating is then applied to the final well using A_{nd} and the observed value, A. Thus, the age-dating procedure depends on three values of ^{14}C activity (1) the ^{14}C value for the initial well, A_0, (2) the adjusted ^{14}C value calculated at the final well by accounting for reaction effects to the initial ^{14}C, A_{nd} and (3) the measured ^{14}C content in the final water, A. The adjusted ^{14}C age is calculated according to the equation:

$$\Delta t(years) = \frac{5730}{\ln 2} \ln\left(\frac{A_{nd}}{A}\right)$$

The ^{14}C age is the travel time, in years, between the initial and final wells.

As discussed previously in the section on methods of ^{14}C dating of ground water, several models have been proposed in the hydrogeochemical literature for estimation of A_0. NETPATH considers nine possible means of defining the initial ^{14}C. These are termed:

1. Original Data
2. Mass Balance
3. Vogel
4. Tamers
5. Ingerson and Pearson
6. Mook
7. Fontes and Garnier
8. Eichinger
9. User-defined

The "original data" method uses the ^{14}C content of dissolved inorganic carbon in the initial well as the value of A_0. The "mass balance" method calculates a chemical mass balance on the initial water composition assuming reaction of pure water with calcite, dolomite, gypsum, and CO_2 gas.

NETPATH has pre-defined default values of parameters associated with each model, but any default value can be altered by the user. NETPATH is capable of calculating the ^{14}C age of a final water based on each model option, or the user can pre-select the model that is most appropriate for the specific reaction conditions.

It is important to note that, unlike the literature models which consider only dissolved inorganic carbon (DIC), NETPATH defines total dissolved carbon as the sum of dissolved inorganic carbon, methane, and dissolved organic carbon - that is,

$$m_{TDC} = m_{TDIC} + m_{CH_4} + m_{DOC}$$

where the subscripts TDC, TDIC, CH_4, and DOC refer to total dissolved carbon, total dissolved inorganic carbon, dissolved methane, and dissolved inorganic carbon. Thus, the values of A_0 are calculated as follows:

$$A_{oTDC} = \frac{A_{oTDIC} m_{TDIC} + {}^{14}C_{CH_4} m_{CH_4} + {}^{14}C_{DOC} m_{DOC}}{m_{TDC}}$$

Therefore, when masses of dissolved methane and dissolved organic carbon are put into the NETPATH database, ^{14}C activities must also be entered, otherwise the A_0 for total dissolved carbon will be in error.

Sample Collection and Analysis

Water Sample Collection

Water samples were collected for the analysis of a full range of parameters during the fall and summer of 1995. An in-line Hydrolab sonde was used to monitor field pH, temperature, conductivity, Eh, and dissolved oxygen. All wells were pumped, either with a portable bladder pump or an existing submersible pump, until these field parameters stabilized. Samples were then collected for ion chemistry, dissolved carbon (inorganic and organic), iron redox species, ^{14}C, $\delta^{13}C$, $\delta^{18}O$. δD, tritium, and ^{34}S. Table 5 lists the details of sample collection, including type of collection bottles and preservatives used. Some samples were filtered with a 0.45 μm in-line filter, as noted.

Water Sample Analysis

Cations were measured by inductively coupled plasma-atomic emission spectroscopy, and anions and iron species were measured by ion chromatography. All organic and inorganic carbon measurements were done on a Dohrmann carbon analyzer. These analyses were performed at Pacific Northwest Laboratories (Richland, WA). Carbon-14 measurements were performed by accelerator mass spectrometry at the Center for Accelerator Mass Spectrometry at Lawrence Livermore National Laboratory (Livermore, CA). All ^{14}C values are reported as percent modern carbon (pmc). The ^{13}C samples were extracted with phosphoric acid, sealed into pyrex tubes, and then measured by mass spectrometry at Duke University (Durham, NC). The $\delta^{13}C$ values are calculated as

$$\delta^{13}C = \left[\frac{^{13}C/^{12}C_{sample}}{^{13}C/^{12}C_{standard}} - 1 \right] \times 1000‰(\text{PDB})$$

Stable isotopes, $\delta^{18}O$ and δD, were measured by mass spectrometry at Washington State University's Stable Isotope Laboratory (Pullman, WA) and at New Mexico Institute of Mining and Technology (Socorro, NM). Reported stable isotope values are the means from the two labs. All stable isotopes are reported as per mil (‰) relative to SMOW (Standard Mean Ocean Water). Enriched tritium analyses were performed by scintillation counting at the Environmental Isotope Laboratory, University of Waterloo (Ontario, Canada), and are expressed in tritium units (TU).

All chemical data are listed in Table 6. Sample locations are listed in Table 3 and are illustrated in Figure 15.

Table 5: Sample collection information

Parameter	Container	Preservative
0.45 μm in-line filter		
Bulk Anion	500 mL glass	none
Bulk Cation	500 mL nalgene	10 mL conc. HNO_3/500 mL
Carbon	5 mL glass w/ septum cap	none
NH_3	glass scintillation vial	40 μL conc. H_2SO_4/20 mL
$Fe^{2/3}$	poly scintillation vial	20 μLconc. HCl/20 mL
Sulfide	amber glass	500 μL 10M NaOH/50 mL
Sulfide	amber glass	500 μL 2N ZnAc/50 mL
NO_2/NO_3	poly scintillation vial	40 μL conc. H_2SO_4/20 mL
Stable Isotopes	100 mL glass w/ cone cap	none
$\delta^{13}C$, ^{14}C	500 mL glass	none
δD, $\delta^{18}O$	40 mL scintillation w/ teflon cap	none
$\delta^{34}S$	1 L nalgene	none
^3H	500 mL glass	none
Unfiltered		
Carbon	5 mL glass w/ septum cap	none
NH_3	glass scintillation vial	40 μL conc. H_2SO_4/20 mL
$Fe^{2/3}$	poly scintillaton vial	20 μL conc. HCl/20mL
Sulfide	amber glass	500 μL 10M NaOH/50 mL
Sulfide	amber glass	500 μL 2N ZnAc/50mL
NO_2/NO_3	ply scintillation vial	40 μLconc. H_2SO_4/20mL
Stable Isotopes	100 mL glass w/ cone cap	none

NOTES: Each sample container was pre-rinsed multiple times with de-ionized water, oven dried and labelled. Preservatives were added in the laboratory prior to sample collection.

Table 6: Water chemistry data. All units mg/L unless otherwise specified.

Sample Name	Presbyteria	Elkins	Bibo	Seboyeta	Moquino	CNV-W2	CNV-W3	CNV-W5	MW-64	MW-65	MW-60	MW-68	L-Bar
Date sampled	10-27-94	10-27-94	10-5-94	10-5-94	10-5-94	7-17-94	7-25-94	7-31-94	5-20-94	5-20-94	5-20-94	5-20-94	10-5-94
Temp (C)	12.48	16.02	19.74	22.9	17.7	20	20	20	19	20	19	19	18.41
DO (mg/L)	6.87	5.91	0.62	0	0.05	0.2	0.18	0.01	-	-	-	-	2.39
Conductivity (mS/cm)	0.170	0.1318	0.839	0.311	0.604	0.93	0.99	1.53	-	-	-	-	1.074
pH	7.27	7.81	8.05	7.94	8.59	8.26	8.17	8.46	7.9	7.8	8.1	8.1	8.26
Eh (mV)	395	229	273	-25	-8	282	231	233	-	-	-	-	103
F	0.17	0.19	1.03	0.23	1.57	1.85	1.38	4.53	1.53	1.81	1.84	1.71	2.15
Cl	2.73	2.96	15	7.75	4.07	13.88	5.25	11.16	34.21	305.43	42.64	61.42	15.12
NO2	<0.01	<0.01	<0.03	<0.03	<0.03	<0.03	<0.03	<.03	<0.01	<0.01	<0.01	<0.01	<0.03
Br	0.05	0.03	<0.02	0.03	<0.02	0.06	0.29	0.3	0.11	0.041	0.13	0.2	0.08
NO3	0.86	1.21	0.22	0.12	<0.02	1.27	0.08	0.07	0.39	0.04	<0.01	0.04	0.31
PO4	0.23	0.17	<0.06	<0.06	<0.06	<0.03	<0.03	<.06	<0.02	<0.02	<0.02	<0.02	<0.06
SO3	<0.05	<0.05	<0.05	<0.05	<0.05	<0.05	<0.05	<.05	-	-	-	-	<0.05
SO4	2.34	2.06	163.2	22.97	<0.05	225.59	80.76	370.42	409.36	260.25	588.92	1131.81	236.24
OX	<0.09	<0.09	<0.07	<0.07	<0.07	<0.07	<0.07	<.07	<0.06	<0.06	<0.06	<0.06	<0.07
HCO3 *	119.80	91.68	362.38	213.53	393.70	464.48	585.80	535.89	653.48	664.11	746.01	612.67	482.11
Zn	0.096	0.05	0.058	0.022	0.08	0.18	0.165	0.065	-	-	-	-	0.028
Ba	0.038	0.018	0.078	0.096	0.046	-	-	-	-	-	-	-	0.02
B	<.0066	<.0066	0.096	<.0066	0.126	0.33	0.34	0.655	-	-	-	-	0.222
Si	23.42	23.492	8.468	9.412	4.408	5.616	4.965	3.96	7.11	7.525	7.575	10.145	4.712
Mn	0.002	0.002	0.006	0.002	0.008	0.005	0.03	0.005	0.01	0.035	0.02	0.01	0.006
Fe	0.008	0.242	0.042	0.008	0.086	0.57	0.95	0	<.012	0.06	<.012	0.725	0.034
Mg	6.418	5.2	4.734	3.232	2.294	1.345	0.77	6.61	2.825	9.77	2.825	4.47	1.322
Al	0.042	0.026	0.034	0.034	<.015	-	-	-	-	-	-	-	0.02
Sr	0.104	0.082	0.576	0.374	0.296	0.185	0.22	0.565	-	-	-	-	0.228
Ca	16.132	13.668	12.78	8.468	4.314	3.335	4.98	17.425	7.97	10.06	7.97	12.995	3.626
Na	10.644	9.072	192.48	68.172	172.84	307	247.2	355.1	568.34	527.12	568.34	724.3	289.24
Li	0.004	0.004	0.044	0.022	0.038	<0.06	0.105	0.09	-	-	-	-	0.054
K	3.848	3.546	2.722	2.012	1.394	6.37	2.17	1.705	3.36	4.095	3.36	4.3	1.704
Fe(tot), (mg/L) onsite	-	-	0.34	.12	1.29	-	-	-	-	-	-	-	0.02
Fe2, (mg/L) onsite	-	-	0	<	0.18	-	-	-	-	-	-	-	0.02
Fe3+ (mg/L) lab	-	<.04	<.04	<.04	<.04	0.11	0.14	<.07	<.13	<.13	<.13	0.14	<.04
Fe2+(mg/L) lab	-	<.1	<.1	<.1	<.1	0.46	0.81	<.04	<.07	<.07	<.07	0.36	<.1
Fe(tot) (mg/L) lab	-	0	0	0	0	0.57	0.95	0	0	0	0	0.5	0
DIC (ppm)	23.6	18.1	71.7	42.2	78.9	92.2	116.1	106.9	129.1	131.1	147.7	121.3	95.7
direct (u) DOC (ppm)	0.78	0.67	0.66	0.75	0.71	5.29	1.84	13.85	-	-	-	-	0.86
del 13C (o/oo)	-13.969	-13.279	-8.669	-11.317	-7.085	-4.43	-3.08	-3.6	-5.65	-6.84	-5.04	-4.67	-5.986
14C (pmc)	73.33±0.48	56.45±0.39	17.84±0.27	23.96±0.29	4.61±0.29	52.29±0.37	0.74±0.30	0.28±0.60	-0.02±0.30	-0.05±0.30	-0.14±0.31	-0.41±0.30	-0.14±0.30
del 18O (o/oo)	-10.90	-11.00	-11.55	-11.30	-11.50	-11.20	-11.20	-	-11.90	-11.60	-12.80	-12.70	-12.60
del D (o/oo)	-91.8	-94.5	-94.5	-89.38	-93.87	-98.6	-100.34	-88.5	-97.88	-89.02	-105.42	-105.39	-105.47
Tritium (TU)	<0.8	0.9	<0.8	<0.8	<0.8	<0.8	<0.8	<0.8	<0.8	<0.8	<0.8	<0.8	<0.8
34S SO4 (o/oo)	nes	nes	-12.15	-2.25	-6.35	-22.09	-9.95	-8.78	-16.61	-14.55	-18.3	-19.18	-8.89
Sample Name	Presbyteria	Elkins	Bibo	Seboyeta	Moquino	CNV-W2	CNV-W3	CNV-W5	MW-64	MW-65	MW-60	MW-68	L-Bar

NOTES ▒▒▒ -Estimated from data on nearby monitor wells
nes -Not enough sample
\- -Not determined
* -Calculated from DIC and pH

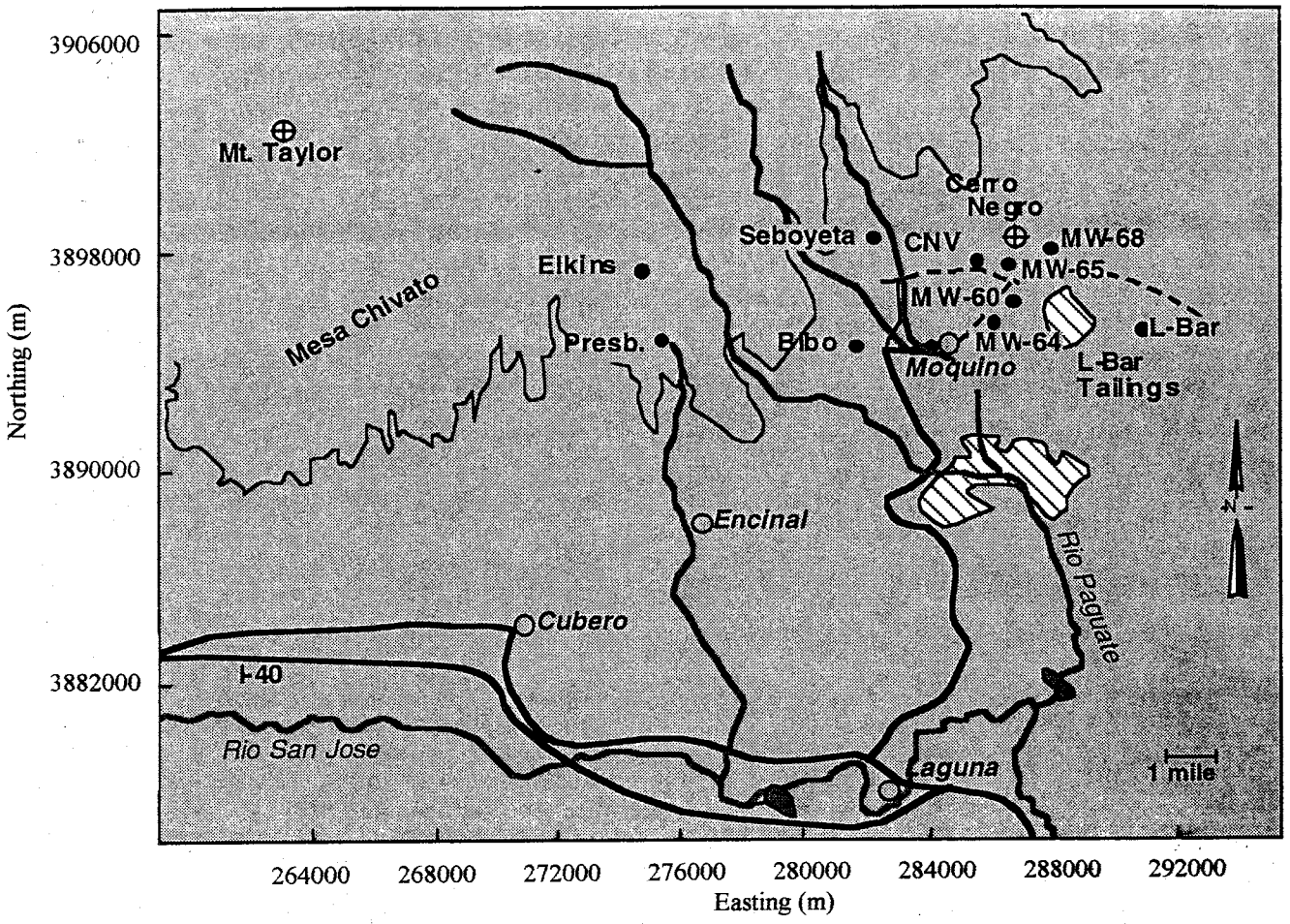

Figure 15: Sample location map.

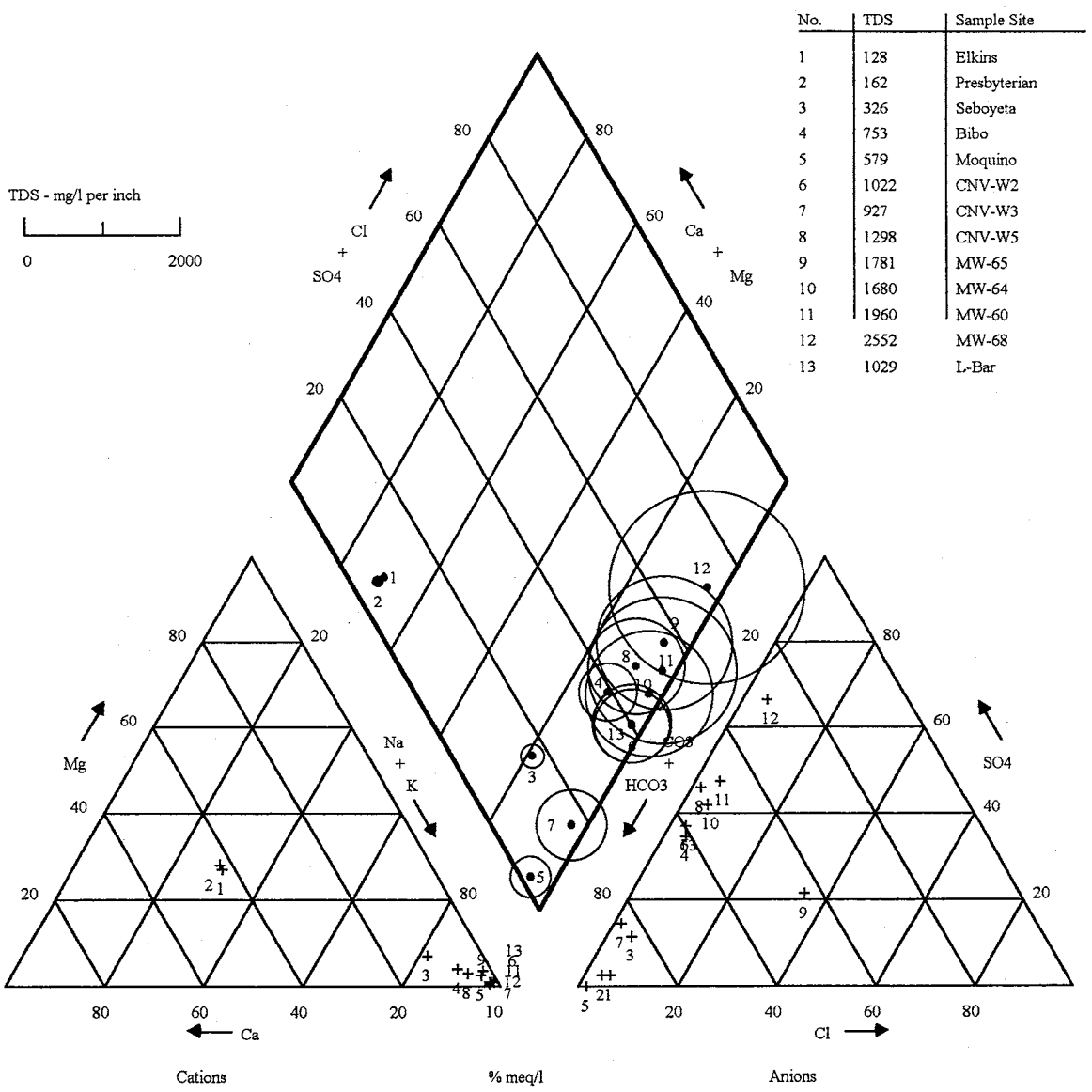

No.	TDS	Sample Site
1	128	Elkins
2	162	Presbyterian
3	326	Seboyeta
4	753	Bibo
5	579	Moquino
6	1022	CNV-W2
7	927	CNV-W3
8	1298	CNV-W5
9	1781	MW-65
10	1680	MW-64
11	1960	MW-60
12	2552	MW-68
13	1029	L-Bar

Figure 16: Piper trilinear diagram of Cerro Negro water samples

Table 7: Major ionic species expressed as a percent of total cations or anions in milli-equivalents per liter.

	Cations								Anions					
	Na^+		K^+		Mg^{2+}		Ca^{2+}		HCO_3^- (calc)		SO_4^{2-}		Cl^-	
Well name	meq/L	% total	meq/L	% total	meq/L	% total	meq/L	% total	meq/L	% total	meq/L	% total	meq/L	% total
Elkins	0.395	24.7	0.091	5.7	0.428	26.8	0.682	42.8	1.503	92.2	0.043	02.6	0.083	5.1
Presbyterian	0.463	24.4	0.098	5.2	0.528	27.9	0.805	42.5	1.963	94.0	0.049	02.3	0.077	3.7
Seboyeta	2.965	80.0	0.051	1.4	0.266	7.2	0.423	11.4	3.499	83.4	0.478	11.4	0.219	5.2
Bibo	8.372	88.4	0.070	0.7	0.389	4.1	0.638	6.7	5.939	60.9	3.398	34.8	0.423	4.3
Moquino	7.518	94.5	0.036	0.4	0.189	2.4	0.215	2.7	6.452	98.3	0	0.0	0.115	1.7
CNV-W2	13.354	96.8	0.163	1.2	0.111	0.8	0.166	1.2	7.612	59.9	4.696	37.0	0.392	3.1
CNV-W3	10.753	96.7	0.056	0.5	0.063	0.6	0.249	2.2	9.601	84.0	1.681	14.7	0.148	1.3
CNV-W5	15.446	91.4	0.044	0.3	0.544	3.2	0.870	5.1	8.782	52.2	7.711	45.9	0.315	1.9
MW-65	22.928	94.2	0.105	0.4	0.804	3.3	0.502	2.1	10.884	43.7	5.418	21.7	8.616	34.6
MW-64	24.721	97.2	0.086	0.3	0.232	0.9	0.398	1.6	10.709	53.0	8.522	42.2	0.965	4.8
MW-60	24.721	97.2	0.086	0.3	0.232	0.9	0.398	1.6	12.226	47.6	12.260	47.	1.203	4.7
MW-68	31.505	96.5	0.110	0.3	0.368	1.1	0.648	2.0	10.063	28.5	23.562	66.6	1.733	4.9
L-Bar	12.581	97.4	0.044	0.3	0.109	0.8	0.181	1.4	7.9011	59.7	4.918	37.1	0.427	3.2

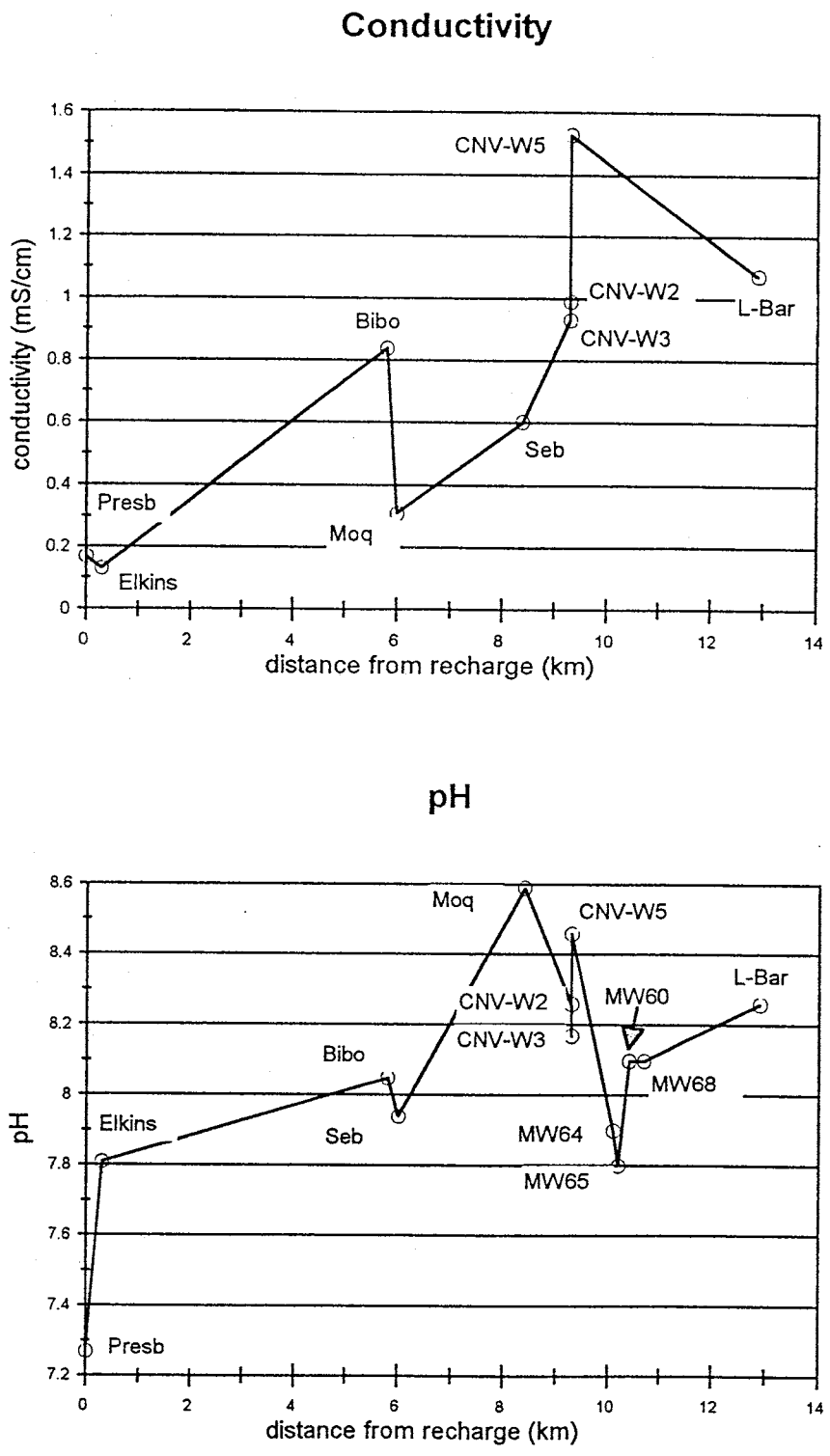

Figure 17: Graphs of conductivity and pH versus distance from recharge.

Water Chemistry - Description and Qualitative Interpretation

Chemistry Trends with Distance From Recharge

The following section presents chemistry data for each significant chemical parameter in the Cerro Negro water samples. A trilinear plot is used to show the major chemical constituents of each sample, and each parameter is plotted against distance from the recharge area to show trends along the flow path. The Presbyterian well is considered the reference recharge well and distances along the flow path are measured from that well, along a line parallel to the flow direction.

Trilinear plot

Piper diagrams are useful tools for showing general trends in chemical composition of natural waters. Figure 16 shows a Piper trilinear diagram of the Cerro Negro flow path chemistry data. The circles plotted in the central field have areas proportional to total dissolved solids concentrations, and are located by extending the points in the lower triangles to their points of intersection. The data points represent the percent of total milli-equivalents per liter (meq/L) and are meant to convey, in a general sense, the predominant cation and anion in each water sample (Hem 1985). Table 7 shows the data used to generate the Piper diagram. These data indicate that, in general, the Cerro Negro samples evolve from calcium-bicarbonate dominated water to sodium-bicarbonate water to sodium-bicarbonate-sulfate water.

Conductivity and pH

The presence of dissolved ionic species allows water to conduct electrical current. Thus, the conductivity of water is a measure of the dissolved ionic concentration (Hem, 1985). As ground water moves along a flow path it tends to increase in conductivity as it dissolves the soluble mineral constituents of the aquifer material through which it flows. Figure 17 shows the conductivity of water along the Cerro Negro flow path. As expected for evolutionary waters, the conductivity increases with distance from the recharge area.

The hydrogen ion concentration in water is expressed in terms of pH. The pH of a solution determines many types of geochemical equilibrium and solubility calculations. Figure 17 shows pH versus distance from recharge at Cerro Negro. The pH of these samples ranges from 7.27 to 8.59 and generally increases with distance from recharge.

Anions

The bicarbonate anion (HCO_3^-)is the dominant carbon species in waters with a pH in the range 6.3 to 10.3. For the Cerro Negro samples, bicarbonate concentrations were calculated from the pH and dissolved inorganic carbon concentration (Appendix A). The graph of bicarbonate concentration versus distance from recharge is shown in Figure 18. Bicarbonate concentration increases uniformly along the flow path. This indicates dissolution of carbonate minerals as ground water flows through the aquifer.

Nitrate (NO_3^-) is the oxidized form of nitrogen found in water. High nitrate concentrations are often a result of nearby animal or human waste sites, or excessive use of nitrogen fertilizers on agricultural land. However, as shown in Figure 18, the nitrate concentrations at Cerro Negro are very low and not likely caused by human interference. The higher values in the recharge wells and in CNV-W2 are an indication of slightly more oxydizing conditions. The concentrations of nitrite (NO_2^-, the reduced form of nitrogen) were below the detection limit in all samples, as listed in Table 6.

Sulfate (SO_4^{2-}) is the most highly oxidized form of sulfur (Hem, 1985). Figure 19 shows sulfate concentrations with distance. Sulfate increases with distance, probably a result of dissolution of gypsum from the Mancos Shale and pyrite from the Gallup Sandstone.

Chloride (Cl^-) concentrations along the flow path are shown in Figure 19. These concentrations are consistently low, except in MW-65, and increase slightly with distance. The increase is most likely a result of diffusion of connate water from low permeability shales. As listed in Table 2, the majority of sandstones and shales in the Cerro Negro area were deposited in a shallow sea. The anomalously high chloride content of MW-65 may be may be a result of tailings pond input, but if that were the case, chloride concentrations would also be high in the other monitor wells. Historical data indicate that chloride concentrations in monitor wells surrounding MW-65 have never exceeded the background level of approximately 100 mg/L. Therefore, the high chloride content in MW-65 is most likely an error.

Cations

Silica (Si) concentrations range from about 4 to 24 mg/L in the Cerro Negro water samples (Figure 20). This is within the normal range of silica concentrations commonly observed in natural waters, which is from 1 to about 30 mg/L (Hem, 1985). The silica concentrations are highest in the recharge wells, and generally decrease along the flow path. This decrease is likely a result of precipitation of silicate minerals.

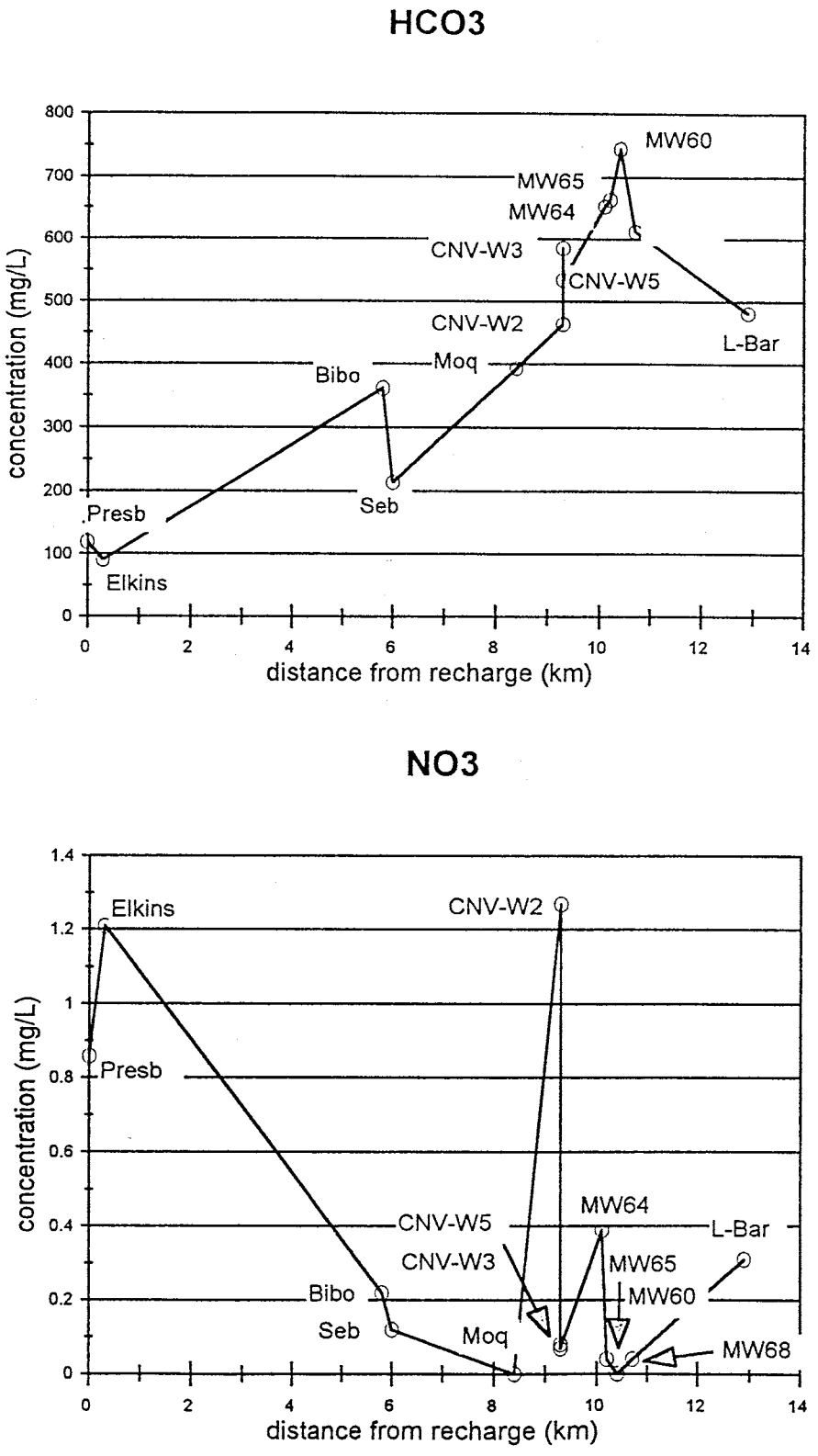

Figure 18: Graphs of bicarbonate (HCO_3^-) and nitrate (NO_3^-) versus distance from recharge.

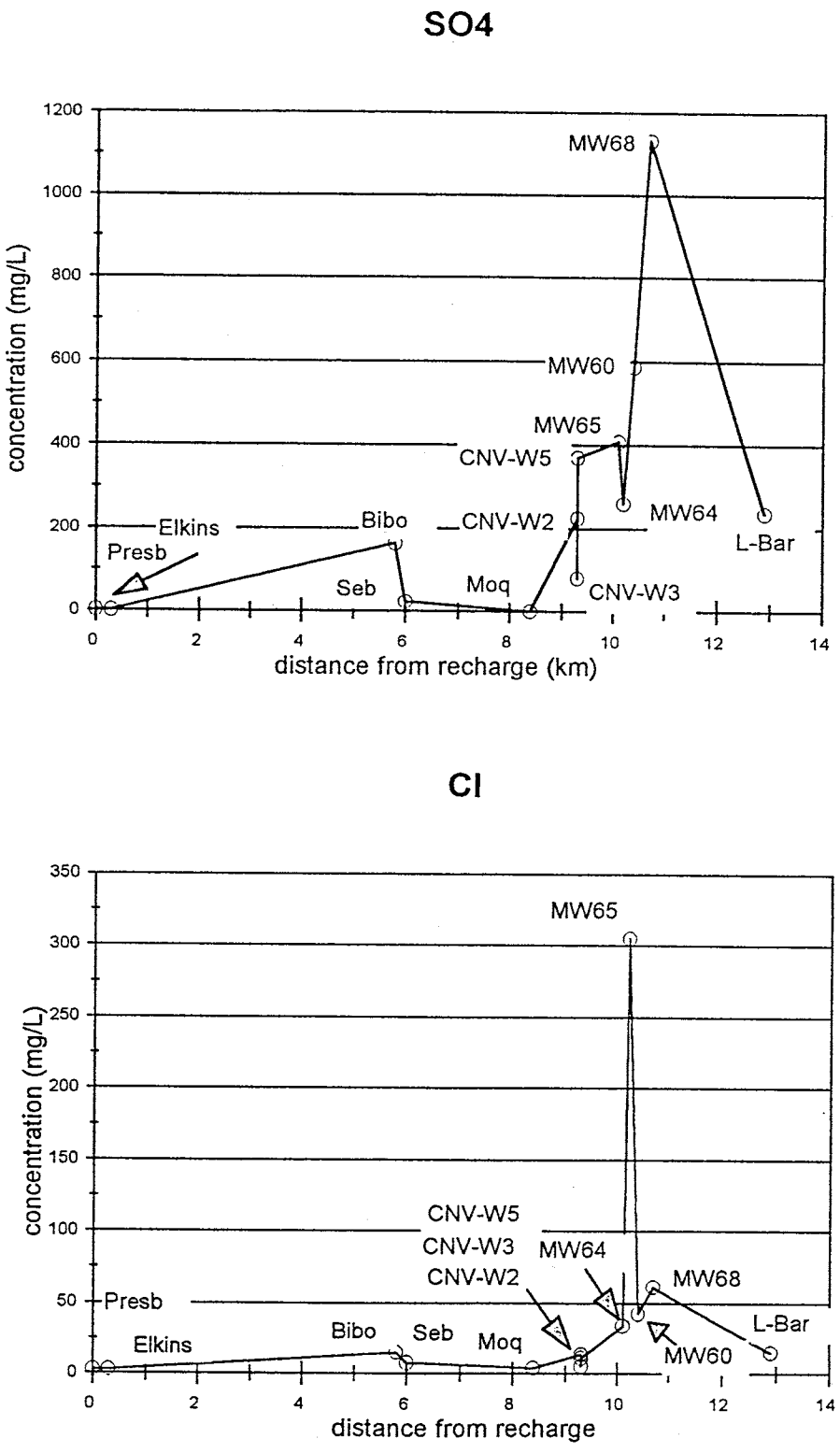

Figure 19: Graphs of sulfate (SO_4^{2-}) and chloride (Cl^-) versus distance from recharge.

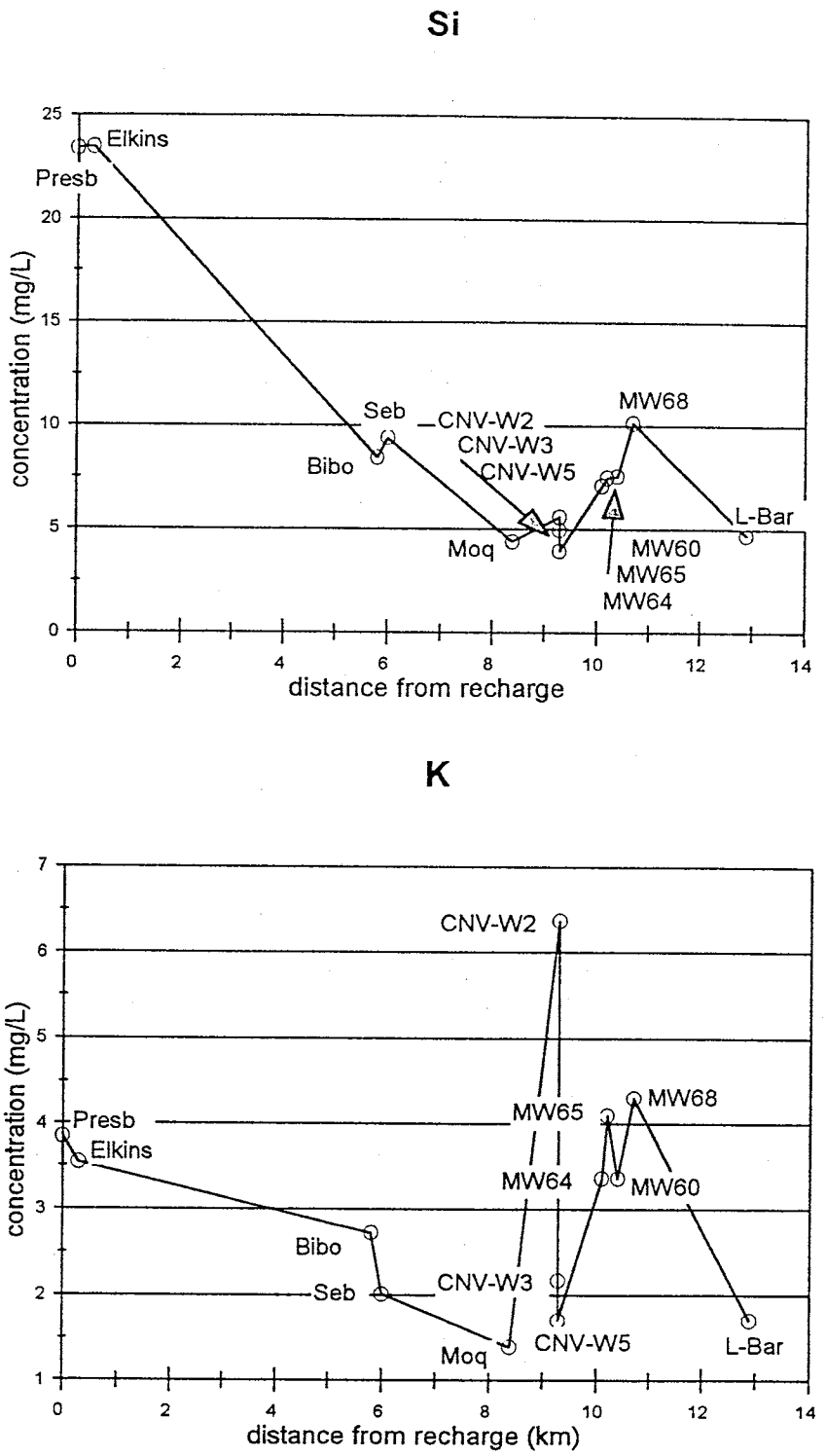

Figure 20: Graphs of silica (Si) and potassium (K^+) versus distance from recharge.

Concentrations of potassium (K^+) versus distance are shown in Figure 20. Reactions involving potassium are not easily quantifiable, but its concentration in ground water is usually low because of the high degree of stability of potassium-bearing aluminosilicate minerals (Hem, 1985). The pattern of concentration with distance for potassium is very similar to that of calcium and magnesium, especially for the monitor wells. The source of potassium in these wells may be the same as the source of calcium and magnesium. The CNV-W2 sample, however, is high in potassium but low in calcium and magnesium. This sample also has an unusually high carbon-14 activity, indicating some vertical leakage from the surface. The potassium in the CNV-W2 may also be a result of vertical leakage.

Figure 21 is a graph of total iron ($Fe^{2+/3+}$) versus distance from recharge. Iron concentrations are very low, in all samples less than 1 mg/L. Table 6 lists iron redox species - ferric (Fe^{3+}) and ferrous (Fe^{2+}) iron. These species indicate whether the environment is oxidizing or reducing. In all samples where iron species were measurable, ferrous iron concentrations are higher than ferric, indicating reducing environments.

Strontium (Sr^{2+}) concentrations are shown in Figure 21. These concentrations are near the average of 0.11 mg/L for U.S. public water supplies (Hem, 1985). Strontium carbonate (strontianite) is common in sedimentary rocks. Both Bibo and CNV-W5 have high strontium concentrations. These wells are both completed in the Paguate Sandstone, indicating that the Paguate may be high in strontianite.

Cation Exchange

Cation exchange is often an important reaction in the evolution of natural waters. This type of reaction is driven by the electrostatic attraction between charged ions in solution and the surface charge on clay minerals. Positively charged cations bind to exchange sites on negatively charged clay surfaces. These cations can exchange with other cations present in solution. The most common cation exchange reaction involves exchange between Ca^{2+} and Mg^{2+} and Na^+. Calcium and magnesium are taken out of the water and replaced with sodium. The main requirement for this process is a large reservoir of exchangeable Na+, which is most often provided by clay minerals deposited in a marine environment. When ion exchange takes place, its effects on the cation chemistry of water should be unmistakable. The concentrations of Ca^{2+} and Mg^{2+} in water samples along a flow path should decrease while concentrations of Na^+ should increase.

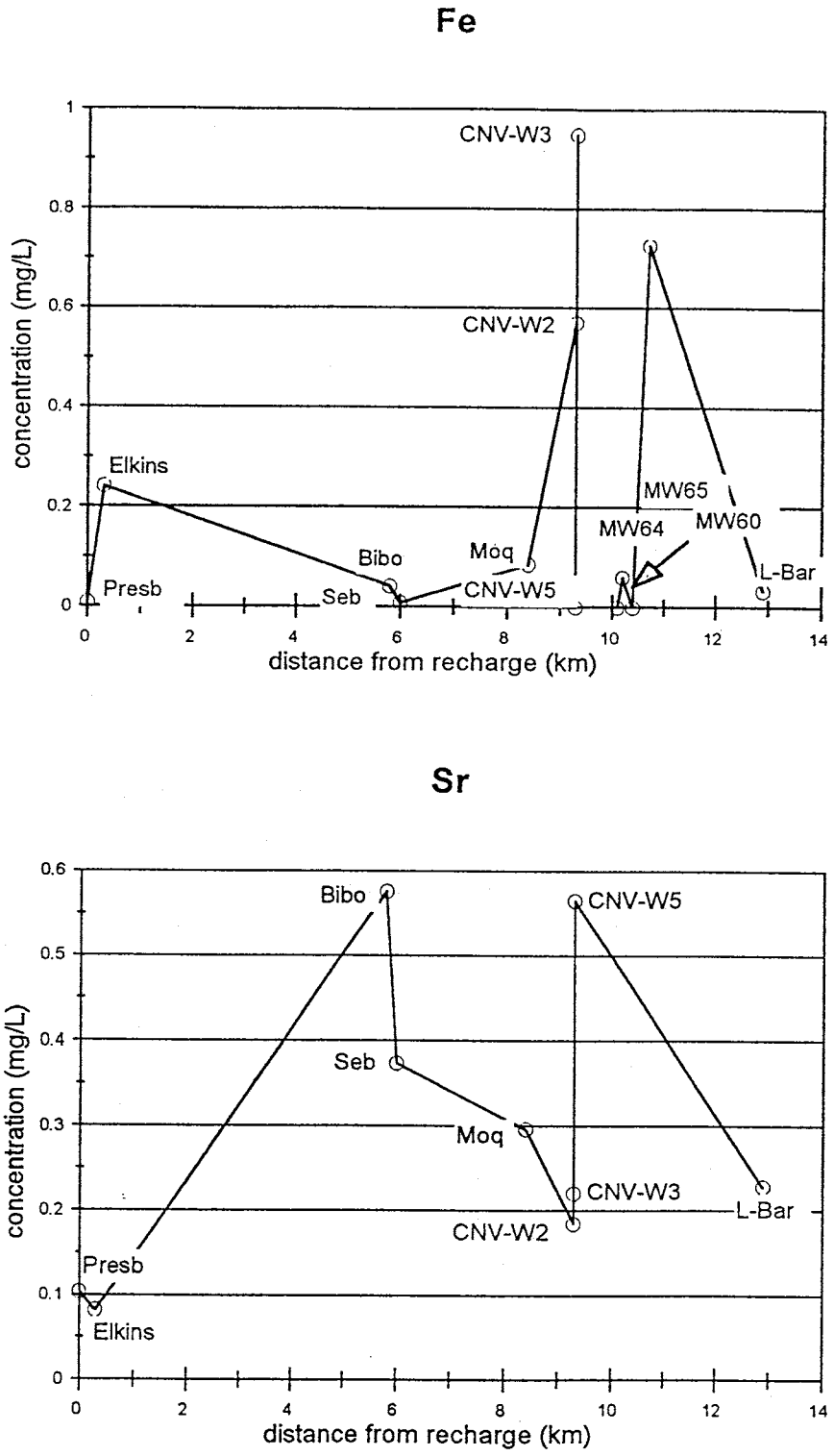

Figure 21: Graphs of iron ($Fe^{2+/3+}$) and strontium (Sr^{2+})versus distance from recharge.

Figure 22 shows the concentrations of Ca^{2+},Mg^{2+} and Na^{+} versus distance along the Cerro Negro flow path. Concentrations of sodium increase uniformly with distance from recharge. Sodium in the L-Bar sample drops relative to the monitor wells, but it is still higher than that in the recharge wells. If the increase in sodium concentrations is a result of exchange with calcium or magnesium, there should be a corresponding decrease in the concentrations of calcium and magnesium. As shown in Figure 22 these two parameters decrease uniformly in the section of the flow path from the recharge wells to the Cerro Negro vertical borehole (CNV), but beyond the CNV samples the trend reverses. The monitor wells, especially, have increased calcium and magnesium concentrations. This may be a result of the reversed hydraulic gradient around the tailings pond introducing high Mg^{2+} and Ca^{2+} water. The L-Bar sample follows the expected trend for cation exchange of relatively high Na concentrations and low Ca^{2+} and Mg^{2+} concentrations.

Quantitative ion exchange test

Cation exchange between Ca^{2+} and Na^{+} often drives dissolution of calcite. Calcium exchanges for sodium on clay mineral surfaces, thus decreasing Ca^{2+} and increasing Na^{+} concentrations in the water. Decreases in aqueous Ca^{2+} concentrations drive the dissolution of mineral $CaCO_3$. Calcite ($CaCO_3$) mineral dissolution increases the concentrations of calcium and carbon in the ground water, thus providing more Ca^{2+} for the exhange process to continue. Carbon concentrations increase in the water as calcite continues to dissolve and cation exchange proceeds. Magnesium (Mg^{2+})can also exchange with sodium on clay surfaces. A simple, quantitative test to determine if cation exchange is a dominant process along a flow path is to analyze the loss (in meq/L) of Ca^{2+} and Mg^{2+} plus the gain (in meq/L) of dissolved inorganic carbon (DIC, as bicarbonate) versus the gain in Na^{+} (in meq/L) between two samples. If the changes in Ca^{2+}, Mg^{2+}, and DIC are approximately equal to the change in Na^{+}, cation exchange is an important process along the flow path.

The solid line in Figure 23 shows the results of the quantitative ion exchange test in terms of the ratio of changes in Ca^{2+}+Mg^{2+}+DIC to changes in Na^{+}, or

$$\frac{\Delta(Ca + Mg + DIC)}{\Delta Na}(meq / L).$$

This ion exchange ratio is plotted against distance from recharge. If cation exchange is important the ratio should be approximately one. The Elkins well is the only point that

plots significantly away from one. All other samples are slightly less than one. In addition, the magnitude of change (in meq/L) of the concentrations of Ca^{2+}, Mg^{2+} and Na^{+} is very large compared to the magnitude of the ratio change. This indicates that cation exchange is a dominant process along the flow path. The high ion exchange ratio in the Elkins sample is a result of a slight decrease in the DIC and Na^{+} concentrations relative to those parameters in the Presbyterian well.

The samples with ion exchange ratios less than one may have a source of Na^{+} in addition to the Na^{+} that comes from ion exchange. It is likely that this excess Na^{+} comes from diffusion of connate water (containing NaCl) from low permeability shales because Cl^{-} concentrations also increase slightly with distance. If the excess Na^{+} does come from diffusion of NaCl in low permeability shales we can assume that the amount of Na^{+} entering the water by diffusion is equal to the amount of Cl^{-} entering the water. We can subtract the change in Cl^{-} from the denominator of the previous equation and test the hypothesis. The dashed line in Figure 23 represents the ratio of changes in Ca^{2+}+Mg^{2+}+DIC to changes in Na^{+}-Cl^{-}or:

$$\frac{\Delta(Ca + Mg + DIC)}{\Delta(Na - Cl)}(meq / L)$$

This ratio is slightly closer to one, indicating that a portion of the increase in Na^{+} concentration is a result of diffusion. However, because the ratios are not exactly equal to one, there may be another mechanism acting to increase Na^{+} and decrease Ca^{+} and Mg^{+} along the flow path.

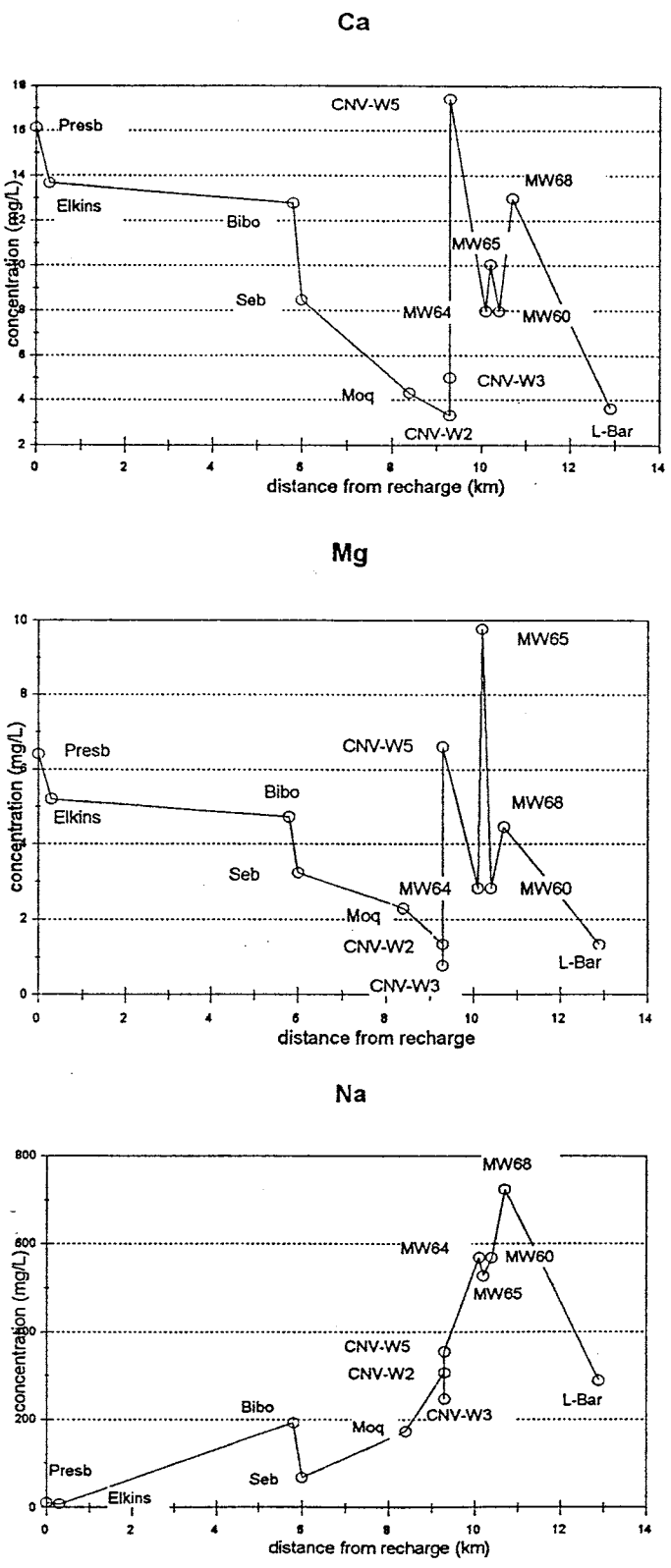

Figure 22: Graphs of calcium (Ca^{2+}), magnesium (Mg^{2+}), and sodium (Na^{+}) versus distance from recharge.

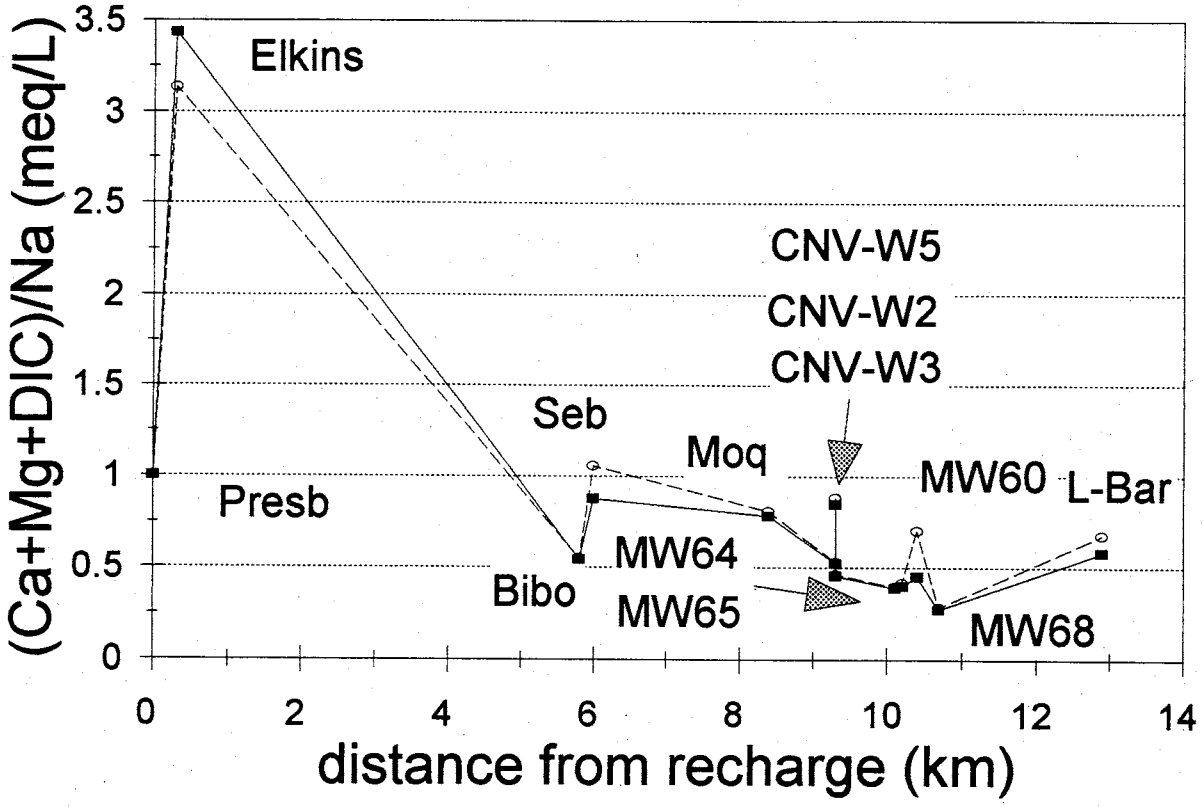

Figure 23: Graph of results of the quantitative ion exchange test. The solid line represents Δ(Ca+Mg+DIC)/ΔNa in meq/L versus distance from recharge, and the dashed line represents Δ(Ca+Mg+DIC)/Δ(Na-Cl) versus distance from recharge.

Carbon Trends

Dissolved organic and inorganic carbon concentrations are shown in Figure 24. Organic carbon concentrations are generally low except in CNV-W5 and CNV-W2. Dissolved inorganic carbon increases uniformly with distance, mainly a result of dissolution of carbonate minerals.

Carbon Isotope Trends

Carbon isotopes $\delta^{13}C$ and ^{14}C are plotted in Figure 25. Carbon-14 activity decreases with distance, to essentially zero at the Cerro Negro vertical borehole and the L-Bar monitor wells. This trend is consistent with increasing ages along a flow path. Carbon-14 activity in the CNV-W2 sample is anomalously high. This sample is taken from the highest unit in that borehole (the Two Wells Sandstone) and the high ^{14}C activity most likely indicates vertical recharge from the surface, which introduces young water into the aquifer in this area. The carbon-13 ratio increases with distance in nearly the same pattern as the dissolved inorganic carbon. Carbon-13 increases from approximately -14 ‰ to -3 ‰. This is most likely a result of dissolution of mineral carbon, with a $\delta^{13}C$ ratio of near zero, into ground water that starts with a $\delta^{13}C$ in equilibrium with that of soil CO_2, approximately -20 ‰.

Tritium

All but one of the samples analyzed for this study contained tritium at or below the detection limit of 0.8 TU. Only the Elkins well, one of the recharge wells, contained detectable tritium at 0.9 TU. These low and barely detectable levels of tritium indicate that there is no post-1952 water in the samples. The samples that contain ^{14}C and are therefore relatively young, such as Presbyterian and CNV-W2, are at least 50 years old. Any recharge in these samples, through fractures or vadose zone infiltration, must take at least 50 years.

Stable Isotope Trends

Stable isotopes of ^{18}O and D are shown in Figure 26 relative to the meteoric water line. In all cases the data points plot to the right of the meteoric water line, most likely indicating evaporation during recharge. The same data are plotted in Figure 27 against the NETPATH generated radiocarbon age of each sample (the NETPATH data are discussed in the following chapter on the NETPATH model). In general, the younger samples are

isotopically enriched in both ^{18}O and D, and the older samples are isotopically depleted. Phillips et al. (1986) found that, in the San Juan Basin, Pleistocene-age samples are characterized by a stable isotope content about 25‰ lighter in D and 3‰ lighter in ^{18}O than modern precipitation and ground water. This difference is attributed to a colder mean annual temperature and perhaps increased winter precipitation in the Pleistocene. The Cerro Negro water samples of Pleistocene age (greater than 10,000 years) are depleted by about 15 ‰ in D and about 2‰ in ^{18}O. While this isotopic depletion is not as great as those found by Phillips et al. (1986) the general isotopic depletion in older samples may be attributed to a colder climate during recharge.

Tailings Pond Tracer Tests

The elevated concentrations of calcium, magnesium, and potassium in the four monitor wells sampled for this study imply the possibility that the plume of tailings pond contaminated water may have reached these wells. Chemical and isotope tracer methods can be used to determine if this is a possibility. The tailings pond water has characteristic chemical and isotopic signatures. If tailings pond water has reached monitor wells 60, 64, 65,and 68, the signatures in these monitor wells will be similar. Ratios of chloride to sulfate, chloride to oxygen-18, and deuterium to oxygen-18 are used as signatures and are graphed in Figure 28 (Kelly Tilford, INTERA, Inc., personal communication, 1995). Monitor wells 2A, 3A, and 69 are know to be contaminated by the tailings pond, and the Bibo and Seboyeta samples are assumed to be uncontaminated. In the case of each signature, monitor wells 60, 64, 65, and 68 plot closer to the known uncontaminated wells than to the contaminated wells or the actual tailings. There is thus no evidence that the elevated calcium, magnesium, and potassium concentrations in monitor wells 60, 64, 65, and 68 are caused by tailings pond contamination.

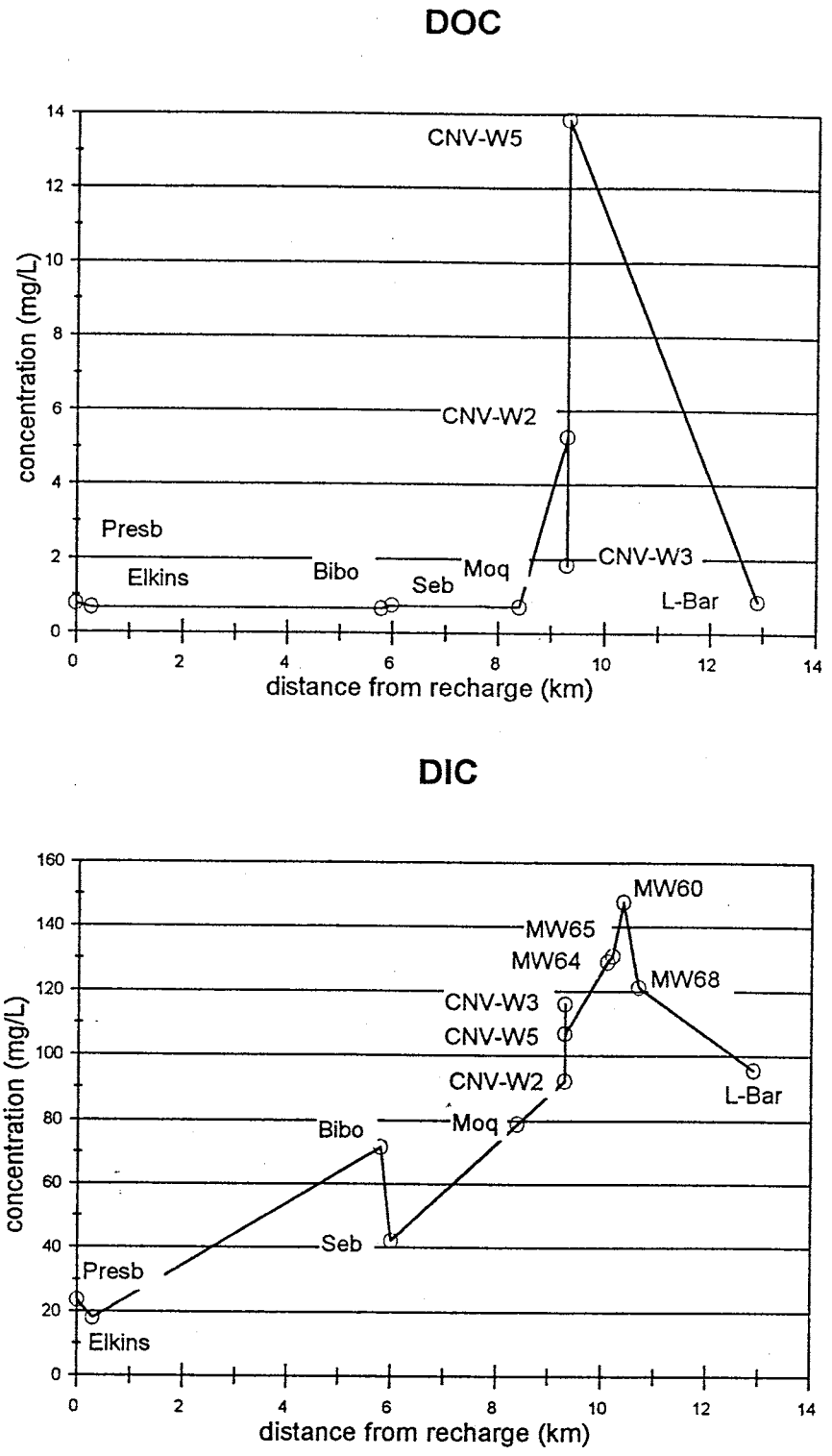

Figure 24: Graphs of dissolved organic carbon (DOC) and dissolved inorganic carbon (DIC) versus distance from recharge.

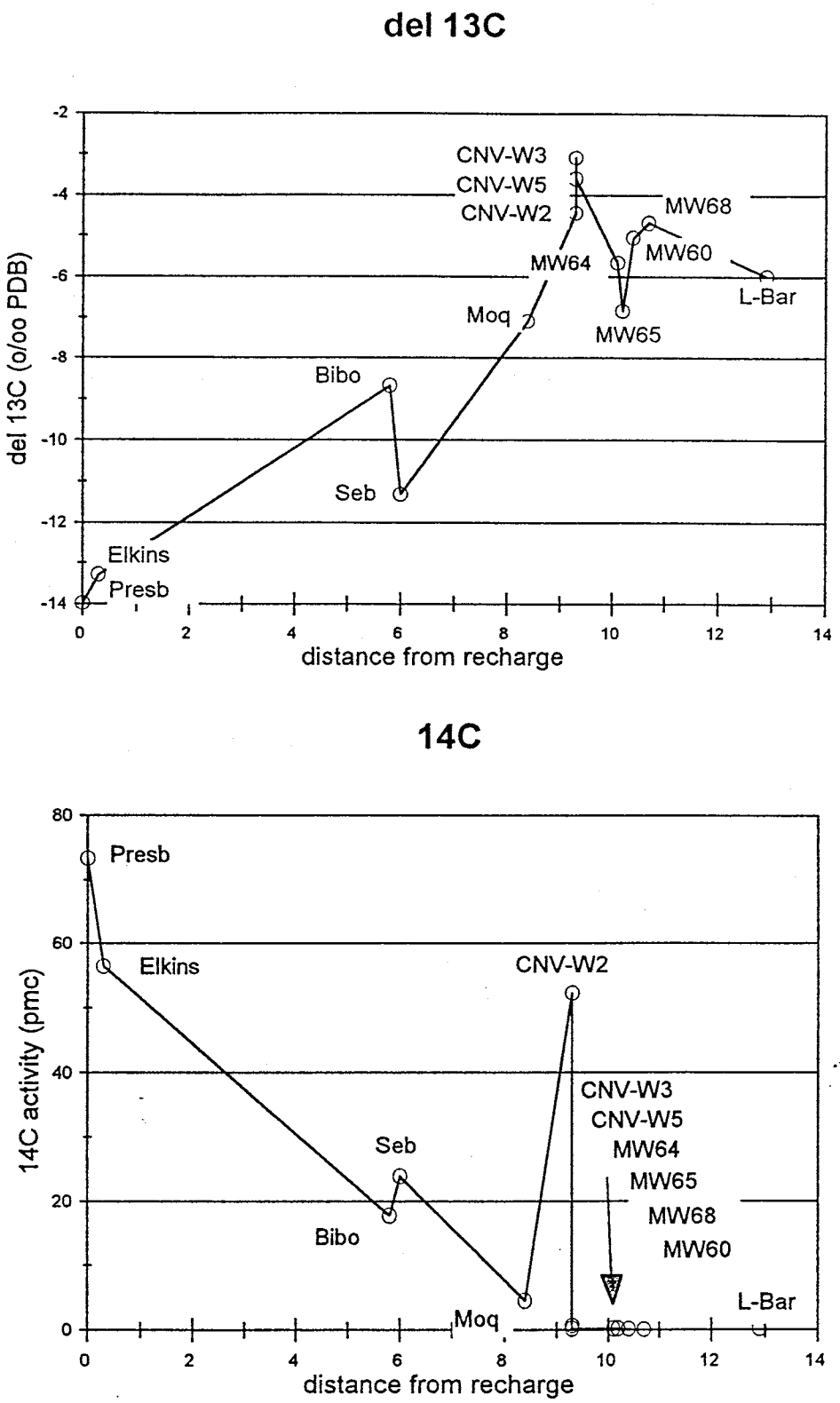

Figure 25: Graphs of $\delta^{13}C$ and ^{14}C versus distance from recharge.

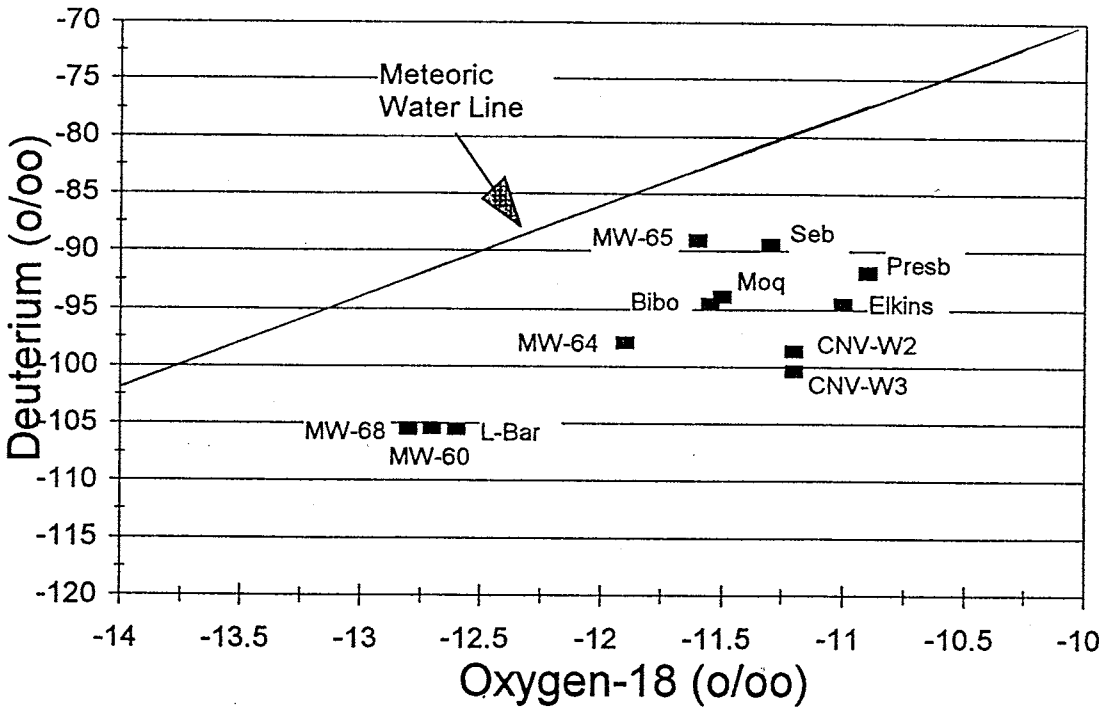

Figure 26: Graphs of $\delta^{18}O$ and δD showing meteoric water line.

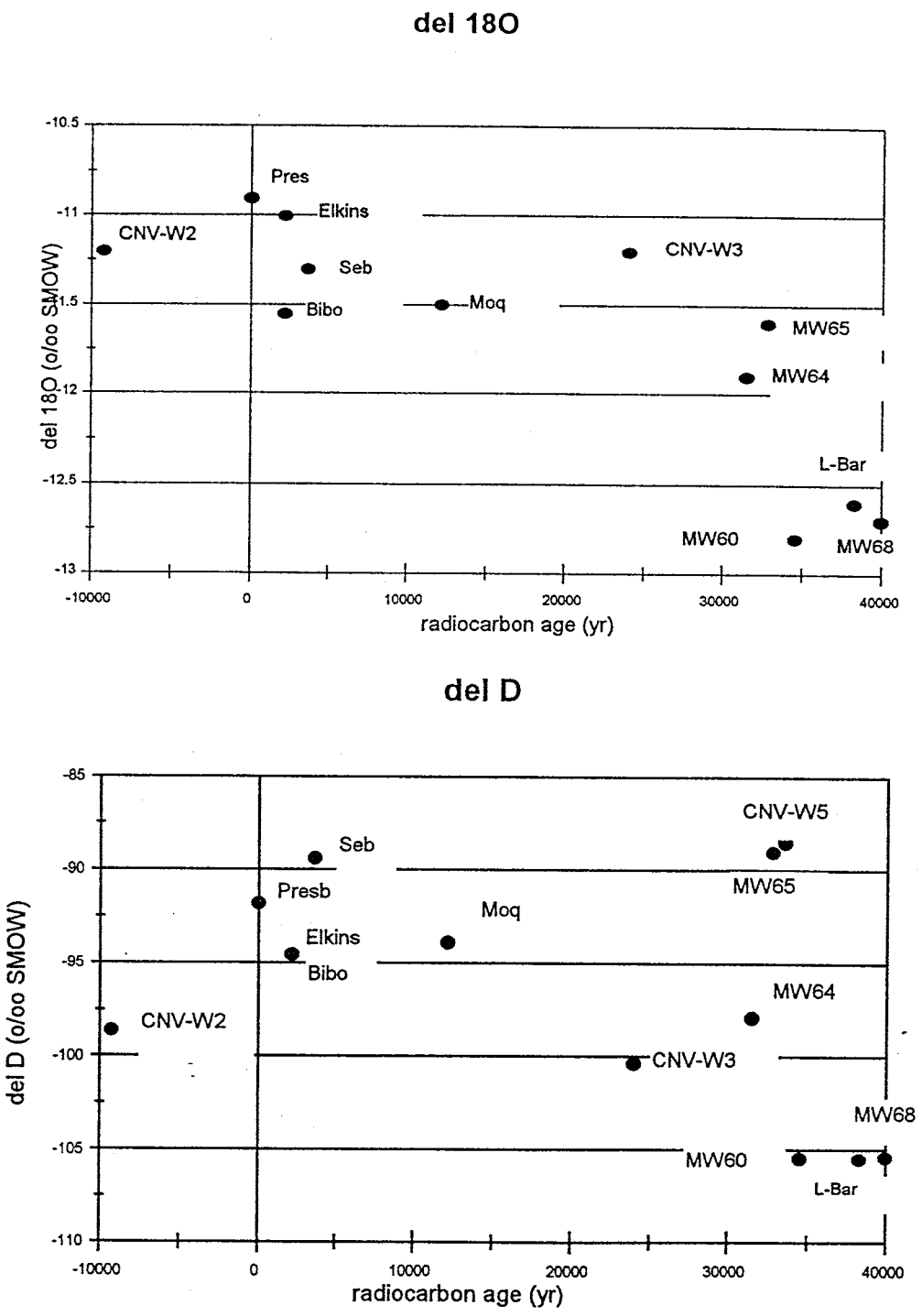

Figure 27: Graphs of $\delta^{18}O$ and δD versus radiocarbon age.

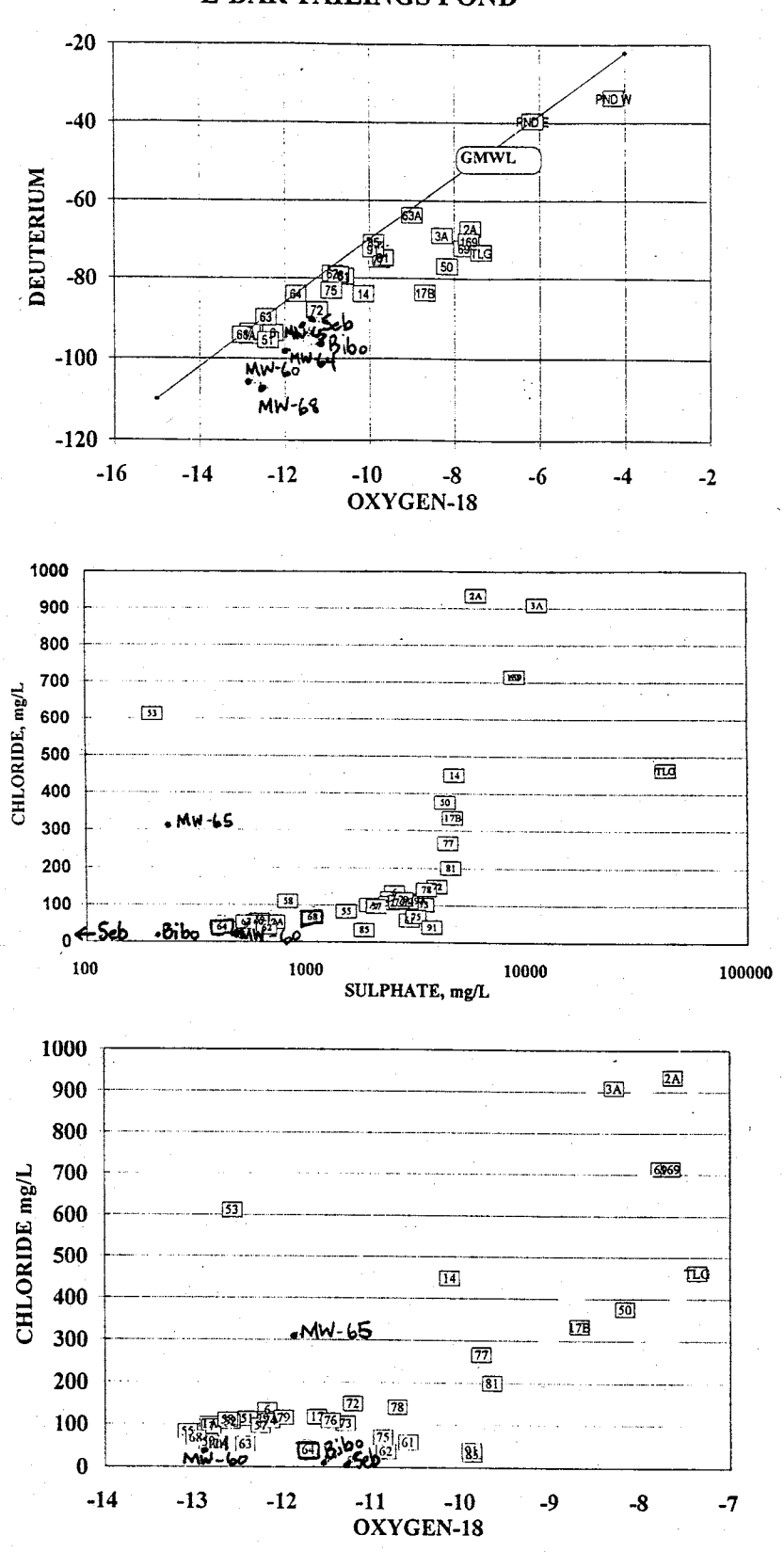

Figure 28: Graphs of deuterium versus $\delta^{18}O$, chloride versus sulfate, and chloride versus $\delta^{18}O$ for water samples taken near the L-Bar tailings pond (from Kelly Tilford, INTERA, Inc., personal communication, 1995).

Carbon-14 Modeling of Cerro Negro Flow Path

Simple Dissolution Model

The simplest case for correction of carbon-14 activities along a flow path is to assume that the only source of carbon entering the ground water is from dissolution of carbonate rocks, and that there is no sink for carbon leaving the ground water. In this case, the increase in dissolved inorganic carbon (DIC), above that of the recharge well (Presbyterian), can be used as a "dilution factor" (DF) to account for input of dead carbon at each down-gradient well. This dilution factor is of the general form:

$$DF_i = \frac{m_c}{\left(m_c + m_{ca}\right)_i}$$

where m_c is the mass of DIC present in the initial recharge well and m_{ca} is the mass of carbon added along the flow path. The subscript i refers to the sample. The total mass of DIC at a given well is then $\left(m_c + m_{ca}\right)_i$. If we also assume the carbon-14 activity in the recharge well to be A_0, and multiply this by the dilution factor at each subsequent well, we will have a reasonable estimate of A_0 for each sample. The equation for A_0 is:

$$\left(A_o\right)_i = A_o\left[\frac{m_c}{\left(m_c + m_{ca}\right)_i}\right]$$

Applying the usual decay equation:

$$time_i = -\frac{1}{\lambda_{14}} \ln \frac{A_i}{\left(A_o\right)_i}$$

where $time_i$ is the travel time between the recharge well and sample *i*, will then give an approximate corrected ^{14}C age.

Table 8 shows the results of these simple dissolution model calculations for the water samples along the Cerro Negro flow path. The corrected ages (relative to the

Table 8: Calculations for simple dissolution model.

Sample Name	DIC (mg/L)	A_i (pmc)	$(A_o)_i$ (pmc)	time (years)
Presbyterian	23.6	73.33	73.33	0
Elkins	18.1	56.45	95.61	4355
Bibo	71.1	17.84	24.34	2568
Seboyeta	42.2	23.96	41.01	4442
Moquino	78.9	4.61	21.93	12,890
CNV-W2	92.2	52.29	18.77	*
CNV-W3	116.1	0.74	14.91	25,161
CNV-W5	106.9	0.28	16.19	33,532
MW64	129.1	0.28	13.41	31,975
MW65	131.1	0.25	13.20	32,781
MW60	147.7	0.17	11.72	34,986
MW68	121.3	0.11	14.27	40,210
L-Bar	95.7	0.16	18.08	39,069

NOTES: *- 14C activity for the CNV-W2 sample is greater than the 14C activity at recharge, yielding a negative age.

Presbyterian sample having a zero age) range from approximately 2500 years to 40,000 years. The ages increase with distance from the recharge area, as expected.

NETPATH Model

Chemical Mass Balance

The results of the NETPATH chemical mass balance modeling are presented in Table 9. The mineral mass transfers were constrained by concentration measurements at the initial and final wells of the elements C, Na, Ca, K, Al, Si, Mg, S, Cl, and Fe. The mass balance calculations determine the amounts (in mmols/kg water) of the phases calcite ($CaCO_3$), quartz (SiO_2), sodium chloride (NaCl), K-spar ($KAlSi_3O_8$), Ca/Na exchange, dolomite ($CaMgCO_3$), gypsum ($CaSO_4 \cdot 2H_2O$), hematite (Fe_2O_3), pyrite (FeS_2) and albite ($NaAlSi_3O_8$) that must dissolve or precipitate to account for the composition of the final water. These mineral phases were chosen because they represent the major mineral constituents of the geologic units through which the water flows (Table 2). The validity of the precipitation/dissolution reactions is checked using the saturation indices calculated by WATEQF (Appendix B)

NETPATH found four models that satisfied all the constraints (Appendix C). Model 3 can be dismissed immediately because it predicts an unreasonably large amount of SiO_2 precipitation. Models 1, 2, and 4 are very similar. The main difference between them is the way they apportion Si between SiO_2, albite and anorthite. All three models predict the same amount of calcite dissolution. Model 1 was chosen as the most appropriate model because it simplifies the Si apportionment by favoring albite over anorthite. Table 9, mentioned above, presents the mass balance transfers generated by Model 1.

In general the NETPATH model indicates that calcite is the main source of carbon along the flow path. Precipitation of dolomite is a minor sink for carbon (except in two cases where small amounts dissolve). The dissolution of large amounts of calcite ($CaCO_3$) forces precipitation of dolomite and gypsum (in most cases). Ion exchange between Ca^{2+} and Na^+ provides the driving force for calcium dissolution. Ion exchange removes calcium from the water, which renders the solution undersaturated with respect to calcium and forces calcite in the aquifer matrix to dissolve. Dissolution of NaCl is another source of Na^+. Silica is lost through SiO_2 precipitation. Hematite is a sink for iron, while pyrite is the main source of sulfur. The aluminosilicates (K-spar and albite) are less uniform in behavior, but in most cases K-spar precipitates where albite dissolves.

Table 9: Chemical mass balance transfer results generated by NETPATH modeling. All units are mmol/kg water. Positive values indicate dissolution and negative values indicate precipitation.

Case	CALCITE	SiO2	NaCl	K-SPAR	EXCHANGE	DOLOMITE	GYPSUM	HEMATITE	PYRITE	ALBITE
					Two Wells Aquifer					
Pres-Bibo	4.14680	-.53222	.34631	-.02798	3.77074	-.06895	-.39004	-.51624	1.03319	.02768
Pres-CNVW2	6.13730	-.62935	.31538	.06513	6.32808	-.20905	.08074	-.55637	1.12285	-.06673
Pres-MW64	9.09726	-.57613	.88961	-.01189	11.69999	-.14791	2.54780	-.42416	.84822	
Pres-MW65	8.69260	-.56108	8.55451	.00715	6.98020	.13862	-2.00174	-1.17240	2.34581	-.00875
Pres-MW60	10.65234	-.55902	1.12836	-.01187	11.58414	-.14788	.87691	-1.31037	2.62063	.01027
Pres-MW68	8.31942	-.46763	1.66043	.01224	14.73814	-.07964	6.09619	-1.41632	2.84556	-.01384
					Paguate Aquifer					
Pres-Bibo	4.14680	-.53222	.34631	-.02798	3.77074	-.06895	-.39004	-.51624	1.03319	.02768
Pres-CNVW5	6.93042	-.68837	.23839	-.05398	7.35622	.00825	.45096	-.84658	1.69306	.05238
					Cubero/Morrison Aquifer					
Pres-Seb	1.81149	-.49834	.14205	-.04702	1.15703	-.13106	-.71450	-.23239	.46478	.04672
Pres-Moq	4.94819	-.67247	.03804	-.06202	3.48043	-.17005	-1.59183	-.39125	.78391	.06042
Pres-CNVW3	8.17451	-.65239	.07111	-.04199	5.09427	-.23208	-3.12622	-.97754	1.97200	.04039
Pres-LBar	6.43121	-.66347	.35045	-.05399	5.86420	-.21005	-.66903	-.77645	1.55339	.05309

Each reaction model was solved in NETPATH by applying constraints to the elemental compositions of the initial and final waters, but without considering isotope measurements. Therefore, the predicted isotopic composition of $\delta^{13}C$ in the final water can be compared to the measured $\delta^{13}C$ to test the accuracy of the model. The predicted $\delta^{13}C$ value of the final water is sensitive to the $\delta^{13}C$ value of mineral sources along the flow path. NETPATH allows the user to specify the isotopic composition of all mineral sources. At Cerro Negro the $\delta^{13}C$ value of calcite cement in all of the geologic units is known, therefore, the mineral $\delta^{13}C$ value used by NETPATH can be varied until the predicted final water $\delta^{13}C$ matches the measured value. If the corresponding mineral $\delta^{13}C$ matches the measured values, the model is verified for carbon. Figure 29 shows graphs of $\delta^{13}C$ values for actual water sample measurements and the corresponding calcite $\delta^{13}C$ value needed for a match between predicted and measured $\delta^{13}C$ of the final water. The error bar at the right side of each graph represents the range of $\delta^{13}C$ values measured in the calcite cement of each geologic unit. In most cases the fitted mineral $\delta^{13}C$ is within the range of measured mineral $\delta^{13}C$.

Both calcite and dolomite are sources of carbon in the Cerro Negro flow path. However, variations in the $\delta^{13}C$ of dolomite produced only slight changes in the final predicted $\delta^{13}C$. Therefore, the $\delta^{13}C$ of dolomite was assumed to be 0 ‰ in all cases, while the $\delta^{13}C$ of calcite varied between -8.5 ‰ and -0.3 ‰ (Figure 29) to fit the measured data.

Carbon-14

NETPATH considers nine models for defining the initial ^{14}C (A_0) of a water sample. Most of these models are appropriately applied in open systems, where the water is exposed to CO_2 at or near the recharge zone. In the Cerro Negro study, all of the samples are presumed to be along a flow path and all are taken from wells completed below the water table. Therefore, the system is closed, and the ^{14}C activity of the sample taken farthest upgradient in the flow path can be considered A_0. Similarly, the ^{14}C activity in the upgradient well of any pair of wells can be considered A_0. In NETPATH the model in which the ^{14}C content of dissolved inorganic carbon in the initial well is used as the value of A_0 is termed "original data."

Table 10 lists the corrected ^{14}C ages generated by NETPATH using the original data model, and the values of ^{14}C activity that NETPATH uses to calculate these adjusted ^{14}C ages. The ages represent the travel time between the Presbyterian well (the sample taken farthest up-gradient in the flow path) and each well down gradient. The ages range from 2179 years at the Bibo well, to 40,000 years at MW-68. The ages

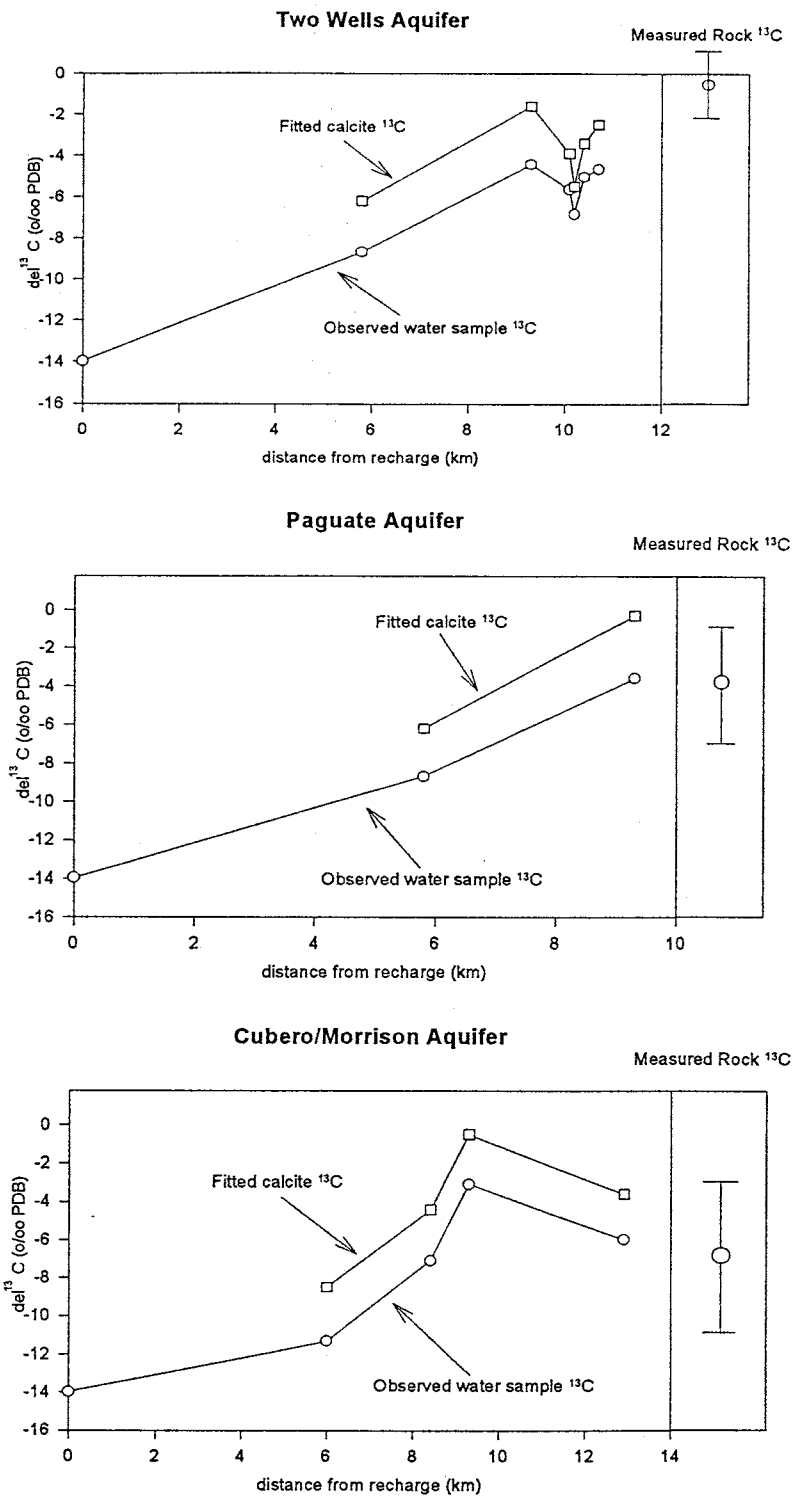

Figure 29: Graph of $\delta^{13}C$ values for actual water sample measurements and the corresponding modeled calcite $\delta^{13}C$ needed for a match between predicted and measured $\delta^{13}C$ of the final water.

Table 10: Corrected radiocarbon ages generated by NETPATH, using the "Original Data" model for determining A_o. Activities are in percent modern carbon (pmc), and age is in years. Distance refers to the distance along the flow path between the samples.

Case	A_o (initial)	A_{nd} (Computed-no decay)	A (observed)	t (age-final)	distance (km)
Two Wells Aquifer					
Pres-Bibo	73.33 ±0.48	23.22	17.84 ±0.27	2179 ±124	5.8
Pres-CNVW2	73.33 ±0.48	16.98	52.29 ±0.37	-9300 ±58	9.3
Pres-MW64	73.33 ±0.48	12.64	< 0.28	> 31497	10.1
Pres-MW65	73.33 ±0.48	13.18	< 0.25	> 32779	10.2
Pres-MW60	73.33 ±0.48	11.10	< 0.17	> 34546	10.4
Pres-MW68	73.33 ±0.48	13.97	< 0.11	> 39936	10.7
Paguate Aquifer					
Pres-Bibo	73.33 ±0.48	23.22	17.84 ±0.27	2179 ±124	5.8
Pres-CNVW5	73.33 ±0.48	16.17	0.28 ±0.60	33533 ±9467	9.3
Cubero/Morrison Aquifer					
Pres-Seb	73.33 ±0.48	37.16	23.96 ±0.29	3628 ±99	6.0
Pres-Moq	73.33 ±0.48	20.06	4.61 ±0.29	12155 ±504	8.4
Pres-CNVW3	73.33 ±0.48	13.53	0.74 ±0.30	24025 ±2814	9.3
Pres-LBar	73.33 ±0.48	16.83	< 0.16	> 38265	12.9

uniformly increase with distance from the initial well, as is expected for samples along a flow path. NETPATH calculates a negative age (-9300 years) for the CNV-W2 sample. This is because the ^{14}C activity in that sample is greater than the ^{14}C activity in the initial well, indicating much younger water in the CNV-W2 sample relative to the initial well.

Flow Rates

The radiocarbon ages calculated by NETPATH and by the simple dissolution model are travel times between an initial well and a final well. The distance between the wells can be divided by the travel time to get a flow rate, or seepage velocity. By calculating travel times between each set of wells along the flow path we can see where travel times are fastest and where they are slowest. Figures 30, 31, and 32 show graphically the NETPATH model-corrected ages and corresponding seepage velocities between every combination of wells. Seepage velocities range from less than 3.49×10^{-9} m/s (0.11 m/yr) to 8.47×10^{-8} m/s (2.67 m/yr). In each aquifer the highest velocities appear to be in the area between the recharge well and the Bibo and Seboyeta wells (wells at the base of Mesa Chivato). The slowest velocities occur in the region between Bibo and the Cerro Negro vertical borehole (CNV), and between CNV and the monitor wells. Table 11 shows the average flow rates for each aquifer in each of three portions of the flow path. The three flow path sections are termed (1) "recharge"-recharge wells to wells at the base of the mesa , (2) "Bibo area"-Bibo well to CNV well, and (3) "tailings area"-CNV well to L-Bar well. The recharge portion of the flow path consistently has the highest seepage velocities. This may indicate increased vertical flow through fractures beneath Mesa Chivato. However, the higher apparent rates are more likely a result of mixing in the wells at the base of the mesa between older ground water traveling along the presumed flow path and younger water that has infiltrated from the surface. As shown by the direction of flow arrows in Figure 6, a small amount of water discharges from springs on the side of Mesa Chivato, especially at the base of the volcanic conglomerate. This discharged water flows into the Rio Paguate drainage and may infiltrate to mix with older water, thus making the water from the wells appear young, and causing the calculated flow rates to be fast. Since the seepage velocities for the Bibo and tailings areas are based on travel times from the wells at the base of the mesa, these velocities are more accurate and better represent the true flow rate near the Cerro Negro intrusion.

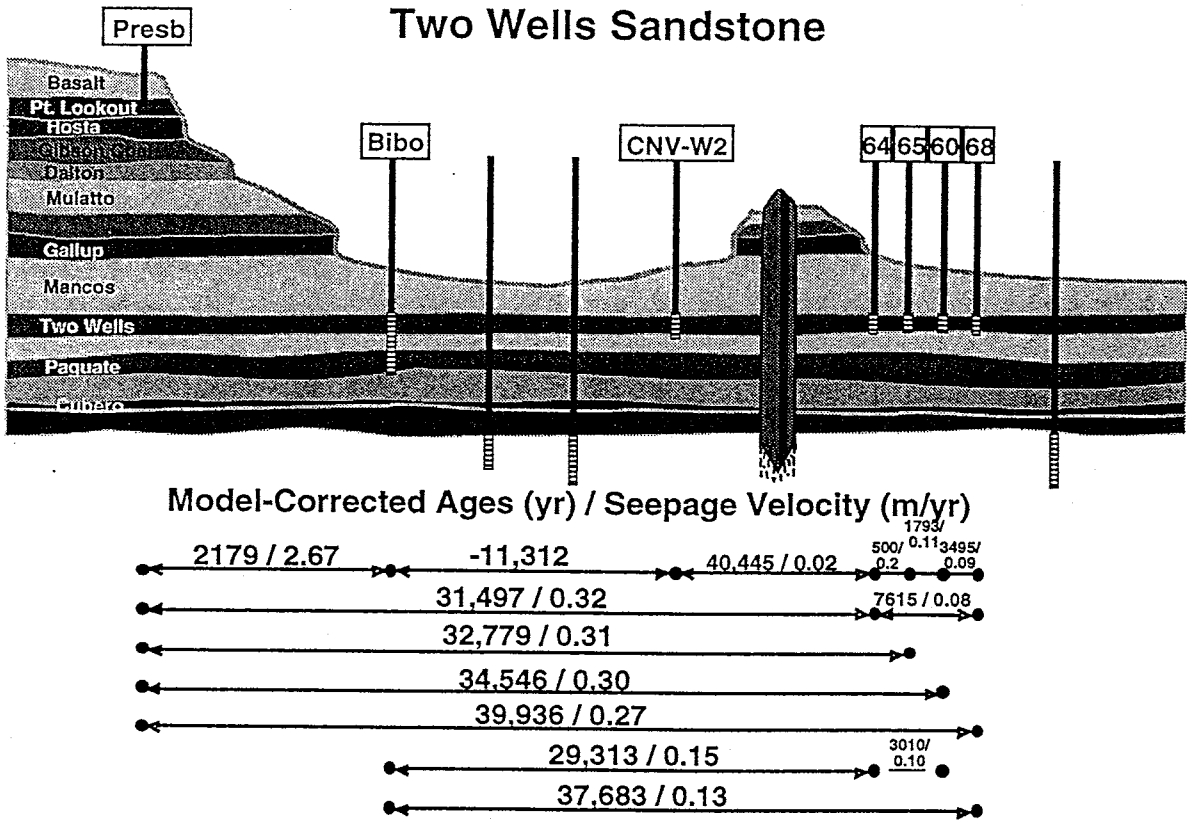

Figure 30: NETPATH model-corrected ages and corresponding seepage velocities for the Two Wells Sandstone

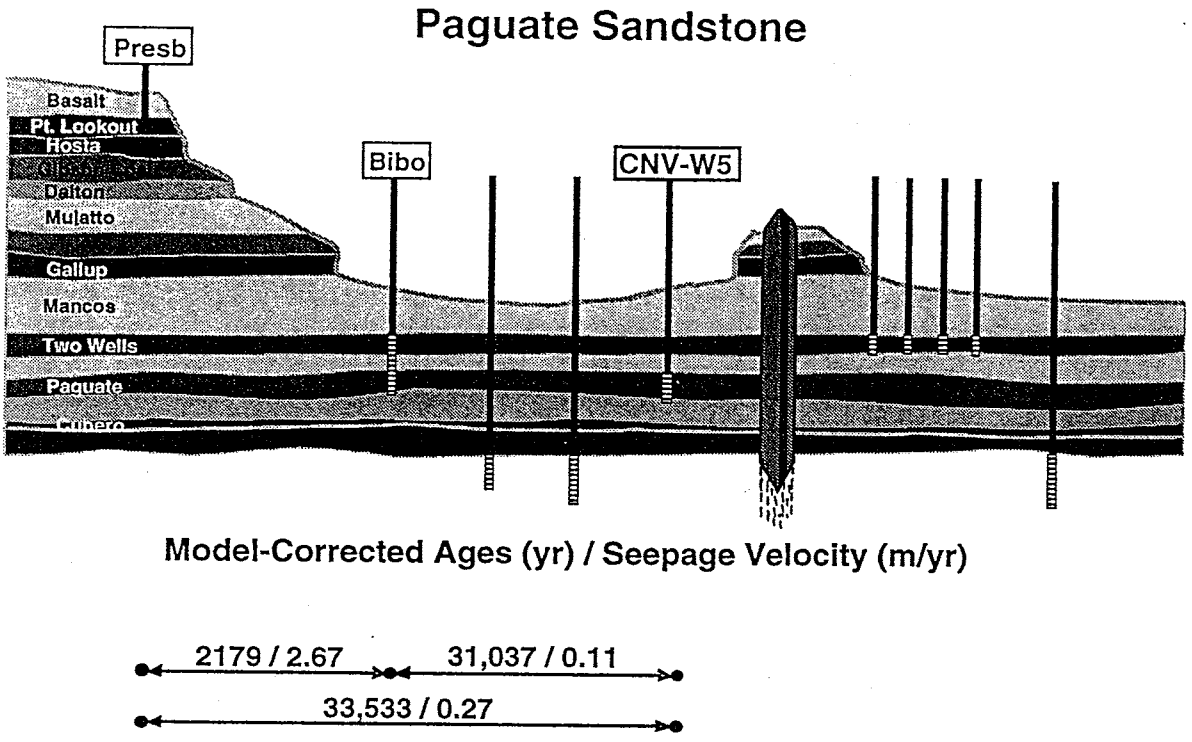

Figure 31: NETPATH model-corrected ages and corresponding seepage velocities for the Paguate Sandstone

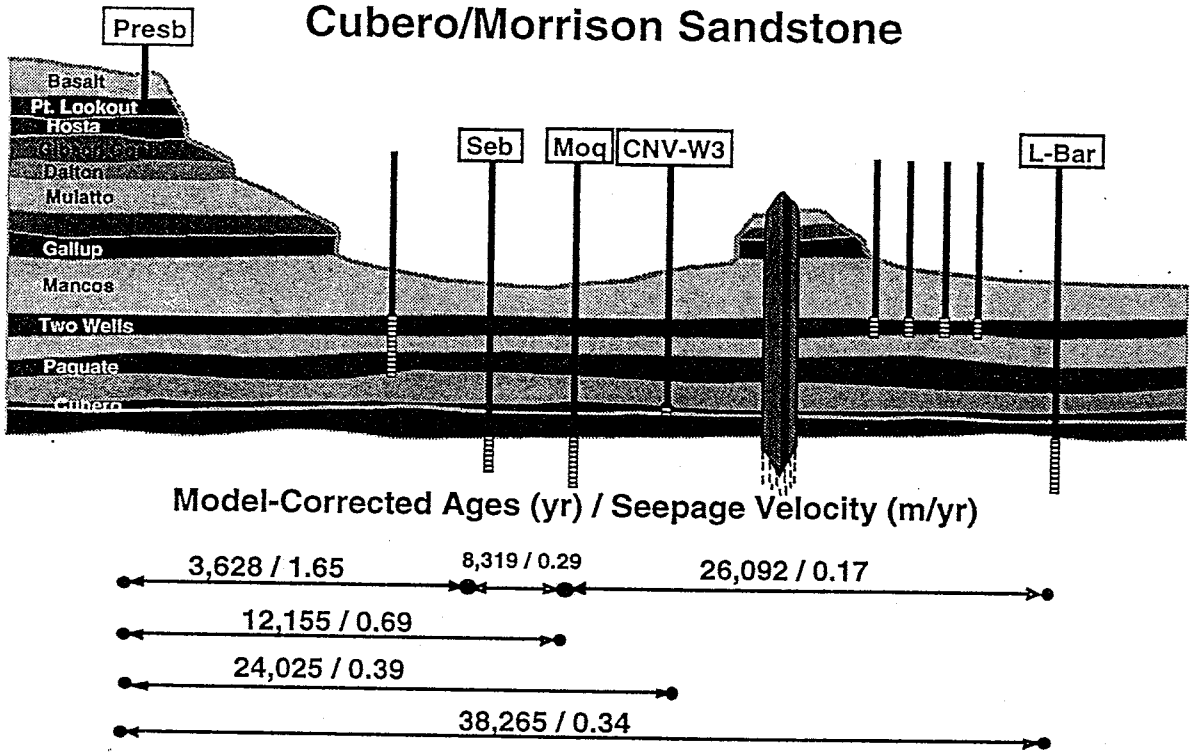

Figure 32: NETPATH model-corrected ages and corresponding seepage velocities for the Cubero/Morrison Sandstone

Table 11: Summary of average flow rates calculated from radiocarbon ages for each aquifer in each section of the flow path.

	Recharge area		Bibo area		Tailings area	
	flow rate		flow rate		flow rate	
	m/s	m/yr	m/s	m/yr	m/s	m/yr
Two Wells	$8.47\pm0.48 \times 10^{-8}$	2.67±0.15	$4.76\pm0.13 \times 10^{-9}$	0.15±0.004	$<3.49 \times 10^{-9}$	<0.11
Paguate	$8.47\pm0.48 \times 10^{-8}$	2.67±0.15	$3.49\pm0.95 \times 10^{-9}$	0.11±0.03	--	--
Cubero/Morrison	$3.71\pm0.13 \times 10^{-8}$	1.17±0.04	$5.71\pm0.63 \times 10^{-9}$	0.18±0.02	$<7.29 \times 10^{-9}$	<0.23

Comparison of NETPATH ages to SDM ages

Figure 33 compares the adjusted ages calculated by NETPATH to the ages predicted by the simple dissolution model. The ages predicted by the simple model are virtually identical to those calculated by the more elaborate NETPATH model. This implies that the carbonate geochemistry of the Cerro Negro ground-water flow path is not complicated. If there were sources and sinks of carbon other than carbonate rocks (such as methane or large amounts of organic carbon) the NETPATH model would not predict the same ground-water ages as the simple dissolution calculations. Therefore, in aquifers with few sources of carbon, a simple "back of the envelope" calculation can nearly match the corrected radiocarbon ages of a more elaborate model.

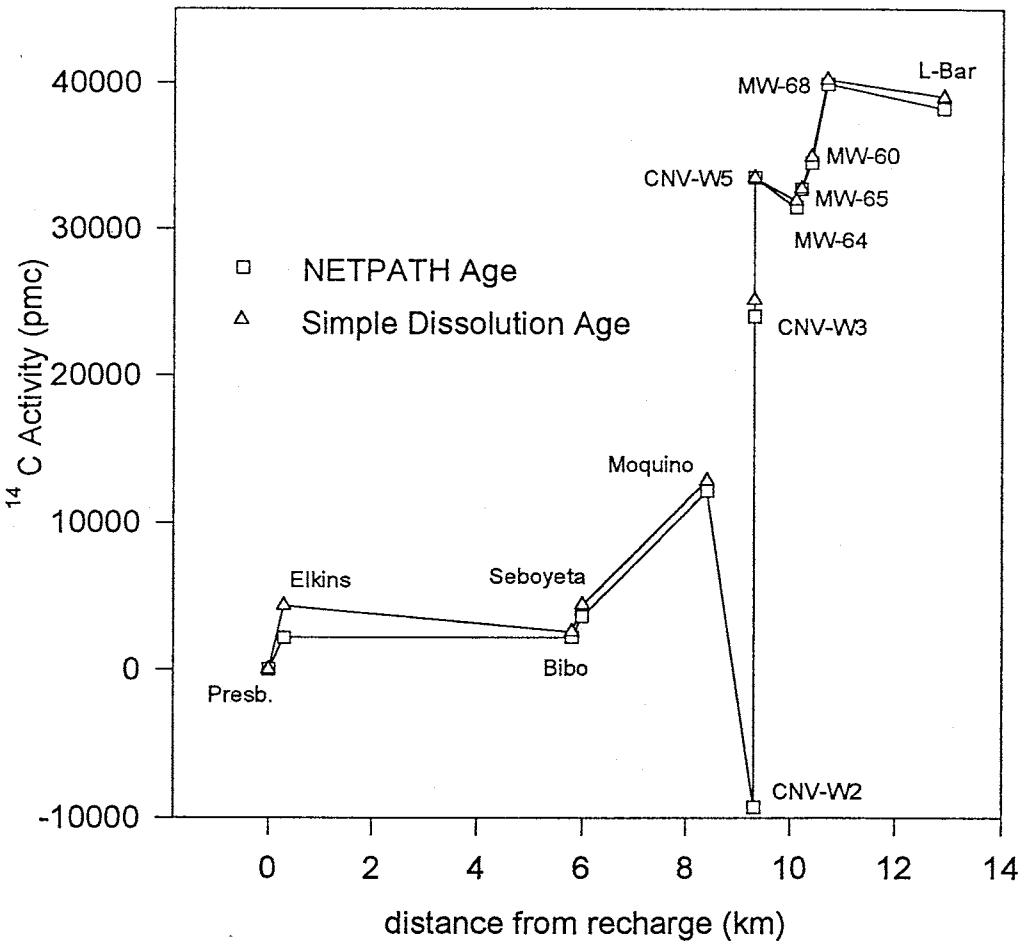

Figure 33: Comparison of radiocarbon ages calculated by NETPATH to those calculated by the Simple Dissolution Model.

Data Synthesis and Interpretation

The goal of this study is to determine accurate flow rates, both horizontal and vertical, near the Cerro Negro intrusion. These flow rates will later be integrated with water level information into a computer model that simulates three dimensional ground-water flow. We can check the flow rates determined in this study against data that have been published for the same rock units in the San Juan Basin. Table 12 shows values of hydraulic conductivity taken from published papers. Most published data is in the form of hydraulic conductivity or transmissivity. With the flow rates determined by radiocarbon dating, we can use Darcy's Law and the local head gradients to calculate hydraulic conductivity and compare these to the published values. Figure 34 graphically shows the comparisons between published conductivity values and those calculated from ^{14}C ages in this study. The following paragraphs provide details of the conductivity calculations.

Table 3 gives water level elevation data for the wells sampled in this study. For wells completed in the Two Wells Sandstone, the most accurate water level information exists for the tailings pond monitor wells. The gradient between MW-65 and MW-68 is 0.0024. The ground-water velocity in this area is $3.49\pm0.95 \times 10^{-9}$ m/s (0.11 ± 0.03 m/yr), and the porosity of the Two Wells is 0.15 (Table 2). Solving Darcy's equation for conductivity (K) yields:

$$K = \frac{vn}{J}$$

where v is the flow rate (seepage velocity), n is the porosity, and J is the hydraulic gradient. For the Two Wells Sandstone this equation gives a horizontal conductivity of $2.18\pm0.6 \times 10^{-7}$ m/s (6.88 ± 1.87 m/yr). Table 12 shows values of hydraulic conductivity taken from published papers. The average of the published values for the Two Wells Sandstone at the L-Bar Mine is 7.83×10^{-6} m/s, only slightly higher than the value calculated from radiocarbon ages. For the Dakota Sandstone in general (of which the Two Wells is a part), the values range from 1×10^{-7} m/s to 3.53×10^{-4} m/s.

For the Cubero/Morrison aquifer, water level information exists for the Moquino and CNV-W3 samples. The gradient between these wells is 0.004, the porosity is 0.15, and the velocity is $5.71\pm0.63 \times 10^{-9}$ m/s (0.18 ± 0.02 m/yr). The calculated hydraulic conductivity is $2.14\pm0.24 \times 10^{-7}$ m/s (6.75 ± 0.75 m/yr). The published values for the Jackpile Sandstone (part of the Morrison) range from 8.82×10^{-8} m/s to 1.38×10^{-6} m/s.

Table 12: Table of published hydraulic conductivity data.

UNIT	CONDUCTIVITY	LOCATION	METHOD OF MEASUREMENT
Alluvium	[1] 8.11×10^{-5} m/s	confluence of Rio Paguate and Rio Moquino	Pump test
	[2] 7.0×10^{-6} m/s -	North of Prewitt, NM	NA
	[3] 8.4×10^{-6} to 1.06×10^{-3} m/s	Rio San Jose	Pump test
Mancos Shale	[2] 1×10^{-10} m/s	North of Prewitt, NM	NA
Two Wells SS	[4] 1.2×10^{-5} m/s	MW-1A, L-Bar Mine	Pump test
	[4] 5.6×10^{-5} m/s	MW-2A, L-Bar Mine	Slug test
	[4] 4.2×10^{-7} m/s	MW-3A, L-Bar Mine	Slug test
	[4] 2.3×10^{-6} m/s	MW-4A, L-Bar Mine	Slug test
	[4] 6.0×10^{-6} m/s	MW-5, L-Bar Mine	Drawdown
	[4] 4.9×10^{-6} m/s	MW-6, L-Bar Mine	Drawdown
	[4] 4.6×10^{-6} m/s	MW-9,10,12, L-Bar Mine	Pump test
	[4] 8.5×10^{-6} m/s	MW-14, L-Bar Mine	Drawdown
	[4] 3.5×10^{-8} m/s	MW-17, L-Bar Mine	Drawdown
	[4] 7.83×10^{-6} m/s	Average, at L-Bar Mine	-
Dakota SS	[2] 1×10^{-7} m/s	North of Prewitt, NM	NA
	[3] 3.53×10^{-4} m/s	Encinal	Pump test
Jackpile SS	[1] 9.17×10^{-7} m/s	South of Rio Paguate - well M2	Pump test
	[1] 1.38×10^{-6} m/s	North Paguate Pit - well M3	Pump test
	[1] 8.82×10^{-8} m/s	Southeast of L-Bar - well M21	Pump test
SS in Brushy Basin Shale	[1] 1.16×10^{-6} m/s	North Paguate Pit - well M25	Slug test
Westwater Canyon	[2] 2.5×10^{-6} to 7.8×10^{-6} m/s	North of Prewitt, NM	NA
	[3] 7.8×10^{-6} m/s	Montano Grant	Pump test

REFERENCES:

[1] Risser, et al (1984)

[2] Stephens (1984)

[3] Risser, Lyford (1983)

[4] Hydro-Engineering (1981)

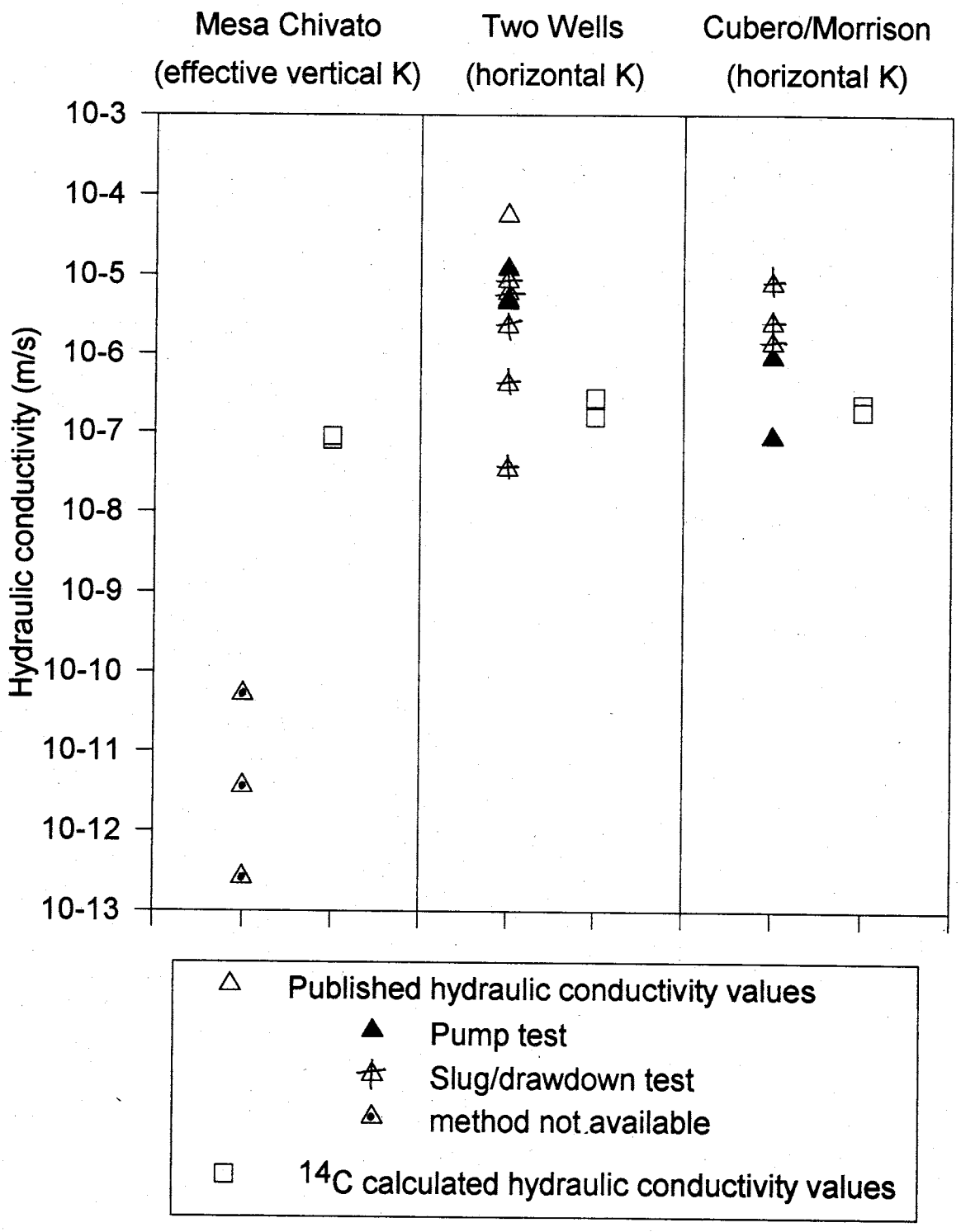

Figure 34: Comparison of published hydraulic conductivity values to conductivities calculated from ^{14}C data.

Thus, the conductivity calculated from radiocarbon ages agrees well with the published data.

As discussed previously in the section on Cerro Negro Site Description, a vertical hydraulic conductivity for the Mancos Shale was calculated as 5.9×10^{-8} m/s. Stephens (1984) reports a horizontal conductivity of 1×10^{-10} m/s. One would expect the horizontal conductivity of a shale to be greater than the vertical conductivity if the shale were intact, with no conduits from the surface. Thus, the higher vertical conductivity seen in the Mancos Shale at the L-Bar tailings pond is probably a result of fractures. Another indication of fracturing in the area is the fact that there is modern water in the sample taken from the Two Wells Sandstone in the Cerro Negro vertical borehole (CNV-W2). This sample has a much higher ^{14}C activity than any of the other samples taken from the same unit. The only explanations for this are sample contamination and input of modern water from the surface. If the sample were contaminated with modern water it would contain some amount of tritium. Since there is no tritium in the sample, and there is no other reason to believe the sample was contaminated, the most likely explanation of the high ^{14}C activity is fracturing in the Mancos Shale above the Two Wells Sandstone in the area of Cerro Negro. This conclusion is reasonable given the proximity to the volcanic intrusion.

We can integrate these horizontal and vertical flow rates and hydraulic conductivities into a final picture of the hydraulic framework in the area surrounding Cerro Negro. It is clear that the recharge area for ground water that flows toward Cerro Negro is on Mount Taylor and the surrounding Mesa Chivato. Rainwater infiltrates the volcanic conglomerate that tops the mesa and flows, in a southeasterly direction, horizontally through the more permeable sandstones and vertically through the less permeable shale underneath the mesa. Some water discharges from springs at the base of the volcanic conglomerate at the edge of the mesa. A portion of this spring discharged water may re-infiltrate through the alluvium in the surface drainage to the east of the mesa. The overall flow rate, based on radiocarbon dating, for this section of the flow path is approximately $8.47 \pm 0.48 \times 10^{-8}$ m/s (2.67 ± 0.15 m/yr). This flow rate includes a large component of vertical flow through various geologic units. Using an estimated average porosity of 0.15 and a hydraulic gradient of 0.082 (calculated from the measured water levels in the Elkins and Bibo#2 wells as shown in Table 3, and the aproximate distance along the flow path) the flow rate can be converted to an effective hydraulic conductivity along the flow path of $1.6 \pm 0.08 \times 10^{-7}$ m/s (4.9 ± 0.28 m/yr). Table 1 lists representative aquifer transmissivities in the San Juan Basin. Converting these transmissivities to hydraulic conductivities gives conductivity values of 2.6×10^{-13} m/s, 3.6×10^{-12} m/s, and

$5.2x10^{-11}$ m/s for the Point Lookout Sandstone, Crevasse Canyon Formation, and Gallup Sandstone respectively. The calculated effective conductivity is at least four orders of magnitude greater than each of these. In addition, the published conductivity values represent only the aquifers and not the aquitards. Therefore, the true effective conductivity is even less, implying that the radiocarbon flow rate and corresponding effective conductivity are high and most likely a result of fracture flow or input of young water at the base of the mesa.

Horizontal flow is probably the main component in the flow path section between the base of Mesa Chivato and the Cerro Negro vertical borehole. In this area the flow rate ranges from $3.5\pm0.95 \times 10^{-9}$ (0.11 ± 0.03 m/yr) in the Paguate Sandstone to $5.7\pm0.63 \times 10^{-9}$ (0.18 ± 0.02 m/yr) in the Cubero/Morrison aquifer. This flow rate corresponds to a hydraulic conductivity of $2.1\pm0.24 \times 10^{-7}$ m/s (6.7 ± 0.75 m/yr) in the Cubero/Morrison aquifer.

In the area of the L-Bar tailings pond the flow is also mainly horizontal, but with a significant vertical component. This is the region closest to the Cerro Negro intrusion, and therefore most important to the microbial transport theory. The flow rates in this area range from less than $3.5x10^{-9}$ m/s (0.11 m/yr) to $7.3\pm0.95 \times 10^{-9}$ m/s (0.23 ± 0.03 m/yr). This corresponds to a hydraulic conductivity of $2.2\pm0.6 \times 10^{-7}$ m/s (6.88 ± 1.87 m/yr) for the Two Wells Sandstone. There is a significant vertical flow component in the Mancos Shale in this area. This vertical component is indicated by seepage of contamination from the L-Bar tailings pond, through the Mancos, and into the Two Wells Sandstone, and also by the presence of an anomalously high ^{14}C activity in the Two Wells sample from the Cerro Negro vertical borehole. In both cases the vertical flow may be through fractures in the shale.

Implications for Cerro Negro Origins Project

The ground water flow rates near Cerro Negro have implications for the microbial transport theory and the timing of re-colonization around the volcanic intrusion after sterilization. Assuming that the pore throat sizes in the aquifer matrix are large enough to allow a microbe to pass through, the re-colonization rate by transport will be closely related to the flow rate. If microbes are assumed to exist immediately adjacent to the sterilized zone, and are transported into this zone with the ground water, the distance they will have to travel to begin re-colonization is simply the radius of the thermal aureole, or sterilized zone. If we assume this radius is approximately 200 m, and the flow rate is approximately 0.11 m/yr, the time necessary for re-colonization by transport is only 1800 years. We could also say that microbes are only transported from the recharge area, and the distance from the recharge area is the distance a microbe would have to travel to re-colonize the sterilized zone. In this case, the distance is approximately 10 km, the slowest possible flow rate is 0.11 m/yr, and the time for re-colonization would be around 91,000 years. In either scenario the flow rates suggest the possibility of relatively rapid re-colonization by transport (within 100,000 years of sterilization), and transport is not ruled out as a mechanism of microbial survival. In fact, assuming ground-water flow patterns have remained relatively the same in the 3.39 million years since sterilization, 34 pore volumes have been replaced in the aquifers around Cerro Negro.

References and Bibliography

Armstrong, A.K., and Mamet, B.L., 1977, Biostratigraphy and paleogeography of the Mississippian system in northern New Mexico and adjacent San Juan Mountains of southwestern Colorado, *Guidebook, New Mexico Geological Society 28th Field Conference*, p. 111-127.

Azimi-Zonooz, A., and Duffy, C.J., 1993, Modeling transport of subsurface salinity from a Mancos Shale hillslope, *Ground Water*, v. 31, p. 972-981.

Craig, H., 1961, Isotopic variations in meteoric water, *Science*, v. 133, p. 795-802.

Craigg, S.D., Dam, W.L., Kernodle, J.M., and Levings, G.W., 1989, Hydrogeology of the Dakota Sandstone in the San Juan structural basin, New Mexico, Colorado, Arizona and Utah, *U. S. Geological Survey Hydrologic Investigations Atlas HA-720-I*, 2 sheets.

Craigg, S.D., Dam, W.L., Kernodle, J.M., Thorn, C.R., and Levings, G.W., 1990, Hydrogeology of the Point Lookout Sandstone in the San Juan structural basin, New Mexico, Colorado, Arizona, and Utah, *U. S. Geological Survey Hydrologic Investigations Atlas HA-720-G*, 2 sheets.

Daniels, D.P., Fritz, S.J., and Leap, D.J., 1991, Estimating recharge rates through unsaturated glacial till by tritium tracing, *Ground Water*, v. 29, p. 26-34.

Dansgaard, W., 1964, Stable isotopes in precipitation, *Tellus*, v. 16, p. 436-468.

Dam, W.L., Kernodle, J.M., Levings, G.W., and Craigg, S.D., 1990, Hydrogeology of the Morrison Formation in the San Juan structural basin, New Mexico, Colorado, Arizona and Utah, *U. S. Geological Survey Hydrologic Investigations Atlas HA 720-J*, 2 sheets.

Dinwiddie, G.A., 1963, Ground water in the vicinity of the Jackpile and Paguate mines, in Geology and Technology of the Grants Uranium Region, *Memoir 15*, New Mexico Bureau of Mines and Mineral Resources, Socorro, NM, p. 217-218.

Domenico, P.A., and Schwartz, F.W., 1990, *Physical and Chemical Hydrogeology*, John Wiley & Sons, New York, 824 p.

Eichinger, L., 1983, A contribution to the interpretation of ^{14}C groundwater ages considering the example of a partially confined sandstone aquifer, *Radiocarbon*, v. 25, p. 347-356.

Fontes, J.-C., 1981, Groundwater, in *Stable isotope hydrology: Deuterium and Oxygen-18 in the water cycle*, edited by J.R. Gat and R. Gonfiantini, IAEA, Vienna, p. 223-240.

Fontes, J.-C., 1980, Environmental isotopes in groundwater hydrology, in *Handbook of Environmental Isotope Geochemistry, vol. 2B*, edited by P. Fritz and J.-C. Fontes, Elsevier, New York, p. 75-140.

Fontes, J.-C., and Garnier,J.M., 1979, Determinatin of the initial ^{14}C activity of the total dissolved carbon - a review of the existing models and a new approach, *Water Resources Research*, p. 399-413.

Freeze, R.A., and Cherry, J.A., 1979, *Groundwater*, Prentice-Hall, Inc., New Jersey, 604 p.

Godwin, H., 1962, Half-life of radiocarbon, *Nature*, v. 195, p. 984.

Hallet, R.B., 1994, Geologic and hydrologic summary of Cerro Negro, 15 p.

Harteck, P., 1954, The relative abundance of HT and HTO in the atmosphere, Journal of Chemistry and Physics, v. 22, p. 1746-1751.

Hem, J.D., 1985, Study and Interpretation of the Chemical Characteristics of Natural Water, *U. S. Geological Survey Water-Supply Paper 2254*, 263 p.

Hydro-Engineering, 1981, Ground-water hydrology near the L-Bar tailings reservoir, prepared for Sohio Western Mining Company by Hydro-Engineering, Casper, Wyoming.

Intera, Inc., 1993, Semi-annual ground-water monitoring report, second half-1993, L-Bar Uranium Mine, Cibola County, New Mexico, prepared for Sohio Western Mining Company by Intera, Inc., Austin, Texas.

Intera, Inc., 1989, Semi-annual environmental monitoring report, first half-1989, L-Bar Uranium mine, Cibola County, New Mexico, prepared for Sohio Western Mining Company by Intera, Inc., Austin, Texas.

Intera, Inc., 1987, Semi-annual environmental monitoring report, first half-1987, L-Bar Uranium mine, Cibola County, New Mexico, prepared for Sohio Western Mining Company by Intera, Inc., Austin, Texas.

International Atomic Energy Agency (IAEA), 1983, Isotope techniques in the hydrogeological assessment of potential sites for the disposal of high-level radioactive wastes, *IAEA Technical Report Series 228*, edited by IAEA, Vienna, p. 57-61.

Jobin, D.A., 1962, Relations of the transmissive character of the sedimentary rocks of the Colorado Plateau to the distribution of uranium deposits, *U. S. Geological Survey Bulletin 1124*, 151 p.

Kaufmann, R.F., Eadie, G.G., and Russell, C.R., 1976, Effects of uranium mining and milling on ground water in the Grants uranium mineral belt, New Mexico, *Ground Water*, v. 14, p. 296-308.

Kaufmann, R.F., Eadie, G.G., and Russell, C.R., 1975, Summary of ground-water quality impacts of uranium mining and milling in the Grants mineral belt, New Mexico, *U.S. Environmental Protection Agency, Office of Radiation Programs-Las Vegas Facility, Technical Note ORP/LV-75-4*, 71 p.

Kernodle, J.M., Levings, G.W., Craigg, S.D., and Dam, W.L., 1989, Hydrogeology of the Gallup Sandstone in the San Juan structural basin, New Mexico, Colorado, Arizona and Utah, *U. S. Geological Survey Hydrologic Investigations Atlas HA-720-H*, 2 sheets.

Libby, W.E., 1955, Radiocarbon Dating, The University of Chicago Press, Chicago,

Long, P.E., Fredrickson, J.K., Onstott, T.C., Bjornstad, B.N., and Colwell, F.S., 1994, Science Investigation Plan for Cerro Negro Field Site, Seboyeta, New Mexico, 37 p.

Longmire, P.A., and Brookins, D.G., 1982, Geochemical studies of discharge water from a uranium acid-leach process, *Guidebook, New Mexico Geological Society 33rd Field Conference, Albuquerque Country II, 1982*, p. 367-370.

Moench, R.H., 1963, Geologic quadrangle map of the Seboyeta Quadrangle, New Mexico, *U. S. Geological Survey Map GQ-207.*

Moench, R.H., and Schlee, J.S., 1967, Geology and uranium deposits of the Laguna district, New Mexico, *U.S. Geological Survey Professional Paper 519*, 116 p.

Molenaar, C.M., 1977b, Stratigraphy and depositional history of Upper Cretaceous rocks of the San Juan Basin area, New Mexico and Colorado, with a note on economic resources, *Guidebook, New Mexico Geological Society 28th field conference*, p. 159-166.

Molenaar, C.M., 1977a, San Juan Basin time-stratigraphic nomenclature chart, *Guidebook, New Mexico Geological Society 28th field conference*, p. xii.

Mook, W.G., 1980, Carbon-14 in hydrogeochemical studies, in *Handbook of Environmental Isotope Geochemistry*, edited by P. Fritz and J.-C. Fontes, Elsevier, New York, p. 49-74.

Mook, W.G., 1976, The dissolution-exchange model for dating ground water with carbon-14, in *Interpretation of Environmental Isotope and Hydrochemical Data in Groundwater Hydrology*, International Atomic Energy Agency, Vienna, p. 213-225.

Mook, W.G., 1972, On the reconstruction of the initial ^{14}C content of ground water from chemical and isotopic composition, in *Proceedings of the VII International Conference on 14C*, Lower Hutt, New Zealand, p. 18-25.

Murphy, E.M., Davis, S.N., Long, A., Donahue, D., and Jull, A.J.T., 1989, Characterization and isotopic composition of organic and inorganic carbon in the Milk River Aquifer, *Water Resources Research*, v. 25, p. 1893-1905.

Murphy, E.M., Schramke, J.A., Fredrickson, J.K., Bledsoe, H.W., Francis, A.J., Sklarew, D.S., and Linehan, J.C., 1992, The influence of microbial activity and sedimentary organic carbon on the isotope geochemistry of the Middendorf Aquifer, *Water Resources Research*, v. 28, p. 723-740.

Parkhurst, D.L., Plummer, L.N., and Thorstenson, D.C., 1982, BALANCE-A computer program for calculating mass transfer for geochemical reactions in ground water, *U.S. Geological Survey Water-Resources Investigations Report 82-14*, 29 p.

Pearson, F.J., Jr., and White, D.E., 1967, Carbon-14 ages and flow rates of water in the Carrizo Sand, Atascosa County, Texas, *Water Resources Research*, v. 3, p. 251-261.

Phelps, T.J., Murphy, E.M., Pfiffner, S.M., and White, D.C., 1994, Comparison between geochemical and biological estimates of subsurface microbial activities, *Microbial Ecology*, v. 28, p. 335-349.

Phillips, F.M., Tansey, M.K., Peeters, L.A., Cheng, S., and Long, A., 1989, An isotopic investigation of groundwater in the central San Juan Basin, New Mexico: Carbon 14 dating as a basis for numerical flow modeling, *Water Resources Research*, v. 25, p. 2259-2273.

Phillips, F.M., Peeters, L.A., Tansey, M.K., and Davis, S.N., 1986, Paleoclimatic inferences from an isotopic investigation of ground water in the central San Juan basin, New Mexico, *Quaternary Research*, v. 26, p. 179-192.

Plummer, L. N., Busby, J.F., Lee, R.W., and Hanshaw, B.B., 1990, Geochemical modeling of the Madison aquifer in parts of Montana, Wyoming, and South Dakota, *Water Resources Research*, v. 26, p. 1981-2014.

Plummer, L.N., 1984, Geochemical modeling: A comparison of forward and inverse methods, in *First Canadian/American Conference on Hydrogeology, Practical Applications of Ground Water Geochemistry*, Hitchon, B., and Wallick, E.I., eds., National Water Well Association, Worthington, Ohio, p. 149-177.

Plummer, L.N., and Back, W., 1980, The mass balance approach: Applications to interpreting the chemical evolution of hydrologic systems, *American Journal of Science*, v. 280, p. 130-142.

Plummer, L.N., Jones, B.F., and Truesdell, A.H., 1976, WATEQF - A FORTRAN IV version of WATEQ, a computer program for calculating chemical equilibria of natural waters, *U.S. Geological Survey Water-Resources Investigations Report 76-13,* 61 p.

Plummer, L.N., Parkhurst, D.L., and Thorstenson, D.C., 1983, Development of reaction models for ground water systems, *Geochimica et Cosmochimica Acta*, v. 47, p. 665-685.

Plummer, L.N., Prestemon, E.C., and Parkhurst, D.L., 1994, An interactive code (NETPATH) for modeling net geochemical reactions along a flow path, Version 2.0, *U.S. Geological Survey Water-Resources Investigations Report 94-4169*, 130 p.

Plummer, L.N., Prestemon, E.C., and Parkhurst, D.L., 1991, An interactive code (NETPATH) for modeling net geochemical reactions along a flow path, *U.S. Geological Survey Water-Resources Investigations Report 91-4078*, 120 p.

Reardon, E.J., and Fritz, P., 1978, Computer modeling of ground water 13C and 14C isotope compositions, *Journal of Hydrology*, v. 36, p. 201-224.

Risser, D.W., Davis, P.A., Baldwin, J.A., and McAda, D.P., 1984, Aquifer tests at the Jackpile-Paguate uranium mine, Pueblo of Laguna, West-Central New Mexico, *U. S. Geological Survey Water-Resources Investigations Report 84-4255*, 26 p.

Risser, D.W., and Lyford, F.P., 1983, Water resources on the Pueblo of Laguna, West-Central New Mexico, *U. S. Geological Survey Water-Resources Investigations Report 83-4038*, 308 p.

Schlee, J.S., and Moench, R.H., 1963, Geologic quadrangle map of the Moquino quadrangle, New Mexico, *U. S. Geological Survey Map GQ-209.*

Solomon, K.K., Poreda, R.J., Schiff, S.L., and Cherry, J.A., 1992, Tritium and helium-3 as ground water age tracers in the Borden aquifer, *Water Resources Research*, v. 28, p. 741-756.

Stephens, D.B., 1983, Ground water flow and implications for groundwater contamination north of Prewitt, New Mexico, U.S.A., *Journal of Hydrology*, v. 61, p. 391-408.

Stone, W.J., Lyford, F.P., Frenzel, P.F., Mizell, N.H. , and Padgett, E.T., 1983, Hydrogeology and water resources of San Juan Basin, New Mexico, *Hydrologic Report 6*, New Mexico Bureau of Mines and Mineral Resources, Socorro, NM, 70 p.

Tamers, M.A., 1975, Validity of radiocarbon dates on ground water, *Geophysical Survey*, v. 2, p. 217-239.

Tamers, M.A., 1967, Radiocarbon ages of groundwater in an arid zone unconfined aquifer, in *Isotope Techniques in the Hydrologic Cycle, Geophysical Monograph Series, v. 11* edited by G.E. Stout, AGU, Washington, D.C., p. 143-152.

United States Department of Energy, 1994, Program Overview of the Subsurface Science Program, *DOE/ER-0640*, 18 p.

Vogel, J.C., 1970, Carbon-14 dating of ground water, in *Isotope Hydrology 1970*, International Atomic Energy Agency, Vienna, p. 225-239.

Vogel, J.C., 1967, Investigation of groundwater flow with radiocarbon, in *Isotopes in Hydrology*, International Atomic Energy Agency, Vienna, p. 235-237.

Ward, J.J., Walter, G.R., Alweis, S.J., Axen, G.J., Bentley, H.W., and Neuman, S.P., 1982, Effects of uranium mine dewatering on the water resources of the Pueblo of Laguna, prepared for the Pueblo of Laguna, Laguna, NM by Hydro Geo Chem, Inc., Tucson, AZ, 250 p.

Wassenaar, L., and Aravena, R., 1991, Radiocarbon in dissolved organic carbon, a possible groundwater dating method: Case studies from western Canada, *Water Resources Research*, v. 27, p. 1975-1986.

Wigley, T.M.L., Plummer, L.N., and Pearson, F.J.,Jr., 1978, Mass transfer and carbon isotope evolution in natural water systems, *Geochimica et Cosmochimica Acta*, v. 42, p. 1117-1139.

Woodward, L.A., and Callendar, J.F., 1977, Tectonic framework of the San Juan Basin, *Guidebook New Mexico Geological Society 28th Field Conference*, p. 209-212.

Appendix A

Calculation of Bicarbonate concentration from pH and DIC

The species of carbon that exist in natural waters are carbonate (CO_3^{2-}), bicarbonate (HCO_3^-), and carbonic acid (H_2CO_3). Dissolved inorganic carbon (DIC) concentration is a measure of the total concentration of carbon species (C_T) in a water sample. The pH of the water controls which species dominates. The predominate carbon species in waters of pH 6.3 to 10.3, the normal range for natural waters, is the bicarbonate ion (HCO_3^-). The bicarbonate concentration (in millimoles per liter) can be calculated when only the pH and DIC concentration are known, as follows:

1) Mass balance equation

$$C_T = \left[H_2CO_3\right] + \left[HCO_3^-\right] + \left[CO_3^{2-}\right] = DIC$$

Assuming $[H_2CO_3]$ is negligible, then

$$\left[CO_3^{2-}\right] = DIC - \left[HCO_3^-\right]$$

2) Equilibrium equation for bicarbonate

$$HCO_3^- \Leftrightarrow H^+ + CO_3^{2-} \qquad \text{pK=10.33}$$

$$pK = \frac{\log\left[HCO_3^{2-}\right]}{\log\left[H^+\right]\left[CO_3^{2-}\right]}$$

$$\log\frac{DIC - \left[HCO_3^-\right]}{\left[HCO_3^-\right]} = pH - 10.33$$

$$\left[HCO_3^-\right] = \frac{DIC}{10^{(pH-10.33)} + 1}$$

Thus, the final equation is solved for bicarbonate knowing only DIC and pH.

Appendix A

Calculation of Bicarbonate concentration from pH and DIC

The species of carbon that exist in natural waters are carbonate (CO_3^{2-}), bicarbonate (HCO_3^-), and carbonic acid (H_2CO_3). Dissolved inorganic carbon (DIC) concentration is a measure of the total concentration of carbon species (C_T) in a water sample. The pH of the water controls which species dominates. The predominate carbon species in waters of pH 6.3 to 10.3, the normal range for natural waters, is the bicarbonate ion (HCO_3^-). The bicarbonate concentration (in millimoles per liter) can be calculated when only the pH and DIC concentration are known, as follows:

1) Mass balance equation

$$C_T = \left[H_2CO_3\right] + \left[HCO_3^-\right] + \left[CO_3^{2-}\right] = DIC$$

Assuming $[H_2CO_3]$ is negligible, then

$$\left[CO_3^{2-}\right] = DIC - \left[HCO_3^-\right]$$

2) Equilibrium equation for bicarbonate

$$HCO_3^- \Leftrightarrow H^+ + CO_3^{2-} \qquad \text{pK=10.33}$$

$$pK = \frac{\log\left[HCO_3^{2-}\right]}{\log\left[H^+\right]\left[CO_3^{2-}\right]}$$

$$\log\frac{DIC - \left[HCO_3^-\right]}{\left[HCO_3^-\right]} = pH - 10.33$$

$$\left[HCO_3^-\right] = \frac{DIC}{10^{(pH-10.33)} + 1}$$

Thus, the final equation is solved for bicarbonate knowing only DIC and pH.

Appendix B

Water sample speciation output from WATEQF

1precip

INITIAL SOLUTION

TEMPERATURE = 20.00 DEGREES C PH = 4.870
ANALYTICAL EPMCAT = .027 ANALYTICAL EPMAN = .034

***** OXIDATION - REDUCTION *****

DISSOLVED OXYGEN = .000 MMOLES/KG H2O
EH MEASURED WITH CALOMEL = 9.9000 VOLTS
MEASURED EH OF ZOBELL SOLUTION = 9.9000 VOLTS
CORRECTED EH = .0000 VOLTS
PE COMPUTED FROM CORRECTED EH = .000

FLAG	CORALK	PECALC	IDAVES
0	0	1	0

*** TOTAL CONCENTRATIONS OF INPUT SPECIES ***

SPECIES		TOTAL MOLALITY	LOG TOTAL MOLALITY	TOTAL MG/LITRE
Ca+2	2.0	4.50001E-06	-5.3468	1.80360E-01
Mg+2	2.0	8.00001E-07	-6.0969	1.94496E-02
Na+	1.0	2.60000E-06	-5.5850	5.97735E-02
K+	1.0	5.00001E-07	-6.3010	1.95510E-02
Cl-	-1.0	2.80000E-06	-5.5528	9.92684E-02
HCO3-	-1.0	1.00000E-08	-8.0000	6.10173E-04
SO4-2	-2.0	8.80001E-06	-5.0555	8.45342E-01
NO3-	-1.0	1.39000E-05	-4.8570	1.94693E-01

precip

****DESCRIPTION OF SOLUTION ****

	ANALYT.	COMP.	PH	ACTIVITY H2O = 1.0000
EPMCAT	.03	.03	4.870	PCO2= 1.120234E-02
EPMAN	.03	.05		LOG PCO2 = -1.9507
			TEMPERATURE	PO2 = 4.298588E-66
EH = .0000	PE =	.000	20.00 DEG C	PCH4 = 5.749739E-18
PE CALC S =	.000			CO2 TOT = 4.525911E-04
PE CALC DOX=	.000		IONIC STRENGTH	DENSITY = 1.0000
PE SATO DOX=	.000		5.166044E-05	TDS = 1.4MG/L

TOT ALK = 1.000E-05 MEQ
ELECT = -2.061E-02 MEQ

CARB ALK = 1.362E-02 MEQ
CHARGE IMBALANCE = -27.4%

IN COMPUTING THE DISTRIBUTION OF SPECIES,
PE = .000 EQUIVALENT EH = .000VOLTS

DISTRIBUTION OF SPECIES

I	SPECIES		MOLALITY	ACTIVITY	LOG ACT	GAMMA
1	H+	1.	1.3601E-05	1.3490E-05	-4.870	9.9182E-01
2	E-	-1.	1.0000E+00	1.0000E+00	.000	1.0000E+00
4	Ca+2	2.	4.4923E-06	4.3459E-06	-5.362	9.6741E-01
5	Mg+2	2.	7.9853E-07	7.7254E-07	-6.112	9.6745E-01
6	Na+	1.	2.5999E-06	2.5784E-06	-5.589	9.9174E-01
7	K+	1.	4.9997E-07	4.9583E-07	-6.305	9.9172E-01
14	Cl-	-1.	2.8000E-06	2.7768E-06	-5.556	9.9172E-01
15	CO3-2	-2.	4.3590E-11	4.2169E-11	-10.375	9.6742E-01
16	SO4-2	-2.	8.7814E-06	8.4950E-06	-5.071	9.6739E-01
17	NO3-	-1.	5.8332E-25	5.7849E-25	-24.238	9.9171E-01
31	OH-	-1.	5.0749E-10	5.0328E-10	-9.298	9.9172E-01
33	H2 AQ	0.	1.3551E-13	1.3552E-13	-12.868	1.0000E+00
34	HCO3-	-1.	1.3620E-05	1.3507E-05	-4.869	9.9175E-01
35	H2CO3	0.	4.3897E-04	4.3898E-04	-3.358	1.0000E+00
40	HSO4-	-1.	1.0096E-08	1.0012E-08	-7.999	9.9173E-01
48	NO2-	-1.	1.3900E-05	1.3785E-05	-4.861	9.9171E-01
75	CaOH+	1.	5.3912E-14	5.3466E-14	-13.272	9.9173E-01
76	CaCO3	0.	2.8108E-13	2.8108E-13	-12.551	1.0000E+00
77	CaHCO3+	1.	6.9368E-10	6.8796E-10	-9.162	9.9175E-01
78	CaSO4	0.	7.0244E-09	7.0245E-09	-8.153	1.0000E+00
79	CaHSO4	1.	5.8729E-13	5.8243E-13	-12.235	9.9173E-01
85	MgOH+	1.	2.0966E-13	2.0793E-13	-12.682	9.9173E-01
86	MgCO3	0.	2.8789E-14	2.8789E-14	-13.541	1.0000E+00
87	MgHCO3+	1.	1.2072E-10	1.1972E-10	-9.922	9.9173E-01
88	MgSO4	0.	1.3496E-09	1.3496E-09	-8.870	1.0000E+00
93	NaOH	0.	1.2628E-15	1.2628E-15	-14.899	1.0000E+00
94	NaCO3-	-1.	1.5796E-15	1.5666E-15	-14.805	9.9173E-01
95	NaHCO3	0.	1.7593E-11	1.7593E-11	-10.755	1.0000E+00
96	NaSO4	-1.	1.0718E-10	1.0629E-10	-9.973	9.9173E-01
99	KOH	0.	1.2745E-16	1.2745E-16	-15.895	1.0000E+00
100	KSO4-	-1.	2.8182E-11	2.7949E-11	-10.554	9.9173E-01

	PHASE	IAP	KT	LOG IAP	LOG KT	IAP/KT	LOG IAP/KT
1	Calcite	1.833E-16	3.521E-09	-15.737	-8.453	5.204E-08	-7.284
2	Aragonit	1.833E-16	4.945E-09	-15.737	-8.306	3.706E-08	-7.431
3	Dolomite	5.970E-33	1.067E-17	-32.224	-16.972	5.598E-16	-15.252
8	Gypsum	3.692E-11	2.623E-05	-10.433	-4.581	1.407E-06	-5.852
9	Anhydrit	3.692E-11	4.531E-05	-10.433	-4.344	8.149E-07	-6.089
42	PCO2	4.390E-04	3.919E-02	-3.358	-1.407	1.120E-02	-1.951
44	H2 gas	1.355E-13	7.447E-04	-12.868	-3.128	1.820E-10	-9.740

1Presbyterian

INITIAL SOLUTION

TEMPERATURE = 12.48 DEGREES C PH = 7.270
ANALYTICAL EPMCAT = 1.903 ANALYTICAL EPMAN = 2.120

***** OXIDATION - REDUCTION *****

DISSOLVED OXYGEN = 6.873 MMOLES/KG H2O
EH MEASURED WITH CALOMEL = 9.9000 VOLTS
MEASURED EH OF ZOBELL SOLUTION = 9.9000 VOLTS
CORRECTED EH = .3950 VOLTS
PE COMPUTED FROM CORRECTED EH = 6.970

FLAG	CORALK	PECALC	IDAVES
0	2	1	0

*** TOTAL CONCENTRATIONS OF INPUT SPECIES ***

SPECIES		TOTAL MOLALITY	LOG TOTAL MOLALITY	TOTAL MG/LITRE
Ca+2	2.0	4.02174E-04	-3.3956	1.61122E+01
Mg+2	2.0	2.64114E-04	-3.5782	6.41837E+00
Na+	1.0	4.63200E-04	-3.3342	1.06443E+01
K+	1.0	9.80424E-05	-4.0086	3.83200E+00
Fe+2	2.0	1.00043E-07	-6.9998	5.58470E-03
Al+3	3.0	1.60069E-06	-5.7957	4.31704E-02
Ba+2	2.0	3.00130E-07	-6.5227	4.12020E-02
Sr+2	2.0	1.20052E-06	-5.9206	1.05144E-01
H4SiO4	.0	8.34361E-04	-3.0786	5.01107E+01
Cl-	-1.0	7.70333E-05	-4.1133	2.72988E+00
HCO3-	-1.0	1.96585E-03	-2.7064	1.19899E+02
SO4-2	-2.0	2.40104E-05	-4.6196	2.30548E+00
NO3-	-1.0	1.39060E-05	-4.8568	1.94693E-01
HPO4-2	-2.0	2.40104E-06	-5.6196	7.43371E-02
F-	-1.0	9.00389E-06	-5.0456	1.70986E-01
Li+	1.0	6.00260E-07	-6.2217	4.16340E-03
Br-	-1.0	6.00260E-07	-6.2217	4.79424E-02
DOX	.0	6.87297E-03	-2.1629	2.19832E+02

****DESCRIPTION OF SOLUTION ****

	ANALYT.	COMP.	PH	
EPMCAT	1.90	1.88	7.270	
EPMAN	2.12	1.87		
			TEMPERATURE	
EH = .3950	PE =	6.970	12.48 DEG C	
PE CALC S =	.000			
PE CALC DOX=	14.792		IONIC STRENGTH	
PE SATO DOX=	3.574		2.555632E-03	
TOT ALK =	1.737E+00 MEQ			
ELECT =	1.458E-02 MEQ			

ACTIVITY H2O =	.9998
PCO2=	4.859141E-03
LOG PCO2 =	-2.3134
PO2 =	2.546432E-31
PCH4 =	4.084605E-92
CO2 TOT =	1.965850E-03
DENSITY =	1.0000
TDS =	432.6MG/L
CARB ALK =	1.727E+00 MEQ
CHARGE IMBALANCE =	.4%

IN COMPUTING THE DISTRIBUTION OF SPECIES,
PE = 6.970 EQUIVALENT EH = .395VOLTS

DISTRIBUTION OF SPECIES

I	SPECIES		MOLALITY	ACTIVITY	LOG ACT	GAMMA
1	H+	1.	5.6499E-08	5.3703E-08	-7.270	9.5052E-01
2	E-	-1.	1.0727E-07	1.0727E-07	-6.970	1.0000E+00
4	Ca+2	2.	3.9511E-04	3.1887E-04	-3.496	8.0704E-01
5	Mg+2	2.	2.5903E-04	2.0943E-04	-3.679	8.0852E-01
6	Na+	1.	4.6286E-04	4.3842E-04	-3.358	9.4721E-01
7	K+	1.	9.8032E-05	9.2784E-05	-4.033	9.4647E-01
8	Fe+2	2.	5.5668E-10	4.5028E-10	-9.347	8.0887E-01
10	Al+3	3.	2.0008E-11	1.2673E-11	-10.897	6.3338E-01
11	Ba+2	2.	2.9524E-07	2.3804E-07	-6.623	8.0625E-01
12	Sr+2	2.	1.1809E-06	9.5361E-07	-6.021	8.0752E-01
13	H4SiO4	0.	8.3286E-04	8.3335E-04	-3.079	1.0006E+00
14	Cl-	-1.	7.7033E-05	7.2910E-05	-4.137	9.4647E-01
15	CO3-2	-2.	1.3066E-06	1.0548E-06	-5.977	8.0731E-01
16	SO4-2	-2.	2.2314E-05	1.7986E-05	-4.745	8.0606E-01
17	NO3-	-1.	4.2909E-07	4.0591E-07	-6.392	9.4598E-01
19	PO4-3	-3.	1.0126E-11	6.1909E-12	-11.208	6.1137E-01
20	F-	-1.	8.8804E-06	8.4043E-06	-5.075	9.4639E-01
21	Li+	1.	6.0021E-07	5.6921E-07	-6.245	9.4835E-01
22	Br-	-1.	6.0026E-07	5.6783E-07	-6.246	9.4598E-01
28	DOX	0.	6.8730E-03	6.8770E-03	-2.163	1.0006E+00
31	OH-	-1.	7.1522E-08	6.7687E-08	-7.169	9.4639E-01
32	O2 AQ	0.	3.5227E-34	3.5248E-34	-33.453	1.0006E+00
33	H2 AQ	0.	2.6743E-32	2.6759E-32	-31.573	1.0006E+00
34	HCO3-	-1.	1.7138E-03	1.6245E-03	-2.789	9.4789E-01
35	H2CO3	0.	2.4032E-04	2.4046E-04	-3.619	1.0006E+00
40	HSO4-	-1.	7.6594E-11	7.2524E-11	-10.140	9.4687E-01
48	NO2-	-1.	1.3477E-05	1.2749E-05	-4.895	9.4598E-01
65	HPO4-2	-2.	1.1917E-06	9.5758E-07	-6.019	8.0357E-01
66	H2PO4-	-1.	9.4090E-07	8.9121E-07	-6.050	9.4719E-01
69	HF AQ	0.	5.4327E-10	5.4359E-10	-9.265	1.0006E+00
70	HF2-	-1.	1.6464E-14	1.5589E-14	-13.807	9.4687E-01
75	CaOH+	1.	1.0405E-09	9.8520E-10	-9.006	9.4687E-01
76	CaCO3	0.	4.6826E-07	4.6854E-07	-6.329	1.0006E+00
77	CaHCO3+	1.	5.4263E-06	5.1435E-06	-5.289	9.4789E-01
78	CaSO4	0.	1.0122E-06	1.0128E-06	-5.994	1.0006E+00
79	CaHSO4	1.	3.8042E-13	3.6021E-13	-12.443	9.4687E-01
80	CaPO4-	-1.	4.7695E-09	4.5161E-09	-8.345	9.4687E-01
81	CaHPO4	0.	1.3107E-07	1.3115E-07	-6.882	1.0006E+00

82	CaH2PO4+	1.	5.9712E-09	5.6539E-09	-8.248	9.4687E-01
83	CaF+	1.	1.8174E-08	1.7208E-08	-7.764	9.4687E-01
85	MgOH+	1.	1.4951E-08	1.4156E-08	-7.849	9.4687E-01
86	MgCO3	0.	1.7383E-07	1.7393E-07	-6.760	1.0006E+00
87	MgHCO3+	1.	4.0449E-06	3.8300E-06	-5.417	9.4687E-01
88	MgSO4	0.	6.3028E-07	6.3065E-07	-6.200	1.0006E+00
89	MgPO4-	-1.	4.2257E-09	4.0012E-09	-8.398	9.4687E-01
90	MgHPO4	0.	1.1639E-07	1.1646E-07	-6.934	1.0006E+00
91	MgH2PO4+	1.	4.9945E-09	4.7291E-09	-8.325	9.4687E-01
92	MgF+	1.	9.6925E-08	9.1775E-08	-7.037	9.4687E-01
93	NaOH	0.	5.3896E-11	5.3928E-11	-10.268	1.0006E+00
94	NaCO3-	-1.	4.7044E-09	4.4545E-09	-8.351	9.4687E-01
95	NaHCO3	0.	2.9773E-07	2.9790E-07	-6.526	1.0006E+00
96	NaSO4-	-1.	3.8420E-08	3.6379E-08	-7.439	9.4687E-01
97	NaHPO4-	-1.	8.6453E-10	8.1859E-10	-9.087	9.4687E-01
98	NaF aq	0.	2.1191E-09	2.1203E-09	-8.674	1.0006E+00
99	KOH	0.	5.9860E-12	5.9895E-12	-11.223	1.0006E+00
100	KSO4-	-1.	1.0564E-08	1.0003E-08	-8.000	9.4687E-01
101	KHPO4-	-1.	1.8296E-10	1.7324E-10	-9.761	9.4687E-01
102	FeOH+	1.	1.0544E-12	9.9836E-13	-12.001	9.4687E-01
105	FeCl+	1.	4.7861E-14	4.5318E-14	-13.344	9.4687E-01
106	FeCO3	0.	1.1387E-11	1.1394E-11	-10.943	1.0006E+00
107	FeHCO3+	1.	5.7461E-11	5.4408E-11	-10.264	9.4687E-01
108	FeSO4	0.	1.1334E-12	1.1341E-12	-11.945	1.0006E+00
109	FeHSO4+	1.	5.3720E-19	5.0866E-19	-18.294	9.4687E-01
112	FeHPO4	0.	1.7155E-12	1.7166E-12	-11.765	1.0006E+00
113	FeH2PO4+	1.	2.1241E-13	2.0112E-13	-12.697	9.4687E-01
114	FeF+	1.	3.9967E-14	3.7843E-14	-13.422	9.4687E-01
115	Fe+3	3.	3.0926E-16	1.9588E-16	-15.708	6.3338E-01
117	FeOH+2	2.	1.3571E-11	1.0908E-11	-10.962	8.0381E-01
118	FeOH2+	1.	4.3263E-08	4.0964E-08	-7.388	9.4687E-01
119	FeOH3	0.	5.5548E-08	5.5580E-08	-7.255	1.0006E+00
120	FeOH4-	-1.	5.8942E-10	5.5811E-10	-9.253	9.4687E-01
121	Fe2OH2+4	4.	1.3166E-20	5.4962E-21	-20.260	4.1747E-01
122	Fe3OH4+5	5.	6.1512E-25	1.5710E-25	-24.804	2.5540E-01
123	FeCl+2	2.	3.5456E-19	2.8500E-19	-18.545	8.0381E-01
124	FeCl2+	1.	1.4835E-22	1.4046E-22	-21.852	9.4687E-01
125	FeCl3	0.	1.0235E-27	1.0241E-27	-26.990	1.0006E+00
126	FeSO4+	1.	3.0550E-17	2.8927E-17	-16.539	9.4687E-01
127	FeHSO4+2	2.	1.4151E-23	1.1375E-23	-22.944	8.0381E-01
128	FeSO42-	-1.	1.1423E-20	1.0816E-20	-19.966	9.4687E-01
129	FeHPO4+	1.	3.4818E-17	3.2968E-17	-16.482	9.4687E-01
130	FeH2P+2	2.	5.7087E-17	4.5887E-17	-16.338	8.0381E-01
131	FeF+2	2.	2.6582E-15	2.1367E-15	-14.670	8.0381E-01
132	FeF2+	1.	6.4637E-16	6.1203E-16	-15.213	9.4687E-01
133	FeF3	0.	7.7937E-18	7.7983E-18	-17.108	1.0006E+00
150	AlOH+2	2.	1.2627E-09	1.0150E-09	-8.994	8.0381E-01
151	AlOH2+	1.	4.8112E-08	4.5556E-08	-7.341	9.4687E-01
152	AlOH3	0.	4.5753E-08	4.5780E-08	-7.339	1.0006E+00
153	AlOH4-	-1.	1.4998E-06	1.4201E-06	-5.848	9.4687E-01
154	AlSO4+	1.	2.1500E-13	2.0358E-13	-12.691	9.4687E-01
155	AlSO42-	-1.	2.9188E-16	2.7637E-16	-15.559	9.4687E-01
156	AlHSO4+2	2.	4.2722E-21	3.4340E-21	-20.464	8.0381E-01
157	AlF+2	2.	1.2250E-09	9.8471E-10	-9.007	8.0381E-01
158	AlF2+	1.	4.0923E-09	3.8748E-09	-8.412	9.4687E-01
159	AlF3	0.	4.0431E-10	4.0455E-10	-9.393	1.0006E+00
160	AlF4-	-1.	1.4253E-12	1.3496E-12	-11.870	9.4687E-01
161	AlF5-2	-2.	2.2967E-16	1.8461E-16	-15.734	8.0381E-01
162	AlF6-3	-3.	3.2881E-21	2.0116E-21	-20.696	6.1179E-01
164	H3SiO4-	-1.	1.5053E-06	1.4253E-06	-5.846	9.4687E-01

165 H2SiO4-2	-2.	9.3282E-13	7.4981E-13	-12.125	8.0381E-01
166 SiF6-2	-2.	1.5327E-32	1.2320E-32	-31.909	8.0381E-01
170 BaOH+	1.	1.5859E-13	1.5017E-13	-12.823	9.4687E-01
171 BaCO3	0.	1.0082E-10	1.0088E-10	-9.996	1.0006E+00
172 BaHCO3	1.	2.6397E-09	2.4995E-09	-8.602	9.4687E-01
173 BaSO4	0.	2.1446E-09	2.1458E-09	-8.668	1.0006E+00
176 SrOH+	1.	9.6089E-13	9.1052E-13	-12.041	9.4758E-01
177 SrHCO3+	1.	1.6285E-08	1.5437E-08	-7.811	9.4789E-01
178 SrCO3	0.	4.4339E-10	4.4365E-10	-9.353	1.0006E+00
179 SrSO4	0.	2.8657E-09	2.8674E-09	-8.543	1.0006E+00
180 LiOH	0.	2.4263E-13	2.4277E-13	-12.615	1.0006E+00
181 LiSO4-	-1.	4.7198E-11	4.4691E-11	-10.350	9.4687E-01

PHASE	IAP	KT	LOG IAP	LOG KT	IAP/KT	LOG IAP/KT
1 Calcite	3.363E-10	3.803E-09	-9.473	-8.420	8.843E-02	-1.053
2 Aragonit	3.363E-10	5.412E-09	-9.473	-8.267	6.215E-02	-1.207
3 Dolomite	7.430E-20	1.634E-17	-19.129	-16.787	4.548E-03	-2.342
4 Siderite	4.750E-16	1.548E-11	-15.323	-10.810	.069E-05	-4.513
6 Strontit	1.006E-12	5.241E-10	-11.997	-9.281	1.919E-03	-2.717
7 Witherit	2.511E-13	2.434E-09	-12.600	-8.614	1.032E-04	-3.987
8 Gypsum	5.733E-09	2.585E-05	-8.242	-4.588	2.218E-04	-3.654
9 Anhydrit	5.735E-09	4.631E-05	-8.241	-4.334	1.238E-04	-3.907
10 Celestit	1.715E-11	2.373E-07	-10.766	-6.625	7.228E-05	-4.141
11 Barite	4.282E-12	6.395E-11	-11.368	-10.194	6.695E-02	-1.174
12 Hydroxap	3.479E-07	5.504E-03	-6.459	-2.259	6.321E-05	-4.199
13 Fluorite	2.252E-14	1.735E-11	-13.647	-10.761	1.298E-03	-2.887
14 SiO2 (a)	8.337E-04	1.516E-03	-3.079	-2.819	5.498E-01	-.260
15 Chalcedy	8.337E-04	1.981E-04	-3.079	-3.703	4.208E+00	.624
16 Quartz	8.337E-04	6.717E-05	-3.079	-4.173	1.241E+01	1.094
17 Gibbs(c)	8.177E+10	6.959E+08	10.913	8.843	1.175E+02	2.070
18 Al(OH)3a	8.177E+10	4.482E+11	10.913	11.651	1.825E-01	-.739
19 Kaolinit	4.648E+15	3.708E+08	15.667	8.569	1.253E+07	7.098
20 Albite	3.609E-19	1.465E-19	-18.443	-18.834	2.463E+00	.391
21 Anorth	4.473E-22	8.202E-21	-21.349	-20.086	5.453E-02	-1.263
22 Kspar	7.637E-20	2.734E-22	-19.117	-21.563	2.794E+02	2.446
23 Kmica	5.477E+26	4.081E+14	26.739	14.611	1.342E+12	12.128
24 Chlorite	7.832E+66	1.768E+73	66.894	73.248	4.430E-07	-6.354
25 Ca-Mont	9.087E-41	1.252E-47	-40.042	-46.903	7.260E+06	6.861
26 Talc	1.848E+20	7.732E+22	20.267	22.888	2.390E-03	-2.622
27 Illite	5.139E-37	9.462E-43	-36.289	-42.024	5.431E+05	5.735
28 Chrysotl	2.659E+26	6.583E+33	26.425	33.818	4.039E-08	-7.394
29 Sepiol c	3.052E+12	1.270E+16	12.485	16.104	2.403E-03	.619
30 Sepiol d	3.052E+12	4.571E+18	12.485	18.660	6.677E-07	-6.175
31 Hematite	1.599E+12	9.617E-04	12.204	-3.017	1.662E+15	15.221
32 Goethite	1.264E+06	1.000E-01	6.102	-1.000	1.264E+07	7.102
33 Fe(OH)3a	1.264E+06	7.780E+04	6.102	4.891	1.625E+01	1.21
37 Vivianit	3.494E-51	1.000E-36	-50.457	-36.000	3.494E-15	-14.457
42 PCO2	2.405E-04	4.949E-02	-3.619	-1.306	4.859E-03	-2.313
43 O2 gas	3.525E-34	1.257E-03	-33.453	-2.901	2.805E-31	-30.552
44 H2 gas	2.676E-32	8.063E-04	-31.573	-3.093	3.319E-29	-28.479
49 Melanter	8.088E-15	4.228E-03	-14.092	-2.374	1.913E-12	-11.718
50 Alunite	2.544E-03	1.639E+00	-2.595	.215	1.552E-03	-2.809
51 K-Jarosi	9.394E-18	6.238E-09	-17.027	-8.205	1.506E-09	-8.822

1Elkins

INITIAL SOLUTION

TEMPERATURE = 18.02 DEGREES C PH = 7.810
ANALYTICAL EPMCAT = 1.611 ANALYTICAL EPMAN = 1.667

***** OXIDATION - REDUCTION *****

DISSOLVED OXYGEN = 5.912 MMOLES/KG H2O
EH MEASURED WITH CALOMEL = 9.9000 VOLTS
MEASURED EH OF ZOBELL SOLUTION = 9.9000 VOLTS
CORRECTED EH = .2290 VOLTS
PE COMPUTED FROM CORRECTED EH = 3.964

FLAG	CORALK	PECALC	IDAVES
0	2	1	0

*** TOTAL CONCENTRATIONS OF INPUT SPECIES ***

SPECIES		TOTAL MOLALITY	LOG TOTAL MOLALITY	TOTAL MG/LITRE
Ca+2	2.0	3.41126E-04	-3.4671	1.36673E+01
Mg+2	2.0	2.14079E-04	-3.6694	5.20277E+00
Na+	1.0	3.95146E-04	-3.4032	9.08097E+00
K+	1.0	9.10336E-05	-4.0408	3.55828E+00
Fe+2	2.0	4.30159E-06	-5.3664	2.40142E-01
Al+3	3.0	1.00037E-06	-5.9998	2.69815E-02
Ba+2	2.0	1.00037E-07	-6.9998	1.37340E-02
Sr+2	2.0	9.00332E-07	-6.0456	7.88580E-02
H4SiO4	.0	8.36308E-04	-3.0776	5.02309E+01
Cl-	-1.0	8.30306E-05	-4.0808	2.94260E+00
HCO3-	-1.0	1.50756E-03	-2.8217	9.19531E+01
SO4-2	-2.0	2.10077E-05	-4.6776	2.01729E+00
NO3-	-1.0	1.95072E-05	-4.7098	2.73131E-01
HPO4-2	-2.0	1.80066E-06	-5.7446	5.57528E-02
F-	-1.0	1.00037E-05	-4.9998	1.89984E-01
Li+	1.0	6.00221E-07	-6.2217	4.16340E-03
Br-	-1.0	4.00148E-07	-6.3978	3.19616E-02
DOX	.0	5.91218E-03	-2.2283	1.89113E+02

Elkins

****DESCRIPTION OF SOLUTION ****

	ANALYT.	COMP.	PH
EPMCAT	1.61	1.58	7.810
EPMAN	1.67	1.61	

EH = .2290 PE = 3.964 TEMPERATURE 18.02 DEG C

ACTIVITY H2O = .9998
PCO2= 1.270341E-03
LOG PCO2 = -2.8961
PO2 = 3.536335E-39
PCH4 = 7.724903E-74

PE CALC S = .000
PE CALC DOX= 13.745
PE SATO DOX= 3.018
TOT ALK = 1.477E+00 MEQ
ELECT = -2.713E-02 MEQ

IONIC STRENGTH
2.169465E-03

CO2 TOT = 1.507556E-03
DENSITY = 1.0000
TDS = 368.7MG/L
CARB ALK = 1.461E+00 MEQ
CHARGE IMBALANCE = -.8%

IN COMPUTING THE DISTRIBUTION OF SPECIES,
PE = 3.964 EQUIVALENT EH = .229VOLTS

DISTRIBUTION OF SPECIES

I	SPECIES		MOLALITY	ACTIVITY	LOG ACT	GAMMA
1	H+	1.	1.6244E-08	1.5488E-08	-7.810	9.5349E-01
2	E-	-1.	1.0872E-04	1.0872E-04	-3.964	1.0000E+00
4	Ca+2	2.	3.3424E-04	2.7352E-04	-3.563	8.1833E-01
5	Mg+2	2.	2.0992E-04	1.7205E-04	-3.764	8.1963E-01
6	Na+	1.	3.9485E-04	3.7533E-04	-3.426	9.5058E-01
7	K+	1.	9.1024E-05	8.6468E-05	-4.063	9.4995E-01
8	Fe+2	2.	2.4857E-07	2.0382E-07	-6.691	8.1996E-01
10	Al+3	3.	2.1396E-14	1.3937E-14	-13.856	6.5139E-01
11	Ba+2	2.	9.8370E-08	8.0432E-08	-7.095	8.1765E-01
12	Sr+2	2.	8.8435E-07	7.2406E-07	-6.140	8.1875E-01
13	H4SiO4	0.	8.2986E-04	8.3027E-04	-3.081	1.0005E+00
14	Cl-	-1.	8.3031E-05	7.8875E-05	-4.103	9.4995E-01
15	CO3-2	-2.	4.3460E-06	3.5576E-06	-5.449	8.1858E-01
16	SO4-2	-2.	1.9609E-05	1.6030E-05	-4.795	8.1749E-01
17	NO3-	-1.	3.1517E-11	2.9926E-11	-10.524	9.4952E-01
19	PO4-3	-3.	4.0384E-11	2.5507E-11	-10.593	6.3162E-01
20	F-	-1.	9.8829E-06	9.3875E-06	-5.027	9.4988E-01
21	Li+	1.	6.0018E-07	5.7112E-07	-6.243	9.5159E-01
22	Br-	-1.	4.0015E-07	3.7995E-07	-6.420	9.4952E-01
28	DOX	0.	5.9122E-03	5.9151E-03	-2.228	1.0005E+00
31	OH-	-1.	3.9335E-07	3.7364E-07	-6.428	9.4988E-01
33	H2 AQ	0.	2.1544E-27	2.1555E-27	-26.666	1.0005E+00
34	HCO3-	-1.	1.4409E-03	1.3705E-03	-2.863	9.5119E-01
35	H2CO3	0.	5.2768E-05	5.2795E-05	-4.277	1.0005E+00
40	HSO4-	-1.	2.1911E-11	2.0821E-11	-10.681	9.5028E-01
48	NO2-	-1.	1.9507E-05	1.8522E-05	-4.732	9.4952E-01
65	HPO4-2	-2.	1.2399E-06	1.0109E-06	-5.995	8.1529E-01
66	H2PO4-	-1.	2.7612E-07	2.6247E-07	-6.581	9.5058E-01
69	HF AQ	0.	1.9257E-10	1.9266E-10	-9.715	1.0005E+00
70	HF2-	-1.	6.8754E-15	6.5335E-15	-14.185	9.5028E-01
75	CaOH+	1.	3.0837E-09	2.9303E-09	-8.533	9.5028E-01
76	CaCO3	0.	1.4470E-06	1.4477E-06	-5.839	1.0005E+00
77	CaHCO3+	1.	4.4428E-06	4.2260E-06	-5.374	9.5119E-01
78	CaSO4	0.	8.1794E-07	8.1835E-07	-6.087	1.0005E+00
79	CaHSO4	1.	8.3576E-14	7.9420E-14	-13.100	9.5028E-01
80	CaPO4-	-1.	1.8635E-08	1.7708E-08	-7.752	9.5028E-01
81	CaHPO4	0.	1.3258E-07	1.3265E-07	-6.877	1.0005E+00
82	CaH2PO4+	1.	1.6845E-09	1.6008E-09	-8.796	9.5028E-01
83	CaF+	1.	1.9920E-08	1.8930E-08	-7.723	9.5028E-01
85	MgOH+	1.	4.2437E-08	4.0327E-08	-7.394	9.5028E-01

86	MgCO3	0.	5.2445E-07	5.2471E-07	-6.280	1.0005E+00
87	MgHCO3+	1.	2.8293E-06	2.6886E-06	-5.570	9.5028E-01
88	MgSO4	0.	5.3758E-07	5.3784E-07	-6.269	1.0005E+00
89	MgPO4-	-1.	1.5813E-08	1.5026E-08	-7.823	9.5028E-01
90	MgHPO4	0.	1.1276E-07	1.1282E-07	-6.948	1.0005E+00
91	MgH2PO4+	1.	1.3495E-09	1.2824E-09	-8.892	9.5028E-01
92	MgF+	1.	9.8659E-08	9.3753E-08	-7.028	9.5028E-01
93	NaOH	0.	1.6000E-10	1.6008E-10	-9.796	1.0005E+00
94	NaCO3-	-1.	1.8245E-08	1.7338E-08	-7.761	9.5028E-01
95	NaHCO3	0.	2.4794E-07	2.4807E-07	-6.605	1.0005E+00
96	NaSO4-	-1.	3.0327E-08	2.8819E-08	-7.540	9.5028E-01
97	NaHPO4-	-1.	7.7850E-10	7.3979E-10	-9.131	9.5028E-01
98	NaF aq	0.	2.0265E-09	2.0275E-09	-8.693	1.0005E+00
99	KOH	0.	1.9345E-11	1.9355E-11	-10.713	1.0005E+00
100	KSO4-	-1.	9.4278E-09	8.9590E-09	-8.048	9.5028E-01
101	KHPO4-	-1.	1.7935E-10	1.7043E-10	-9.768	9.5028E-01
102	FeOH+	1.	2.5667E-09	2.4390E-09	-8.613	9.5028E-01
105	FeCl+	1.	2.3352E-11	2.2191E-11	-10.654	9.5028E-01
106	FeCO3	0.	1.7385E-08	1.7394E-08	-7.760	1.0005E+00
107	FeHCO3+	1.	2.5208E-08	2.3955E-08	-7.621	9.5028E-01
108	FeSO4	0.	5.0957E-10	5.0983E-10	-9.293	1.0005E+00
109	FeHSO4+	1.	6.2277E-17	5.9181E-17	-16.228	9.5028E-01
112	FeHPO4	0.	8.1981E-10	8.2022E-10	-9.086	1.0005E+00
113	FeH2PO4+	1.	2.8215E-11	2.6812E-11	-10.572	9.5028E-01
114	FeF+	1.	2.0134E-11	1.9133E-11	-10.718	9.5028E-01
115	Fe+3	3.	1.8577E-16	1.2101E-16	-15.917	6.5139E-01
117	FeOH+2	2.	4.0607E-11	3.3114E-11	-10.480	8.1546E-01
118	FeOH2+	1.	5.6801E-07	5.3977E-07	-6.268	9.5028E-01
119	FeOH3	0.	3.2856E-06	3.2872E-06	-5.483	1.0005E+00
120	FeOH4-	-1.	1.5281E-07	1.4521E-07	-6.838	9.5028E-01
121	Fe2OH2+4	4.	8.9676E-20	3.9654E-20	-19.402	4.4219E-01
122	Fe3OH4+5	5.	3.0949E-23	8.6480E-24	-23.063	2.7943E-01
123	FeCl+2	2.	2.8181E-19	2.2980E-19	-18.639	8.1546E-01
124	FeCl2+	1.	1.0687E-22	1.0155E-22	-21.993	9.5028E-01
125	FeCl3	0.	8.0061E-28	8.0101E-28	-27.096	1.0005E+00
126	FeSO4+	1.	1.9108E-17	1.8158E-17	-16.741	9.5028E-01
127	FeHSO4+2	2.	1.6013E-24	1.3058E-24	-23.884	8.1546E-01
128	FeSO42-	-1.	6.5167E-21	6.1927E-21	-20.208	9.5028E-01
129	FeHPO4+	1.	2.7444E-17	2.6080E-17	-16.584	9.5028E-01
130	FeH2P+2	2.	1.0349E-17	8.4389E-18	-17.074	8.1546E-01
131	FeF+2	2.	1.9794E-15	1.6141E-15	-14.792	8.1546E-01
132	FeF2+	1.	5.8308E-16	5.5409E-16	-15.256	9.5028E-01
133	FeF3	0.	8.0421E-18	8.0461E-18	-17.094	1.0005E+00
150	AlOH+2	2.	6.9121E-12	5.6366E-12	-11.249	8.1546E-01
151	AlOH2+	1.	1.5898E-09	1.5108E-09	-8.821	9.5028E-01
152	AlOH3	0.	8.3817E-09	8.3859E-09	-8.076	1.0005E+00
153	AlOH4-	-1.	9.9038E-07	9.4114E-07	-6.026	9.5028E-01
154	AlSO4+	1.	2.2567E-16	2.1445E-16	-15.669	9.5028E-01
155	AlSO42-	-1.	2.7944E-19	2.6555E-19	-18.576	9.5028E-01
156	AlHSO4+2	2.	1.1904E-24	9.7075E-25	-24.013	8.1546E-01
157	AlF+2	2.	1.5370E-12	1.2534E-12	-11.902	8.1546E-01
158	AlF2+	1.	5.9789E-12	5.6816E-12	-11.246	9.5028E-01
159	AlF3	0.	6.6626E-13	6.6659E-13	-12.176	1.0005E+00
160	AlF4-	-1.	2.6173E-15	2.4872E-15	-14.604	9.5028E-01
161	AlF5-2	-2.	4.6045E-19	3.7548E-19	-18.425	8.1546E-01
162	AlF6-3	-3.	6.4291E-24	4.0627E-24	-23.391	6.3191E-01
164	H3SiO4-	-1.	6.4510E-06	6.1302E-06	-5.213	9.5028E-01
165	H2SiO4-2	-2.	2.0556E-11	1.6763E-11	-10.776	8.1546E-01
166	SiF6-2	-2.	1.1725E-34	9.5614E-35	-34.019	8.1546E-01
170	BaOH+	1.	1.8514E-13	1.7594E-13	-12.755	9.5028E-01

171	BaCO3	0.	1.2843E-10	1.2849E-10	-9.891	1.0005E+00
172	BaHCO3+	1.	8.9264E-10	8.4825E-10	-9.071	9.5028E-01
173	BaSO4	0.	6.4589E-10	6.4621E-10	-9.190	1.0005E+00
176	SrOH+	1.	2.5209E-12	2.3972E-12	-11.620	9.5092E-01
177	SrHCO3+	1.	1.2567E-08	1.1953E-08	-7.923	9.5119E-01
178	SrCO3	0.	1.3374E-09	1.3381E-09	-8.874	1.0005E+00
179	SrSO4	0.	2.0795E-09	2.0805E-09	-8.682	1.0005E+00
180	LiOH	0.	8.4419E-13	8.4461E-13	-12.073	1.0005E+00
181	LiSO4-	-1.	4.2055E-11	3.9964E-11	-10.398	9.5028E-01

	PHASE	IAP	KT	LOG IAP	LOG KT	IAP/KT	LOG IAP/KT
1	Calcite	9.731E-10	3.600E-09	-9.012	-8.444	2.703E-01	-.568
2	Aragonit	9.731E-10	5.072E-09	-9.012	-8.295	1.918E-01	-.717
3	Dolomite	5.956E-19	1.191E-17	-18.225	-16.924	5.002E-02	-1.301
4	Siderite	7.251E-13	1.424E-11	-12.140	-10.846	5.091E-02	-1.293
6	Strontit	2.576E-12	5.365E-10	-11.589	-9.270	4.801E-03	-2.319
7	Witherit	2.861E-13	2.613E-09	-12.543	-8.583	1.095E-04	-3.961
8	Gypsum	4.383E-09	2.618E-05	-8.358	-4.582	1.674E-04	-3.776
9	Anhydrit	4.385E-09	4.577E-05	-8.358	-4.339	9.580E-05	-4.019
10	Celestit	1.161E-11	2.394E-07	-10.935	-6.621	4.849E-05	-4.314
11	Barite	1.289E-12	8.167E-11	-11.890	-10.088	1.579E-02	-1.802
12	Hydroxap	2.748E-05	1.638E-03	-4.561	-2.786	1.677E-02	-1.775
13	Fluorite	2.410E-14	2.064E-11	-13.618	-10.685	1.168E-03	-2.933
14	SiO2 (a)	8.305E-04	1.696E-03	-3.081	-2.771	4.897E-01	-.310
15	Chalcedy	8.305E-04	2.321E-04	-3.081	-3.634	3.578E+00	.554
16	Quartz	8.305E-04	8.210E-05	-3.081	-4.086	1.012E+01	1.005
17	Gibbs(c)	3.749E+09	3.241E+08	9.574	8.511	1.157E+01	1.063
18	Al(OH)3a	3.749E+09	1.844E+11	9.574	11.266	2.034E-02	-1.692
19	Kaolinit	9.698E+12	1.136E+08	12.987	8.055	8.539E+04	4.931
20	Albite	2.024E-19	3.491E-19	-18.694	-18.457	5.799E-01	-.237
21	Anorth	1.672E-22	1.209E-20	-21.777	-19.917	1.383E-02	-1.859
22	Kspar	4.664E-20	7.681E-22	-19.331	-21.115	6.071E+01	1.783
23	Kmica	1.687E+23	5.576E+13	23.227	13.746	3.025E+09	9.481
24	Chlorite	1.530E+69	1.102E+71	69.185	71.042	1.389E-02	-1.857
25	Ca-Mont	2.787E-42	8.857E-47	-41.555	-46.053	3.146E+04	4.498
26	Talc	1.755E+23	1.635E+22	23.244	22.213	1.073E+01	1.031
27	Illite	4.041E-38	5.917E-42	-37.394	-41.228	6.829E+03	3.834
28	Chrysotl	2.543E+29	1.220E+33	29.405	33.086	2.085E-04	-3.681
29	Sepiol c	2.945E+14	8.872E+15	14.469	15.948	3.319E-02	-1.479
30	Sepiol d	2.945E+14	4.571E+18	14.469	18.660	6.442E-05	-4.191
31	Hematite	1.060E+15	3.420E-04	15.025	-3.466	3.101E+18	18.491
32	Goethite	3.256E+07	1.000E-01	7.513	-1.000	3.256E+08	8.513
33	Fe(OH)3a	3.255E+07	7.780E+04	7.513	4.891	4.184E+02	2.622
37	Vivianit	5.502E-42	1.000E-36	-41.260	-36.000	5.502E-06	-5.260
42	PCO2	5.279E-05	4.156E-02	-4.277	-1.381	1.270E-03	-2.896
44	H2 gas	2.155E-27	7.602E-04	-26.666	-3.119	2.836E-24	-23.547
49	Melanter	3.264E-12	5.040E-03	-11.486	-2.298	6.476E-10	-9.189
50	Alunite	4.353E-09	3.041E-01	-8.361	-.517	1.432E-08	-7.844
51	K-Jarosi	2.850E-15	2.186E-09	-14.545	-8.660	1.304E-06	-5.885

1Bibo

INITIAL SOLUTION

TEMPERATURE = 19.74 DEGREES C PH = 8.050
ANALYTICAL EPMCAT = 9.512 ANALYTICAL EPMAN = 9.865
***** OXIDATION - REDUCTION *****
DISSOLVED OXYGEN = .620 MMOLES/KG H2O
EH MEASURED WITH CALOMEL = 9.9000 VOLTS
MEASURED EH OF ZOBELL SOLUTION = 9.9000 VOLTS
CORRECTED EH = .2730 VOLTS
PE COMPUTED FROM CORRECTED EH = 4.698

FLAG	CORALK	PECALC	IDAVES
0	2	1	0

*** TOTAL CONCENTRATIONS OF INPUT SPECIES ***

SPECIES		TOTAL MOLALITY	LOG TOTAL MOLALITY	TOTAL MG/LITRE
Ca+2	2.0	3.19254E-04	-3.4959	1.27855E+01
Mg+2	2.0	1.95155E-04	-3.7096	4.74084E+00
Na+	1.0	8.37866E-03	-2.0768	1.92471E+02
K+	1.0	7.00557E-05	-4.1546	2.73714E+00
Fe+2	2.0	8.00637E-07	-6.0966	4.46776E-02
Mn+2	2.0	1.00080E-07	-6.9997	5.49380E-03
Al+3	3.0	1.30103E-06	-5.8857	3.50760E-02
Ba+2	2.0	6.00477E-07	-6.2215	8.24040E-02
Sr+2	2.0	6.60525E-06	-5.1801	5.78292E-01
H4Si04	.0	3.01240E-04	-3.5211	1.80855E+01
Cl-	-1.0	4.23337E-04	-3.3733	1.49966E+01
HCO3-	-1.0	5.97475E-03	-2.2237	3.64273E+02
SO4-2	-2.0	1.70035E-03	-2.7695	1.63209E+02
NO3-	-1.0	3.50279E-06	-5.4556	4.90235E-02
H3BO3	.0	8.90708E-06	-5.0503	9.62090E-02
F-	-1.0	5.40430E-05	-4.2673	1.02591E+00
Li+	1.0	6.30501E-06	-5.2003	4.37157E-02
DOX	.0	6.20493E-04	-3.2073	1.98393E+01

Bibo

****DESCRIPTION OF SOLUTION ****

	ANALYT.	COMP.
EPMCAT	9.51	9.27
EPMAN	9.87	9.57

PH 8.050
TEMPERATURE 19.74 DEG C
ACTIVITY H2O = .9997
PCO2= 2.839428E-03
LOG PCO2 = -2.5468
PO2 = 1.126677E-34
PCH4 = 1.525096E-81
CO2 TOT = 5.974750E-03

EH = .2730 PE = 4.698
PE CALC S = .000

PE CALC DOX= 13.112 IONIC STRENGTH DENSITY = 1.0000
PE SATO DOX= 2.533 1.150212E-02 TDS = 795.1MG/L
TOT ALK = 5.924E+00 MEQ CARB ALK = 5.912E+00 MEQ
ELECT = -3.023E-01 MEQ CHARGE IMBALANCE = -1.6%

IN COMPUTING THE DISTRIBUTION OF SPECIES,
PE = 4.698 EQUIVALENT EH = .273VOLTS

DISTRIBUTION OF SPECIES

I	SPECIES		MOLALITY	ACTIVITY	LOG ACT	GAMMA
1	H+	1.	9.8008E-09	8.9125E-09	-8.050	9.0937E-01
2	E-	-1.	2.0067E-05	2.0067E-05	-4.698	1.0000E+00
4	Ca+2	2.	2.6635E-04	1.7481E-04	-3.757	6.5632E-01
5	Mg+2	2.	1.6248E-04	1.0741E-04	-3.969	6.6105E-01
6	Na+	1.	8.3140E-03	7.4654E-03	-2.127	8.9793E-01
7	K+	1.	6.9576E-05	6.2268E-05	-4.206	8.9497E-01
8	Fe+2	2.	1.5620E-09	1.0334E-09	-8.986	6.6158E-01
9	Mn+2	2.	3.7086E-08	2.4535E-08	-7.610	6.6158E-01
10	Al+3	3.	2.8820E-15	1.2256E-15	-14.912	4.2526E-01
11	Ba+2	2.	4.3538E-07	2.8450E-07	-6.546	6.5345E-01
12	Sr+2	2.	5.5850E-06	3.6733E-06	-5.435	6.5771E-01
13	H4SiO4	0.	2.9670E-04	2.9749E-04	-3.527	1.0027E+00
14	Cl-	-1.	4.2334E-04	3.7887E-04	-3.422	8.9497E-01
15	CO3-2	-2.	3.7185E-05	2.4421E-05	-4.612	6.5675E-01
16	SO4-2	-2.	1.5995E-03	1.0441E-03	-2.981	6.5276E-01
17	NO3-	-1.	7.8190E-10	6.9826E-10	-9.156	8.9303E-01
18	H3BO3	0.	8.3596E-06	8.3818E-06	-5.077	1.0027E+00
20	F-	-1.	5.3423E-05	4.7792E-05	-4.321	8.9461E-01
21	Li+	1.	6.2762E-06	5.6604E-06	-5.247	9.0187E-01
28	DOX	0.	6.2049E-04	6.2214E-04	-3.206	1.0027E+00
31	OH-	-1.	8.3375E-07	7.4588E-07	-6.127	8.9461E-01
32	O2 AQ	0.	1.3622E-37	1.3658E-37	-36.865	1.0027E+00
33	H2 AQ	0.	2.3822E-29	2.3885E-29	-28.622	1.0027E+00
34	HCO3-	-1.	5.7753E-03	5.1991E-03	-2.284	9.0022E-01
35	H2CO3	0.	1.1182E-04	1.1212E-04	-3.950	1.0027E+00
40	HSO4-	-1.	9.0171E-10	8.0864E-10	-9.092	8.9679E-01
48	NO2-	-1.	3.5020E-06	3.1274E-06	-5.505	8.9303E-01
57	H2BO3-	-1.	5.4727E-07	4.9079E-07	-6.309	8.9679E-01
58	BFOH3-	-1.	1.6813E-10	1.5078E-10	-9.822	8.9679E-01
59	BF2OH2-	-1.	7.7303E-15	6.9325E-15	-14.159	8.9679E-01
60	BF3OH-	-1.	3.9832E-21	3.5721E-21	-20.447	8.9679E-01
61	BF4-	-1.	6.9627E-27	6.2441E-27	-26.205	8.9679E-01
69	HF AQ	0.	5.8016E-10	5.8170E-10	-9.235	1.0027E+00
70	HF2-	-1.	1.1380E-13	1.0205E-13	-12.991	8.9679E-01
75	CaOH+	1.	3.6287E-09	3.2541E-09	-8.488	8.9679E-01
76	CaCO3	0.	6.5030E-06	6.5203E-06	-5.186	1.0027E+00
77	CaHCO3+	1.	1.1774E-05	1.0599E-05	-4.975	9.0022E-01
78	CaSO4	0.	3.4549E-05	3.4641E-05	-4.460	1.0027E+00
79	CaHSO4	1.	2.1214E-12	1.9024E-12	-11.721	8.9679E-01
83	CaF+	1.	7.1615E-08	6.4223E-08	-7.192	8.9679E-01
85	MgOH+	1.	4.8777E-08	4.3743E-08	-7.359	8.9679E-01
86	MgCO3	0.	2.3027E-06	2.3088E-06	-5.637	1.0027E+00
87	MgHCO3+	1.	7.1382E-06	6.4015E-06	-5.194	8.9679E-01

88	MgSO4	0.	2.2842E-05	2.2902E-05	-4.640	1.0027E+00
92	MgF+	1.	3.4323E-07	3.0780E-07	-6.512	8.9679E-01
93	NaOH	0.	5.5179E-09	5.5325E-09	-8.257	1.0027E+00
94	NaCO3-	-1.	2.8896E-06	2.5913E-06	-5.586	8.9679E-01
95	NaHCO3	0.	1.9439E-05	1.9490E-05	-4.710	1.0027E+00
96	NaSO4-	-1.	4.2107E-05	3.7761E-05	-4.423	8.9679E-01
98	NaF aq	0.	2.0477E-07	2.0531E-07	-6.688	1.0027E+00
99	KOH	0.	2.4154E-11	2.4218E-11	-10.616	1.0027E+00
100	KSO4-	-1.	4.7940E-07	4.2992E-07	-6.367	8.9679E-01
102	FeOH+	1.	2.7395E-11	2.4568E-11	-10.610	8.9679E-01
105	FeCl+	1.	6.0265E-13	5.4045E-13	-12.267	8.9679E-01
106	FeCO3	0.	6.0378E-10	6.0538E-10	-9.218	1.0027E+00
107	FeHCO3+	1.	5.3498E-10	4.7976E-10	-9.319	8.9679E-01
108	FeSO4	0.	1.7351E-10	1.7397E-10	-9.760	1.0027E+00
109	FeHSO4+	1.	1.2540E-17	1.1246E-17	-16.949	8.9679E-01
114	FeF+	1.	5.5072E-13	4.9388E-13	-12.306	8.9679E-01
115	Fe+3	3.	8.6237E-18	3.6673E-18	-17.436	4.2526E-01
117	FeOH+2	2.	2.9960E-12	1.9378E-12	-11.713	6.4679E-01
118	FeOH2+	1.	6.5507E-08	5.8746E-08	-7.231	8.9679E-01
119	FeOH3	0.	6.7040E-07	6.7217E-07	-6.173	1.0027E+00
120	FeOH4-	-1.	6.1829E-08	5.5448E-08	-7.256	8.9679E-01
121	Fe2OH2+4	4.	7.2053E-22	1.2610E-22	-21.899	1.7501E-01
122	Fe3OH4+5	5.	3.8635E-26	2.5367E-27	-26.596	6.5657E-02
123	FeCl+2	2.	5.4746E-20	3.5410E-20	-19.451	6.4679E-01
124	FeCl2+	1.	7.9185E-23	7.1012E-23	-22.149	8.9679E-01
125	FeCl3	0.	2.6833E-27	2.6905E-27	-26.570	1.0027E+00
126	FeSO4+	1.	4.1583E-17	3.7292E-17	-16.428	8.9679E-01
127	FeHSO4+2	2.	2.0785E-24	1.3444E-24	-23.871	6.4679E-01
128	FeSO42-	-1.	9.3020E-19	8.3419E-19	-18.079	8.9679E-01
131	FeF+2	2.	3.9573E-16	2.5595E-16	-15.592	6.4679E-01
132	FeF2+	1.	5.0955E-16	4.5696E-16	-15.340	8.9679E-01
133	FeF3	0.	3.3899E-17	3.3989E-17	-16.469	1.0027E+00
134	MnOH+	1.	5.0981E-11	4.5719E-11	-10.340	8.9679E-01
136	MnCl+	1.	4.2227E-11	3.7869E-11	-10.422	8.9679E-01
137	MnCl2	0.	6.2464E-15	6.2629E-15	-14.203	1.0027E+00
138	MnCl3-	-1.	7.2875E-19	6.5354E-19	-18.185	8.9679E-01
139	MnCO3	0.	4.7468E-08	4.7594E-08	-7.322	1.0027E+00
140	MnHCO3+	1.	1.1320E-08	1.0152E-08	-7.993	8.9679E-01
141	MnSO4	0.	4.1022E-09	4.1131E-09	-8.386	1.0027E+00
142	Mn(NO3)2	0.	4.8071E-26	4.8199E-26	-25.317	1.0027E+00
143	MnF+	1.	9.0461E-12	8.1124E-12	-11.091	8.9679E-01
144	Mn+3	3.	4.6073E-29	1.7285E-29	-28.762	3.7516E-01
150	AlOH+2	2.	1.4937E-12	9.6608E-13	-12.015	6.4679E-01
151	AlOH2+	1.	5.8967E-10	5.2881E-10	-9.277	8.9679E-01
152	AlOH3	0.	5.8367E-09	5.8522E-09	-8.233	1.0027E+00
153	AlOH4-	-1.	1.2946E-06	1.1610E-06	-5.935	8.9679E-01
154	AlSO4+	1.	1.3999E-15	1.2554E-15	-14.901	8.9679E-01
155	AlSO42-	-1.	1.1369E-16	1.0196E-16	-15.992	8.9679E-01
156	AlHSO4+2	2.	4.9467E-24	3.1995E-24	-23.495	6.4679E-01
157	AlF+2	2.	8.7696E-13	5.6721E-13	-12.246	6.4679E-01
158	AlF2+	1.	1.4733E-11	1.3213E-11	-10.879	8.9679E-01
159	AlF3	0.	7.8856E-12	7.9065E-12	-11.102	1.0027E+00
160	AlF4-	-1.	1.6754E-13	1.5025E-13	-12.823	8.9679E-01
161	AlF5-2	-2.	1.7789E-16	1.1506E-16	-15.939	6.4679E-01
162	AlF6-3	-3.	1.6303E-20	6.1162E-21	-20.214	3.7516E-01
164	H3SiO4-	-1.	4.5413E-06	4.0726E-06	-5.390	8.9679E-01
165	H2SiO4-2	-2.	3.3750E-11	2.1829E-11	-10.661	6.4679E-01
166	SiF6-2	-2.	8.5789E-32	5.5488E-32	-31.256	6.4679E-01
170	BaOH+	1.	1.2058E-12	1.0813E-12	-11.966	8.9679E-01
171	BaCO3	0.	3.2210E-09	3.2295E-09	-8.491	1.0027E+00

172	BaHCO3+	1.	1.3398E-08	1.2015E-08	-7.920	8.9679E-01
173	BaSO4	0.	1.4848E-07	1.4887E-07	-6.827	1.0027E+00
176	SrOH+	1.	2.3503E-11	2.1131E-11	-10.675	8.9909E-01
177	SrHCO3+	1.	2.7104E-07	2.4399E-07	-6.613	9.0022E-01
178	SrCO3	0.	4.8897E-08	4.9026E-08	-7.310	1.0027E+00
179	SrSO4	0.	7.0027E-07	7.0212E-07	-6.154	1.0027E+00
180	LiOH	0.	1.4506E-11	1.4545E-11	-10.837	1.0027E+00
181	LiSO4-	-1.	2.8767E-08	2.5798E-08	-7.588	8.9679E-01

	PHASE	IAP	KT	LOG IAP	LOG KT	IAP/KT	LOG IAP/KT
1	Calcite	4.269E-09	3.532E-09	-8.370	-8.452	1.209E+00	.082
2	Aragonit	4.269E-09	4.962E-09	-8.370	-8.304	8.604E-01	-.065
3	Dolomite	1.120E-17	1.082E-17	-16.951	-16.966	1.035E+00	.015
4	Siderite	2.524E-14	1.389E-11	-13.598	-10.857	1.817E-03	-2.741
5	Rhodochr	5.992E-13	7.741E-12	-12.222	-11.111	7.740E-02	-1.111
6	Strontit	8.971E-11	5.381E-10	-10.047	-9.269	1.667E-01	-.778
7	Witherit	6.948E-12	2.656E-09	-11.158	-8.576	2.616E-03	-2.582
8	Gypsum	1.824E-07	2.623E-0	-6.739	-4.581	6.954E-03	-2.158
9	Anhydrit	1.825E-07	4.537E-05	-6.739	-4.343	4.022E-03	-2.396
10	Celestit	3.835E-09	2.386E-07	-8.416	-6.622	1.607E-02	-1.794
11	Barite	2.970E-10	8.763E-11	-9.527	-10.057	3.390E+00	.530
13	Fluorite	3.993E-13	2.172E-11	-12.399	-10.663	1.839E-02	-1.735
14	SiO2 (a)	2.977E-04	1.755E-03	-3.526	-2.756	1.696E-01	-.770
15	Chalcedy	2.977E-04	2.435E-04	-3.526	-3.614	1.222E+00	.087
16	Quartz	2.977E-04	8.725E-05	-3.526	-4.059	3.412E+00	.533
17	Gibbs(c)	1.730E+09	2.571E+08	9.238	8.410	6.727E+00	.828
18	Al(OH)3a	1.730E+09	1.409E+11	9.238	11.149	1.228E-02	-1.911
19	Kaolinit	2.651E+11	7.938E+07	11.423	7.900	3.340E+03	3.524
20	Albite	2.287E-19	4.540E-19	-18.641	-18.343	5.038E-01	-.298
21	Anorth	2.090E-23	1.360E-20	-22.680	-19.866	1.537E-03	-2.813
22	Kspar	1.908E-21	1.050E-21	-20.719	-20.979	1.817E+00	.259
23	Kmica	9.543E+20	3.052E+13	20.980	13.485	3.126E+07	7.495
24	Chlorite	3.573E+68	2.367E+70	68.553	70.374	1.509E-02	-1.821
25	Ca-Mont	3.238E-44	1.602E-46	-43.490	-45.795	2.022E+02	2.306
26	Talc	1.939E+22	1.021E+22	22.288	22.009	1.898E+00	.278
27	Illite	6.792E-40	1.031E-41	-39.168	-40.987	6.590E+01	1.819
28	Chrysotl	2.187E+29	7.317E+32	29.340	32.864	2.989E-04	-3.524
29	Sepiol c	4.814E+13	7.959E+15	13.683	15.901	6.049E-03	-2.218
30	Sepiol d	4.814E+13	4.571E+18	13.683	18.660	1.053E-05	-4.977
31	Hematite	2.681E+13	2.501E-04	13.428	-3.602	1.072E+17	17.030
32	Goethite	5.177E+06	1.000E-01	6.714	-1.000	5.177E+07	7.714
33	Fe(OH)3a	5.175E+06	7.780E+04	6.714	4.891	6.652E+01	1.823
38	Pyrolusi	9.651E+33	1.726E+42	33.985	42.237	5.590E-09	-8.253
39	Hausmani	9.202E+50	2.264E+62	50.964	62.355	4.065E-12	-11.391
40	Manganit	1.726E+21	2.188E+25	21.237	25.340	7.889E-05	-4.103
41	Pyrochro	3.087E+08	1.585E+15	8.490	15.200	1.948E-07	-6.710
42	PCO2	1.121E-04	3.949E-02	-3.950	-1.404	2.839E-03	-2.547
43	O2 gas	1.366E-37	1.160E-03	-36.865	-2.936	1.178E-34	-33.929
44	H2 gas	2.389E-29	7.467E-04	-28.622	-3.127	3.199E-26	-25.495
49	Melanter	1.077E-12	5.308E-03	-11.968	-2.275	2.028E-10	-9.693
50	Alunite	2.489E-07	1.826E-01	-6.604	-.739	1.363E-06	-5.866
51	K-Jarosi	6.668E-15	1.591E-09	-14.176	-8.798	4.190E-06	-5.378

1Moquino

INITIAL SOLUTION

TEMPERATURE = 17.70 DEGREES C PH = 8.590
ANALYTICAL EPMCAT = 7.984 ANALYTICAL EPMAN = 6.780
***** OXIDATION - REDUCTION *****
DISSOLVED OXYGEN = .050 MMOLES/KG H2O
EH MEASURED WITH CALOMEL = 9.9000 VOLTS
MEASURED EH OF ZOBELL SOLUTION = 9.9000 VOLTS
CORRECTED EH = -.0080 VOLTS
PE COMPUTED FROM CORRECTED EH =-.139

FLAG	CORALK	PECALC	IDAVES
0	2	1	0

*** TOTAL CONCENTRATIONS OF INPUT SPECIES ***

SPECIES		TOTAL MOLALITY	LOG TOTAL MOLALITY	TOTAL MG/LITRE
Ca+2	2.0	1.08065E-04	-3.9663	4.32864E+00
Mg+2	2.0	9.40563E-05	-4.0266	2.28533E+00
Na+	1.0	7.52251E-03	-2.1236	1.72837E+02
K+	1.0	3.60216E-05	-4.4434	1.40767E+00
Fe+2	2.0	1.50090E-06	-5.8236	8.37705E-02
Mn+2	2.0	1.00060E-07	-6.9997	5.49380E-03
Ba+2	2.0	3.00180E-07	-6.5226	4.12020E-02
Sr+2	2.0	3.40204E-06	-5.4683	2.97908E-01
H4SiO4	.0	1.57094E-04	-3.8038	9.43331E+00
Cl-	-1.0	1.15069E-04	-3.9390	4.07710E+00
HCO3-	-1.0	6.57394E-03	-2.1822	4.00884E+02
H3BO3	.0	1.17070E-05	-4.9316	1.26477E-01
F-	-1.0	8.30497E-05	-4.0807	1.57687E+00
Li+	1.0	5.50330E-06	-5.2594	3.81645E-02
DOX	.0	5.00300E-05	-4.3008	1.59994E+00

Moquino

****DESCRIPTION OF SOLUTION ****

	ANALYT.	COMP.		
EPMCAT	7.98	7.91	PH 8.590	ACTIVITY H2O = .9997
EPMAN	6.78	6.83		PCO2= 8.914678E-04
				LOG PCO2 = -3.0499
			TEMPERATURE	PO2 = 1.397601E-52
EH = -.0080	PE = -.139		17.70 DEG C	PCH4 = 2.300819E-47
PE CALC S =	.000			CO2 TOT = 6.573938E-03
PE CALC DOX=	12.475		IONIC STRENGTH	DENSITY = 1.0000
PE SATO DOX=	1.720		7.683425E-03	TDS = 599.0MG/L
TOT ALK =	6.700E+00 MEQ			CARB ALK = 6.688E+00 MEQ

ELECT = 1.081E+00 MEQ CHARGE IMBALANCE = 7.3%

IN COMPUTING THE DISTRIBUTION OF SPECIES,
PE = -.139 EQUIVALENT EH = -.008VOLTS

DISTRIBUTION OF SPECIES

I	SPECIES		MOLALITY	ACTIVITY	LOG ACT	GAMMA
1	H+	1.	2.7872E-09	2.5704E-09	-8.590	9.2222E-01
2	E-	-1.	1.3760E+00	1.3760E+00	.139	1.0000E+00
4	Ca+2	2.	9.4443E-05	6.6322E-05	-4.178	7.0224E-01
5	Mg+2	2.	8.4737E-05	5.9807E-05	-4.223	7.0579E-01
6	Na+	1.	7.4945E-03	6.8490E-03	-2.164	9.1387E-01
7	K+	1.	3.6022E-05	3.2845E-05	-4.484	9.1181E-01
8	Fe+2	2.	4.6776E-07	3.3040E-07	-6.481	7.0633E-01
9	Mn+2	2.	1.5621E-08	1.1034E-08	-7.957	7.0633E-01
11	Ba+2	2.	2.8261E-07	1.9788E-07	-6.704	7.0020E-01
12	Sr+2	2.	3.1329E-06	2.2034E-06	-5.657	7.0332E-01
13	H4SiO4	0.	1.4987E-04	1.5013E-04	-3.824	1.0018E+00
14	Cl-	-1.	1.1507E-04	1.0492E-04	-3.979	9.1181E-01
15	CO3-2	-2.	1.2855E-04	9.0327E-05	-4.044	7.0268E-01
18	H3BO3	0.	9.6409E-06	9.6580E-06	-5.015	1.0018E+00
20	F-	-1.	8.2429E-05	7.5140E-05	-4.124	9.1157E-01
21	Li+	1.	5.5033E-06	5.0451E-06	-5.297	9.1675E-01
28	DOX	0.	5.0030E-05	5.0119E-05	-4.300	1.0018E+00
31	OH-	-1.	2.4059E-06	2.1932E-06	-5.659	9.1157E-01
33	H2 AQ	0.	9.5244E-21	9.5412E-21	-20.020	1.0018E+00
34	HCO3-	-1.	6.3566E-03	5.8199E-03	-2.235	9.1557E-01
35	H2CO3	0.	3.7343E-05	3.7409E-05	-4.427	1.0018E+00
57	H2BO3-	-1.	2.0658E-06	1.8861E-06	-5.724	9.1302E-01
58	BFOH3-	-1.	2.9258E-10	2.6713E-10	-9.573	9.1302E-01
59	BF2OH2-	-1.	6.1164E-15	5.5844E-15	-14.253	9.1302E-01
60	BF3OH-	-1.	1.4857E-21	1.3565E-21	-20.868	9.1302E-01
61	BF4-	-1.	1.1808E-27	1.0781E-27	-26.967	9.1302E-01
69	HF AQ	0.	2.5405E-10	2.5450E-10	-9.594	1.0018E+00
70	HF2-	-1.	7.5432E-14	6.8871E-14	-13.162	9.1302E-01
75	CaOH+	1.	4.6889E-09	4.2810E-09	-8.368	9.1302E-01
76	CaCO3	0.	8.8561E-06	8.8718E-06	-5.052	1.0018E+00
77	CaHCO3+	1.	4.7214E-06	4.3227E-06	-5.364	9.1557E-01
83	CaF+	1.	3.9925E-08	3.6453E-08	-7.438	9.1302E-01
85	MgOH+	1.	9.2504E-08	8.4458E-08	-7.073	9.1302E-01
86	MgCO3	0.	4.6001E-06	4.6083E-06	-5.336	1.0018E+00
87	MgHCO3+	1.	4.3426E-06	3.9649E-06	-5.402	9.1302E-01
92	MgF+	1.	2.8397E-07	2.5927E-07	-6.586	9.1302E-01
93	NaOH	0.	1.7569E-08	1.7600E-08	-7.754	1.0018E+00
94	NaCO3-	-1.	8.6505E-06	7.8981E-06	-5.102	9.1302E-01
95	NaHCO3	0.	1.9041E-05	1.9074E-05	-4.720	1.0018E+00
98	NaF aq	0.	2.9562E-07	2.9614E-07	-6.528	1.0018E+00
99	KOH	0.	4.4217E-11	4.4296E-11	-10.354	1.0018E+00
102	FeOH+	1.	2.5445E-08	2.3232E-08	-7.634	9.1302E-01
105	FeCl+	1.	5.2411E-11	4.7852E-11	-10.320	9.1302E-01
106	FeCO3	0.	7.1464E-07	7.1591E-07	-6.145	1.0018E+00
107	FeHCO3+	1.	1.7922E-07	1.6363E-07	-6.786	9.1302E-01
114	FeF+	1.	2.7191E-10	2.4826E-10	-9.605	9.1302E-01

115	Fe+3	3.	3.1536E-20	1.5217E-20	-19.818	4.8253E-01
117	FeOH+2	2.	3.5396E-14	2.4597E-14	-13.609	6.9490E-01
118	FeOH2+	1.	2.6123E-09	2.3851E-09	-8.622	9.1302E-01
119	FeOH3	0.	8.6093E-08	8.6246E-08	-7.064	1.0018E+00
120	FeOH4-	-1.	2.4804E-08	2.2647E-08	-7.645	9.1302E-01
121	Fe2OH2+4	4.	9.5144E-26	2.2185E-26	-25.654	2.3318E-01
122	Fe3OH4+5	5.	2.1451E-31	2.2052E-32	-31.657	1.0280E-01
123	FeCl+2	2.	5.4732E-23	3.8033E-23	-22.420	6.9490E-01
124	FeCl2+	1.	2.4750E-26	2.2597E-26	-25.646	9.1302E-01
125	FeCl3	0.	2.3667E-31	2.3709E-31	-30.625	1.0018E+00
131	FeF+2	2.	2.3260E-18	1.6163E-18	-17.791	6.9490E-01
132	FeF2+	1.	4.8449E-18	4.4235E-18	-17.354	9.1302E-01
133	FeF3	0.	5.1266E-19	5.1357E-19	-18.289	1.0018E+00
134	MnOH+	1.	6.5646E-11	5.9936E-11	-10.222	9.1302E-01
136	MnCl+	1.	5.1655E-12	4.7162E-12	-11.326	9.1302E-01
137	MnCl2	0.	2.1562E-16	2.1600E-16	-15.666	1.0018E+00
138	MnCl3-	-1.	6.8366E-21	6.2419E-21	-20.205	9.1302E-01
139	MnCO3	0.	7.9027E-08	7.9167E-08	-7.101	1.0018E+00
140	MnHCO3+	1.	5.3342E-09	4.8702E-09	-8.312	9.1302E-01
143	MnF+	1.	6.2823E-12	5.7359E-12	-11.241	9.1302E-01
144	Mn+3	3.	1.8842E-34	8.3070E-35	-34.081	4.4088E-01
164	H3SiO4-	-1.	7.2268E-06	6.5982E-06	-5.181	9.1302E-01
165	H2SiO4-2	-2.	1.5294E-10	1.0628E-10	-9.974	6.9490E-01
166	SiF6-2	-2.	5.1212E-33	3.5587E-33	-32.449	6.9490E-01
170	BaOH+	1.	2.8564E-12	2.6079E-12	-11.584	9.1302E-01
171	BaCO3	0.	7.9608E-09	7.9749E-09	-8.098	1.0018E+00
172	BaHCO3+	1.	9.6087E-09	8.7729E-09	-8.057	9.1302E-01
176	SrOH+	1.	4.8049E-11	4.3953E-11	-10.357	9.1476E-01
177	SrHCO3+	1.	1.6687E-07	1.5278E-07	-6.816	9.1557E-01
178	SrCO3	0.	1.0223E-07	1.0241E-07	-6.990	1.0018E+00
180	LiOH	0.	4.4874E-11	4.4953E-11	-10.347	1.0018E+00

	PHASE	IAP	KT	LOG IAP	LOG KT	IAP/KT	LOG IAP/KT
1	Calcite	5.991E-09	3.612E-09	-8.223	-8.442	1.658E+00	.220
2	Aragonit	5.991E-09	5.092E-09	-8.223	-8.293	1.176E+00	.071
3	Dolomite	3.236E-17	1.212E-17	-16.490	-16.916	2.670E+00	.426
4	Siderite	2.984E-11	1.431E-11	-10.525	-10.844	2.086E+00	.319
5	Rhodochr	9.967E-13	7.876E-12	-12.001	-11.104	1.265E-01	-.898
6	Strontit	1.990E-10	5.361E-10	-9.701	-9.271	3.713E-01	-.430
7	Witherit	1.787E-11	2.605E-09	-10.748	-8.584	6.862E-03	-2.164
13	Fluorite	3.745E-13	2.044E-11	-12.427	-10.689	1.832E-02	-1.737
14	SiO2 (a)	1.502E-04	1.685E-03	-3.823	-2.773	8.913E-02	-1.050
15	Chalcedy	1.502E-04	2.300E-04	-3.823	-3.638	6.530E-01	-.185
16	Quartz	1.502E-04	8.117E-05	-3.823	-4.091	1.851E+00	.267
26	Talc	3.772E+23	1.786E+22	23.577	22.252	2.113E+01	1.325
28	Chrysotl	1.671E+31	1.342E+33	31.223	33.128	1.245E-02	-1.905
29	Sepiol c	2.773E+14	9.054E+15	14.443	15.957	3.063E-02	-1.514
30	Sepiol d	2.773E+14	4.571E+18	14.443	18.660	6.067E-05	-4.217
31	Hematite	8.023E+11	3.626E-04	11.904	-3.441	2.212E+15	15.345
32	Goethite	8.956E+05	1.000E-01	5.952	-1.000	8.956E+06	6.952
33	Fe(OH)3a	8.954E+05	7.780E+04	5.952	4.891	1.151E+01	1.061
38	Pyrolusi	1.334E+26	3.783E+42	26.125	42.578	3.527E-17	-16.453
39	Hausmani	3.720E+44	7.613E+62	44.571	62.882	4.886E-19	-18.311
40	Manganit	4.719E+17	2.188E+25	17.674	25.340	2.157E-08	7.666
41	Pyrochro	1.669E+09	1.585E+15	9.223	15.200	1.053E-06	-5.977
42	PCO2	3.741E-05	4.196E-02	-4.427	-1.377	8.915E-04	-3.050
44	H2 gas	9.541E-21	7.627E-04	-20.020	-3.118	1.251E-17	-16.903

1Seboyeta

INITIAL SOLUTION

TEMPERATURE = 22.90 DEGREES C PH = 7.940
ANALYTICAL EPMCAT = 3.724 ANALYTICAL EPMAN = 4.229
***** OXIDATION - REDUCTION *****
DISSOLVED OXYGEN = .000 MMOLES/KG H2O
EH MEASURED WITH CALOMEL = 9.9000 VOLTS
MEASURED EH OF ZOBELL SOLUTION = 9.9000 VOLTS
CORRECTED EH = -.0250 VOLTS
PE COMPUTED FROM CORRECTED EH = -.426

FLAG	CORALK	PECALC	IDAVES
0	2	1	0

*** TOTAL CONCENTRATIONS OF INPUT SPECIES ***

SPECIES		TOTAL MOLALITY	LOG TOTAL MOLALITY	TOTAL MG/LITRE
Ca+2	2.0	2.11073E-04	-3.6756	8.45688E+00
Mg+2	2.0	1.33046E-04	-3.8760	3.23350E+00
Na+	1.0	2.96603E-03	-2.5278	6.81648E+01
K+	1.0	5.10178E-05	-4.2923	1.99420E+00
Fe+2	2.0	1.00035E-07	-6.9998	5.58470E-03
Al+3	3.0	1.30045E-06	-5.8859	3.50760E-02
Ba+2	2.0	7.00244E-07	-6.1548	9.61380E-02
Sr+2	2.0	4.30150E-06	-5.3664	3.76766E-01
H4SiO4	.0	3.35117E-04	-3.4748	2.01284E+01
Cl-	-1.0	2.19076E-04	-3.6594	7.76421E+00
HCO3-	-1.0	3.51522E-03	-2.4540	2.14415E+02
SO4-2	-2.0	2.39083E-04	-3.6215	2.29587E+01
NO3-	-1.0	1.90066E-06	-5.7211	2.66127E-02
F-	-1.0	1.20042E-05	-4.9207	2.27981E-01
Li+	1.0	3.20111E-06	-5.4947	2.22048E-02
Br-	-1.0	4.00139E-07	-6.3978	3.19616E-02

Seboyeta

****DESCRIPTION OF SOLUTION ****

	ANALYT.	COMP.
EPMCAT	3.72	3.67
EPMAN	4.23	4.13

EH = -.0250 PE = -.426
PE CALC S = .000
PE CALC DOX= .000
PE SATO DOX= .000

PH
7.940

TEMPERATURE
22.90 DEG C

IONIC STRENGTH
4.471093E-03

ACTIVITY H2O = .9999
PCO2= 2.328384E-03
LOG PCO2 = -2.6329
PO2 = 1.656203E-54
PCH4 = 3.054457E-40
CO2 TOT = 3.515223E-03
DENSITY = 1.0000
TDS = 347.9MG/L

TOT ALK = 3.463E+00 MEQ
ELECT = -4.516E-01 MEQ

CARB ALK = 3.452E+00 MEQ
CHARGE IMBALANCE = -5.8%

IN COMPUTING THE DISTRIBUTION OF SPECIES,
PE = -.426 EQUIVALENT EH = -.025VOLTS

DISTRIBUTION OF SPECIES

I	SPECIES		MOLALITY	ACTIVITY	LOG ACT	GAMMA
1	H+	1.	1.2258E-08	1.1482E-08	-7.940	9.3665E-01
2	E-	-1.	2.6643E+00	2.6643E+00	.426	1.0000E+00
4	Ca+2	2.	1.9687E-04	1.4867E-04	-3.828	7.5517E-01
5	Mg+2	2.	1.2455E-04	9.4351E-05	-4.025	7.5753E-01
6	Na+	1.	2.9582E-03	2.7547E-03	-2.560	9.3120E-01
7	K+	1.	5.0958E-05	4.7387E-05	-4.324	9.2994E-01
8	Fe+2	2.	6.5925E-08	4.9973E-08	-7.301	7.5803E-01
10	Al+3	3.	2.8933E-15	1.6053E-15	-14.794	5.5486E-01
11	Ba+2	2.	6.4100E-07	4.8324E-07	-6.316	7.5389E-01
12	Sr+2	2.	4.0321E-06	3.0480E-06	-5.516	7.5592E-01
13	H4SiO4	0.	3.3087E-04	3.3121E-04	-3.480	1.0010E+00
14	Cl-	-1.	2.1908E-04	2.0373E-04	-3.691	9.2994E-01
15	CO3-2	-2.	1.6385E-05	1.2380E-05	-4.907	7.5556E-01
16	SO4-2	-2.	2.2779E-04	1.7165E-04	-3.765	7.5358E-01
17	NO3-	-1.	3.2371E-20	3.0075E-20	-19.522	9.2910E-01
20	F-	-1.	1.1900E-05	1.1065E-05	-4.956	9.2980E-01
21	Li+	1.	3.1987E-06	2.9847E-06	-5.525	9.3309E-01
22	Br-	-1.	4.0014E-07	3.7177E-07	-6.430	9.2910E-01
31	OH-	-1.	7.9850E-07	7.4244E-07	-6.129	9.2980E-01
33	H2 AQ	0.	6.7587E-19	6.7657E-19	-18.170	1.0010E+00
34	HCO3-	-1.	3.3954E-03	3.1656E-03	-2.500	9.3232E-01
35	H2CO3	0.	8.3895E-05	8.3982E-05	-4.076	1.0010E+00
40	HSO4-	-1.	1.9675E-10	1.8310E-10	-9.737	9.3063E-01
48	NO2-	-1.	1.9007E-06	1.7659E-06	-5.753	9.2910E-01
69	HF AQ	0.	1.8330E-10	1.8349E-10	-9.736	1.0010E+00
70	HF2-	-1.	8.2314E-15	7.6603E-15	-14.116	9.3063E-01
75	CaOH+	1.	2.3089E-09	2.1487E-09	-8.668	9.3063E-01
76	CaCO3	0.	2.9659E-06	2.9690E-06	-5.527	1.0010E+00
77	CaHCO3+	1.	6.2285E-06	5.8070E-06	-5.236	9.3232E-01
78	CaSO4	0.	4.9873E-06	4.9924E-06	-5.302	1.0010E+00
79	CaHSO4	1.	3.6822E-13	3.4268E-13	-12.465	9.3063E-01
83	CaF+	1.	1.4655E-08	1.3638E-08	-7.865	9.3063E-01
85	MgOH+	1.	3.2057E-08	2.9833E-08	-7.525	9.3063E-01
86	MgCO3	0.	1.0781E-06	1.0792E-06	-5.967	1.0010E+00
87	MgHCO3+	1.	3.7221E-06	3.4639E-06	-5.460	9.3063E-01
88	MgSO4	0.	3.5917E-06	3.5954E-06	-5.444	1.0010E+00
92	MgF+	1.	7.1332E-08	6.6384E-08	-7.178	9.3063E-01
93	NaOH	0.	1.5833E-09	1.5849E-09	-8.800	1.0010E+00
94	NaCO3-	-1.	6.1330E-07	5.7076E-07	-6.244	9.3063E-01
95	NaHCO3	0.	4.6917E-06	4.6965E-06	-5.328	1.0010E+00
96	NaSO4-	-1.	2.5126E-06	2.3383E-06	-5.631	9.3063E-01
98	NaF aq	0.	1.7522E-08	1.7540E-08	-7.756	1.0010E+00
99	KOH	0.	1.4294E-11	1.4309E-11	-10.844	1.0010E+00
100	KSO4-	-1.	6.0234E-08	5.6056E-08	-7.251	9.3063E-01
102	FeOH+	1.	1.2626E-09	1.1750E-09	-8.930	9.3063E-01
105	FeCl+	1.	1.5101E-11	1.4053E-11	-10.852	9.3063E-01
106	FeCO3	0.	1.4825E-08	1.4840E-08	-7.829	1.0010E+00

107	FeHCO3+	1.	1.6280E-08	1.5151E-08	-7.820	9.3063E-01
108	FeSO4	0.	1.4660E-09	1.4676E-09	-8.833	1.0010E+00
109	FeHSO4+	1.	1.2377E-16	1.1518E-16	-15.939	9.3063E-01
114	FeF+	1.	5.9417E-12	5.5295E-12	-11.257	9.3063E-01
115	Fe+3	3.	2.8750E-21	1.5952E-21	-20.797	5.5486E-01
117	FeOH+2	2.	1.0558E-15	7.9193E-16	-15.101	7.5007E-01
118	FeOH2+	1.	2.2647E-11	2.1076E-11	-10.676	9.3063E-01
119	FeOH3	0.	2.1540E-10	2.1563E-10	-9.666	1.0010E+00
120	FeOH4-	-1.	1.6903E-11	1.5730E-11	-10.803	9.3063E-01
121	Fe2OH2+4	4.	5.8199E-29	1.8422E-29	-28.735	3.1653E-01
122	Fe3OH4+5	5.	5.9495E-37	9.8600E-38	-37.006	1.6573E-01
123	FeCl+2	2.	1.2236E-23	9.1781E-24	-23.037	7.5007E-01
124	FeCl2+	1.	9.5972E-27	8.9314E-27	-26.049	9.3063E-01
125	FeCl3	0.	1.8177E-31	1.8196E-31	-30.740	1.0010E+00
126	FeSO4+	1.	3.0787E-21	2.8651E-21	-20.543	9.3063E-01
127	FeHSO4+2	2.	1.3826E-28	1.0371E-28	-27.984	7.5007E-01
128	FeSO42-	-1.	1.1467E-23	1.0671E-23	-22.972	9.3063E-01
131	FeF+2	2.	3.6110E-20	2.7085E-20	-19.567	7.5007E-01
132	FeF2+	1.	1.2502E-20	1.1635E-20	-19.934	9.3063E-01
133	FeF3	0.	2.0237E-22	2.0258E-22	-21.693	1.0010E+00
150	AlOH+2	2.	1.6140E-12	1.2106E-12	-11.917	7.5007E-01
151	AlOH2+	1.	7.3751E-10	6.8635E-10	-9.163	9.3063E-01
152	AlOH3	0.	7.5220E-09	7.5298E-09	-8.123	1.0010E+00
153	AlOH4-	-1.	1.2922E-06	1.2025E-06	-5.920	9.3063E-01
154	AlSO4+	1.	3.0218E-16	2.8122E-16	-15.551	9.3063E-01
155	AlSO42-	-1.	4.0863E-18	3.8029E-18	-17.420	9.3063E-01
156	AlHSO4+2	2.	1.1834E-24	8.8761E-25	-24.052	7.5007E-01
157	AlF+2	2.	2.3383E-13	1.7539E-13	-12.756	7.5007E-01
158	AlF2+	1.	1.0337E-12	9.6201E-13	-12.017	9.3063E-01
159	AlF3	0.	1.3358E-13	1.3372E-13	-12.874	1.0010E+00
160	AlF4-	-1.	6.3265E-16	5.8876E-16	-15.230	9.3063E-01
161	AlF5-2	-2.	1.3825E-19	1.0370E-19	-18.984	7.5007E-01
162	AlF6-3	-3.	2.2855E-24	1.1966E-24	-23.922	5.2358E-01
164	H3SiO4-	-1.	4.2444E-06	3.9500E-06	-5.403	9.3063E-01
165	H2SiO4-2	-2.	2.7165E-11	2.0376E-11	-10.691	7.5007E-01
166	SiF6-2	-2.	2.5911E-35	1.9435E-35	-34.711	7.5007E-01
170	BaOH+	1.	1.5323E-12	1.4260E-12	-11.846	9.3063E-01
171	BaCO3	0.	2.9599E-09	2.9630E-09	-8.528	1.0010E+00
172	BaHCO3+	1.	1.4749E-08	1.3726E-08	-7.862	9.3063E-01
173	BaSO4	0.	4.1531E-08	4.1574E-08	-7.381	1.0010E+00
176	SrOH+	1.	1.4609E-11	1.3613E-11	-10.866	9.3181E-01
177	SrHCO3+	1.	1.4733E-07	1.3736E-07	-6.862	9.3232E-01
178	SrCO3	0.	2.2616E-08	2.2639E-08	-7.645	1.0010E+00
179	SrSO4	0.	9.9404E-08	9.9506E-08	-7.002	1.0010E+00
180	LiOH	0.	5.9483E-12	5.9544E-12	-11.225	1.0010E+00
181	LiSO4-	-1.	2.4031E-09	2.2364E-09	-8.650	9.3063E-01

	PHASE	IAP	KT	LOG IAP	LOG KT	IAP/KT	LOG IAP/KT
1	Calcite	1.841E-09	3.402E-09	-8.735	-8.468	5.410E-01	-.267
2	Aragonit	1.841E-09	4.754E-09	-8.735	-8.323	3.872E-01	-.412
3	Dolomite	2.150E-18	9.100E-18	-17.668	-17.041	2.362E-01	-.627
4	Siderite	6.186E-13	1.327E-11	-12.209	-10.877	4.662E-02	-1.331
6	Strontit	3.773E-11	5.382E-10	-10.423	-9.269	7.011E-02	-1.154
7	Witherit	5.982E-12	2.716E-09	-11.223	-8.566	2.203E-03	-2.657
8	Gypsum	2.551E-08	2.626E-05	-7.593	-4.581	9.714E-04	-3.013
9	Anhydrit	2.552E-08	4.439E-05	-7.593	-4.353	5.749E-04	-3.240

10 Celestit	5.232E-10	2.359E-07	-9.281	-6.627	2.218E-03	-2.654
11 Barite	8.295E-11	9.910E-11	-10.081	-10.004	8.371E-01	-.077
13 Fluorite	1.820E-14	2.375E-11	-13.740	-10.624	7.665E-04	-3.116
14 SiO2 (a)	3.313E-04	1.866E-03	-3.480	-2.729	1.776E-01	-.751
15 Chalcedy	3.313E-04	2.655E-04	-3.480	-3.576	1.248E+00	.096
16 Quartz	3.313E-04	9.738E-05	-3.480	-4.012	3.402E+00	.532
17 Gibbs(c)	1.060E+09	1.693E+08	9.025	8.229	6.264E+00	.797
18 Al(OH)3a	1.060E+09	8.665E+10	9.025	10.938	1.224E-02	-1.912
19 Kaolinit	1.234E+11	4.155E+07	11.091	7.619	2.970E+03	3.473
20 Albite	1.205E-19	7.301E-19	-18.919	-18.137	1.650E-01	-.782
21 Anorth	2.361E-23	1.682E-20	-22.627	-19.774	1.404E-03	-2.853
22 Kspar	2.073E-21	1.848E-21	-20.683	-20.733	1.121E+00	.050
23 Kmica	1.789E+20	1.027E+13	20.253	13.012	1.742E+07	7.241
24 Chlorite	7.683E+66	1.471E+69	66.886	69.168	5.222E-03	-2.282
25 Ca-Mont	8.405E-44	4.672E-46	-43.075	-45.331	1.799E+02	2.255
26 Talc	4.415E+21	4.365E+21	21.645	21.640	1.011E+00	.005
27 Illite	1.192E-39	2.810E-41	-38.924	-40.551	4.243E+01	1.628
28 Chrysotl	4.022E+28	2.905E+32	28.604	32.463	1.384E-04	-3.859
29 Sepiol c	1.861E+13	6.541E+15	13.270	15.816	2.846E-03	-2.546
30 Sepiol d	1.861E+13	4.571E+18	13.270	18.660	4.072E-06	-5.390
31 Hematite	1.110E+06	1.420E-04	6.045	-3.848	7.818E+09	9.893
32 Goethite	1.054E+03	1.000E-01	3.023	-1.000	1.054E+04	4.023
33 Fe(OH)3a	1.054E+03	7.780E+04	3.023	4.891	1.354E-02	-1.868
42 PCO2	8.398E-05	3.607E-02	-4.076	-1.443	2.328E-03	-2.633
44 H2 gas	6.766E-19	7.230E-04	-18.170	-3.141	9.358E-16	-15.029
49 Melanter	8.570E-12	5.821E-03	-11.067	-2.235	1.472E-09	-8.832
50 Alunite	2.520E-09	7.266E-02	-8.599	-1.139	3.468E-08	-7.460
51 K-Jarosi	2.472E-27	8.967E-10	-26.607	-9.047	2.757E-18	-17.560

1CNV-W2

INITIAL SOLUTION

TEMPERATURE = 20.00 DEGREES C PH = 8.260
ANALYTICAL EPMCAT = 13.847 ANALYTICAL EPMAN = 12.912

***** OXIDATION - REDUCTION *****

DISSOLVED OXYGEN = .200 MMOLES/KG H2O
EH MEASURED WITH CALOMEL = 9.9000 VOLTS
MEASURED EH OF ZOBELL SOLUTION = 9.9000 VOLTS
CORRECTED EH = .2820 VOLTS
PE COMPUTED FROM CORRECTED EH = 4.848

FLAG	CORALK	PECALC	IDAVES
0	2	1	0

*** TOTAL CONCENTRATIONS OF INPUT SPECIES ***

SPECIES		TOTAL MOLALITY	LOG TOTAL MOLALITY	TOTAL MG/LITRE
Ca+2	2.0	8.30870E-05	-4.0805	3.32664E+00
Mg+2	2.0	5.50577E-05	-4.2592	1.33716E+00
Na+	1.0	1.33680E-02	-1.8739	3.07006E+02
K+	1.0	1.63171E-04	-3.7874	6.37363E+00
Fe+2	2.0	1.02107E-05	-4.9909	5.69639E-01
Mn+2	2.0	1.00105E-07	-6.9995	5.49380E-03
Sr+2	2.0	2.10220E-06	-5.6773	1.84002E-01
H4SiO4	.0	2.00210E-04	-3.6985	1.20170E+01
Cl-	-1.0	3.92411E-04	-3.4063	1.38976E+01
HCO3-	-1.0	7.68505E-03	-2.1144	4.68430E+02
SO4-2	-2.0	2.35046E-03	-2.6288	2.25553E+02
NO3-	-1.0	2.05215E-05	-4.6878	2.87137E-01
H3BO3	.0	3.05320E-05	-4.5152	3.29705E-01
F-	-1.0	9.71017E-05	-4.0128	1.84284E+00
Br-	-1.0	8.00839E-07	-6.0965	6.39232E-02
DOX	.0	2.00210E-04	-3.6985	6.39976E+00

CNV-W2

****DESCRIPTION OF SOLUTION ****

	ANALYT.	COMP.	PH	ACTIVITY H2O = .9996
EPMCAT	13.85	13.61	8.260	PCO2= 2.236861E-03
EPMAN	12.91	12.71		LOG PCO2 = -2.6504
			TEMPERATURE	PO2 = 3.848239E-33
EH = .2820	PE =	4.848	20.00 DEG C	PCH4 = 1.431369E-84
PE CALC S =	.000			CO2 TOT = 7.685051E-03
PE CALC DOX=	12.757		IONIC STRENGTH	DENSITY = 1.0000
PE SATO DOX=	2.200		1.560673E-02	TDS = 1047.6MG/L
TOT ALK =	7.714E+00 MEQ			CARB ALK = 7.694E+00 MEQ
ELECT =	8.963E-01 MEQ			CHARGE IMBALANCE = 3.4%

IN COMPUTING THE DISTRIBUTION OF SPECIES,
PE = 4.848 EQUIVALENT EH = .282VOLTS

DISTRIBUTION OF SPECIES

I	SPECIES		MOLALITY	ACTIVITY	LOG ACT	GAMMA
1	H+	1.	6.1129E-09	5.4954E-09	-8.260	8.9898E-01
2	E-	-1.	1.4188E-05	1.4188E-05	-4.848	1.0000E+00
4	Ca+2	2.	6.5686E-05	4.0728E-05	-4.390	6.2005E-01
5	Mg+2	2.	4.3600E-05	2.7288E-05	-4.564	6.2587E-01
6	Na+	1.	1.3230E-02	1.1704E-02	-1.932	8.8467E-01

7	K+	1.	1.6169E-04	1.4242E-04	-3.846	8.8079E-01
8	Fe+2	2.	3.2569E-09	2.0397E-09	-8.690	6.2626E-01
9	Mn+2	2.	2.4827E-08	1.5548E-08	-7.808	6.2626E-01
12	Sr+2	2.	1.7035E-06	1.0591E-06	-5.975	6.2170E-01
13	H4SiO4	0.	1.9524E-04	1.9594E-04	-3.708	1.0036E+00
14	Cl-	-1.	3.9241E-04	3.4563E-04	-3.461	8.8079E-01
15	CO3-2	-2.	8.1749E-05	5.0717E-05	-4.295	6.2039E-01
16	SO4-2	-2.	2.2416E-03	1.3797E-03	-2.860	6.1549E-01
17	NO3-	-1.	2.5735E-08	2.2602E-08	-7.646	8.7827E-01
18	H3BO3	0.	2.7544E-05	2.7644E-05	-4.558	1.0036E+00
20	F-	-1.	9.6343E-05	8.4812E-05	-4.072	8.8032E-01
22	Br-	-1.	8.0084E-07	7.0335E-07	-6.153	8.7827E-01
28	DOX	0.	2.0021E-04	2.0093E-04	-3.697	1.0036E+00
31	OH-	-1.	1.4028E-06	1.2349E-06	-5.908	8.8032E-01
32	O2 AQ	0.	4.6257E-36	4.6424E-36	-35.333	1.0036E+00
33	H2 AQ	0.	4.5111E-30	4.5274E-30	-29.344	1.0036E+00
34	HCO3-	-1.	7.4568E-03	6.6179E-03	-2.179	8.8750E-01
35	H2CO3	0.	8.7339E-05	8.7654E-05	-4.057	1.0036E+00
40	HSO4-	-1.	7.5000E-10	6.6247E-10	-9.179	8.8329E-01
48	NO2-	-1.	2.0496E-05	1.8001E-05	-4.745	8.7827E-01
57	H2BO3-	-1.	2.9866E-06	2.6381E-06	-5.579	8.8329E-01
58	BFOH3-	-1.	1.0019E-09	8.8496E-10	-9.053	8.8329E-01
59	BF2OH2-	-1.	5.0391E-14	4.4510E-14	-13.352	8.8329E-01
60	BF3OH-	-1.	2.8275E-20	2.4975E-20	-19.602	8.8329E-01
61	BF4-	-1.	5.4068E-26	4.7758E-26	-25.321	8.8329E-01
69	HF AQ	0.	6.3713E-10	6.3942E-10	-9.194	1.0036E+00
70	HF2-	-1.	2.2591E-13	1.9954E-13	-12.700	8.8329E-01
75	CaOH+	1.	1.3919E-09	1.2295E-09	-8.910	8.8329E-01
76	CaCO3	0.	3.1567E-06	3.1681E-06	-5.499	1.0036E+00
77	CaHCO3+	1.	3.5593E-06	3.1589E-06	-5.500	8.8750E-01
78	CaSO4	0.	1.0654E-05	1.0692E-05	-4.971	1.0036E+00
79	CaHSO4	1.	4.0886E-13	3.6114E-13	-12.442	8.8329E-01
83	CaF+	1.	3.0251E-08	2.6720E-08	-7.573	8.8329E-01
85	MgOH+	1.	2.0403E-08	1.8022E-08	-7.744	8.8329E-01
86	MgCO3	0.	1.2186E-06	1.2230E-06	-5.913	1.0036E+00
87	MgHCO3+	1.	2.3458E-06	2.0720E-06	-5.684	8.8329E-01
88	MgSO4	0.	7.7146E-06	7.7424E-06	-5.111	1.0036E+00
92	MgF+	1.	1.5788E-07	1.3945E-07	-6.856	8.8329E-01
93	NaOH	0.	1.4015E-08	1.4066E-08	-7.852	1.0036E+00
94	NaCO3-	-1.	9.6827E-06	8.5527E-06	-5.068	8.8329E-01
95	NaHCO3	0.	3.8988E-05	3.9129E-05	-4.408	1.0036E+00
96	NaSO4-	-1.	8.8721E-05	7.8366E-05	-4.106	8.8329E-01
98	NaF aq	0.	5.6917E-07	5.7122E-07	-6.243	1.0036E+00
99	KOH	0.	8.9501E-11	8.9823E-11	-10.047	1.0036E+00
100	KSO4-	-1.	1.4761E-06	1.3038E-06	-5.885	8.8329E-01
102	FeOH+	1.	9.0834E-11	8.0233E-11	-10.096	8.8329E-01
105	FeCl+	1.	1.1017E-12	9.7314E-13	-12.012	8.8329E-01
106	FeCO3	0.	2.4726E-09	2.4815E-09	-8.605	1.0036E+00
107	FeHCO3+	1.	1.3728E-09	1.2126E-09	-8.916	8.8329E-01
108	FeSO4	0.	4.5437E-10	4.5600E-10	-9.341	1.0036E+00
109	FeHSO4+	1.	2.0476E-17	1.8086E-17	-16.743	8.8329E-01
114	FeF+	1.	1.9585E-12	1.7299E-12	-11.762	8.8329E-01
115	Fe+3	3.	2.7093E-17	1.0390E-17	-16.983	3.8350E-01
117	FeOH+2	2.	1.4859E-11	9.0450E-12	-11.044	6.0872E-01
118	FeOH2+	1.	5.0858E-07	4.4922E-07	-6.348	8.8329E-01
119	FeOH3	0.	8.4033E-06	8.4336E-06	-5.074	1.0036E+00
120	FeOH4-	-1.	1.2911E-06	1.1404E-06	-5.943	8.8329E-01
121	Fe2OH2+4	4.	1.9789E-20	2.7170E-21	-20.566	1.3730E-01
122	Fe3OH4+5	5.	9.0726E-24	4.0769E-25	-24.390	4.4936E-02
123	FeCl+2	2.	1.5163E-19	9.2302E-20	-19.035	6.0872E-01

124	FeCl2+	1.	1.8956E-22	1.6743E-22	-21.776	8.8329E-01
125	FeCl3	0.	5.7663E-27	5.7870E-27	-26.238	1.0036E+00
126	FeSO4+	1.	1.5901E-16	1.4045E-16	-15.852	8.8329E-01
127	FeHSO4+2	2.	5.0235E-24	3.0579E-24	-23.515	6.0872E-01
128	FeSO42-	-1.	4.7051E-18	4.1560E-18	-17.381	8.8329E-01
131	FeF+2	2.	2.1227E-15	1.2922E-15	-14.889	6.0872E-01
132	FeF2+	1.	4.6496E-15	4.1069E-15	-14.386	8.8329E-01
133	FeF3	0.	5.4065E-16	5.4259E-16	-15.266	1.0036E+00
134	MnOH+	1.	5.4370E-11	4.8025E-11	-10.319	8.8329E-01
136	MnCl+	1.	2.4785E-11	2.1892E-11	-10.660	8.8329E-01
137	MnCl2	0.	3.2911E-15	3.3030E-15	-14.481	1.0036E+00
138	MnCl3-	-1.	3.5597E-19	3.1443E-19	-18.502	8.8329E-01
139	MnCO3	0.	6.2412E-08	6.2637E-08	-7.203	1.0036E+00
140	MnHCO3+	1.	9.3267E-09	8.2382E-09	-8.084	8.8329E-01
141	MnSO4	0.	3.4496E-09	3.4620E-09	-8.461	1.0036E+00
142	Mn(NO3)2	0.	3.1870E-23	3.1985E-23	-22.495	1.0036E+00
143	MnF+	1.	1.0328E-11	9.1230E-12	-11.040	8.8329E-01
144	Mn+3	3.	4.9233E-29	1.6114E-29	-28.793	3.2729E-01
164	H3SiO4-	-1.	4.9731E-06	4.3927E-06	-5.357	8.8329E-01
165	H2SiO4-2	-2.	6.3869E-11	3.8878E-11	-10.410	6.0872E-01
166	SiF6-2	-2.	2.6452E-31	1.6102E-31	-30.793	6.0872E-01
176	SrOH+	1.	1.1150E-11	9.8797E-12	-11.005	8.8606E-01
177	SrHCO3+	1.	1.0180E-07	9.0346E-08	-7.044	8.8750E-01
178	SrCO3	0.	2.9475E-08	2.9582E-08	-7.529	1.0036E+00
179	SrSO4	0.	2.6739E-07	2.6835E-07	-6.571	1.0036E+00

	PHASE	IAP	KT	LOG IAP	LOG KT	IAP/KT	LOG IAP/KT
1	Calcite	2.066E-09	3.521E-09	-8.685	-8.453	5.866E-01	-.232
2	Aragonit	2.066E-09	4.945E-09	-8.685	-8.306	4.177E-01	-.379
3	Dolomite	2.859E-18	1.067E-17	-17.544	-16.972	2.680E-01	-.572
4	Siderite	1.034E-13	1.384E-11	-12.985	-10.859	7.477E-03	-2.126
5	Rhodochr	7.886E-13	7.725E-12	-12.103	-11.112	1.021E-01	-.991
6	Strontit	5.371E-11	5.382E-10	-10.270	-9.269	9.980E-02	-1.001
8	Gypsum	5.615E-08	2.623E-05	-7.251	-4.581	2.140E-03	-2.670
9	Anhydrit	5.619E-08	4.531E-05	-7.250	-4.344	1.240E-03	-2.906
10	Celestit	1.461E-09	2.385E-07	-8.835	-6.623	6.127E-03	-2.213
13	Fluorite	2.930E-13	2.188E-11	-12.533	-10.660	1.339E-02	-1.873
14	SiO2 (a)	1.961E-04	1.764E-03	-3.708	-2.754	1.112E-01	-.954
15	Chalcedy	1.961E-04	2.453E-04	-3.708	-3.610	7.996E-01	-.097
16	Quartz	1.961E-04	8.805E-05	-3.708	-4.055	2.227E+00	.348
26	Talc	1.089E+21	9.517E+21	21.037	21.979	1.145E-01	-.941
28	Chrysotl	2.831E+28	6.776E+32	28.452	32.831	4.178E-05	-4.379
29	Sepiol c	6.143E+12	7.830E+15	12.788	15.894	7.846E-04	-3.105
30	Sepiol d	6.143E+12	4.571E+18	12.788	18.660	1.344E-06	-5.872
31	Hematite	3.915E+15	2.386E-04	15.593	-3.622	1.641E+19	19.215
32	Goethite	6.255E+07	1.000E-01	7.796	-1.000	6.255E+08	8.796
33	Fe(OH)3a	6.253E+07	7.780E+04	7.796	4.891	8.037E+02	2.905
38	Pyrolusi	8.462E+34	1.563E+42	34.927	42.194	5.413E-08	-7.267
39	Hausmani	2.241E+52	1.942E+62	52.350	62.288	1.154E-10	-9.938
40	Manganit	6.598E+21	2.188E+25	21.819	25.340	3.016E-04	-3.521
41	Pyrochro	5.144E+08	1.585E+15	8.711	15.200	3.246E-07	-6.489
42	PCO2	8.765E-05	3.919E-02	-4.057	-1.407	2.237E-03	-2.650
43	O2 gas	4.642E-36	1.156E-03	-35.333	-2.937	4.015E-33	-32.396
44	H2 gas	4.527E-30	7.447E-04	-29.344	-3.128	6.079E-27	-26.216
49	Melanter	2.806E-12	5.349E-03	-11.552	-2.272	5.245E-10	-9.280

51 K-Jarosi	1.101E-11	1.517E-09	-10.958	-8.819	7.258E-03	-2.139

1CNV-W3

INITIAL SOLUTION

TEMPERATURE = 20.00 DEGREES C PH = 8.170
ANALYTICAL EPMCAT = 11.197 ANALYTICAL EPMAN = 11.598
***** OXIDATION - REDUCTION *****
DISSOLVED OXYGEN = .180 MMOLES/KG H2O
EH MEASURED WITH CALOMEL = 9.9000 VOLTS FLAG CORALK PECALC IDAVES
MEASURED EH OF ZOBELL SOLUTION = 9.9000 VOLTS 0 2 1 0
CORRECTED EH = .2310 VOLTS
PE COMPUTED FROM CORRECTED EH = 3.971

*** TOTAL CONCENTRATIONS OF INPUT SPECIES ***

SPECIES		TOTAL MOLALITY	LOG TOTAL MOLALITY	TOTAL MG/LITRE
Ca+2	2.0	1.24118E-04	-3.9062	4.96992E+00
Mg+2	2.0	3.20305E-05	-4.4944	7.77984E-01
Na+	1.0	1.07632E-02	-1.9681	2.47209E+02
K+	1.0	5.60533E-05	-4.2514	2.18971E+00
Fe+2	2.0	1.70162E-05	-4.7691	9.49399E-01
Mn+2	2.0	5.00476E-07	-6.3006	2.74690E-02
Sr+2	2.0	2.50238E-06	-5.6016	2.19050E-01
H4SiO4	.0	1.77168E-04	-3.7516	1.06350E+01
Cl-	-1.0	1.48141E-04	-3.8293	5.24704E+00
HCO3-	-1.0	9.67620E-03	-2.0143	5.89854E+02
SO4-2	-2.0	8.41800E-04	-3.0748	8.07878E+01
NO3-	-1.0	1.30124E-06	-5.8856	1.82087E-02
H3BO3	.0	3.15300E-05	-4.5013	3.40515E-01
F-	-1.0	7.30695E-05	-4.1363	1.38688E+00
Li+	1.0	1.51144E-05	-4.8206	1.04779E-01
Br-	-1.0	3.60343E-06	-5.4433	2.87654E-01
DOX	.0	1.80171E-04	-3.7443	5.75978E+00

CNV-W3

****DESCRIPTION OF SOLUTION ****

	ANALYT.	COMP.	PH	ACTIVITY H2O = .9996
EPMCAT	11.20	11.03	8.170	PCO2= 3.506008E-03
EPMAN	11.60	11.43		LOG PCO2 = -2.4552

	TEMPERATURE	PO2 = 5.226147E-37
EH = .2310 PE = 3.971	20.00 DEG C	PCH4 = 1.216529E-76
PE CALC S = .000		CO2 TOT = 9.676200E-03
PE CALC DOX= 12.835	IONIC STRENGTH	DENSITY = 1.0000
PE SATO DOX= 2.279	1.225774E-02	TDS = 950.8MG/L
TOT ALK = 9.660E+00 MEQ		CARB ALK = 9.635E+00 MEQ
ELECT = -3.995E-01 MEQ		CHARGE IMBALANCE = -1.8%

IN COMPUTING THE DISTRIBUTION OF SPECIES,
PE = 3.971 EQUIVALENT EH = .231VOLTS

DISTRIBUTION OF SPECIES

I	SPECIES		MOLALITY	ACTIVITY	LOG ACT	GAMMA
1	H+	1.	7.4522E-09	6.7608E-09	-8.170	9.0723E-01
2	E-	-1.	1.0683E-04	1.0683E-04	-3.971	1.0000E+00
4	Ca+2	2.	1.0448E-04	6.7789E-05	-4.169	6.4879E-01
5	Mg+2	2.	2.7285E-05	1.7837E-05	-4.749	6.5374E-01
6	Na+	1.	1.0687E-02	9.5675E-03	-2.019	8.9523E-01
7	K+	1.	5.5861E-05	4.9833E-05	-4.302	8.9209E-01
8	Fe+2	2.	7.3112E-08	4.7834E-08	-7.320	6.5425E-01
9	Mn+2	2.	1.1712E-07	7.6627E-08	-7.116	6.5425E-01
12	Sr+2	2.	2.1584E-06	1.4034E-06	-5.853	6.5024E-01
13	H4SiO4	0.	1.7362E-04	1.7411E-04	-3.759	1.0028E+00
14	Cl-	-1.	1.4814E-04	1.3216E-04	-3.879	8.9209E-01
15	CO3-2	-2.	8.0901E-05	5.2522E-05	-4.280	6.4922E-01
16	SO4-2	-2.	8.0585E-04	5.1981E-04	-3.284	6.4505E-01
17	NO3-	-1.	1.9040E-11	1.6947E-11	-10.771	8.9005E-01
18	H3BO3	0.	2.9005E-05	2.9087E-05	-4.536	1.0028E+00
20	F-	-1.	7.2597E-05	6.4736E-05	-4.189	8.9172E-01
21	Li+	1.	1.5080E-05	1.3562E-05	-4.868	8.9937E-01
22	Br-	-1.	3.6034E-06	3.2072E-06	-5.494	8.9005E-01
28	DOX	0.	1.8017E-04	1.8068E-04	-3.743	1.0028E+00
31	OH-	-1.	1.1257E-06	1.0038E-06	-5.998	8.9172E-01
33	H2 AQ	0.	3.8742E-28	3.8851E-28	-27.411	1.0028E+00
34	HCO3-	-1.	9.3932E-03	8.4316E-03	-2.074	8.9763E-01
35	H2CO3	0.	1.3700E-04	1.3739E-04	-3.862	1.0028E+00
40	HSO4-	-1.	3.4345E-10	3.0706E-10	-9.513	8.9404E-01
48	NO2-	-1.	1.3012E-06	1.1581E-06	-5.936	8.9005E-01
57	H2BO3-	-1.	2.5237E-06	2.2563E-06	-5.647	8.9404E-01
58	BFOH3-	-1.	7.9499E-10	7.1076E-10	-9.148	8.9404E-01
59	BF2OH2-	-1.	3.7547E-14	3.3568E-14	-13.474	8.9404E-01
60	BF3OH-	-1.	1.9783E-20	1.7687E-20	-19.752	8.9404E-01
61	BF4-	-1.	3.5522E-26	3.1758E-26	-25.498	8.9404E-01
69	HF AQ	0.	5.9875E-10	6.0045E-10	-9.222	1.0028E+00
70	HF2-	-1.	1.5997E-13	1.4302E-13	-12.845	8.9404E-01
75	CaOH+	1.	1.8605E-09	1.6634E-09	-8.779	8.9404E-01
76	CaCO3	0.	5.4454E-06	5.4608E-06	-5.263	1.0028E+00
77	CaHCO3+	1.	7.4627E-06	6.6987E-06	-5.174	8.9763E-01
78	CaSO4	0.	6.6857E-06	6.7046E-06	-5.174	1.0028E+00
79	CaHSO4	1.	3.1163E-13	2.7861E-13	-12.555	8.9404E-01
83	CaF+	1.	3.7969E-08	3.3946E-08	-7.469	8.9404E-01
85	MgOH+	1.	1.0710E-08	9.5756E-09	-8.019	8.9404E-01
86	MgCO3	0.	8.2558E-07	8.2791E-07	-6.082	1.0028E+00
87	MgHCO3+	1.	1.9301E-06	1.7256E-06	-5.763	8.9404E-01

88	MgSO4	0.	1.9014E-06	1.9067E-06	-5.720	1.0028E+00
92	MgF+	1.	7.7823E-08	6.9577E-08	-7.158	8.9404E-01
93	NaOH	0.	9.3198E-09	9.3462E-09	-8.029	1.0028E+00
94	NaCO3-	-1.	8.0982E-06	7.2401E-06	-5.140	8.9404E-01
95	NaHCO3	0.	4.0636E-05	4.0751E-05	-4.390	1.0028E+00
96	NaSO4-	-1.	2.6995E-05	2.4135E-05	-4.617	8.9404E-01
98	NaF aq	0.	3.5540E-07	3.5640E-07	-6.448	1.0028E+00
99	KOH	0.	2.5476E-11	2.5548E-11	-10.593	1.0028E+00
100	KSO4-	-1.	1.9225E-07	1.7188E-07	-6.765	8.9404E-01
102	FeOH+	1.	1.7107E-09	1.5295E-09	-8.815	8.9404E-01
105	FeCl+	1.	9.7603E-12	8.7261E-12	-11.059	8.9404E-01
106	FeCO3	0.	6.0097E-08	6.0267E-08	-7.220	1.0028E+00
107	FeHCO3+	1.	4.0525E-08	3.6231E-08	-7.441	8.9404E-01
108	FeSO4	0.	4.0177E-09	4.0290E-09	-8.395	1.0028E+00
109	FeHSO4+	1.	2.1990E-16	1.9660E-16	-15.706	8.9404E-01
114	FeF+	1.	3.4636E-11	3.0966E-11	-10.509	8.9404E-01
115	Fe+3	3.	7.7723E-17	3.2360E-17	-16.490	4.1635E-01
117	FeOH+2	2.	3.5842E-11	2.2899E-11	-10.640	6.3890E-01
118	FeOH2+	1.	1.0340E-06	9.2447E-07	-6.034	8.9404E-01
119	FeOH3	0.	1.4068E-05	1.4108E-05	-4.851	1.0028E+00
120	FeOH4-	-1.	1.7345E-06	1.5507E-06	-5.809	8.9404E-01
121	Fe2OH2+4	4.	1.0451E-19	1.7414E-20	-19.759	1.6662E-01
122	Fe3OH4+5	5.	8.8437E-23	5.3776E-24	-23.269	6.0807E-02
123	FeCl+2	2.	1.7205E-19	1.0992E-19	-18.959	6.3890E-01
124	FeCl2+	1.	8.5275E-23	7.6239E-23	-22.118	8.9404E-01
125	FeCl3	0.	1.0047E-27	1.0075E-27	-26.997	1.0028E+00
126	FeSO4+	1.	1.8434E-16	1.6480E-16	-15.783	8.9404E-01
127	FeHSO4+2	2.	6.9094E-24	4.4144E-24	-23.355	6.3890E-01
128	FeSO42-	-1.	2.0551E-18	1.8373E-18	-17.736	8.9404E-01
131	FeF+2	2.	4.8080E-15	3.0718E-15	-14.513	6.3890E-01
132	FeF2+	1.	8.3354E-15	7.4522E-15	-14.128	8.9404E-01
133	FeF3	0.	7.4938E-16	7.5150E-16	-15.124	1.0028E+00
134	MnOH	1.	2.1519E-10	1.9239E-10	-9.716	8.9404E-01
136	MnCl+	1.	4.6143E-11	4.1254E-11	-10.385	8.9404E-01
137	MnCl2	0.	2.3732E-15	2.3799E-15	-14.623	1.0028E+00
138	MnCl3-	-1.	9.6890E-20	8.6624E-20	-19.062	8.9404E-01
139	MnCO3	0.	3.1879E-07	3.1969E-07	-6.495	1.0028E+00
140	MnHCO3+	1.	5.7858E-08	5.1728E-08	-7.286	8.9404E-01
141	MnSO4	0.	6.4101E-09	6.4283E-09	-8.192	1.0028E+00
142	Mn(NO3)2	0.	8.8364E-29	8.8614E-29	-28.052	1.0028E+00
143	MnF+	1.	3.8386E-11	3.4318E-11	-10.464	8.9404E-01
144	Mn+3	3.	2.8900E-29	1.0547E-29	-28.977	3.6494E-01
164	H3SiO4-	-1.	3.5487E-06	3.1727E-06	-5.499	8.9404E-01
165	H2SiO4-2	-2.	3.5725E-11	2.2825E-11	-10.642	6.3890E-01
166	SiF6-2	-2.	1.0144E-31	6.4808E-32	-31.188	6.3890E-01
176	SrOH+	1.	1.1872E-11	1.0642E-11	-10.973	8.9644E-01
177	SrHCO3+	1.	1.6993E-07	1.5253E-07	-6.817	8.9763E-01
178	SrCO3	0.	4.0481E-08	4.0596E-08	-7.392	1.0028E+00
179	SrSO4	0.	1.3360E-07	1.3398E-07	-6.873	1.0028E+00
180	LiOH	0.	4.5809E-11	4.5938E-11	-10.338	1.0028E+00
181	LiSO4-	-1.	3.4421E-08	3.0774E-08	-7.512	8.9404E-01

PHASE	IAP	KT	LOG IAP	LOG KT	IAP/KT	LOG IAP/KT
1 Calcite	3.560E-09	3.521E-09	-8.448	-8.453	1.011E+00	.005
2 Aragonit	3.560E-09	4.945E-09	-8.448	-8.306	7.201E-01	-.143
3 Dolomite	3.336E-18	1.067E-17	-17.477	-16.972	3.128E-01	-.505
4 Siderite	2.512E-12	1.384E-11	-11.600	-10.859	1.816E-01	-.741
5 Rhodochr	4.025E-12	7.725E-12	-11.395	-11.112	5.210E-01	-.283
6 Strontit	7.371E-11	5.382E-10	-10.132	-9.269	1.370E-01	-.863
8 Gypsum	3.521E-08	2.623E-05	-7.453	-4.581	1.342E-03	-2.872
9 Anhydrit	3.524E-08	4.531E-05	-7.453	-4.344	7.778E-04	-3.109
10 Celestit	7.295E-10	2.385E-07	-9.137	-6.623	3.059E-03	-2.514
13 Fluorite	2.841E-13	2.188E-11	-12.547	-10.660	1.298E-02	-1.887
14 SiO2 (a)	1.742E-04	1.764E-03	-3.759	-2.754	9.880E-02	-1.005
15 Chalcedy	1.742E-04	2.453E-04	-3.759	-3.610	.104E-01	-.148
16 Quartz	1.742E-04	8.805E-05	-3.759	-4.055	1.979E+00	.296
26 Talc	5.469E+19	9.517E+21	19.738	21.979	5.747E-03	-2.241
28 Chrysotl	1.801E+27	6.776E+32	27.255	32.831	2.658E-06	-5.576
29 Sepiol c	8.039E+11	7.830E+15	11.905	15.894	1.027E-04	-3.989
30 Sepiol d	8.039E+11	4.571E+18	11.905	18.660	1.759E-07	-6.755
31 Hematite	1.095E+16	2.386E-04	16.040	3.622	4.591E+19	19.662
32 Goethite	1.046E+08	1.000E-01	8.020	-1.000	1.046E+09	9.020
33 Fe(OH)3a	1.046E+08	7.780E+04	8.020	4.891	1.344E+03	3.129
38 Pyrolusi	3.211E+33	1.563E+42	33.507	42.194	2.054E-09	-8.687
39 Hausmani	9.017E+51	1.942E+62	51.955	62.288	4.644E-11	-10.333
40 Manganit	2.319E+21	2.188E+25	21.365	25.340	1.060E-04	-3.975
41 Pyrochro	1.675E+09	1.585E+15	9.224	15.200	1.057E-06	-5.976
42 PCO2	1.374E-04	3.919E-02	-3.862	-1.407	3.506E-03	-2.455
43 O2 gas	6.305E-40	1.156E-03	-39.200	-2.937	5.453E-37	-36.263
44 H2 gas	3.885E-28	7.447E-04	-27.411	-3.128	5.217E-25	-24.283
49 Melanter	2.480E-11	5.349E-03	-10.606	-2.272	4.636E-09	-8.334
51 K-Jarosi	4.767E-12	1.517E-09	-11.322	-8.819	3.142E-03	-2.503

1CNV-W5

INITIAL SOLUTION

TEMPERATURE = 20.00 DEGREES C PH = 8.460
ANALYTICAL EPMCAT = 16.975 ANALYTICAL EPMAN = 17.219

***** OXIDATION - REDUCTION *****

DISSOLVED OXYGEN = .010 MMOLES/KG H2O
EH MEASURED WITH CALOMEL = 9.9000 VOLTS
MEASURED EH OF ZOBELL SOLUTION = 9.9000 VOLTS
CORRECTED EH = .2330 VOLTS
PE COMPUTED FROM CORRECTED EH = 4.006

FLAG	CORALK	PECALC	IDAVES
0	2	1	0

*** TOTAL CONCENTRATIONS OF INPUT SPECIES ***

SPECIES		TOTAL MOLALITY	LOG TOTAL MOLALITY	TOTAL MG/LITRE
Ca+2	2.0	4.35575E-04	-3.3609	1.74348E+01
Mg+2	2.0	2.72360E-04	-3.5649	6.61286E+00
Na+	1.0	1.54664E-02	-1.8106	3.55100E+02
K+	1.0	4.40582E-05	-4.3560	1.72049E+00
Mn+2	2.0	1.00132E-07	-6.9994	5.49380E-03
Sr+2	2.0	6.40846E-06	-5.1932	5.60768E-01
H4SiO4	.0	1.41186E-04	-3.8502	8.47196E+00
Cl-	-1.0	3.15417E-04	-3.5011	1.11677E+01
HCO3-	-1.0	8.91277E-03	-2.0500	5.43115E+02
SO4-2	-2.0	3.86110E-03	-2.4133	3.70414E+02
NO3-	-1.0	1.10145E-06	-5.9580	1.54074E-02
H3BO3	.0	6.06801E-05	-4.2170	6.55086E-01
F-	-1.0	2.38315E-04	-3.6228	4.52162E+00
Li+	1.0	1.30172E-05	-4.8855	9.02070E-02
Br-	-1.0	3.80502E-06	-5.4196	3.03635E-01
DOX	.0	1.00132E-05	-4.9994	3.19988E-01

CNV-W5

****DESCRIPTION OF SOLUTION ****

	ANALYT.	COMP.		
EPMCAT	16.97	16.35	PH 8.460	ACTIVITY H2O = .9995
EPMAN	17.22	16.76		PCO2= 1.596351E-03
				LOG PCO2 = -2.7969
			TEMPERATURE	PO2 = 1.036589E-35
EH = .2330	PE = 4.006		20.00 DEG C	PCH4 = 1.407603E-79
PE CALC S =	.000			CO2 TOT = 8.912769E-03
PE CALC DOX= 12.232			IONIC STRENGTH	DENSITY = 1.0000
PE SATO DOX= 1.675			2.083821E-02	TDS = 1320.5MG/L
TOT ALK = 9.078E+00 MEQ				CARB ALK = 9.061E+00 MEQ
ELECT = -4.069E-01 MEQ				CHARGE IMBALANCE = -1.2%

IN COMPUTING THE DISTRIBUTION OF SPECIES,
PE = 4.006 EQUIVALENT EH = .233VOLTS

DISTRIBUTION OF SPECIES

I	SPECIES		MOLALITY	ACTIVITY	LOG ACT	GAMMA
1	H+	1.	3.9020E-09	3.4674E-09	-8.460	8.8860E-01
2	E-	-1.	9.8701E-05	9.8701E-05	-4.006	1.0000E+00
4	Ca+2	2.	3.1784E-04	1.8581E-04	-3.731	5.8460E-01
5	Mg+2	2.	1.9940E-04	1.1797E-04	-3.928	5.9160E-01

6	Na+	1.	1.5241E-02	1.3277E-02	-1.877	8.7109E-01
7	K+	1.	4.3462E-05	3.7643E-05	-4.424	8.6610E-01
9	Mn+2	2.	1.7080E-08	1.0107E-08	-7.995	5.9175E-01
12	Sr+2	2.	4.8687E-06	2.8555E-06	-5.544	5.8651E-01
13	H4SiO4	0.	1.3562E-04	1.3627E-04	-3.866	1.0048E+00
14	Cl-	-1.	3.1542E-04	2.7318E-04	-3.564	8.6610E-01
15	CO3-2	-2.	1.5546E-04	9.0909E-05	-4.041	5.8477E-01
16	SO4-2	-2.	3.5826E-03	2.0739E-03	-2.683	5.7888E-01
17	NO3-	-1.	7.1775E-11	6.1934E-11	-10.208	8.6288E-01
18	H3BO3	0.	5.1648E-05	5.1896E-05	-4.285	1.0048E+00
20	F-	-1.	2.3477E-04	2.0318E-04	-3.692	8.6547E-01
21	Li+	1.	1.2899E-05	1.1314E-05	-4.946	8.7707E-01
22	Br-	-1.	3.8050E-06	3.2833E-06	-5.484	8.6288E-01
28	DOX	0.	1.0013E-05	1.0061E-05	-4.997	1.0048E+00
31	OH-	-1.	2.2612E-06	1.9570E-06	-5.708	8.6547E-01
32	O2 AQ	0.	1.2445E-38	1.2505E-38	-37.903	1.0048E+00
33	H2 AQ	0.	8.6807E-29	8.7224E-29	-28.059	1.0048E+00
34	HCO3-	-1.	8.5591E-03	7.4847E-03	-2.126	8.7447E-01
35	H2CO3	0.	6.2255E-05	6.2555E-05	-4.204	1.0048E+00
40	HSO4-	-1.	7.2262E-10	6.2829E-10	-9.202	8.6947E-01
48	NO2-	-1.	1.1014E-06	9.5037E-07	-6.022	8.6288E-01
57	H2BO3-	-1.	9.0277E-06	7.8493E-06	-5.105	8.6947E-01
58	BFOH3-	-1.	4.5777E-09	3.9801E-09	-8.400	8.6947E-01
59	BF2OH2-	-1.	3.4806E-13	3.0263E-13	-12.519	8.6947E-01
60	BF3OH-	-1.	2.9524E-19	2.5670E-19	-18.591	8.6947E-01
61	BF4-	-1.	8.5345E-25	7.4204E-25	-24.130	8.6947E-01
69	HF AQ	0.	9.6192E-10	9.6654E-10	-9.015	1.0048E+00
70	HF2-	-1.	8.3108E-13	7.2260E-13	-12.141	8.6947E-01
75	CaOH+	1.	1.0223E-08	8.8889E-09	-8.051	8.6947E-01
76	CaCO3	0.	2.5783E-05	2.5907E-05	-4.587	1.0048E+00
77	CaHCO3+	1.	1.8639E-05	1.6299E-05	-4.788	8.7447E-01
78	CaSO4	0.	7.2969E-05	7.3320E-05	-4.135	1.0048E+00
79	CaHSO4	1.	1.7972E-12	1.5626E-12	-11.806	8.6947E-01
83	CaF+	1.	3.3589E-07	2.9204E-07	-6.535	8.6947E-01
85	MgOH+	1.	1.4200E-07	1.2347E-07	-6.908	8.6947E-01
86	MgCO3	0.	9.4318E-06	9.4772E-06	-5.023	1.0048E+00
87	MgHCO3+	1.	1.1651E-05	1.0131E-05	-4.994	8.6947E-01
88	MgSO4	0.	5.0070E-05	5.0311E-05	-4.298	1.0048E+00
92	MgF+	1.	1.6611E-06	1.4443E-06	-5.840	8.6947E-01
93	NaOH	0.	2.5164E-08	2.5285E-08	-7.597	1.0048E+00
94	NaCO3-	-1.	2.0001E-05	1.7390E-05	-4.760	8.6947E-01
95	NaHCO3	0.	4.9958E-05	5.0198E-05	-4.299	1.0048E+00
96	NaSO4-	-1.	1.5368E-04	1.3362E-04	-3.874	8.6947E-01
98	NaF aq	0.	1.5449E-06	1.5523E-06	-5.809	1.0048E+00
99	KOH	0.	3.7444E-11	3.7624E-11	-10.425	1.0048E+00
100	KSO4-	-1.	5.9577E-07	5.1800E-07	-6.286	8.6947E-01
134	MnOH+	1.	5.6901E-11	4.9473E-11	-10.306	8.6947E-01
136	MnCl+	1.	1.2936E-11	1.1248E-11	-10.949	8.6947E-01
137	MnCl2	0.	1.3349E-15	1.3413E-15	-14.872	1.0048E+00
138	MnCl3-	-1.	1.1607E-19	1.0092E-19	-18.996	8.6947E-01
139	MnCO3	0.	7.2634E-08	7.2983E-08	-7.137	1.0048E+00
140	MnHCO3+	1.	6.9658E-09	6.0565E-09	-8.218	8.6947E-01
141	MnSO4	0.	3.3666E-09	3.3827E-09	-8.471	1.0048E+00
142	Mn(NO3)2	0.	1.5536E-28	1.5611E-28	-27.807	1.0048E+00
143	MnF+	1.	1.6340E-11	1.4207E-11	-10.847	8.6947E-01
144	Mn+3	3.	5.3023E-30	1.5057E-30	-29.822	2.8397E-01
164	H3SiO4-	-1.	5.5687E-06	4.8418E-06	-5.315	8.6947E-01
165	H2SiO4-2	-2.	1.1884E-10	6.7918E-11	-10.168	5.7149E-01
166	SiF6-2	-2.	5.8734E-30	3.3566E-30	-29.474	5.7149E-01
176	SrOH+	1.	4.8374E-11	4.2215E-11	-10.375	8.7268E-01

177	SrHCO3+	1.	3.1505E-07	2.7550E-07	-6.560	8.7447E-01
178	SrCO3	0.	1.4228E-07	1.4297E-07	-6.845	1.0048E+00
179	SrSO4	0.	1.0824E-06	1.0876E-06	-5.964	1.0048E+00
180	LiOH	0.	7.4354E-11	7.4711E-11	-10.127	1.0048E+00
181	LiSO4-	-1.	1.1780E-07	1.0242E-07	-6.990	8.6947E-01

	PHASE	IAP	KT	LOG IAP	LOG KT	IAP/KT	LOG IAP/KT
1	Calcite	1.689E-08	3.521E-09	-7.772	-8.453	4.797E+00	.681
2	Aragonit	1.689E-08	4.945E-09	-7.772	-8.306	3.416E+00	.534
3	Dolomite	1.812E-16	1.067E-17	-15.742	-16.972	1.699E+01	1.230
5	Rhodochr	9.188E-13	7.725E-12	-12.037	-11.112	1.189E-01	-.925
6	Strontit	2.596E-10	5.382E-10	-9.586	-9.269	4.823E-01	-.317
8	Gypsum	3.850E-07	2.623E-05	-6.415	-4.581	1.467E-02	-1.833
9	Anhydrit	3.853E-07	4.531E-05	-6.414	-4.344	8.505E-03	-2.070
10	Celestit	5.922E-09	2.385E-07	-8.228	-6.623	2.483E-02	-1.605
13	Fluorite	7.671E-12	2.188E-11	-11.115	-10.660	3.506E-01	-.455
14	SiO2 (a)	1.364E-04	1.764E-03	-3.865	-2.754	7.735E-02	-1.112
15	Chalcedy	1.364E-04	2.453E-04	-3.865	-3.610	5.562E-01	-.255
16	Quartz	1.364E-04	8.805E-05	-3.865	-4.055	1.549E+00	.190
26	Talc	3.264E+23	9.517E+21	23.514	21.979	3.430E+01	1.535
28	Chrysotl	1.753E+31	6.776E+32	31.244	32.831	2.587E-02	-1.587
29	Sepiol c	2.437E+14	7.830E+15	14.387	15.894	3.112E-02	-1.507
30	Sepiol d	2.437E+14	4.571E+18	14.387	18.660	5.331E-05	-4.273
38	Pyrolusi	7.170E+33	1.563E+42	33.856	42.194	4.587E-09	-8.338
39	Hausmani	5.062E+51	1.942E+62	51.704	62.288	2.607E-11	-10.584
40	Manganit	2.454E+21	2.188E+25	21.390	25.340	1.122E-04	-3.950
41	Pyrochro	8.398E+08	1.585E+15	8.924	15.200	5.299E-07	-6.276
42	PCO2	6.255E-05	3.919E-02	-4.204	-1.407	1.596E-03	-2.797
43	O2 gas	1.251E-38	1.156E-03	-37.903	-2.937	1.082E-35	-34.966
44	H2 gas	8.722E-29	7.447E-04	-28.059	-3.128	1.171E-25	-24.931

1MW-64

INITIAL SOLUTION

TEMPERATURE = 19.00 DEGREES C PH = 7.900
ANALYTICAL EPMCAT = 25.524 ANALYTICAL EPMAN = 20.395

***** OXIDATION - REDUCTION *****

DISSOLVED OXYGEN = .000 MMOLES/KG H2O
EH MEASURED WITH CALOMEL = 9.9000 VOLTS
MEASURED EH OF ZOBELL SOLUTION = 9.9000 VOLTS
CORRECTED EH = .0000 VOLTS
PE COMPUTED FROM CORRECTED EH = .000

FLAG	CORALK	PECALC	IDAVES
0	2	1	0

*** TOTAL CONCENTRATIONS OF INPUT SPECIES ***

SPECIES		TOTAL MOLALITY	LOG TOTAL MOLALITY	TOTAL MG/LITRE
Ca+2	2.0	1.99339E-04	-3.7004	7.97592E+00
Mg+2	2.0	1.16197E-04	-3.9348	2.82019E+00
Na+	1.0	2.47631E-02	-1.6062	5.68331E+02
K+	1.0	8.61464E-05	-4.0648	3.36277E+00
Mn+2	2.0	2.00340E-07	-6.6982	1.09876E-02
H4SiO4	.0	2.53431E-04	-3.5961	1.52015E+01
Cl-	-1.0	9.66642E-04	-3.0147	3.42121E+01
HCO3-	-1.0	1.07673E-02	-1.9679	6.55875E+02
SO4-2	-2.0	4.26825E-03	-2.3698	4.09318E+02
NO3-	-1.0	6.31072E-06	-5.1999	8.82422E-02
F-	-1.0	8.11378E-05	-4.0908	1.53887E+00
Br-	-1.0	1.40238E-06	-5.8531	1.11866E-01

MW-64

****DESCRIPTION OF SOLUTION ****

	ANALYT.	COMP.		
EPMCAT	25.52	24.94	PH 7.900	ACTIVITY H2O = .9993
EPMAN	20.39	19.63		PCO2= 6.803365E-03
				LOG PCO2 = -2.1673
			TEMPERATURE	PO2 = 2.515602E-54
EH = .0000	PE = .000		19.00 DEG C	PCH4 = 2.858993E-42
PE CALC S =	.000			CO2 TOT = 1.076729E-02
PE CALC DOX=	.000		IONIC STRENGTH	DENSITY = 1.0000
PE SATO DOX=	.000		2.657080E-02	TDS = 1698.8MG/L
TOT ALK =	1.056E+01 MEQ			CARB ALK = 1.056E+01 MEQ
ELECT =	5.324E+00 MEQ			CHARGE IMBALANCE = 11.9%

IN COMPUTING THE DISTRIBUTION OF SPECIES,
PE = .000 EQUIVALENT EH = .000VOLTS

DISTRIBUTION OF SPECIES

I	SPECIES		MOLALITY	ACTIVITY	LOG ACT	GAMMA
1	H+	1.	1.4312E-08	1.2589E-08	-7.900	8.7966E-01
2	E-	-1.	1.0000E+00	1.0000E+00	.000	1.0000E+00
4	Ca+2	2.	1.5153E-04	8.4055E-05	-4.075	5.5473E-01
5	Mg+2	2.	8.7590E-05	4.9299E-05	-4.307	5.6284E-01
6	Na+	1.	2.4405E-02	2.0967E-02	-1.678	8.5912E-01
7	K+	1.	8.4947E-05	7.2456E-05	-4.140	8.5296E-01
9	Mn+2	2.	6.8020E-08	3.8270E-08	-7.417	5.6263E-01
13	H4SiO4	0.	2.5066E-04	2.5220E-04	-3.598	1.0061E+00
14	Cl-	-1.	9.6664E-04	8.2451E-04	-3.084	8.5296E-01
15	CO3-2	-2.	5.2484E-05	2.9110E-05	-4.536	5.5464E-01
16	SO4-2	-2.	3.9561E-03	2.1672E-03	-2.664	5.4781E-01
17	NO3-	-1.	2.3497E-19	1.9950E-19	-18.700	8.4905E-01

20	F-	-1.	8.0036E-05	6.8205E-05	-4.166	8.5218E-01
22	Br-	-1.	1.4024E-06	1.1907E-06	-5.924	8.4905E-01
31	OH-	-1.	5.8367E-07	4.9739E-07	-6.303	8.5218E-01
33	H2 AQ	0.	1.1853E-19	1.1926E-19	-18.924	1.0061E+00
34	HCO3-	-1.	1.0320E-02	8.9057E-03	-2.050	8.6298E-01
35	H2CO3	0.	2.7290E-04	2.7457E-04	-3.561	1.0061E+00
40	HSO4-	-1.	2.7234E-09	2.3348E-09	-8.632	8.5730E-01
48	NO2-	-1.	6.3107E-06	5.3581E-06	-5.271	8.4905E-01
69	HF AQ	0.	1.1504E-09	1.1575E-09	-8.936	1.0061E+00
70	HF2-	-1.	3.3574E-13	2.8783E-13	-12.541	8.5730E-01
75	CaOH+	1.	1.2916E-09	1.1073E-09	-8.956	8.5730E-01
76	CaCO3	0.	3.6714E-06	3.6940E-06	-5.433	1.0061E+00
77	CaHCO3+	1.	9.9725E-06	8.6061E-06	-5.065	8.6298E-01
78	CaSO4	0.	3.4117E-05	3.4326E-05	-4.464	1.0061E+00
79	CaHSO4	1.	3.1285E-12	2.6820E-12	-11.572	8.5730E-01
83	CaF+	1.	5.0493E-08	4.3287E-08	-7.364	8.5730E-01
85	MgOH+	1.	1.6573E-08	1.4208E-08	-7.847	8.5730E-01
86	MgCO3	0.	1.2412E-06	1.2489E-06	-5.903	1.0061E+00
87	MgHCO3+	1.	5.8567E-06	5.0209E-06	-5.299	8.5730E-01
88	MgSO4	0.	2.1261E-05	2.1392E-05	-4.670	1.0061E+00
92	MgF+	1.	2.3193E-07	1.9883E-07	-6.702	8.5730E-01
93	NaOH	0.	1.0929E-08	1.0996E-08	-7.959	1.0061E+00
94	NaCO3-	-1.	9.7344E-06	8.3453E-06	-5.079	8.5730E-01
95	NaHCO3	0.	9.1604E-05	9.2167E-05	-4.035	1.0061E+00
96	NaSO4-	-1.	2.5553E-04	2.1907E-04	-3.659	8.5730E-01
98	NaF aq	0.	8.1790E-07	8.2291E-07	-6.085	1.0061E+00
99	KOH	0.	1.9821E-11	1.9942E-11	-10.700	1.0061E+00
100	KSO4-	-1.	1.1994E-06	1.0283E-06	-5.988	8.5730E-01
134	MnOH+	1.	5.5290E-11	4.7400E-11	-10.324	8.5730E-01
136	MnCl+	1.	1.4994E-10	1.2854E-10	-9.891	8.5730E-01
137	MnCl2	0.	4.5982E-14	4.6265E-14	-13.335	1.0061E+00
138	MnCl3-	-1.	1.2255E-17	1.0506E-17	-16.979	8.5730E-01
139	MnCO3	0.	8.7951E-08	8.8491E-08	-7.053	1.0061E+00
140	MnHCO3+	1.	3.1100E-08	2.6662E-08	-7.574	8.5730E-01
141	MnSO4	0.	1.3043E-08	1.3123E-08	-7.882	1.0061E+00
143	MnF+	1.	2.1064E-11	1.8058E-11	-10.743	8.5730E-01
144	Mn+3	3.	1.9332E-33	4.8358E-34	-33.316	2.5014E-01
164	H3SiO4-	-1.	2.7732E-06	2.3775E-06	-5.624	8.5730E-01
165	H2SiO4-2	-2.	1.5863E-11	8.5685E-12	-11.067	5.4016E-01
166	SiF6-2	-2.	3.1486E-30	1.7007E-30	-29.769	5.4016E-01

	PHASE	IAP	KT	LOG IAP	LOG KT	IAP/KT	LOG IAP/KT
1	Calcite	2.447E-09	3.561E-09	-8.611	-8.448	6.871E-01	-.163
2	Aragonit	2.447E-09	5.009E-09	-8.611	-8.300	4.885E-01	-.311
3	Dolomite	3.511E-18	1.127E-17	-17.455	-16.948	3.115E-01	-.507
5	Rhodochr	1.114E-12	7.790E-12	-11.953	-11.108	1.430E-01	-.845
8	Gypsum	1.819E-07	2.621E-05	-6.740	-4.582	6.941E-03	-2.159
9	Anhydrit	1.822E-07	4.556E-05	-6.740	-4.341	3.999E-03	-2.398
13	Fluorite	3.910E-13	2.125E-11	-12.408	-10.673	1.840E-02	-1.735
14	SiO2 (a)	2.525E-04	1.729E-03	-3.598	-2.762	1.460E-01	-.836
15	Chalcedy	2.525E-04	2.385E-04	-3.598	-3.622	1.059E+00	.025
16	Quartz	2.525E-04	8.500E-05	-3.598	-4.071	2.971E+00	.473
26	Talc	1.221E+20	1.250E+22	20.087	22.097	9.770E-03	-2.010
28	Chrysotl	1.913E+27	9.109E+32	27.282	32.959	2.100E-06	-5.678
29	Sepiol c	1.553E+12	8.338E+15	12.191	15.921	1.862E-04	-3.730

30 Sepiol d	1.553E+12	4.571E+18	12.191	18.660	3.397E-07	-6.469
38 Pyrolusi	1.521E+24	2.292E+42	24.182	42.360	6.639E-19	-18.178
39 Hausmani	8.859E+40	3.508E+62	40.947	62.545	2.525E-22	-21.598
40 Manganit	1.915E+16	2.188E+25	16.282	25.340	8.755E-10	-9.058
41 Pyrochro	2.411E+08	1.585E+15	8.382	15.200	1.521E-07	-6.818
42 PCO2	2.746E-04	4.036E-02	-3.561	-1.394	6.803E-03	-2.167
44 H2 gas	1.193E-19	7.525E-04	-18.924	-3.124	1.585E-16	-15.800

1MW-65

INITIAL SOLUTION

TEMPERATURE = 20.00 DEGREES C PH = 7.800
ANALYTICAL EPMCAT = 24.430 ANALYTICAL EPMAN = 25.137
***** OXIDATION - REDUCTION *****
DISSOLVED OXYGEN = .000 MMOLES/KG H2O
EH MEASURED WITH CALOMEL = 9.9000 VOLTS FLAG CORALK PECALC IDAVES
MEASURED EH OF ZOBELL SOLUTION = 9.9000 VOLTS 0 2 1 0
CORRECTED EH = .0000 VOLTS
PE COMPUTED FROM CORRECTED EH = .000

*** TOTAL CONCENTRATIONS OF INPUT SPECIES ***

SPECIES		TOTAL MOLALITY	LOG TOTAL MOLALITY	TOTAL MG/LITRE
Ca+2	2.0	2.51453E-04	-3.5995	1.00601E+01
Mg+2	2.0	4.02725E-04	-3.3950	9.77342E+00
Na+	1.0	2.29694E-02	-1.6389	5.27110E+02
K+	1.0	1.05189E-04	-3.9780	4.10571E+00
Fe+2	2.0	1.10198E-06	-5.9578	6.14317E-02
Mn+2	2.0	6.01082E-07	-6.2211	3.29628E-02
H4SiO4	.0	2.68484E-04	-3.5711	1.61027E+01
Cl-	-1.0	8.63154E-03	-2.0639	3.05463E+02
HCO3-	-1.0	1.09357E-02	-1.9612	6.66065E+02
SO4-2	-2.0	2.71389E-03	-2.5664	2.60231E+02
NO3-	-1.0	6.01082E-07	-6.2211	8.40402E-03
F-	-1.0	9.51714E-05	-4.0215	1.80485E+00
Br-	-1.0	5.00902E-07	-6.3002	3.99520E-02

MW-65

****DESCRIPTION OF SOLUTION ****

	ANALYT.	COMP.	PH	ACTIVITY H2O = .9992
EPMCAT	24.43	23.88	7.800	PCO2= 8.748353E-03
EPMAN	25.14	24.31		LOG PCO2 = -2.0581
			TEMPERATURE	PO2 = 2.252448E-54
EH = .0000	PE =	.000	20.00 DEG C	PCH4 = 1.632810E-41
PE CALC S =	.000			CO2 TOT = 1.093569E-02
PE CALC DOX=	.000	IONIC STRENGTH		DENSITY = 1.0000
PE SATO DOX=	.000	2.719894E-02		TDS = 1800.9MG/L
TOT ALK = 1.066E+01 MEQ				CARB ALK = 1.065E+01 MEQ
ELECT = -4.267E-01 MEQ				CHARGE IMBALANCE = -.9%

IN COMPUTING THE DISTRIBUTION OF SPECIES,
PE = .000 EQUIVALENT EH = .000VOLTS

DISTRIBUTION OF SPECIES

I	SPECIES		MOLALITY	ACTIVITY	LOG ACT	GAMMA
1	H+	1.	1.8039E-08	1.5849E-08	-7.800	8.7860E-01
2	E-	-1.	1.0000E+00	1.0000E+00	.000	1.0000E+00
4	Ca+2	2.	2.0466E-04	1.1283E-04	-3.948	5.5129E-01
5	Mg+2	2.	3.2560E-04	1.8218E-04	-3.740	5.5951E-01
6	Na+	1.	2.2723E-02	1.9490E-02	-1.710	8.5770E-01
7	K+	1.	1.0426E-04	8.8768E-05	-4.052	8.5142E-01
8	Fe+2	2.	5.5545E-07	3.1065E-07	-6.508	5.5928E-01
9	Mn+2	2.	2.2565E-07	1.2620E-07	-6.899	5.5928E-01
13	H4SiO4	0.	2.6605E-04	2.6772E-04	-3.572	1.0063E+00
14	Cl-	-1.	8.6315E-03	7.3491E-03	-2.134	8.5142E-01
15	CO3-2	-2.	4.3250E-05	2.3839E-05	-4.623	5.5118E-01
16	SO4-2	-2.	2.4843E-03	1.3521E-03	-2.869	5.4425E-01
17	NO3-	-1.	1.8260E-20	1.5474E-20	-19.810	8.4743E-01
20	F-	-1.	9.3188E-05	7.9268E-05	-4.101	8.5062E-01
22	Br-	-1.	5.0090E-07	4.2448E-07	-6.372	8.4743E-01
31	OH-	-1.	5.0320E-07	4.2803E-07	-6.369	8.5062E-01
33	H2 AQ	0.	1.8590E-19	1.8706E-19	-18.728	1.0063E+00
34	HCO3-	-1.	1.0412E-02	8.9711E-03	-2.047	8.6163E-01
35	H2CO3	0.	3.4067E-04	3.4281E-04	-3.465	1.0063E+00
40	HSO4-	-1.	2.1876E-09	1.8723E-09	-8.728	8.5586E-01
48	NO2-	-1.	6.0108E-07	5.0937E-07	-6.293	8.4743E-01
69	HF AQ	0.	1.7128E-09	1.7236E-09	-8.764	1.0063E+00
70	HF2-	-1.	5.8736E-13	5.0270E-13	-12.299	8.5586E-01
75	CaOH+	1.	1.3793E-09	1.1805E-09	-8.928	8.5586E-01
76	CaCO3	0.	4.0994E-06	4.1252E-06	-5.385	1.0063E+00
77	CaHCO3+	1.	1.3767E-05	1.1863E-05	-4.926	8.6163E-01
78	CaSO4	0.	2.8844E-05	2.9025E-05	-4.537	1.0063E+00
79	CaHSO4	1.	3.3037E-12	2.8275E-12	-11.549	8.5586E-01
83	CaF+	1.	8.0834E-08	6.9183E-08	-7.160	8.5586E-01
85	MgOH+	1.	4.8725E-08	4.1702E-08	-7.380	8.5586E-01
86	MgCO3	0.	3.8139E-06	3.8378E-06	-5.416	1.0063E+00
87	MgHCO3+	1.	2.1910E-05	1.8752E-05	-4.727	8.5586E-01
88	MgSO4	0.	5.0337E-05	5.0653E-05	-4.295	1.0063E+00
92	MgF+	1.	1.0167E-06	8.7013E-07	-6.060	8.5586E-01
93	NaOH	0.	8.0678E-09	8.1184E-09	-8.091	1.0063E+00
94	NaCO3-	-1.	7.8216E-06	6.6942E-06	-5.174	8.5586E-01

95	NaHCO3	0.	8.7775E-05	8.8327E-05	-4.054	1.0063E+00
96	NaSO4-	-1.	1.4942E-04	1.2788E-04	-3.893	8.5586E-01
98	NaF aq	0.	8.8347E-07	8.8902E-07	-6.051	1.0063E+00
99	KOH	0.	1.9284E-11	1.9405E-11	-10.712	1.0063E+00
100	KSO4-	-1.	9.3051E-07	7.9639E-07	-6.099	8.5586E-01
102	FeOH+	1.	4.9488E-09	4.2355E-09	-8.373	8.5586E-01
105	FeCl+	1.	3.6822E-09	3.1514E-09	-8.501	8.5586E-01
106	FeCO3	0.	1.7654E-07	1.7765E-07	-6.750	1.0063E+00
107	FeHCO3+	1.	2.9252E-07	2.5035E-07	-6.601	8.5586E-01
108	FeSO4	0.	6.7634E-08	6.8059E-08	-7.167	1.0063E+00
109	FeHSO4+	1.	9.0964E-15	7.7852E-15	-14.109	8.5586E-01
114	FeF+	1.	2.8772E-10	2.4625E-10	-9.609	8.5586E-01
115	Fe+3	3.	7.1965E-20	2.2452E-20	-19.649	3.1198E-01
117	FeOH+2	2.	1.2626E-14	6.7747E-15	-14.169	5.3655E-01
118	FeOH2+	1.	1.3626E-10	1.1662E-10	-9.933	8.5586E-01
119	FeOH3	0.	7.5414E-10	7.5888E-10	-9.120	1.0063E+00
120	FeOH4-	-1.	4.1559E-11	3.5569E-11	-10.449	8.5586E-01
121	Fe2OH2+4	4.	1.8391E-26	1.5242E-27	-26.817	8.2878E-02
122	Fe3OH4+5	5.	2.9077E-33	5.9376E-35	-34.226	2.0420E-02
123	FeCl+2	2.	7.9042E-21	4.2410E-21	-20.373	5.3655E-01
124	FeCl2+	1.	1.9112E-22	1.6357E-22	-21.786	8.5586E-01
125	FeCl3	0.	1.1946E-25	1.2021E-25	-24.920	1.0063E+00
126	FeSO4+	1.	3.4751E-19	2.9742E-19	-18.527	8.5586E-01
127	FeHSO4+2	2.	3.4807E-26	1.8675E-26	-25.729	5.3655E-01
128	FeSO42-	-1.	1.0077E-20	8.6245E-21	-20.064	8.5586E-01
131	FeF+2	2.	4.8639E-18	2.6097E-18	-17.583	5.3655E-01
132	FeF2+	1.	9.0580E-18	7.7524E-18	-17.111	8.5586E-01
133	FeF3	0.	9.5128E-19	9.5726E-19	-18.019	1.0063E+00
134	MnOH+	1.	1.5787E-10	1.3511E-10	-9.869	8.5586E-01
136	MnCl+	1.	4.4147E-09	3.7784E-09	-8.423	8.5586E-01
137	MnCl2	0.	1.2045E-11	1.2121E-11	-10.916	1.0063E+00
138	MnCl3-	-1.	2.8666E-14	2.4534E-14	-13.610	8.5586E-01
139	MnCO3	0.	2.3748E-07	2.3898E-07	-6.622	1.0063E+00
140	MnHCO3+	1.	1.0591E-07	9.0647E-08	-7.043	8.5586E-01
141	MnSO4	0.	2.7366E-08	2.7538E-08	-7.560	1.0063E+00
143	MnF+	1.	8.0866E-11	6.9210E-11	-10.160	8.5586E-01
144	Mn+3	3.	7.5317E-33	1.8557E-33	-32.731	2.4639E-01
164	H3SiO4-	-1.	2.4316E-06	2.0811E-06	-5.682	8.5586E-01
165	H2SiO4-2	-2.	1.1903E-11	6.3866E-12	-11.195	5.3655E-01
166	SiF6-2	-2.	1.8937E-29	1.0161E-29	-28.993	5.3655E-01

	PHASE	IAP	KT	LOG IAP	LOG KT	IAP/KT	LOG IAP/KT
1	Calcite	2.690E-09	3.521E-09	-8.570	-8.453	7.638E-01	-.117
2	Aragonit	2.690E-09	4.945E-09	-8.570	-8.306	5.439E-01	-.264
3	Dolomite	1.168E-17	1.067E-17	-16.933	-16.972	1.095E+00	.039
4	Siderite	7.405E-12	1.384E-11	-11.130	-10.859	5.352E-01	-.271
5	Rhodochr	3.009E-12	7.725E-12	-11.522	-11.112	3.895E-01	-.410
8	Gypsum	1.523E-07	2.623E-05	-6.817	-4.581	5.806E-03	-2.236
9	Anhydrit	1.525E-07	4.531E-05	-6.817	-4.344	3.367E-03	-2.473
13	Fluorite	7.089E-13	2.188E-11	-12.149	-10.660	3.240E-02	-1.489
14	SiO2 (a)	2.681E-04	1.764E-03	-3.572	-2.754	1.520E-01	-.818
15	Chalcedy	2.681E-04	2.453E-04	-3.572	-3.610	1.093E+00	.039
16	Quartz	2.681E-04	8.805E-05	-3.572	-4.055	3.045E+00	.484
26	Talc	1.966E+21	9.517E+21	21.294	21.979	2.066E-01	-.685
28	Chrysotl	2.732E+28	6.776E+32	28.437	32.831	4.032E-05	-4.394
29	Sepiol c	1.010E+13	7.830E+15	13.004	15.894	1.290E-03	-2.890

30 Sepiol d	1.010E+13	4.571E+18	13.004	18.660	2.209E-06	-5.656
31 Hematite	3.173E+07	2.386E-04	7.501	-3.622	1.330E+11	11.124
32 Goethite	5.631E+03	1.000E-01	3.751	-1.000	5.631E+04	4.751
33 Fe(OH)3a	5.626E+03	7.780E+04	3.750	4.891	7.232E-02	-1.141
38 Pyrolusi	1.997E+24	1.563E+42	24.300	42.194	1.278E-18	-17.894
39 Hausmani	5.033E+41	1.942E+62	41.702	62.288	2.592E-21	-20.586
40 Manganit	3.165E+16	2.188E+25	16.500	25.340	1.447E-09	-8.840
41 Pyrochro	5.016E+08	1.585E+15	8.700	15.200	3.165E-07	-6.500
42 PCO2	3.428E-04	3.919E-02	-3.465	-1.407	8.748E-03	-2.058
44 H2 gas	1.871E-19	7.447E-04	-18.728	-3.128	2.512E-16	-15.600
49 Melanter	4.177E-10	5.349E-03	-9.379	-2.272	7.809E-08	-7.107
51 K-Jarosi	1.153E-22	1.517E-09	-21.938	-8.819	7.601E-14	-13.119

1MW-60

INITIAL SOLUTION

TEMPERATURE = 19.00 DEGREES C PH = 8.100
ANALYTICAL EPMCAT = 25.539 ANALYTICAL EPMAN = 25.964
***** OXIDATION - REDUCTION *****
DISSOLVED OXYGEN = .000 MMOLES/KG H2O
EH MEASURED WITH CALOMEL = 9.9000 VOLTS FLAG CORALK PECALC IDAVES
MEASURED EH OF ZOBELL SOLUTION = 9.9000 VOLTS 0 2 1 0
CORRECTED EH = .0000 VOLTS
PE COMPUTED FROM CORRECTED EH = .000

*** TOTAL CONCENTRATIONS OF INPUT SPECIES ***

SPECIES		TOTAL MOLALITY	LOG TOTAL MOLALITY	TOTAL MG/LITRE
Ca+2	2.0	1.99395E-04	-3.7003	7.97592E+00
Mg+2	2.0	1.16230E-04	-3.9347	2.82019E+00
Na+	1.0	2.47701E-02	-1.6061	5.68331E+02
K+	1.0	8.61708E-05	-4.0646	3.36277E+00
Mn+2	2.0	4.00795E-07	-6.3971	2.19752E-02
H4SiO4	.0	2.70536E-04	-3.5678	1.62229E+01
Cl-	-1.0	1.20539E-03	-2.9189	4.26500E+01
HCO3-	-1.0	1.23224E-02	-1.9093	7.50391E+02
SO4-2	-2.0	6.14218E-03	-2.2117	5.88858E+02
F-	-1.0	9.71927E-05	-4.0124	1.84284E+00
Br-	-1.0	1.60318E-06	-5.7950	1.27846E-01

MW-60

****DESCRIPTION OF SOLUTION ****

	ANALYT.	COMP.	PH
EPMCAT	25.54	24.79	8.100
EPMAN	25.96	25.15	

TEMPERATURE
EH = .0000 PE = .000 19.00 DEG C
PE CALC S = .000
PE CALC DOX= .000 IONIC STRENGTH
PE SATO DOX= .000 3.105643E-02
TOT ALK = 1.226E+01 MEQ
ELECT = -3.562E-01 MEQ

ACTIVITY H2O = .9992
PCO2= 4.898230E-03
LOG PCO2 = -2.3100
PO2 = 1.587049E-53
PCH4 = 5.171052E-44
CO2 TOT = 1.232243E-02
DENSITY = 1.0000
TDS = 1982.6MG/L
CARB ALK = 1.225E+01 MEQ
CHARGE IMBALANCE = -.7%

IN COMPUTING THE DISTRIBUTION OF SPECIES,
PE = .000 EQUIVALENT EH = .000VOLTS

DISTRIBUTION OF SPECIES

I	SPECIES		MOLALITY	ACTIVITY	LOG ACT	GAMMA
1	H+	1.	9.0920E-09	7.9433E-09	-8.100	8.7366E-01
2	E-	-1.	1.0000E+00	1.0000E+00	.000	1.0000E+00
4	Ca+2	2.	1.4066E-04	7.5268E-05	-4.123	5.3510E-01
5	Mg+2	2.	8.1360E-05	4.4259E-05	-4.354	5.4398E-01
6	Na+	1.	2.4295E-02	2.0674E-02	-1.685	8.5096E-01
7	K+	1.	8.4512E-05	7.1323E-05	-4.147	8.4393E-01
9	Mn+2	2.	9.9531E-08	5.4092E-08	-7.267	5.4347E-01
13	H4SiO4	0.	2.6582E-04	2.6773E-04	-3.572	1.0072E+00
14	Cl-	-1.	1.2054E-03	1.0173E-03	-2.993	8.4393E-01
15	CO3-2	-2.	9.8434E-05	5.2641E-05	-4.279	5.3479E-01
16	SO4-2	-2.	5.7176E-03	3.0149E-03	-2.521	5.2731E-01
20	F-	-1.	9.5933E-05	8.0874E-05	-4.092	8.4303E-01
22	Br-	-1.	1.6032E-06	1.3459E-06	-5.871	8.3949E-01
31	OH-	-1.	9.3504E-07	7.8826E-07	-6.103	8.4303E-01
33	H2 AQ	0.	4.7138E-20	4.7477E-20	-19.324	1.0072E+00
34	HCO3-	-1.	1.1883E-02	1.0162E-02	-1.993	8.5516E-01
35	H2CO3	0.	1.9627E-04	1.9768E-04	-3.704	1.0072E+00
40	HSO4-	-1.	2.4138E-09	2.0494E-09	-8.688	8.4903E-01
69	HF AQ	0.	8.5980E-10	8.6598E-10	-9.062	1.0072E+00
70	HF2-	-1.	3.0075E-13	2.5534E-13	-12.593	8.4903E-01
75	CaOH+	1.	1.8508E-09	1.5714E-09	-8.804	8.4903E-01
76	CaCO3	0.	5.9391E-06	5.9817E-06	-5.223	1.0072E+00
77	CaHCO3+	1.	1.0282E-05	8.7931E-06	-5.056	8.5516E-01
78	CaSO4	0.	4.2456E-05	4.2761E-05	-4.369	1.0072E+00
79	CaHSO4	1.	2.4829E-12	2.1081E-12	-11.676	8.4903E-01
83	CaF+	1.	5.4135E-08	4.5962E-08	-7.338	8.4903E-01
85	MgOH+	1.	2.3809E-08	2.0215E-08	-7.694	8.4903E-01
86	MgCO3	0.	2.0131E-06	2.0275E-06	-5.693	1.0072E+00
87	MgHCO3+	1.	6.0577E-06	5.1432E-06	-5.289	8.4903E-01
88	MgSO4	0.	2.6526E-05	2.6717E-05	-4.573	1.0072E+00
92	MgF+	1.	2.4929E-07	2.1166E-07	-6.674	8.4903E-01
93	NaOH	0.	1.7060E-08	1.7183E-08	-7.765	1.0072E+00
94	NaCO3-	-1.	1.7526E-05	1.4880E-05	-4.827	8.4903E-01
95	NaHCO3	0.	1.0295E-04	1.0369E-04	-3.984	1.0072E+00
96	NaSO4-	-1.	3.5393E-04	3.0050E-04	-3.522	8.4903E-01
98	NaF aq	0.	9.5528E-07	9.6213E-07	-6.017	1.0072E+00

99	KOH	0.	3.0888E-11	3.1110E-11	-10.507	1.0072E+00
100	KSO4-	-1.	1.6585E-06	1.4081E-06	-5.851	8.4903E-01
134	MnOH+	1.	1.2506E-10	1.0618E-10	-9.974	8.4903E-01
136	MnCl+	1.	2.6403E-10	2.2417E-10	-9.649	8.4903E-01
137	MnCl2	0.	9.8833E-14	9.9543E-14	-13.002	1.0072E+00
138	MnCl3-	-1.	3.2849E-17	2.7890E-17	-16.555	8.4903E-01
139	MnCO3	0.	2.2457E-07	2.2618E-07	-6.646	1.0072E+00
140	MnHCO3+	1.	5.0645E-08	4.2999E-08	-7.367	8.4903E-01
141	MnSO4	0.	2.5620E-08	2.5804E-08	-7.588	1.0072E+00
143	MnF+	1.	3.5647E-11	3.0266E-11	-10.519	8.4903E-01
144	Mn+3	3.	2.9815E-33	6.8350E-34	-33.165	2.2924E-01
164	H3SiO4-	-1.	4.7114E-06	4.0001E-06	-5.398	8.4903E-01
165	H2SiO4-2	-2.	4.3973E-11	2.2849E-11	-10.641	5.1962E-01
166	SiF6-2	-2.	1.5310E-30	7.9555E-31	-30.099	5.1962E-01

	PHASE	IAP	KT	LOG IAP	LOG KT	IAP/KT	LOG IAP/KT
1	Calcite	3.962E-09	3.561E-09	-8.402	-8.448	1.113E+00	.046
2	Aragonit	3.962E-09	5.009E-09	-8.402	-8.300	7.910E-01	-.102
3	Dolomite	9.231E-18	1.127E-17	-17.035	-16.948	8.189E-01	-.087
5	Rhodochr	2.847E-12	7.790E-12	-11.546	-11.108	3.655E-01	-.437
8	Gypsum	2.266E-07	2.621E-05	-6.645	-4.582	8.645E-03	-2.063
9	Anhydrit	2.269E-07	4.556E-05	-6.644	-4.341	4.981E-03	-2.303
13	Fluorite	4.923E-13	2.125E-11	-12.308	-10.673	2.317E-02	-1.635
14	SiO2 (a)	2.681E-04	1.729E-03	-3.572	-2.762	1.551E-01	-.809
15	Chalcedy	2.681E-04	2.385E-04	-3.572	-3.622	1.124E+00	.051
16	Quartz	2.681E-04	8.500E-05	-3.572	-4.071	3.155E+00	.499
26	Talc	1.779E+21	1.250E+22	21.250	22.097	1.423E-01	-.847
28	Chrysotl	2.472E+28	9.109E+32	28.393	32.959	2.714E-05	-4.566
29	Sepiol c	9.446E+12	8.338E+15	12.975	15.921	1.133E-03	-2.946
30	Sepiol d	9.446E+12	4.571E+18	12.975	18.660	2.067E-06	-5.685
38	Pyrolusi	1.357E+25	2.292E+42	25.132	42.360	5.920E-18	-17.228
39	Hausmani	9.956E+42	3.508E+62	42.998	62.545	2.838E-20	-19.547
40	Manganit	1.078E+17	2.188E+25	17.032	25.340	4.926E-09	-8.308
41	Pyrochro	8.560E+08	1.585E+15	8.932	15.200	5.401E-07	-6.268
42	PCO2	1.977E-04	4.036E-02	-3.704	-1.394	4.898E-03	-2.310
44	H2 gas	4.748E-20	7.525E-04	-19.324	-3.124	6.310E-17	-16.200

1MW-68

INITIAL SOLUTION

TEMPERATURE = 19.00 DEGREES C PH = 8.100
ANALYTICAL EPMCAT = 32.174 ANALYTICAL EPMAN = 35.672

***** OXIDATION - REDUCTION *****

DISSOLVED OXYGEN = .000 MMOLES/KG H2O

EH MEASURED WITH CALOMEL = 9.9000 VOLTS
MEASURED EH OF ZOBELL SOLUTION = 9.9000 VOLTS
CORRECTED EH = .0000 VOLTS
PE COMPUTED FROM CORRECTED EH = .000

FLAG	CORALK	PECALC	IDAVES
0	2	1	0

*** TOTAL CONCENTRATIONS OF INPUT SPECIES ***

SPECIES		TOTAL MOLALITY	LOG TOTAL MOLALITY	TOTAL MG/LITRE
Mg+2	2.0	1.84474E-04	-3.7341	4.47341E+00
Na+	1.0	3.15861E-02	-1.5005	7.24294E+02
K+	1.0	1.10283E-04	-3.9575	4.30122E+00
Fe+2	2.0	1.30335E-05	-4.8849	7.26011E-01
Mn+2	2.0	2.00515E-07	-6.6979	1.09876E-02
H4SiO4	.0	3.61929E-04	-3.4414	2.16906E+01
Cl-	-1.0	1.73746E-03	-2.7601	6.14401E+01
HCO3-	-1.0	1.01260E-02	-1.9946	6.16275E+02
SO4-2	-2.0	1.18113E-02	-1.9277	1.13170E+03
NO3-	-1.0	6.01544E-07	-6.2207	8.40402E-03
F-	-1.0	9.02316E-05	-4.0446	1.70986E+00
Br-	-1.0	2.50643E-06	-5.6009	1.99760E-01

MW-68

****DESCRIPTION OF SOLUTION ****

	ANALYT.	COMP.
EPMCAT	32.17	30.96
EPMAN	35.67	34.40

PH 8.100

TEMPERATURE 19.00 DEG C

IONIC STRENGTH 4.393246E-02

ACTIVITY H2O = .9991
PCO2= 3.933574E-03
LOG PCO2 = -2.4052
PO2 = 1.586488E-53
PCH4 = 4.154137E-44
CO2 TOT = 1.012599E-02
DENSITY = 1.0000
TDS = 2566.8MG/L
CARB ALK = 1.008E+01 MEQ
CHARGE IMBALANCE = -5.3%

EH = .0000 PE = .000
PE CALC S = .000
PE CALC DOX= .000
PE SATO DOX= .000
TOT ALK = 1.009E+01 MEQ
ELECT = -3.447E+00 MEQ

IN COMPUTING THE DISTRIBUTION OF SPECIES,
PE = .000 EQUIVALENT EH = .000VOLTS

DISTRIBUTION OF SPECIES

I	SPECIES		MOLALITY	ACTIVITY	LOG ACT	GAMMA
1	H+	1.	9.2368E-09	7.9433E-09	-8.100	8.5996E-01
2	E-	-1.	1.0000E+00	1.0000E+00	.000	1.0000E+00
5	Mg+2	2.	1.1507E-04	5.7801E-05	-4.238	5.0230E-01
6	Na+	1.	3.0683E-02	2.5528E-02	-1.593	8.3199E-01
7	K+	1.	1.0663E-04	8.7712E-05	-4.057	8.2258E-01
8	Fe+2	2.	5.4829E-06	2.7458E-06	-5.561	5.0080E-01
9	Mn+2	2.	5.7809E-08	2.8950E-08	-7.538	5.0080E-01
13	H4SiO4	0.	3.5546E-04	3.5908E-04	-3.445	1.0102E+00
14	Cl-	-1.	1.7375E-03	1.4292E-03	-2.845	8.2258E-01
15	CO3-2	-2.	8.6171E-05	4.2267E-05	-4.374	4.9050E-01
16	SO4-2	-2.	1.0962E-02	5.2777E-03	-2.278	4.8145E-01
17	NO3-	-1.	5.6246E-20	4.5939E-20	-19.338	8.1675E-01
20	F-	-1.	8.8866E-05	7.2989E-05	-4.137	8.2134E-01
22	Br-	-1.	2.5064E-06	2.0471E-06	-5.689	8.1675E-01
31	OH-	-1.	9.5956E-07	7.8812E-07	-6.103	8.2134E-01
33	H2 AQ	0.	4.6999E-20	4.7477E-20	-19.324	1.0102E+00
34	HCO3-	-1.	9.7493E-03	8.1589E-03	-2.088	8.3687E-01
35	H2CO3	0.	1.5715E-04	1.5875E-04	-3.799	1.0102E+00
40	HSO4-	-1.	4.3229E-09	3.5875E-09	-8.445	8.2987E-01
48	NO2-	-1.	6.0154E-07	4.9131E-07	-6.309	8.1675E-01
69	HF AQ	0.	7.7368E-10	7.8154E-10	-9.107	1.0102E+00
70	HF2-	-1.	2.5062E-13	2.0798E-13	-12.682	8.2987E-01
85	MgOH+	1.	3.1807E-08	2.6396E-08	-7.578	8.2987E-01
86	MgCO3	0.	2.1047E-06	2.1261E-06	-5.672	1.0102E+00
87	MgHCO3+	1.	6.4988E-06	5.3932E-06	-5.268	8.2987E-01
88	MgSO4	0.	6.0464E-05	6.1079E-05	-4.214	1.0102E+00
92	MgF+	1.	3.0062E-07	2.4947E-07	-6.603	8.2987E-01
93	NaOH	0.	2.1000E-08	2.1213E-08	-7.673	1.0102E+00
94	NaCO3-	-1.	1.7777E-05	1.4753E-05	-4.831	8.2987E-01
95	NaHCO3	0.	1.0177E-04	1.0280E-04	-3.988	1.0102E+00
96	NaSO4-	-1.	7.8269E-04	6.4953E-04	-3.187	8.2987E-01
98	NaF aq	0.	1.0614E-06	1.0722E-06	-5.970	1.0102E+00
99	KOH	0.	3.7867E-11	3.8252E-11	-10.417	1.0102E+00
100	KSO4-	-1.	3.6528E-06	3.0314E-06	-5.518	8.2987E-01
102	FeOH+	1.	8.3280E-08	6.9112E-08	-7.160	8.2987E-01
105	FeCl+	1.	6.5276E-09	5.4171E-09	-8.266	8.2987E-01
106	FeCO3	0.	2.7560E-06	2.7840E-06	-5.555	1.0102E+00
107	FeHCO3+	1.	2.3695E-06	1.9664E-06	-5.706	8.2987E-01
108	FeSO4	0.	2.2809E-06	2.3041E-06	-5.638	1.0102E+00
109	FeHSO4+	1.	1.6222E-13	1.3462E-13	-12.871	8.2987E-01
114	FeF+	1.	2.4150E-09	2.0042E-09	-8.698	8.2987E-01
115	Fe+3	3.	7.2887E-19	1.8748E-19	-18.727	2.5722E-01
117	FeOH+2	2.	2.2384E-13	1.0616E-13	-12.974	4.7429E-01
118	FeOH2+	1.	4.2238E-09	3.5052E-09	-8.455	8.2987E-01
119	FeOH3	0.	4.3052E-08	4.3490E-08	-7.362	1.0102E+00
120	FeOH4-	-1.	4.6999E-09	3.9003E-09	-8.409	8.2987E-01
121	Fe2OH2+4	4.	7.7212E-24	3.9071E-25	-24.408	5.0602E-02
122	Fe3OH4+5	5.	5.3294E-29	5.0344E-31	-30.298	9.4464E-03
123	FeCl+2	2.	1.4051E-20	6.6641E-21	-20.176	4.7429E-01
124	FeCl2+	1.	6.2248E-23	5.1658E-23	-22.287	8.2987E-01
125	FeCl3	0.	7.3086E-27	7.3829E-27	-26.132	1.0102E+00
126	FeSO4+	1.	1.1416E-17	9.4740E-18	-17.023	8.2987E-01
127	FeHSO4+2	2.	6.8089E-25	3.2294E-25	-24.491	4.7429E-01

128	FeSO42-	-1.	1.2870E-18	1.0681E-18	-17.971	8.2987E-01
131	FeF+2	2.	4.1641E-17	1.9750E-17	-16.704	4.7429E-01
132	FeF2+	1.	6.4298E-17	5.3359E-17	-16.273	8.2987E-01
133	FeF3	0.	5.9847E-18	6.0455E-18	-17.219	1.0102E+00
134	MnOH+	1.	6.8464E-11	5.6816E-11	-10.246	8.2987E-01
136	MnCl+	1.	2.0311E-10	1.6856E-10	-9.773	8.2987E-01
137	MnCl2	0.	1.0410E-13	1.0516E-13	-12.978	1.0102E+00
138	MnCl3-	-1.	4.9880E-17	4.1394E-17	-16.383	8.2987E-01
139	MnCO3	0.	9.6219E-08	9.7197E-08	-7.012	1.0102E+00
140	MnHCO3+	1.	2.2266E-08	1.8478E-08	-7.733	8.2987E-01
141	MnSO4	0.	2.3932E-08	2.4175E-08	-7.617	1.0102E+00
143	MnF+	1.	1.7616E-11	1.4619E-11	-10.835	8.2987E-01
144	Mn+3	3.	1.9596E-33	3.6581E-34	-33.437	1.8668E-01
164	H3SiO4-	-1.	6.4648E-06	5.3649E-06	-5.270	8.2987E-01
165	H2SiO4-2	-2.	6.4612E-11	3.0645E-11	-10.514	4.7429E-01
166	SiF6-2	-2.	1.2165E-30	5.7696E-31	-30.239	4.7429E-01

	PHASE	IAP	KT	LOG IAP	LOG KT	IAP/KT	LOG IAP/KT
4	Siderite	1.161E-10	1.404E-11	-9.935	-10.853	8.267E+00	.917
5	Rhodochr	1.224E-12	7.790E-12	-11.912	-11.108	1.571E-01	-.804
14	SiO2 (a)	3.598E-04	1.729E-03	-3.444	-2.762	2.080E-01	-.682
15	Chalcedy	3.598E-04	2.385E-04	-3.444	-3.622	1.508E+00	.178
16	Quartz	3.598E-04	8.500E-05	-3.444	-4.071	4.232E+00	.627
26	Talc	1.283E+22	1.250E+22	22.108	22.097	1.027E+00	.011
28	Chrysotl	9.904E+28	9.109E+32	28.996	32.959	1.087E-04	-3.964
29	Sepiol c	3.887E+13	8.338E+15	13.590	15.921	4.662E-03	-2.331
30	Sepiol d	3.887E+13	4.571E+18	13.590	18.660	8.505E-06	-5.070
31	Hematite	1.395E+11	2.860E-04	11.145	-3.544	4.879E+14	14.688
32	Goethite	3.734E+05	1.000E-01	5.572	-1.000	3.734E+06	6.572
33	Fe(OH)3a	3.730E+05	7.780E+04	5.572	4.891	4.794E+00	.681
38	Pyrolusi	7.258E+24	2.292E+42	24.861	42.360	3.167E-18	-17.499
39	Hausmani	1.525E+42	3.508E+62	42.183	62.545	4.348E-21	-20.362
40	Manganit	5.766E+16	2.188E+25	16.761	25.340	2.635E-09	-8.579
41	Pyrochro	4.580E+08	1.585E+15	8.661	15.200	2.890E-07	-6.539
42	PCO2	1.588E-04	4.036E-02	-3.799	-1.394	3.934E-03	-2.405
44	H2 gas	4.748E-20	7.525E-04	-19.324	-3.124	6.310E-17	-16.200
49	Melanter	1.440E-08	5.192E-03	-7.842	-2.285	2.773E-06	-5.557
51	K-Jarosi	6.373E-17	1.823E-09	-16.196	-8.739	3.495E-08	-7.457

1L-Bar

INITIAL SOLUTION

TEMPERATURE = 18.41 DEGREES C PH = 8.260
ANALYTICAL EPMCAT = 12.959 ANALYTICAL EPMAN = 13.464

***** OXIDATION - REDUCTION *****

DISSOLVED OXYGEN = 2.393 MMOLES/KG H2O
EH MEASURED WITH CALOMEL = 9.9000 VOLTS
MEASURED EH OF ZOBELL SOLUTION = 9.9000 VOLTS
CORRECTED EH = .1030 VOLTS

FLAG	CORALK	PECALC	IDAVES
0	2	1	0

PE COMPUTED FROM CORRECTED EH = 1.780

*** TOTAL CONCENTRATIONS OF INPUT SPECIES ***

SPECIES		TOTAL MOLALITY	LOG TOTAL MOLALITY	TOTAL MG/LITRE
Ca+2	2.0	9.01012E-05	-4.0453	3.60720E+00
Mg+2	2.0	5.40607E-05	-4.2671	1.31285E+00
Na+	1.0	1.25951E-02	-1.8998	2.89235E+02
K+	1.0	4.40495E-05	-4.3561	1.72049E+00
Fe+2	2.0	6.00675E-07	-6.2214	3.35082E-02
Mn+2	2.0	1.00112E-07	-6.9995	5.49380E-03
Al+3	3.0	7.00787E-07	-6.1544	1.88870E-02
Ba+2	2.0	1.00112E-07	-6.9995	1.37340E-02
Sr+2	2.0	2.60292E-06	-5.5845	2.27812E-01
H4SiO4	.0	1.68189E-04	-3.7742	1.00942E+01
Cl-	-1.0	4.27480E-04	-3.3691	1.51384E+01
HCO3-	-1.0	7.97696E-03	-2.0982	4.86186E+02
SO4-2	-2.0	2.46176E-03	-2.6088	2.36215E+02
NO3-	-1.0	5.00562E-06	-5.3005	7.00335E-02
H3BO3	.0	2.05230E-05	-4.6878	2.21605E-01
F-	-1.0	1.13127E-04	-3.9464	2.14682E+00
Li+	1.0	7.80877E-06	-5.1074	5.41242E-02
Br-	-1.0	1.00112E-06	-5.9995	7.99040E-02
DOX	.0	2.39269E-03	-2.6211	7.64771E+01

L-Bar

****DESCRIPTION OF SOLUTION ****

	ANALYT.	COMP.		
EPMCAT	12.96	12.74	PH	ACTIVITY H2O = .9996
EPMAN	13.46	13.25		PCO2= 2.274401E-03
				LOG PCO2 = -2.6431
			TEMPERATURE	PO2 = 5.671232E-46
EH = .1030	PE = 1.780		18.41 DEG C	PCH4 = 8.857763E-60
PE CALC S =	.000			CO2 TOT = 7.976957E-03
PE CALC DOX=	13.163		IONIC STRENGTH	DENSITY = 1.0000
PE SATO DOX=	2.470		1.556184E-02	TDS = 1122.9MG/L
TOT ALK =	7.989E+00 MEQ			CARB ALK = 7.979E+00 MEQ
ELECT	= -5.151E-01 MEQ			CHARGE IMBALANCE = -2.0%

IN COMPUTING THE DISTRIBUTION OF SPECIES,
PE = 1.780 EQUIVALENT EH = .103VOLTS

DISTRIBUTION OF SPECIES

I	SPECIES		MOLALITY	ACTIVITY	LOG ACT	GAMMA
1	H+	1.	6.1107E-09	5.4954E-09	-8.260	8.9931E-01
2	E-	-1.	1.6580E-02	1.6580E-02	-1.780	1.0000E+00
4	Ca+2	2.	7.0915E-05	4.4047E-05	-4.356	6.2112E-01
5	Mg+2	2.	4.2691E-05	2.6764E-05	-4.572	6.2692E-01
6	Na+	1.	1.2462E-02	1.1030E-02	-1.957	8.8508E-01
7	K+	1.	4.3639E-05	3.8455E-05	-4.415	8.8121E-01
8	Fe+2	2.	1.4008E-07	8.7875E-08	-7.056	6.2731E-01
9	Mn+2	2.	2.4759E-08	1.5532E-08	-7.809	6.2731E-01
10	Al+3	3.	3.4178E-16	1.3150E-16	-15.881	3.8475E-01
11	Ba+2	2.	6.6777E-08	4.1232E-08	-7.385	6.1746E-01
12	Sr+2	2.	2.1030E-06	1.3097E-06	-5.883	6.2276E-01
13	H4SiO4	0.	1.6425E-04	1.6484E-04	-3.783	1.0036E+00
14	Cl-	-1.	4.2748E-04	3.7670E-04	-3.424	8.8121E-01
15	CO3-2	-2.	8.1718E-05	5.0784E-05	-4.294	6.2146E-01
16	SO4-2	-2.	2.3543E-03	1.4516E-03	-2.838	6.1658E-01
17	NO3-	-1.	3.0554E-15	2.6848E-15	-14.571	8.7870E-01
18	H3BO3	0.	1.8570E-05	1.8636E-05	-4.730	1.0036E+00
20	F-	-1.	1.1229E-04	9.8896E-05	-4.005	8.8073E-01
21	Li+	1.	7.7592E-06	6.9054E-06	-5.161	8.8996E-01
22	Br-	-1.	1.0011E-06	8.7969E-07	-6.056	8.7870E-01
28	DOX	0.	2.3927E-03	2.4013E-03	-2.620	1.0036E+00
31	OH-	-1.	1.2338E-06	1.0867E-06	-5.964	8.8073E-01
33	H2 AQ	0.	6.2629E-24	6.2854E-24	-23.202	1.0036E+00
34	HCO3-	-1.	7.7458E-03	6.8773E-03	-2.163	8.8788E-01
35	H2CO3	0.	9.3087E-05	9.3421E-05	-4.030	1.0036E+00
40	HSO4-	-1.	7.6313E-10	6.7438E-10	-9.171	8.8370E-01
48	NO2-	-1.	5.0056E-06	4.3984E-06	-5.357	8.7870E-01
57	H2BO3-	-1.	1.9527E-06	1.7256E-06	-5.763	8.8370E-01
58	BFOH3-	-1.	7.7371E-10	6.8373E-10	-9.165	8.8370E-01
59	BF2OH2-	-1.	4.5477E-14	4.0188E-14	-13.396	8.8370E-01
60	BF3OH-	-1.	3.0670E-20	2.7103E-20	-19.567	8.8370E-01
61	BF4-	-1.	6.8538E-26	6.0567E-26	-25.218	8.8370E-01
69	HF AQ	0.	7.2248E-10	7.2508E-10	-9.140	1.0036E+00
70	HF2-	-1.	2.9422E-13	2.6000E-13	-12.585	8.8370E-01
75	CaOH+	1.	1.5046E-09	1.3296E-09	-8.876	8.8370E-01
76	CaCO3	0.	3.3351E-06	3.3470E-06	-5.475	1.0036E+00
77	CaHCO3+	1.	3.8767E-06	3.4420E-06	-5.463	8.8788E-01
78	CaSO4	0.	1.1936E-05	1.1979E-05	-4.922	1.0036E+00
79	CaHSO4	1.	4.6501E-13	4.1093E-13	-12.386	8.8370E-01
83	CaF+	1.	3.6688E-08	3.2421E-08	-7.489	8.8370E-01
85	MgOH+	1.	2.0001E-08	1.7675E-08	-7.753	8.8370E-01
86	MgCO3	0.	1.1680E-06	1.1722E-06	-5.931	1.0036E+00
87	MgHCO3+	1.	2.3776E-06	2.1011E-06	-5.678	8.8370E-01
88	MgSO4	0.	7.6290E-06	7.6563E-06	-5.116	1.0036E+00
92	MgF+	1.	1.7515E-07	1.5478E-07	-6.810	8.8370E-01
93	NaOH	0.	1.3208E-08	1.3255E-08	-7.878	1.0036E+00
94	NaCO3-	-1.	8.4020E-06	7.4249E-06	-5.129	8.8370E-01
95	NaHCO3	0.	3.6792E-05	3.6924E-05	-4.433	1.0036E+00
96	NaSO4-	-1.	8.7010E-05	7.6891E-05	-4.114	8.8370E-01
98	NaF aq	0.	6.2546E-07	6.2771E-07	-6.202	1.0036E+00
99	KOH	0.	2.4166E-11	2.4253E-11	-10.615	1.0036E+00
100	KSO4-	-1.	4.1041E-07	3.6268E-07	-6.440	8.8370E-01
102	FeOH+	1.	3.4567E-09	3.0547E-09	-8.515	8.8370E-01

105	FeCl+	1.	5.1707E-11	4.5694E-11	-10.340	8.8370E-01
106	FeCO3	0.	1.0667E-07	1.0705E-07	-6.970	1.0036E+00
107	FeHCO3+	1.	5.9195E-08	5.2311E-08	-7.281	8.8370E-01
108	FeSO4	0.	1.9982E-08	2.0054E-08	-7.698	1.0036E+00
109	FeHSO4+	1.	9.2771E-16	8.1982E-16	-15.086	8.8370E-01
114	FeF+	1.	9.8341E-11	8.6904E-11	-10.061	8.8370E-01
115	Fe+3	3.	9.0931E-19	3.4986E-19	-18.456	3.8475E-01
117	FeOH+2	2.	4.5307E-13	2.7631E-13	-12.559	6.0985E-01
118	FeOH2+	1.	1.4584E-08	1.2888E-08	-7.890	8.8370E-01
119	FeOH3	0.	2.2432E-07	2.2513E-07	-6.648	1.0036E+00
120	FeOH4-	-1.	3.2233E-08	2.8484E-08	-7.545	8.8370E-01
121	Fe2OH2+4	4.	1.9626E-23	2.7148E-24	-23.566	1.3833E-01
122	Fe3OH4+5	5.	2.9945E-28	1.3614E-29	-28.866	4.5464E-02
123	FeCl+2	2.	5.2708E-21	3.2144E-21	-20.493	6.0985E-01
124	FeCl2+	1.	7.5783E-24	6.6970E-24	-23.174	8.8370E-01
125	FeCl3	0.	2.5137E-28	2.5227E-28	-27.598	1.0036E+00
126	FeSO4+	1.	5.4282E-18	4.7970E-18	-17.319	8.8370E-01
127	FeHSO4+2	2.	1.9449E-25	1.1861E-25	-24.926	6.0985E-01
128	FeSO42-	-1.	1.6791E-19	1.4838E-19	-18.829	8.8370E-01
131	FeF+2	2.	8.1117E-17	4.9469E-17	-16.306	6.0985E-01
132	FeF2+	1.	2.0343E-16	1.7977E-16	-15.745	8.8370E-01
133	FeF3	0.	2.7441E-17	2.7540E-17	-16.560	1.0036E+00
134	MnOH+	1.	4.7439E-11	4.1922E-11	-10.378	8.8370E-01
136	MnCl+	1.	2.6971E-11	2.3835E-11	-10.623	8.8370E-01
137	MnCl2	0.	3.9052E-15	3.9192E-15	-14.407	1.0036E+00
138	MnCl3-	-1.	4.6014E-19	4.0663E-19	-18.391	8.8370E-01
139	MnCO3	0.	6.2429E-08	6.2653E-08	-7.203	1.0036E+00
140	MnHCO3+	1.	9.3248E-09	8.2403E-09	-8.084	8.8370E-01
141	MnSO4	0.	3.5130E-09	3.5256E-09	-8.453	1.0036E+00
142	Mn(NO3)2	0.	4.5085E-37	4.5247E-37	-36.344	1.0036E+00
143	MnF+	1.	1.2025E-11	1.0627E-11	-10.974	8.8370E-01
144	Mn+3	3.	3.2916E-32	1.0819E-32	-31.966	3.2867E-01
150	AlOH+2	2.	2.5222E-13	1.5382E-13	-12.813	6.0985E-01
151	AlOH2+	1.	1.3640E-10	1.2053E-10	-9.919	8.8370E-01
152	AlOH3	0.	1.9384E-09	1.9453E-09	-8.711	1.0036E+00
153	AlOH4-	-1.	6.9870E-07	6.1744E-07	-6.209	8.8370E-01
154	AlSO4+	1.	2.0838E-16	1.8415E-16	-15.735	8.8370E-01
155	AlSO42-	-1.	2.3403E-17	2.0682E-17	-16.684	8.8370E-01
156	AlHSO4+2	2.	4.8257E-25	2.9430E-25	-24.531	6.0985E-01
157	AlF+2	2.	2.0480E-13	1.2490E-13	-12.903	6.0985E-01
158	AlF2+	1.	6.7636E-12	5.9770E-12	-11.224	8.8370E-01
159	AlF3	0.	7.3641E-12	7.3906E-12	-11.131	1.0036E+00
160	AlF4-	-1.	3.2877E-13	2.9053E-13	-12.537	8.8370E-01
161	AlF5-2	-2.	7.5703E-16	4.6168E-16	-15.336	6.0985E-01
162	AlF6-3	-3.	1.5882E-19	5.2200E-20	-19.282	3.2867E-01
164	H3SiO4-	-1.	3.9396E-06	3.4814E-06	-5.458	8.8370E-01
165	H2SiO4-2	-2.	4.5222E-11	2.7579E-11	-10.559	6.0985E-01
166	SiF6-2	-2.	6.5023E-31	3.9655E-31	-30.402	6.0985E-01
170	BaOH+	1.	2.8757E-13	2.5412E-13	-12.595	8.8370E-01
171	BaCO3	0.	9.4429E-10	9.4768E-10	-9.023	1.0036E+00
172	BaHCO3+	1.	2.4997E-09	2.2090E-09	-8.656	8.8370E-01
173	BaSO4	0.	2.9891E-08	2.9998E-08	-7.523	1.0036E+00
176	SrOH+	1.	1.3782E-11	1.2217E-11	-10.913	8.8645E-01
177	SrHCO3+	1.	1.2384E-07	1.0995E-07	-6.959	8.8788E-01
178	SrCO3	0.	3.4825E-08	3.4950E-08	-7.457	1.0036E+00
179	SrSO4	0.	3.4120E-07	3.4242E-07	-6.465	1.0036E+00
180	LiOH	0.	2.8671E-11	2.8774E-11	-10.541	1.0036E+00
181	LiSO4-	-1.	4.9515E-08	4.3757E-08	-7.359	8.8370E-01

	PHASE	IAP	KT	LOG IAP	LOG KT	IAP/KT	LOG IAP/KT
1	Calcite	2.237E-09	3.584E-09	-8.650	-8.446	6.240E-01	-.205
2	Aragonit	2.237E-09	5.047E-09	-8.650	-8.297	4.432E-01	-.353
3	Dolomite	3.040E-18	1.165E-17	-17.517	-16.934	2.610E-01	-.583
4	Siderite	4.463E-12	1.416E-11	-11.350	-10.849	3.151E-01	-.501
5	Rhodochr	7.888E-13	7.829E-12	-12.103	-11.106	1.008E-01	-.997
6	Strontit	6.651E-11	5.369E-10	-10.177	-9.270	1.239E-01	-.907
7	Witherit	2.094E-12	2.624E-09	-11.679	-8.581	7.981E-04	-3.098
8	Gypsum	6.388E-08	2.619E-05	-7.195	-4.582	2.439E-03	-2.613
9	Anhydrit	6.394E-08	4.569E-05	-7.194	-4.340	1.399E-03	-2.854
10	Celestit	1.901E-09	2.393E-07	-8.721	-6.621	7.946E-03	-2.100
11	Barite	5.985E-11	8.300E-11	-10.223	-10.081	7.211E-01	-.142
13	Fluorite	4.308E-13	2.088E-11	-12.366	-10.680	2.063E-02	-1.686
14	SiO2 (a)	1.650E-04	1.709E-03	-3.783	-2.767	9.653E-02	-1.015
15	Chalcedy	1.650E-04	2.346E-04	-3.783	-3.630	7.031E-01	-.153
16	Quartz	1.650E-04	8.324E-05	-3.783	-4.080	1.982E+00	.297
17	Gibbs(c)	7.913E+08	3.074E+08	8.898	8.488	2.574E+00	.411
18	Al(OH)3a	7.913E+08	1.734E+11	8.898	11.239	4.564E-03	-2.341
19	Kaolinit	1.705E+10	1.047E+08	10.232	8.020	1.629E+02	2.212
20	Albite	3.061E-20	3.706E-19	-19.514	-18.431	8.259E-02	-1.083
21	Anorth	4.579E-25	1.242E-20	-24.339	-19.906	3.687E-05	-4.433
22	Kspar	1.067E-22	8.249E-22	-21.972	-21.084	1.294E-01	-.888
23	Kmica	1.559E+19	4.861E+13	19.193	13.687	3.208E+05	5.506
24	Chlorite	1.542E+66	7.761E+70	66.188	70.890	1.986E-05	-4.702
25	Ca-Mont	2.584E-46	1.014E-46	-45.588	-45.994	2.549E+00	.406
26	Talc	5.148E+20	1.469E+22	20.712	22.167	3.505E-02	-1.455
27	Illite	5.972E-42	6.714E-42	-41.224	-41.173	8.894E-01	-.051
28	Chrysotl	1.891E+28	1.086E+33	28.277	33.036	1.741E-05	-4.759
29	Sepiol c	3.519E+12	8.655E+15	12.546	15.937	4.065E-04	-3.391
30	Sepiol d	3.519E+12	4.571E+18	12.546	18.660	7.698E-07	-6.114
31	Hematite	4.438E+12	3.184E-04	12.647	-3.497	1.394E+16	16.144
32	Goethite	2.106E+06	1.000E-01	6.324	-1.000	2.106E+07	7.324
33	Fe(OH)3a	2.105E+06	7.780E+04	6.323	4.891	2.706E+01	1.432
38	Pyrolusi	6.189E+28	2.876E+42	28.792	42.459	2.152E-14	-13.667
39	Hausmani	1.636E+46	4.982E+62	46.214	62.697	3.283E-17	-16.484
40	Manganit	5.639E+18	2.188E+25	18.751	25.340	2.578E-07	-6.589
41	Pyrochro	5.138E+08	1.585E+15	8.711	15.200	3.242E-07	-6.489
42	PCO2	9.342E-05	4.107E-02	-4.030	-1.386	2.274E-03	-2.643
44	H2 gas	6.285E-24	7.571E-04	-23.202	-3.121	8.302E-21	-20.081
49	Melanter	1.272E-10	5.100E-03	-9.896	-2.292	2.493E-08	-7.603
50	Alunite	6.673E-09	2.707E-01	-8.176	-.567	2.465E-08	-7.608
51	K-Jarosi	1.257E-16	2.033E-09	-15.901	-8.692	6.179E-08	-7.209

Appendix C
NETPATH model output

```
Initial Well : Presbyterian
Final Well   : Bibo
          Final      Initial
C        5.9748       1.9659
NA       8.3787        .4632
CA        .3193        .4022
K         .0701        .0980
AL        .0013        .0016
SI        .3012        .8344
MG        .1952        .2641
S        1.7004        .0240
CL        .4233        .0770
FE        .0008        .0001

CALCITE  CA    1.0000 C     1.0000 RS   4.0000 I1   -6.2000 I2
.0000
SiO2     SI    1.0000
NaCl     NA    1.0000 CL    1.0000
K-SPAR   K     1.0000 AL    1.0000 SI    3.0000
EXCHANGE CA   -1.0000 NA    2.0000 MG     .0000
DOLOMITE CA    1.0000 MG    1.0000 C    2.0000 RS    8.0000 I1
.0000
         I2     .0000
GYPSUM   CA    1.0000 S     1.0000 RS    6.0000 I3   22.0000
HEMATITE FE    2.0000 RS    6.0000
PYRITE   FE    1.0000 S     2.0000 RS     .0000 I3  -60.0000
ALBITE   NA    1.0000 AL    1.0000 SI    3.0000
ANORTH   CA    1.0000 AL    2.0000 SI    2.0000

                    11 models checked
                     4 models found
           MODEL    1
 CALCITE                 4.14680
 SiO2                    -.53222
 NaCl       +             .34631
 K-SPAR                  -.02798
 EXCHANGE                3.77074
 DOLOMITE                -.06895
 GYPSUM                  -.39004
 HEMATITE                -.51624
 PYRITE                  1.03319
 ALBITE                   .02768
                Computed    Observed
Carbon-13       -8.6791     -8.6690
C-14 (% mod)    23.2208*    17.8400
Sulfur-34      -29.8428    -12.1500
Strontium-87    .000000   Undefined
```

Nitrogen-15 .0000 Undefined

---------Adjusted C-14 age in years: 2179.* * = based on Original Data

Model (for initial A0)	A0 (initial)	Computed (no decay)	Observed	age (final)
Original Data	73.33	23.22	17.84	2179.
Mass Balance	67.33	21.32	17.84	1473.
Vogel	85.00	26.92	17.84	3400.
Tamers	56.12	17.77	17.84	-32.
Ingerson and Pearson	55.88	17.69	17.84	-68.
Mook	42.38	13.42	17.84	-2354.
Fontes and Garnier	55.87	17.69	17.84	-68.
Eichinger	53.18	16.84	17.84	-478.
User-defined	100.00	31.67	17.84	4743.

Data used for Carbon-13

Initial Value: -13.9690 Modeled Final Value: -8.6791

1 dissolving phases:

Phase	Delta C	Isotopic composition (o/oo)
CALCITE	4.14680	-6.2000

1 precipitating phases:

Phase	Delta C	Fractionation factor	Average Isotopic composition (o/oo)
DOLOMITE	-.13790	.8337	-9.5432

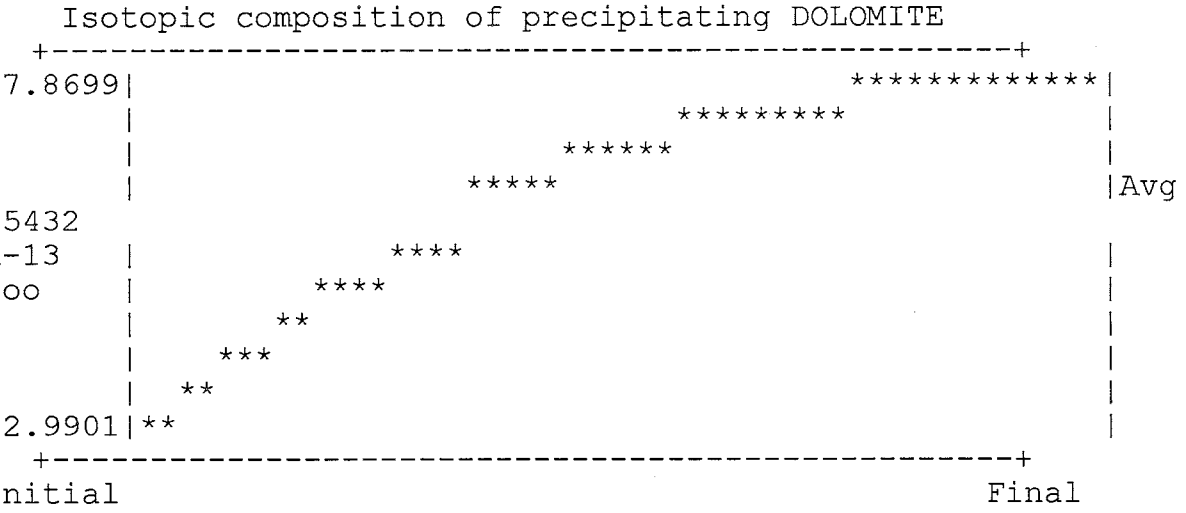

Data used for C-14 (% mod)

Initial Value: 73.3300 Modeled Final Value: 23.2208

1 dissolving phases:

Phase	Delta C	Isotopic composition (% modern)
CALCITE	4.14680	.0000

1 precipitating phases: Average

Phase	Delta C	Fractionation factor	Isotopic composition (% modern)
DOLOMITE	-.13790	1.6673	39.2868

Isotopic composition of precipitating DOLOMITE

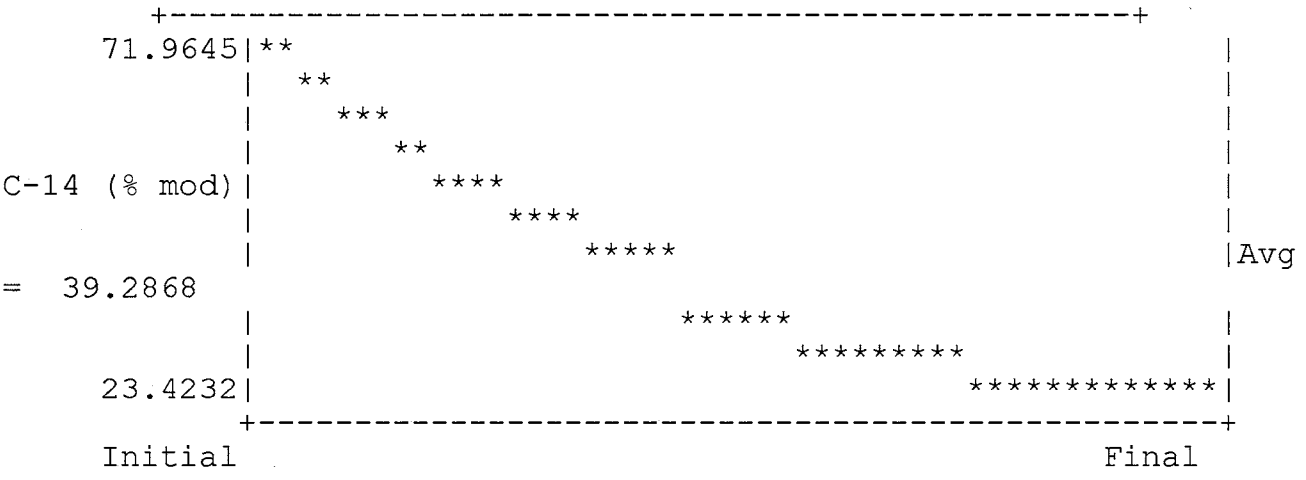

Data used for Sulfur-34

Initial Value: .0000 Modeled Final Value: -29.8428

1 dissolving phases:

Phase	Delta S	Isotopic composition (o/oo)
PYRITE	2.06638	-30.0000

1 precipitating phases:

Phase	Delta S	Fractionation factor	Average Isotopic composition (o/oo)
GYPSUM	-.39004	.0000	-28.7645

Isotopic composition of precipitating GYPSUM

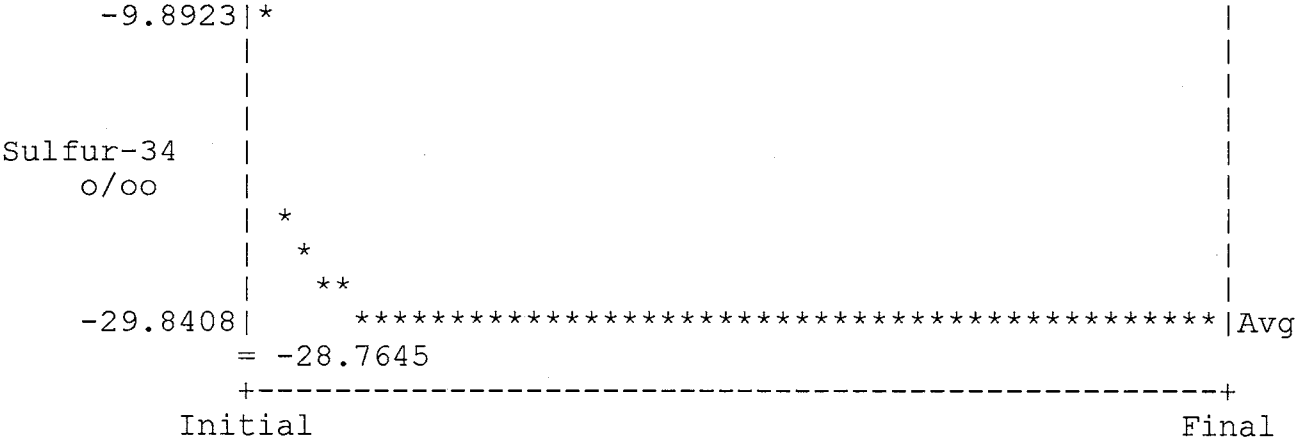

Data used for Strontium-87

Initial Value: .0000 Modeled Final Value: .0000

No incoming or outgoing phases

Data used for Nitrogen-15

Initial Value: .0000 Modeled Final Value: .0000

No incoming or outgoing phases

MODEL 2

CALCITE		4.14680
SiO2		-.47686
NaCl	+	.34631
K-SPAR		-.02798
EXCHANGE		3.78458
DOLOMITE		-.06895
GYPSUM		-.39004
HEMATITE		-.51624
PYRITE		1.03319
ANORTH		.01384

	Computed	Observed
Carbon-13	-8.6791	-8.6690
C-14 (% mod)	23.2208*	17.8400
Sulfur-34	-29.8428	-12.1500
Strontium-87	.000000	Undefined
Nitrogen-15	.0000	Undefined

---------Adjusted C-14 age in years: 2179.* * = based on Original Data

Model (for initial A0)	A0 (initial)	Computed (no decay)	Observed	age (final)
Original Data	73.33	23.22	17.84	2179.
Mass Balance	67.33	21.32	17.84	1473.
Vogel	85.00	26.92	17.84	3400.
Tamers	56.12	17.77	17.84	-32.
Ingerson and Pearson	55.88	17.69	17.84	-68.
Mook	42.38	13.42	17.84	-2354.
Fontes and Garnier	55.87	17.69	17.84	-68.
Eichinger	53.18	16.84	17.84	-478.
User-defined	100.00	31.67	17.84	4743.

Data used for Carbon-13

Initial Value: -13.9690 Modeled Final Value: -8.6791

1 dissolving phases:

Phase	Delta C	Isotopic composition (o/oo)
CALCITE	4.14680	-6.2000

```
 1 precipitating phases:                                    Average
Phase        Delta C     Fractionation factor Isotopic composition (o/oo)
DOLOMITE     -.13790              .8337                  -9.5432
```

Isotopic composition of precipitating DOLOMITE

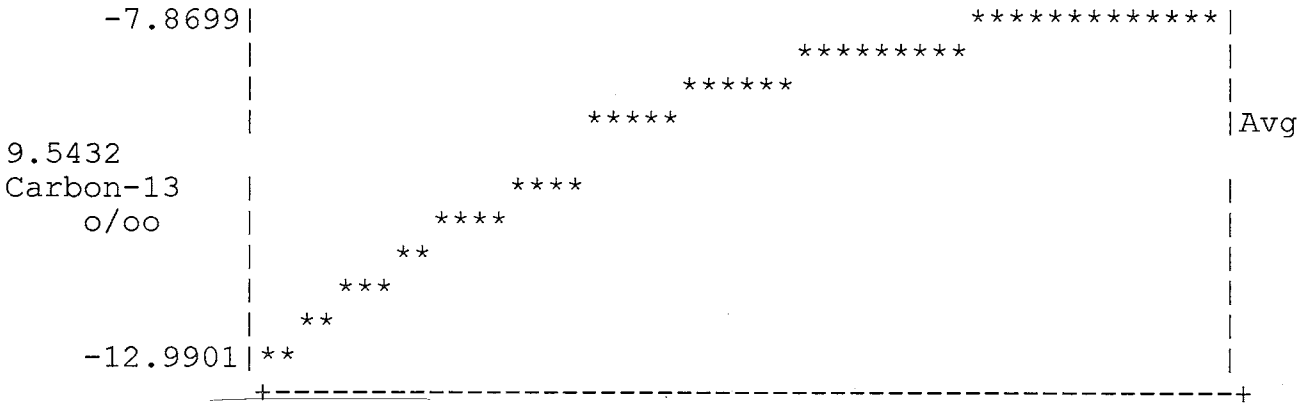

Data used for C-14 (% mod)

Initial Value: 73.3300 Modeled Final Value: 23.2208

```
 1 dissolving phases:
Phase        Delta C     Isotopic composition (% modern)
CALCITE      4.14680              .0000

 1 precipitating phases:                                    Average
Phase        Delta C     Fractionation factor Isotopic composition (% mod
DOLOMITE     -.13790             1.6673                  39.2868
```

Isotopic composition of precipitating DOLOMITE

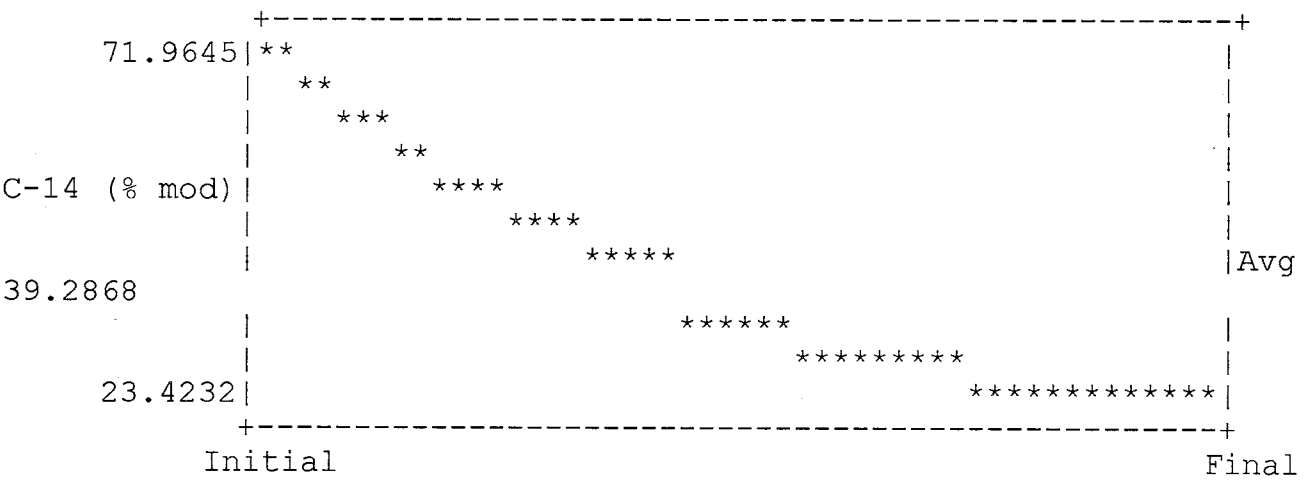

Data used for Sulfur-34

Initial Value: .0000 Modeled Final Value: -29.8428

1 dissolving phases:

Phase	Delta S	Isotopic composition (o/oo)
PYRITE	2.06638	-30.0000

1 precipitating phases:

Phase	Delta S	Fractionation factor	Average Isotopic composition (o/oo)
GYPSUM	-.39004	.0000	-28.7645

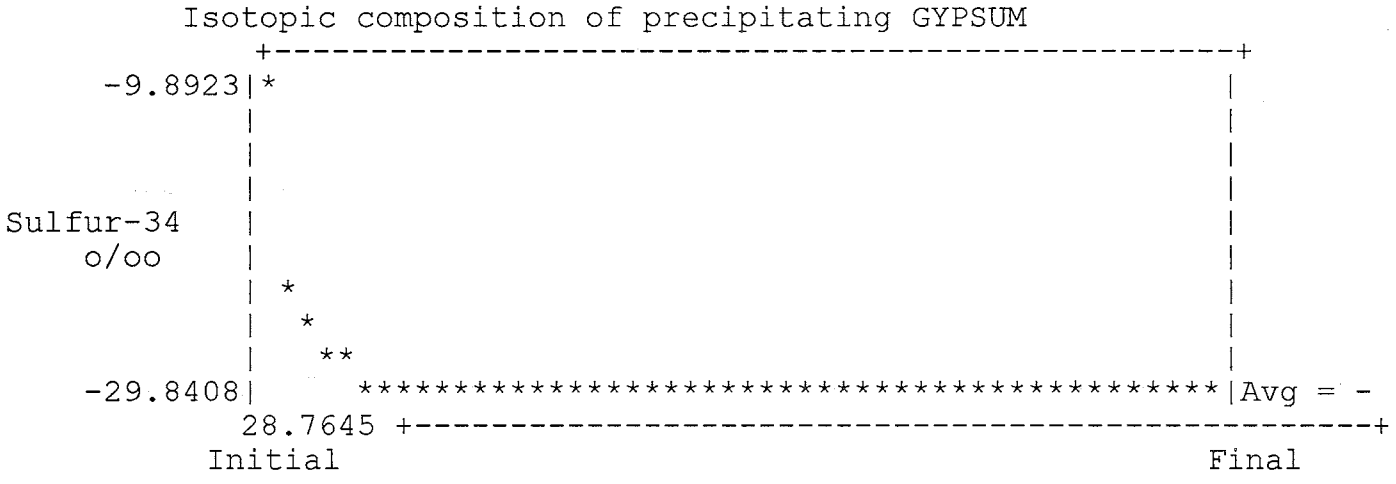

Data used for Strontium-87

Initial Value: .0000 Modeled Final Value: .0000

No incoming or outgoing phases

Data used for Nitrogen-15

Initial Value: .0000 Modeled Final Value: .0000

No incoming or outgoing phases

MODEL 3

CALCITE		4.14680
SiO2		-15.61516
NaCl	+	.34631
K-SPAR		-.02798
DOLOMITE		-.06895
GYPSUM		-.39004
HEMATITE		-.51624

```
 PYRITE                1.03319
 ALBITE                7.56915
 ANORTH               -3.77074
                Computed    Observed
Carbon-13        -8.6791     -8.6690
C-14 (% mod)     23.2208*    17.8400
Sulfur-34       -29.8428    -12.1500
Strontium-87     .000000   Undefined
Nitrogen-15        .0000   Undefined
```

Adjusted C-14 age in years: 2179.* * = based on Original Data

Model (for initial A0)	A0 (initial)	Computed (no decay)	Observed	age (final)
Original Data	73.33	23.22	17.84	2179.
Mass Balance	67.33	21.32	17.84	1473.
Vogel	85.00	26.92	17.84	3400.
Tamers	56.12	17.77	17.84	-32.
Ingerson and Pearson	55.88	17.69	17.84	-68.
Mook	42.38	13.42	17.84	-2354.
Fontes and Garnier	55.87	17.69	17.84	-68.
Eichinger	53.18	16.84	17.84	-478.
User-defined	100.00	31.67	17.84	4743.

Data used for Carbon-13

Initial Value: -13.9690 Modeled Final Value: -8.6791

1 dissolving phases:

Phase	Delta C	Isotopic composition (o/oo)
CALCITE	4.14680	-6.2000

1 precipitating phases:

Phase	Delta C	Fractionation factor	Average Isotopic composition (o/oo)
DOLOMITE	-.13790	.8337	-9.5432

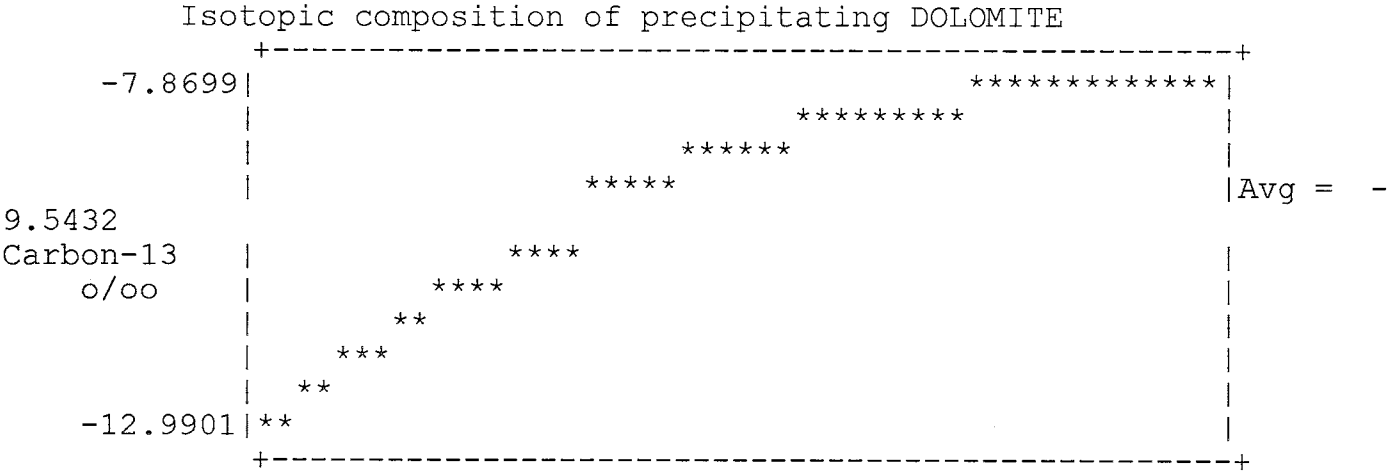

Initial Final

Data used for C-14 (% mod)

Initial Value: 73.3300 Modeled Final Value: 23.2208

1 dissolving phases:

Phase	Delta C	Isotopic composition (% modern)
CALCITE	4.14680	.0000

1 precipitating phases:

Phase	Delta C	Fractionation factor	Average Isotopic composition (% mod
DOLOMITE	-.13790	1.6673	39.2868

Isotopic composition of precipitating DOLOMITE

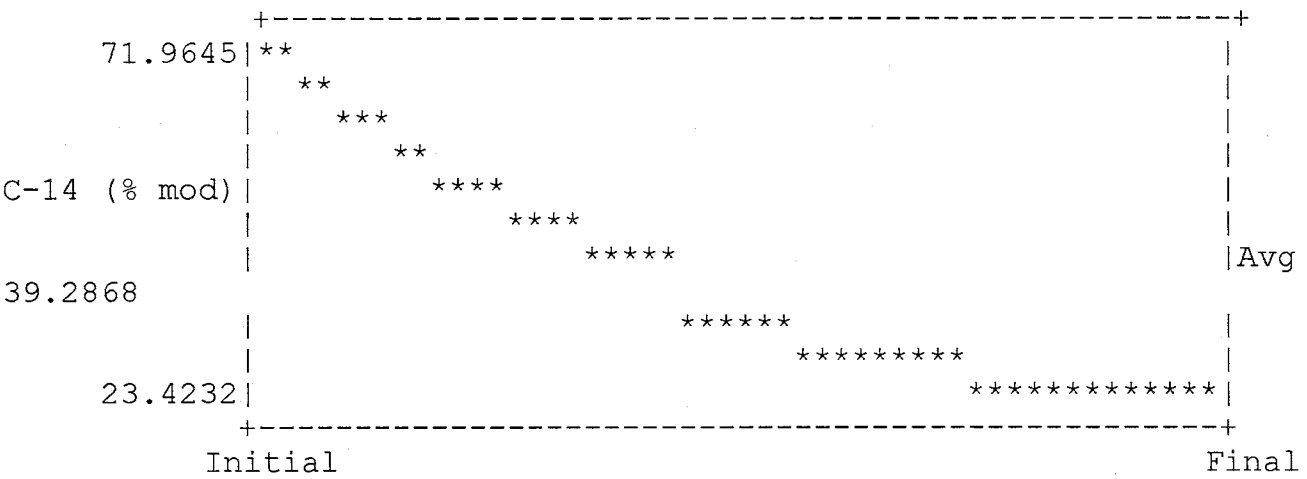

Data used for Sulfur-34

Initial Value: .0000 Modeled Final Value: -29.8428

1 dissolving phases:

Phase	Delta S	Isotopic composition (o/oo)
PYRITE	2.06638	-30.0000

1 precipitating phases:

Phase	Delta S	Fractionation factor	Average Isotopic composition (o/oo)
GYPSUM	-.39004	.0000	-28.7645

Isotopic composition of precipitating GYPSUM

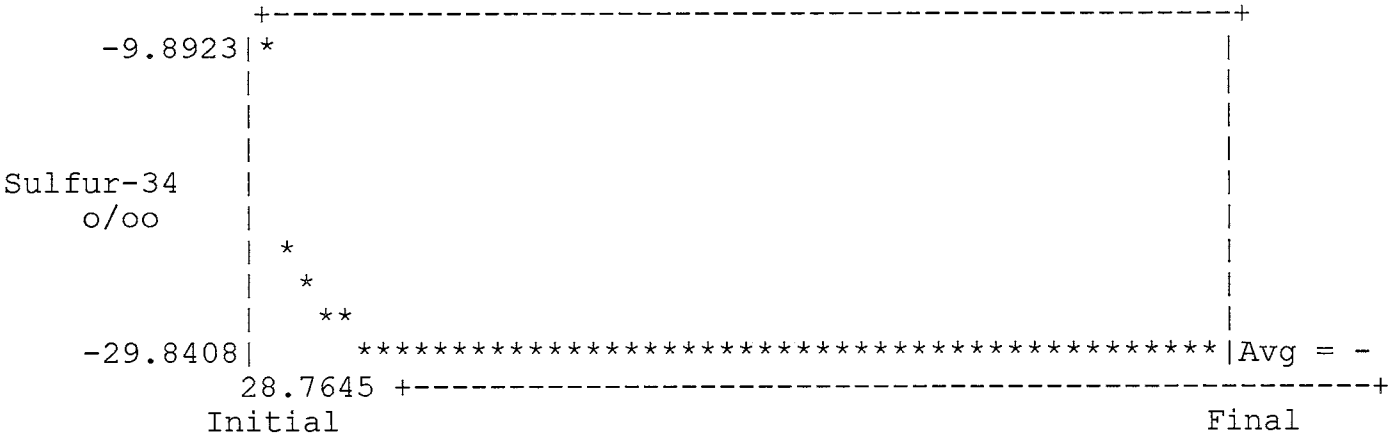

Data used for Strontium-87

Initial Value: .0000 Modeled Final Value: .0000

No incoming or outgoing phases

Data used for Nitrogen-15

Initial Value: .0000 Modeled Final Value: .0000

No incoming or outgoing phases

	MODEL 4	
CALCITE		4.14680
NaCl	+	.34631
K-SPAR		-.02798
EXCHANGE		3.90379
DOLOMITE		-.06895
GYPSUM		-.39004
HEMATITE		-.51624
PYRITE		1.03319
ALBITE		-.23843
ANORTH		.13306

	Computed	Observed
Carbon-13	-8.6791	-8.6690
C-14 (% mod)	23.2208*	17.8400
Sulfur-34	-29.8428	-12.1500
Strontium-87	.000000	Undefined
Nitrogen-15	.0000	Undefined

Adjusted C-14 age in years: 2179.* * = based on Original Data

Model (for initial A0)	A0 (initial)	Computed (no decay)	Observed	age (final)
Original Data	73.33	23.22	17.84	2179.
Mass Balance	67.33	21.32	17.84	1473.
Vogel	85.00	26.92	17.84	3400.
Tamers	56.12	17.77	17.84	-32.
Ingerson and Pearson	55.88	17.69	17.84	-68.
Mook	42.38	13.42	17.84	-2354.
Fontes and Garnier	55.87	17.69	17.84	-68.
Eichinger	53.18	16.84	17.84	-478.
User-defined	100.00	31.67	17.84	4743.

Data used for Carbon-13

Initial Value: -13.9690 Modeled Final Value: -8.6791

1 dissolving phases:

Phase	Delta C	Isotopic composition (o/oo)
CALCITE	4.14680	-6.2000

1 precipitating phases:

Phase	Delta C	Fractionation factor	Average Isotopic composition (o/oo)
DOLOMITE	-.13790	.8337	-9.5432

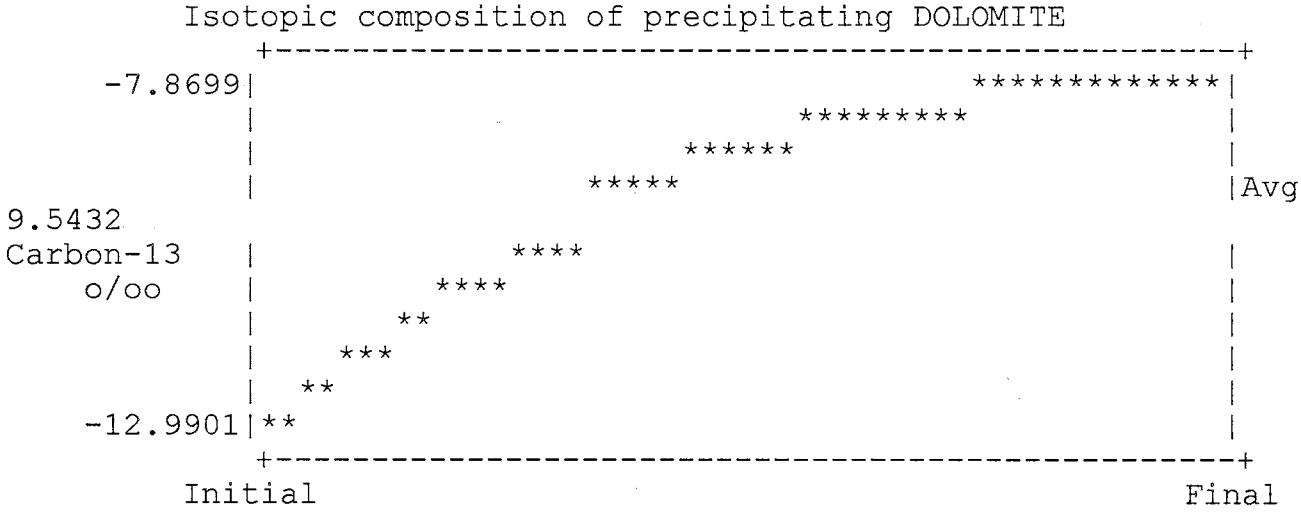

Data used for C-14 (% mod)

Initial Value: 73.3300 Modeled Final Value: 23.2208

1 dissolving phases:

Phase	Delta C	Isotopic composition (% modern)
CALCITE	4.14680	.0000

1 precipitating phases:

Phase	Delta C	Fractionation factor	Average Isotopic composition (% mod
DOLOMITE	-.13790	1.6673	39.2868

Isotopic composition of precipitating DOLOMITE

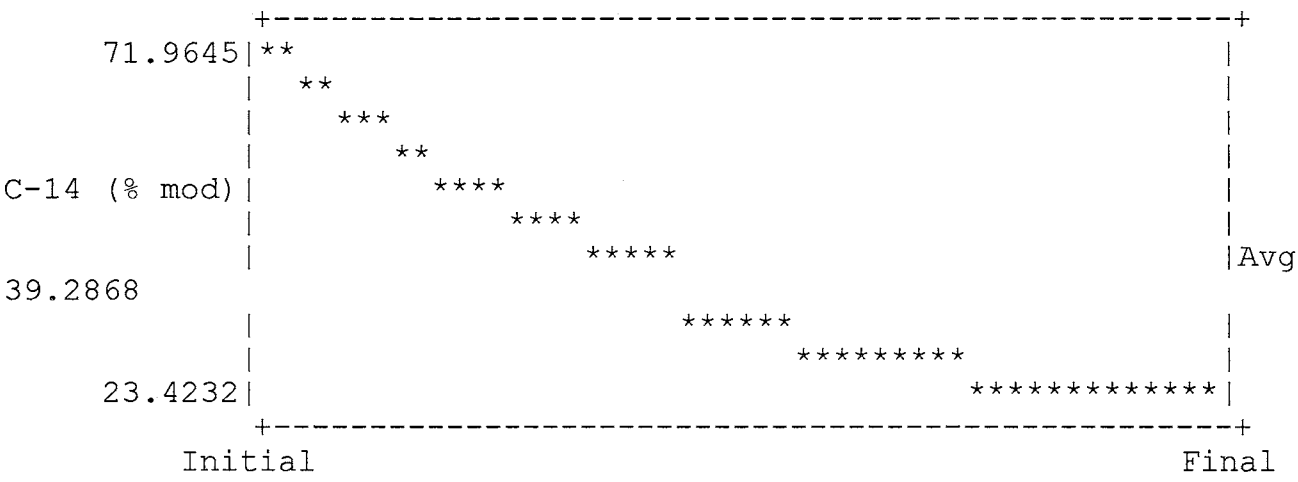

Data used for Sulfur-34

Initial Value: .0000 Modeled Final Value: -29.8428

1 dissolving phases:

Phase	Delta S	Isotopic composition (o/oo)
PYRITE	2.06638	-30.0000

1 precipitating phases:

Phase	Delta S	Fractionation factor	Average Isotopic composition (o/oo)
GYPSUM	-.39004	.0000	-28.7645

Isotopic composition of precipitating GYPSUM

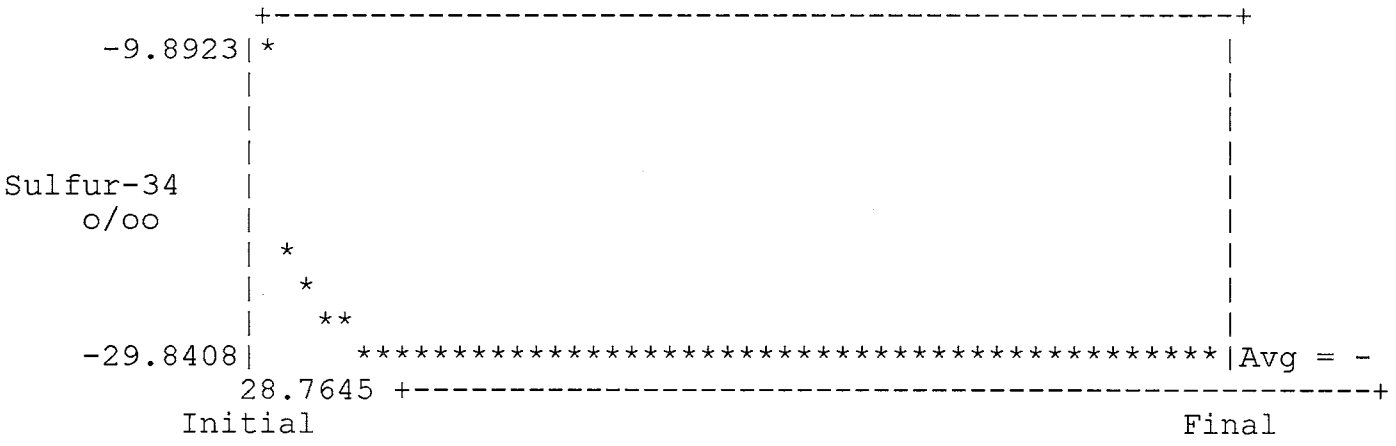

Data used for Strontium-87

Initial Value: .0000 Modeled Final Value: .0000
No incoming or outgoing phases

```
Initial Well : Presbyterian
Final Well   : Seboyeta
          Final      Initial
C        3.5152       1.9659
NA       2.9660        .4632
CA        .2111        .4022
K         .0510        .0980
AL        .0013        .0016
SI        .3351        .8344
MG        .1331        .2641
S         .2391        .0240
CL        .2191        .0770
FE        .0001        .0001

CALCITE  CA   1.0000 C    1.0000 RS   4.0000 I1  -8.5000 I2    .0000
SiO2     SI   1.0000
NaCl     NA   1.0000 CL   1.0000
K-SPAR   K    1.0000 AL   1.0000 SI   3.0000
EXCHANGE CA  -1.0000 NA   2.0000 MG    .0000
DOLOMITE CA   1.0000 MG   1.0000 C    2.0000 RS   8.0000 I1    .0000
         I2    .0000
GYPSUM   CA   1.0000 S    1.0000 RS   6.0000 I3  22.0000
HEMATITE FE   2.0000 RS   6.0000
PYRITE   FE   1.0000 S    2.0000 RS    .0000 I3 -60.0000
ALBITE   NA   1.0000 AL   1.0000 SI   3.0000
ANORTH   CA   1.0000 AL   2.0000 SI   2.0000

                  11 models checked
                   4 models found
          MODEL   1
 CALCITE              1.81149
 SiO2                 -.49834
 NaCl      +           .14205
 K-SPAR               -.04702
 EXCHANGE             1.15703
 DOLOMITE             -.13106
 GYPSUM               -.71450
 HEMATITE             -.23239
 PYRITE                .46478
 ALBITE                .04672
              Computed    Observed
Carbon-13     -11.3445    -11.3170
C-14 (% mod)   37.1613*    23.9600
Sulfur-34     -29.9985     -2.2500
Strontium-87   .000000   Undefined
Nitrogen-15      .0000   Undefined
-------------------------------------------------------------------------
Adjusted C-14 age in years:   3628.*     * = based on Original Data
```

Model (for initial A0)	A0 (initial)	Computed (no decay)	Observed	age (final)
Original Data	73.33	37.16	23.96	3628.
Mass Balance	67.33	34.12	23.96	2922.
Vogel	85.00	43.08	23.96	4849.
Tamers	56.12	28.44	23.96	1417.
Ingerson and Pearson	55.88	28.32	23.96	1381.
Mook	42.38	21.48	23.96	-905.
Fontes and Garnier	55.87	28.31	23.96	1380.
Eichinger	53.18	26.95	23.96	971.
User-defined	100.00	50.68	23.96	6192.

Data used for Carbon-13

Initial Value: -13.9690 Modeled Final Value: -11.3445

1 dissolving phases:

Phase	Delta C	Isotopic composition (o/oo)
CALCITE	1.81149	-8.5000

1 precipitating phases:

Phase	Delta C	Fractionation factor	Average Isotopic composition (o/oo)
DOLOMITE	-.26212	1.0275	-11.3700

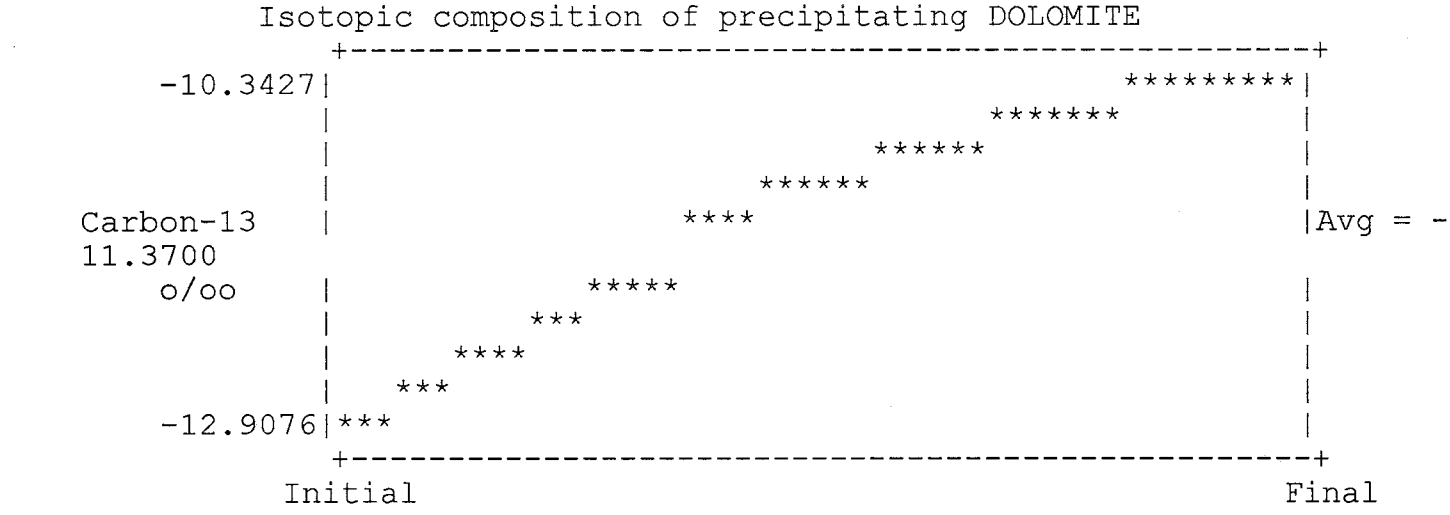

Data used for C-14 (% mod)

Initial Value: 73.3300 Modeled Final Value: 37.1613

1 dissolving phases:

Phase	Delta C	Isotopic composition (% modern)
CALCITE	1.81149	.0000

1 precipitating phases:

Phase	Delta C	Fractionation factor	Average Isotopic composition (% mod
DOLOMITE	-.26212	2.0550	51.6027

Isotopic composition of precipitating DOLOMITE

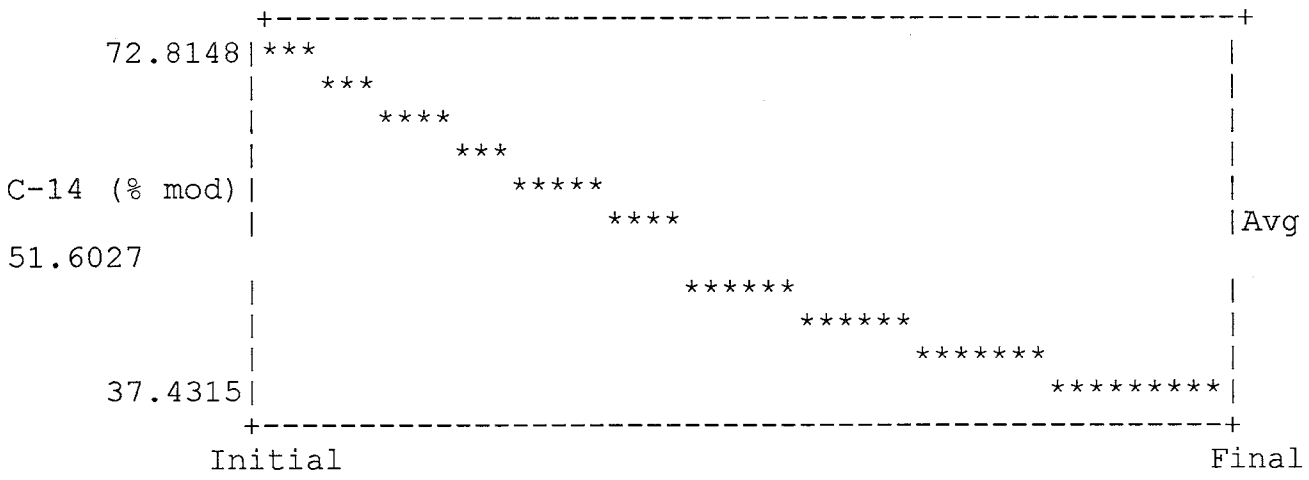

Data used for Sulfur-34

Initial Value: .0000 Modeled Final Value: -29.9985

1 dissolving phases:

Phase	Delta S	Isotopic composition (o/oo)
PYRITE	.92957	-30.0000

1 precipitating phases:

Phase	Delta S	Fractionation factor	Average Isotopic composition (o/oo)
GYPSUM	-.71450	.0000	-28.9543

Isotopic composition of precipitating GYPSUM

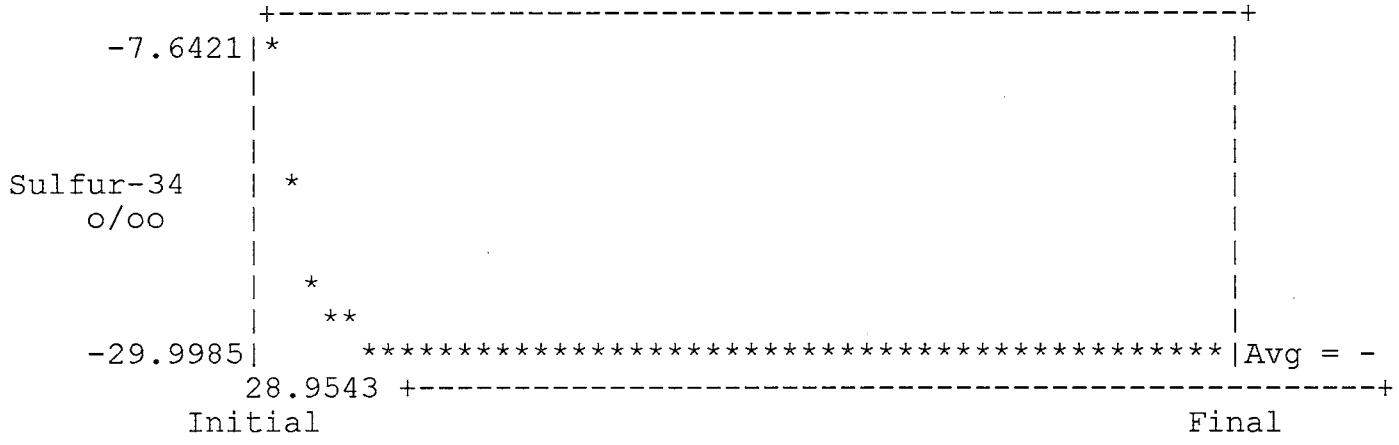

Data used for Strontium-87

Initial Value: .0000 Modeled Final Value: .0000

No incoming or outgoing phases

```
Initial Well : Presbyterian
Final Well   : Moquino
          Final      Initial
C        6.5739       1.9659
NA       7.5225        .4632
CA        .1081        .4022
K         .0360        .0980
AL        .0000        .0016
SI        .1571        .8344
MG        .0941        .2641
S         .0000        .0240
CL        .1151        .0770
FE        .0015        .0001

CALCITE  CA   1.0000 C    1.0000 RS   4.0000 I1  -4.4000 I2    .0000
SiO2     SI   1.0000
NaCl     NA   1.0000 CL   1.0000
K-SPAR   K    1.0000 AL   1.0000 SI   3.0000
EXCHANGE CA  -1.0000 NA   2.0000 MG    .0000
DOLOMITE CA   1.0000 MG   1.0000 C    2.0000 RS   8.0000 I1    .0000
         I2    .0000
GYPSUM   CA   1.0000 S    1.0000 RS   6.0000 I3  22.0000
HEMATITE FE   2.0000 RS   6.0000
PYRITE   FE   1.0000 S    2.0000 RS    .0000 I3 -60.0000
ALBITE   NA   1.0000 AL   1.0000 SI   3.0000
ANORTH   CA   1.0000 AL   2.0000 SI   2.0000

                  11 models checked
                   4 models found
           MODEL   1
 CALCITE              4.94819
 SiO2                 -.67247
 NaCl      +           .03804
 K-SPAR               -.06202
 EXCHANGE             3.48043
 DOLOMITE             -.17005
 GYPSUM              -1.59183
 HEMATITE             -.39125
 PYRITE                .78391
 ALBITE                .06042
               Computed    Observed
Carbon-13      -7.0480     -7.0850
C-14 (% mod)   20.0569*     4.6100
Sulfur-34     -30.0000       .0000
Strontium-87   .000000   Undefined
Nitrogen-15      .0000   Undefined
-------------------------------------------------------------------------
Adjusted C-14 age in years:  12155.*     * = based on Original Data
```

Model (for initial A0)	A0 (initial)	Computed (no decay)	Observed	age (final)
Original Data	73.33	20.06	4.61	12155.
Mass Balance	67.33	18.42	4.61	11449.
Vogel	85.00	23.25	4.61	13376.
Tamers	56.12	15.35	4.61	9943.
Ingerson and Pearson	55.88	15.28	4.61	9908.
Mook	42.38	11.59	4.61	7622.
Fontes and Garnier	55.87	15.28	4.61	9907.
Eichinger	53.18	14.54	4.61	9498.
User-defined	100.00	27.35	4.61	14719.

Data used for Carbon-13

Initial Value: -13.9690 Modeled Final Value: -7.0480

1 dissolving phases:

Phase	Delta C	Isotopic composition (o/oo)
CALCITE	4.94819	-4.4000

1 precipitating phases:

Phase	Delta C	Fractionation factor	Average Isotopic composition (o/oo)
DOLOMITE	-.34010	.6159	-8.5266

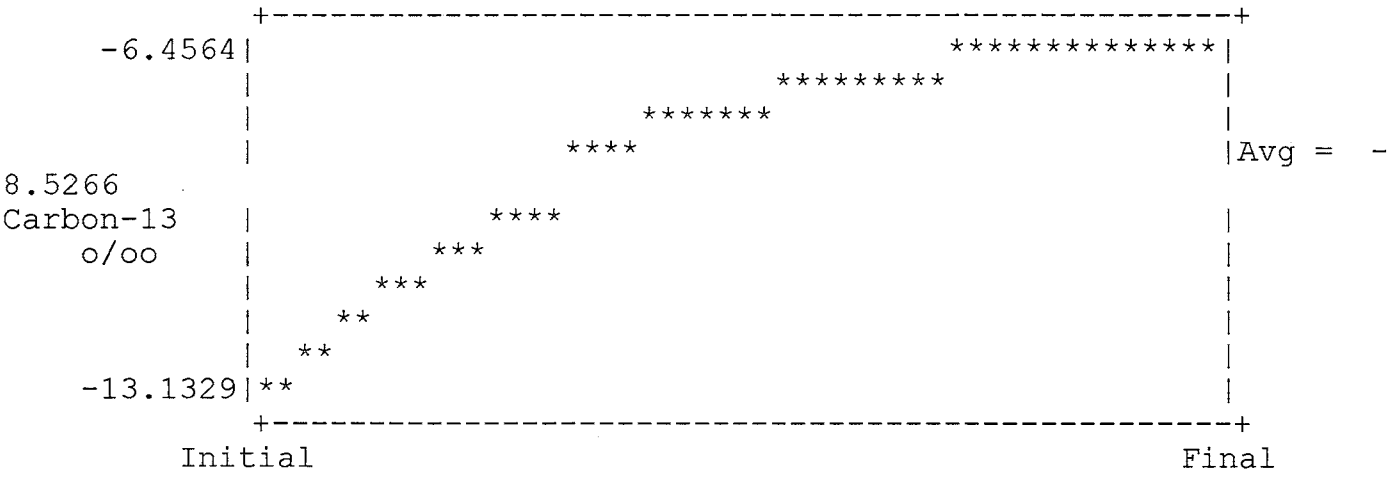

Data used for C-14 (% mod)

Initial Value: 73.3300 Modeled Final Value: 20.0569

1 dissolving phases:

Phase	Delta C	Isotopic composition (% modern)
CALCITE	4.94819	.0000

1 precipitating phases:

Phase	Delta C	Fractionation factor	Average Isotopic composition (% mod
DOLOMITE	-.34010	1.2318	36.1794

Isotopic composition of precipitating DOLOMITE

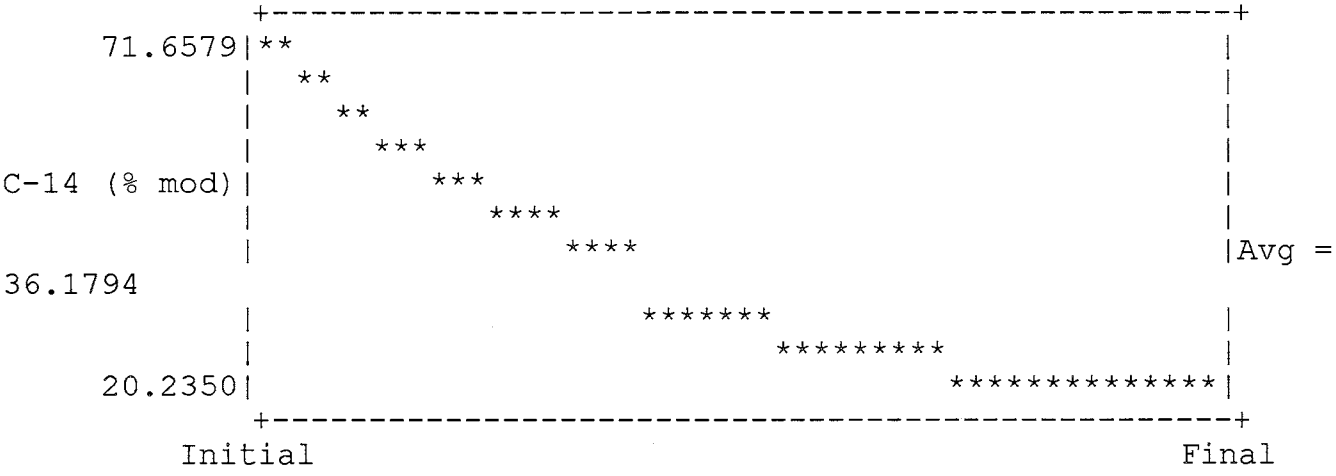

Data used for Sulfur-34

Initial Value: .0000 Modeled Final Value: -30.0000

1 dissolving phases:

Phase	Delta S	Isotopic composition (o/oo)
PYRITE	1.56782	-30.0000

1 precipitating phases:

Phase	Delta S	Fractionation factor	Average Isotopic composition (o/oo)

```
Initial Well : Presbyterian
Final Well   : CNV-W2
          Final      Initial
C        7.6851       1.9659
NA      13.3680        .4632
CA        .0831        .4022
K         .1632        .0980
AL        .0000        .0016
SI        .2002        .8344
MG        .0551        .2641
S        2.3505        .0240
CL        .3924        .0770
FE        .0102        .0001

CALCITE  CA   1.0000 C    1.0000 RS   4.0000 I1  -1.6000 I2    .0000
SiO2     SI   1.0000
NaCl     NA   1.0000 CL   1.0000
K-SPAR   K    1.0000 AL   1.0000 SI   3.0000
EXCHANGE CA  -1.0000 NA   2.0000 MG    .0000
DOLOMITE CA   1.0000 MG   1.0000 C    2.0000 RS   8.0000 I1    .0000
         I2    .0000
GYPSUM   CA   1.0000 S    1.0000 RS   6.0000 I3  22.0000
HEMATITE FE   2.0000 RS   6.0000
PYRITE   FE   1.0000 S    2.0000 RS    .0000 I3 -60.0000
ALBITE   NA   1.0000 AL   1.0000 SI   3.0000
ANORTH   CA   1.0000 AL   2.0000 SI   2.0000

                  11 models checked
                   4 models found
          MODEL   1
 CALCITE              6.13730
 SiO2                 -.62935
 NaCl      +           .31538
 K-SPAR                .06513
 EXCHANGE             6.32808
 DOLOMITE             -.20905
 GYPSUM                .08074
 HEMATITE             -.55637
 PYRITE               1.12285
 ALBITE               -.06673
                Computed    Observed
Carbon-13       -4.5043     -4.4300
C-14 (% mod)    16.9759*    52.2900
Sulfur-34      -27.9072    -22.0900
Strontium-87    .000000   Undefined
Nitrogen-15       .0000   Undefined
-------------------------------------------------------------------
Adjusted C-14 age in years:  -9300.*     * = based on Original Data
```

Model (for initial A0)	A0 (initial)	Computed (no decay)	Observed	age (final)
Original Data	73.33	16.98	52.29	-9300
Mass Balance	67.33	15.59	52.29	-10006
Vogel	85.00	19.68	52.29	--8079
Tamers	56.12	12.99	52.29	-11511
Ingerson and Pearson	55.88	12.94	52.29	-11547
Mook	42.38	9.81	52.29	-13833
Fontes and Garnier	55.87	12.93	52.29	-11548
Eichinger	53.18	12.31	52.29	-11957
User-defined	100.00	23.15	52.29	-6736

Data used for Carbon-13

Initial Value: -13.9690 Modeled Final Value: -4.5043

1 dissolving phases:

Phase	Delta C	Isotopic composition (o/oo)
CALCITE	6.13730	-1.6000

1 precipitating phases:

Phase	Delta C	Fractionation factor	Average Isotopic composition (o/oo)
DOLOMITE	-.41810	.7776	-6.3751

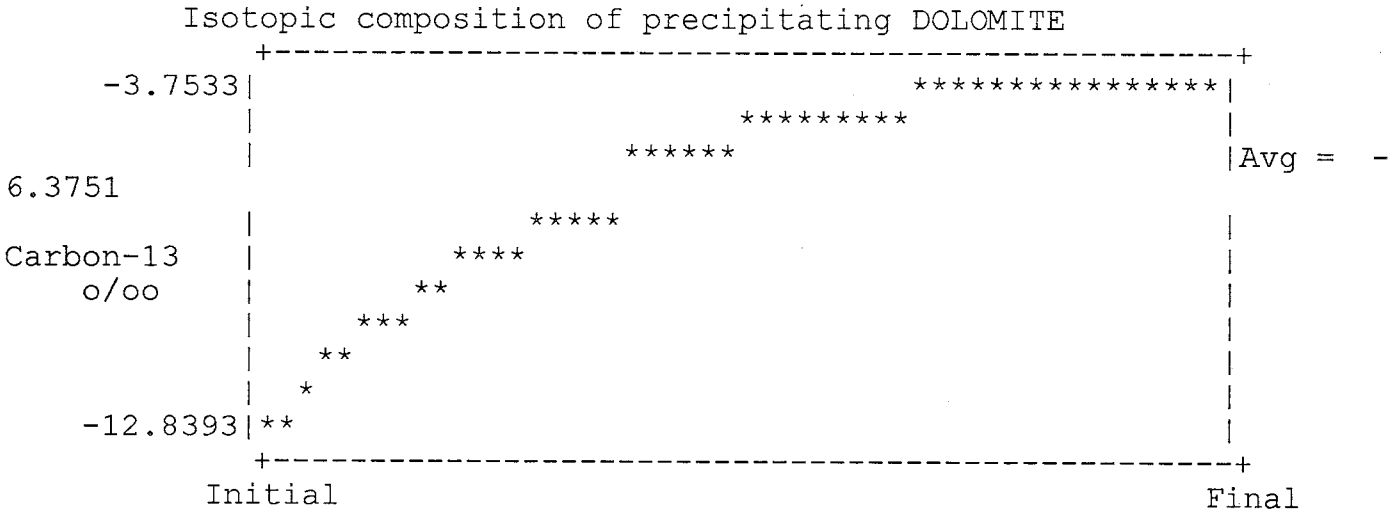

Data used for C-14 (% mod)

Initial Value: 73.3300 Modeled Final Value: 16.9759

1 dissolving phases:

Phase	Delta C	Isotopic composition (% modern)
CALCITE	6.13730	.0000

1 precipitating phases:

Phase	Delta C	Fractionation factor	Average Isotopic composition (% mod
DOLOMITE	-.41810	1.5552	32.7627

Isotopic composition of precipitating DOLOMITE

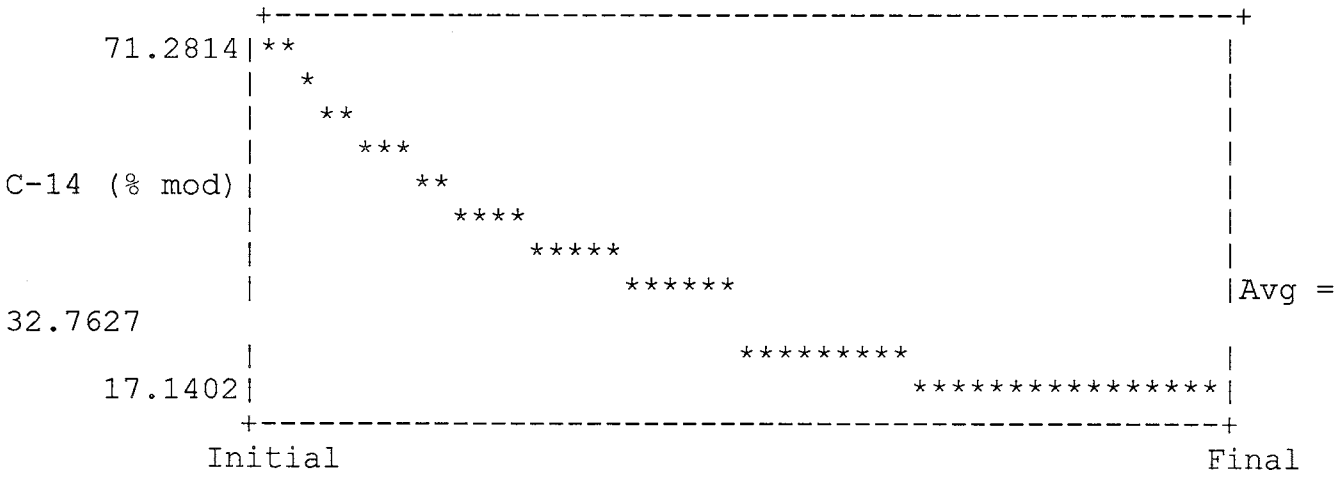

Data used for Sulfur-34

Initial Value: .0000 Modeled Final Value: -27.9072

2 dissolving phases:

Phase	Delta S	Isotopic composition (o/oo)
GYPSUM	.08074	22.000
PYRITE	2.24571	-30.0000

Data used for Strontium-87

Initial Value: .0000 Modeled Final Value: .0000

No incoming or outgoing phases

Data used for Nitrogen-15

Initial Value: .0000 Modeled Final Value: .0000

No incoming or outgoing phases

```
Initial Well : Presbyterian
Final Well   : CNV-W3
          Final      Initial
C        9.6762       1.9659
NA      10.7632        .4632
CA        .1241        .4022
K         .0561        .0980
AL        .0000        .0016
SI        .1772        .8344
MG        .0320        .2641
S         .8418        .0240
CL        .1481        .0770
FE        .0170        .0001

CALCITE  CA   1.0000 C    1.0000 RS   4.0000 I1   -.5000 I2    .0000
SiO2     SI   1.0000
NaCl     NA   1.0000 CL   1.0000
K-SPAR   K    1.0000 AL   1.0000 SI   3.0000
EXCHANGE CA  -1.0000 NA   2.0000 MG    .0000
DOLOMITE CA   1.0000 MG   1.0000 C    2.0000 RS   8.0000 I1    .0000
         I2    .0000
GYPSUM   CA   1.0000 S    1.0000 RS   6.0000 I3  22.0000
HEMATITE FE   2.0000 RS   6.0000
PYRITE   FE   1.0000 S    2.0000 RS    .0000 I3 -60.0000
ALBITE   NA   1.0000 AL   1.0000 SI   3.0000
ANORTH   CA   1.0000 AL   2.0000 SI   2.0000

                  11 models checked
                   4 models found
           MODEL   1
 CALCITE              8.17451
 SiO2                -.65239
 NaCl      +          .07111
 K-SPAR               -.04199
 EXCHANGE             5.09427
 DOLOMITE             -.23208
 GYPSUM              -3.12622
 HEMATITE             -.97754
 PYRITE               1.97200
 ALBITE                .04039
                Computed    Observed
Carbon-13       -3.0230     -3.0800
C-14 (% mod)    13.5330*      .7400
Sulfur-34      -30.0000     -9.9500
Strontium-87    .000000   Undefined
Nitrogen-15       .0000   Undefined
-------------------------------------------------------------------------
Adjusted C-14 age in years:  24025.*     * = based on Original Data
```

Model (for initial A0)	A0 (initial)	Computed (no decay)	Observed	age (final)
Original Data	73.33	13.53	.74	24025.
Mass Balance	67.33	12.43	.74	23319.
Vogel	85.00	15.69	.74	25246.
Tamers	56.12	10.36	.74	21813.
Ingerson and Pearson	55.88	10.31	.74	21778.
Mook	42.38	7.82	.74	19492.
Fontes and Garnier	55.87	10.31	.74	21777.
Eichinger	53.18	9.81	.74	21368.
User-defined	100.00	18.45	.74	26589.

Data used for Carbon-13

Initial Value: -13.9690 Modeled Final Value: -3.0230

1 dissolving phases:

Phase	Delta C	Isotopic composition (o/oo)
CALCITE	8.17451	-.5000

1 precipitating phases:

Phase	Delta C	Fractionation factor	Average Isotopic composition (o/oo)
DOLOMITE	-.46416	.8031	-4.9497

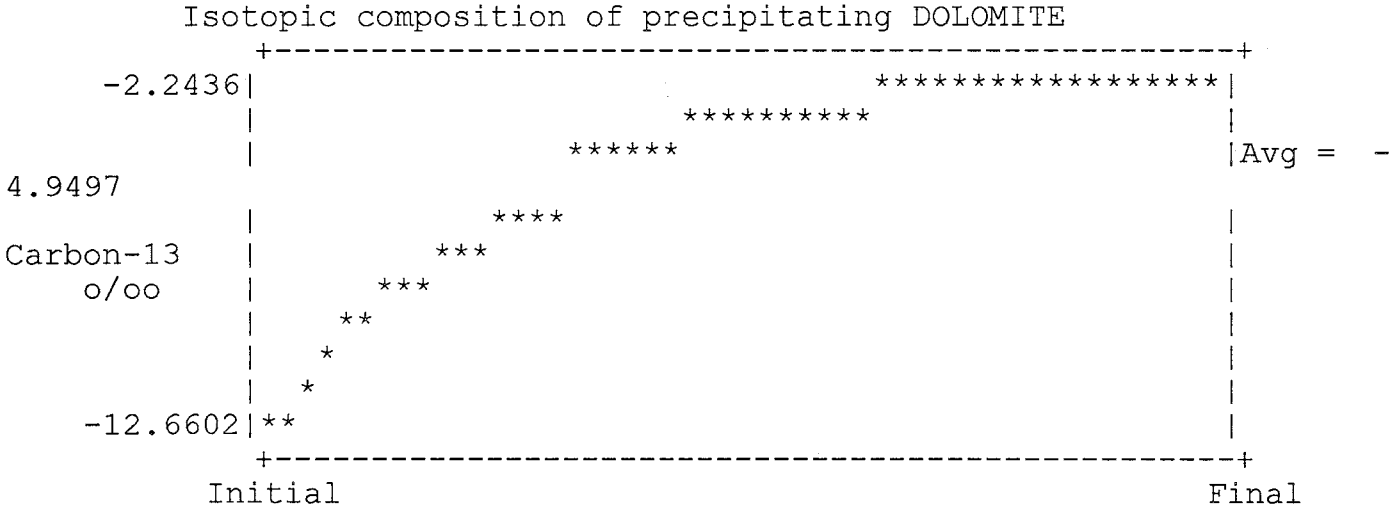

Data used for C-14 (% mod)

Initial Value: 73.3300 Modeled Final Value: 13.5330

1 dissolving phases:

Phase	Delta C	Isotopic composition (% modern)
CALCITE	8.17451	.0000

1 precipitating phases:

Phase	Delta C	Fractionation factor	Average Isotopic composition (% mod
DOLOMITE	-.46416	1.6063	28.4658

Isotopic composition of precipitating DOLOMITE

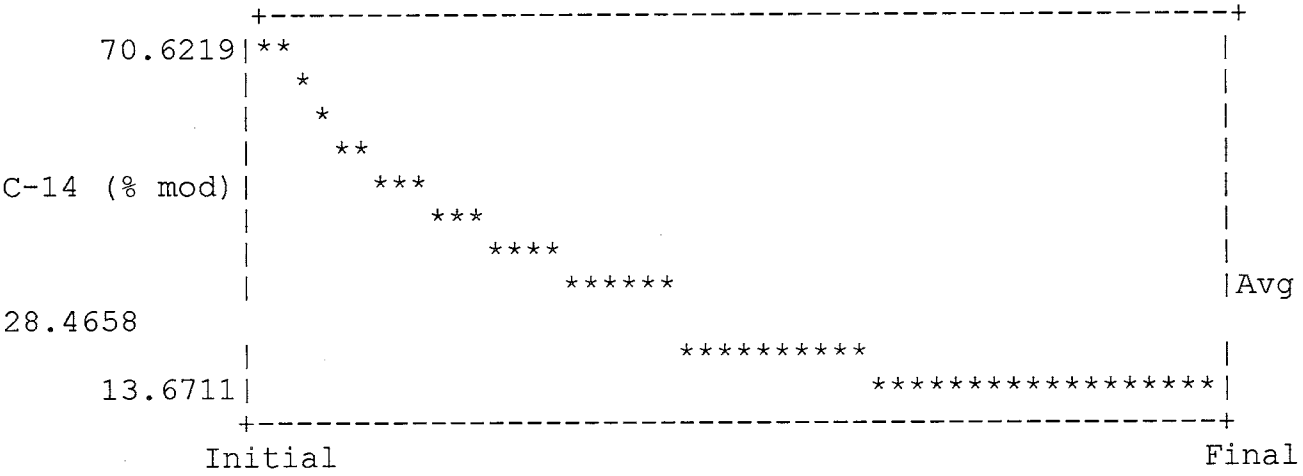

Data used for Sulfur-34

Initial Value: .0000 Modeled Final Value: -30.0000

1 dissolving phases:

Phase	Delta S	Isotopic composition (o/oo)
PYRITE	3.94401	-30.0000

1 precipitating phases:

Phase	Delta S	Fractionation factor	Average Isotopic composition (o/oo)
GYPSUM	-3.12622	.0000	-29.6366

Isotopic composition of precipitating GYPSUM

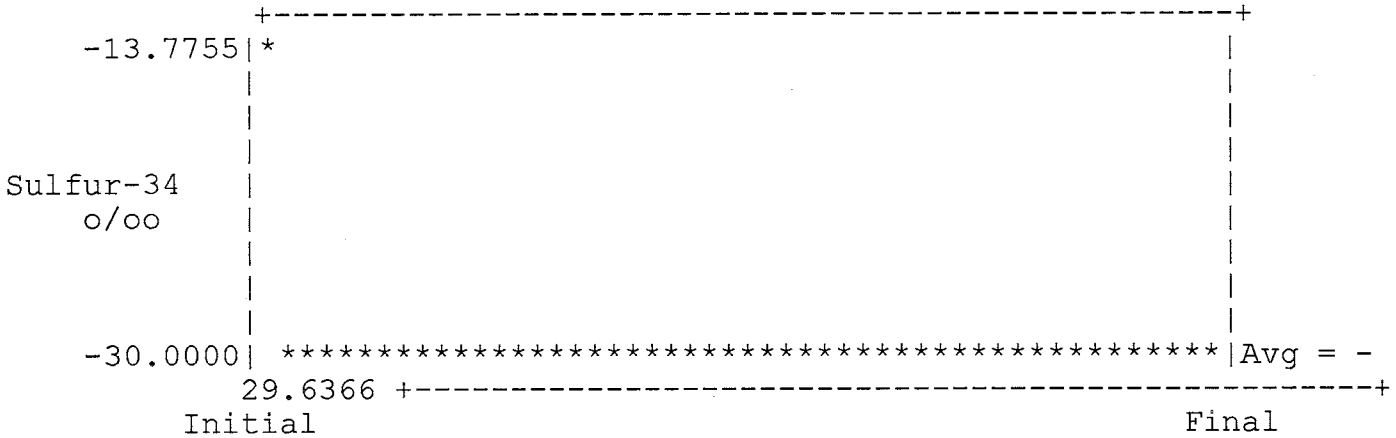

Data used for Strontium-87

Initial Value: .0000 Modeled Final Value: .0000

No incoming or outgoing phases

```
Initial Well : Presbyterian
Final Well   : CNV-W5
          Final      Initial
C        8.9128       1.9659
NA      15.4664        .4632
CA        .4356        .4022
K         .0441        .0980
AL        .0000        .0016
SI        .1412        .8344
MG        .2724        .2641
S        3.8611        .0240
CL        .3154        .0770
FE        .0000        .0001

CALCITE   CA    1.0000 C    1.0000 RS   4.0000 I1   -.3000 I2    .0000
SiO2      SI    1.0000
NaCl      NA    1.0000 CL   1.0000
K-SPAR    K     1.0000 AL   1.0000 SI   3.0000
EXCHANGE  CA   -1.0000 NA   2.0000 MG    .0000
DOLOMITE  CA    1.0000 MG   1.0000 C    2.0000 RS   8.0000 I1    .0000
          I2     .0000
GYPSUM    CA    1.0000 S    1.0000 RS   6.0000 I3  22.0000
HEMATITE  FE    2.0000 RS   6.0000
PYRITE    FE    1.0000 S    2.0000 RS    .0000 I3 -60.0000
ALBITE    NA    1.0000 AL   1.0000 SI   3.0000

ANORTH    CA    1.0000 AL   2.0000 SI   2.0000

                   11 models checked
                    4 models found
            MODEL   1
 CALCITE                  6.93042
 SiO2                    -.68837
 NaCl        +            .23839
 K-SPAR                  -.05398
 EXCHANGE                7.35622
 DOLOMITE                 .00825
 GYPSUM                   .45096
 HEMATITE                -.84658
 PYRITE                  1.69306
 ALBITE                   .05238
                 Computed    Observed
Carbon-13         -3.3144     -3.3000
C-14 (% mod)      16.1741*      .2800
Sulfur-34        -23.7400     -8.7800
Strontium-87      .000000   Undefined
Nitrogen-15         .0000   Undefined
-------------------------------------------------------------------------
Adjusted C-14 age in years:  33533.*     * = based on Original Data
```

Model (for initial A0)	A0 (initial)	Computed (no decay)	Observed	age (final)
Original Data	73.33	16.17	.28	33533.
Mass Balance	67.33	14.85	.28	32827.
Vogel	85.00	18.75	.28	34753.
Tamers	56.12	12.38	.28	31321.
Ingerson and Pearson	55.88	12.32	.28	31285.
Mook	42.38	9.35	.28	29000.
Fontes and Garnier	55.87	12.32	.28	31285.
Eichinger	53.18	11.73	.28	30876.
User-defined	100.00	22.06	.28	36097.

Data used for Carbon-13

Initial Value: -13.9690 Modeled Final Value: -3.3144

2 dissolving phases:

Phase	Delta C	Isotopic composition (o/oo)
CALCITE	6.93042	-.3000
DOLOMITE	.01650	.0000

Data used for C-14 (% mod)

Initial Value: 73.3300 Modeled Final Value: 16.1741

2 dissolving phases:

Phase	Delta C	Isotopic composition (% modern)
CALCITE	6.93042	.0000
DOLOMITE	.01650	.0000

Data used for Sulfur-34

Initial Value: .0000 Modeled Final Value: -23.7400

2 dissolving phases:

Phase	Delta S	Isotopic composition (o/oo)
GYPSUM	.45096	22.0000
PYRITE	3.38613	-30.0000

Data used for Strontium-87

Initial Value: .0000 Modeled Final Value: .0000

No incoming or outgoing phases

```
Initial Well : Presbyterian
Final Well   : MW-64
          Final      Initial
C       10.7673       1.9659
NA      24.7631        .4632
CA        .1993        .4022
K         .0862        .0980
AL        .0000        .0016
SI        .2534        .8344
MG        .1162        .2641
S        4.2683        .0240
CL        .9666        .0770
FE        .0000        .0001

CALCITE  CA    1.0000 C     1.0000 RS    4.0000 I1   -3.9000 I2     .0000
SiO2     SI    1.0000
NaCl     NA    1.0000 CL    1.0000
K-SPAR   K     1.0000 AL    1.0000 SI    3.0000
EXCHANGE CA   -1.0000 NA    2.0000 MG     .0000
DOLOMITE CA    1.0000 MG    1.0000 C     2.0000 RS    8.0000 I1     .0000
         I2     .0000
GYPSUM   CA    1.0000 S     1.0000 RS    6.0000 I3   22.0000
HEMATITE FE    2.0000 RS    6.0000
PYRITE   FE    1.0000 S     2.0000 RS     .0000 I3  -60.0000
ALBITE   NA    1.0000 AL    1.0000 SI    3.0000
ANORTH   CA    1.0000 AL    2.0000 SI    2.0000

                    11 models checked
                     4 models found
           MODEL   1
 CALCITE              9.09726
 SiO2                -.57613
 NaCl      +          .88961
 K-SPAR              -.01189
 EXCHANGE           11.69999
 DOLOMITE            -.14791
 GYPSUM              2.54780
 HEMATITE            -.42416
 PYRITE               .84822
 ALBITE               .01029
                Computed    Observed
Carbon-13       -5.6592     -5.6500
C-14 (% mod)    12.6433*       .2800
Sulfur-34        1.2086    -16.6100
Strontium-87    .000000   Undefined
Nitrogen-15       .0000   Undefined
-------------------------------------------------------------------------
Adjusted C-14 age in years:  31497.*     * = based on Original Data
```

Model (for initial A0)	A0 (initial)	Computed (no decay)	Observed	age (final)
Original Data	73.33	12.64	.28	31497.
Mass Balance	67.33	11.61	.28	30791.
Vogel	85.00	14.66	.28	32717.
Tamers	56.12	9.68	.28	29285.
Ingerson and Pearson	55.88	9.63	.28	29250.
Mook	42.38	7.31	.28	26964.
Fontes and Garnier	55.87	9.63	.28	29249.
Eichinger	53.18	9.17	.28	28840.
User-defined	100.00	17.24	.28	34061.

Data used for Carbon-13

Initial Value: -13.9690 Modeled Final Value: -5.6592

1 dissolving phases:

Phase	Delta C	Isotopic composition (o/oo)
CALCITE	9.09726	-3.9000

1 precipitating phases:

Phase	Delta C	Fractionation factor	Average Isotopic composition (o/oo)
DOLOMITE	-.29582	.8619	-6.7810

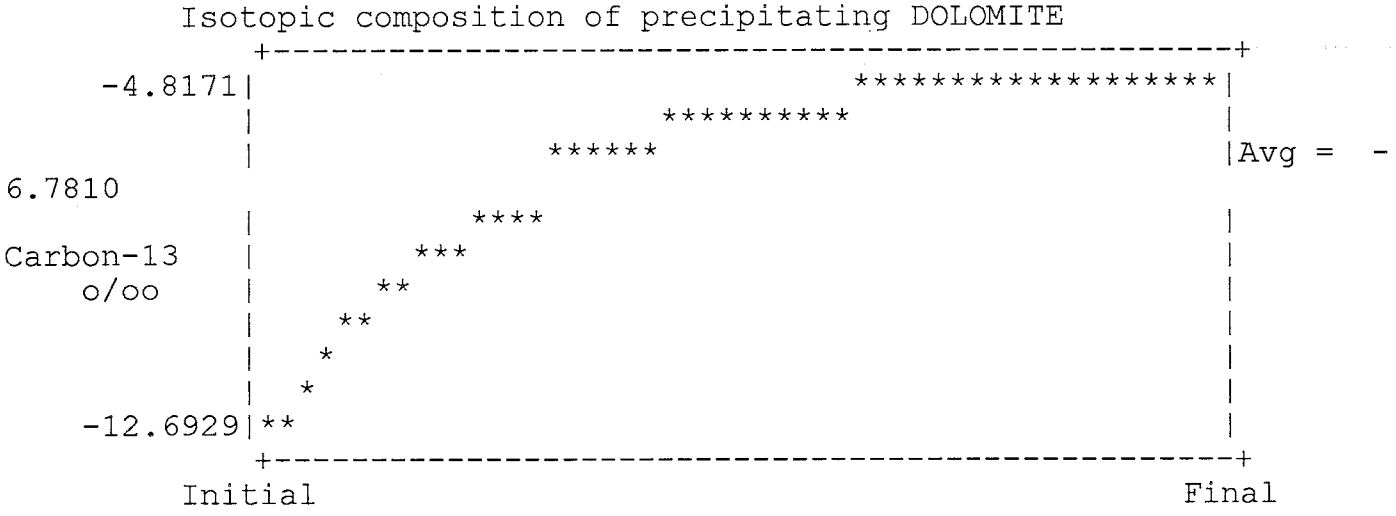

Data used for C-14 (% mod)

Initial Value: 73.3300 Modeled Final Value: 12.6433

1 dissolving phases:

Phase	Delta C	Isotopic composition (% modern)
CALCITE	9.09726	.0000

1 precipitating phases:

Phase	Delta C	Fractionation factor	Average Isotopic composition (% mod
DOLOMITE	-.29582	1.7238	27.1286

Isotopic composition of precipitating DOLOMITE

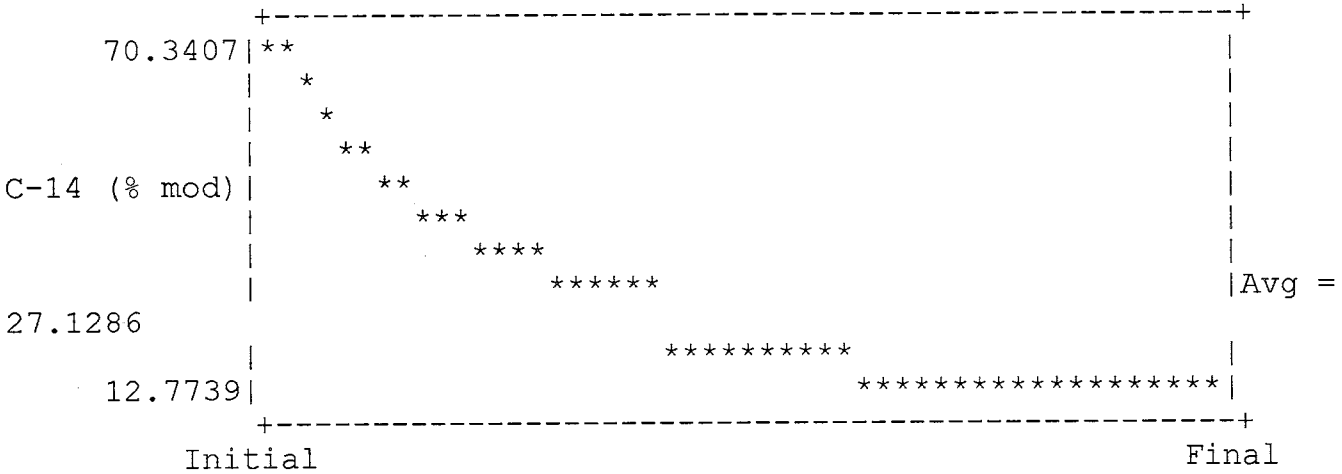

Data used for Sulfur-34

Initial Value: .0000 Modeled Final Value: 1.2086

2 dissolving phases:

Phase	Delta S	Isotopic composition (o/oo)
GYPSUM	2.54780	22.0000
PYRITE	1.69644	-30.0000

Data used for Strontium-87

Initial Value: .0000 Modeled Final Value: .0000

No incoming or outgoing phases

Data used for Nitrogen-15

Initial Value: .0000 Modeled Final Value: .0000

No incoming or outgoing phases

```
Initial Well : Presbyterian
Final Well   : MW-65
          Final      Initial
C       10.9357       1.9659
NA      22.9694        .4632
CA        .2515        .4022
K         .1052        .0980
AL        .0000        .0016
SI        .2685        .8344
MG        .4027        .2641
S        2.7139        .0240
CL       8.6315        .0770
FE        .0011        .0001

CALCITE  CA    1.0000 C    1.0000 RS   4.0000 I1  -5.5000 I2    .0000
SiO2     SI    1.0000
NaCl     NA    1.0000 CL   1.0000
K-SPAR   K     1.0000 AL   1.0000 SI   3.0000
EXCHANGE CA   -1.0000 NA   2.0000 MG    .0000
DOLOMITE CA    1.0000 MG   1.0000 C    2.0000 RS   8.0000 I1    .0000
         I2     .0000
GYPSUM   CA    1.0000 S    1.0000 RS   6.0000 I3  22.0000
HEMATITE FE    2.0000 RS   6.0000
PYRITE   FE    1.0000 S    2.0000 RS    .0000 I3 -60.0000
ALBITE   NA    1.0000 AL   1.0000 SI   3.0000
ANORTH   CA    1.0000 AL   2.0000 SI   2.0000

                   11 models checked
                    4 models found
            MODEL   1
 CALCITE                 8.69260
 SiO2                    -.56108
 NaCl        +           8.55451
 K-SPAR                   .00715
 EXCHANGE                6.98020
 DOLOMITE                 .13862
 GYPSUM                 -2.00174
 HEMATITE               -1.17240
 PYRITE                  2.34581
 ALBITE                  -.00875
                 Computed    Observed
Carbon-13        -6.8830     -6.8400
C-14 (% mod)     13.1821*       .2500
Sulfur-34       -29.9921    -14.5500
Strontium-87     .000000   Undefined
Nitrogen-15        .0000   Undefined
-------------------------------------------------------------------------
Adjusted C-14 age in years:  32779.*     * = based on Original Data
```

Model (for initial A0)	A0 (initial)	Computed (no decay)	Observed	age (final)
Original Data	73.33	13.18	.25	32779.
Mass Balance	67.33	12.10	.25	32073.
Vogel	85.00	15.28	.25	33999.
Tamers	56.12	10.09	.25	30567.
Ingerson and Pearson	55.88	10.04	.25	30531.
Mook	42.38	7.62	.25	28246.
Fontes and Garnier	55.87	10.04	.25	30531.
Eichinger	53.18	9.56	.25	30122.
User-defined	100.00	17.98	.25	35343.

Data used for Carbon-13

Initial Value: -13.9690 Modeled Final Value: -6.8830

2 dissolving phases:

Phase	Delta C	Isotopic composition (o/oo)
CALCITE	8.69260	-5.5000
DOLOMITE	.27724	.0000

Data used for C-14 (% mod)

Initial Value: 73.3300 Modeled Final Value: 13.1821

2 dissolving phases:

Phase	Delta C	Isotopic composition (% modern)
CALCITE	8.69260	.0000
DOLOMITE	.27724	.0000

Data used for Sulfur-34

Initial Value: .0000 Modeled Final Value: -29.9921

1 dissolving phases:

Phase	Delta S	Isotopic composition (o/oo)
PYRITE	4.69162	-30.0000

1 precipitating phases:

Phase	Delta S	Fractionation factor	Average Isotopic composition (o/oo)
GYPSUM	-2.00174	.0000	-29.5148

Isotopic composition of precipitating GYPSUM

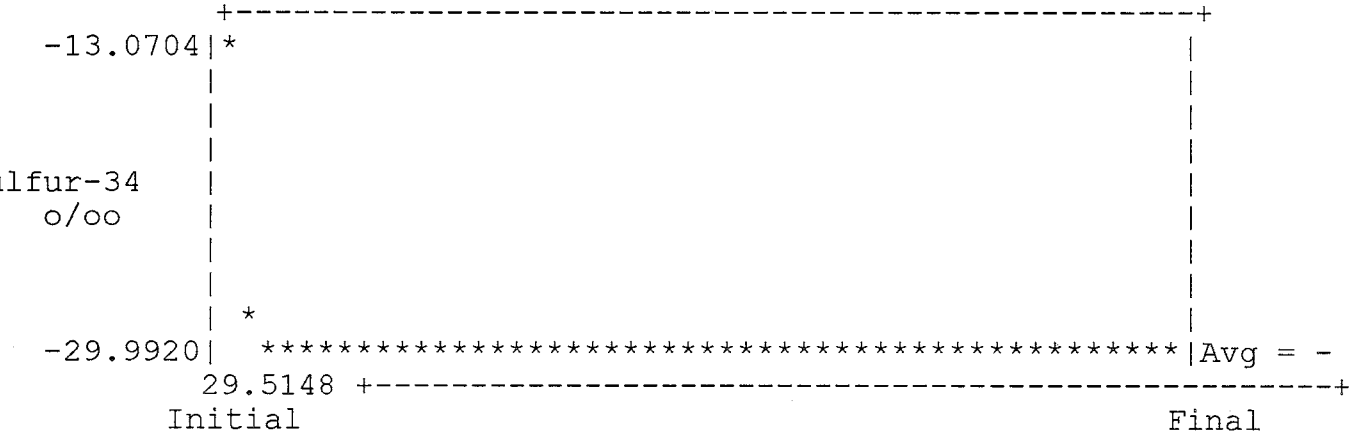

Data used for Strontium-87

Initial Value: .0000 Modeled Final Value: .0000

No incoming or outgoing phases

Data used for Nitrogen-15

Initial Value: .0000 Modeled Final Value: .0000

No incoming or outgoing phases

```
Initial Well : Presbyterian
Final Well   : MW-60
          Final      Initial
C       12.3224       1.9659
NA      24.7701        .4632
CA        .1994        .4022
K         .0862        .0980
AL        .0000        .0016
SI        .2705        .8344
MG        .1162        .2641
S        6.1422        .0240
CL       1.2054        .0770
FE        .0000        .0001

CALCITE  CA    1.0000 C    1.0000 RS   4.0000 I1  -3.4000 I2    .0000
SiO2     SI    1.0000
NaCl     NA    1.0000 CL   1.0000
K-SPAR   K     1.0000 AL   1.0000 SI   3.0000
EXCHANGE CA   -1.0000 NA   2.0000 MG    .0000
DOLOMITE CA    1.0000 MG   1.0000 C    2.0000 RS   8.0000 I1    .0000
         I2     .0000
GYPSUM   CA    1.0000 S    1.0000 RS   6.0000 I3  22.0000
HEMATITE FE    2.0000 RS   6.0000
PYRITE   FE    1.0000 S    2.0000 RS    .0000 I3 -60.0000
ALBITE   NA    1.0000 AL   1.0000 SI   3.0000
ANORTH   CA    1.0000 AL   2.0000 SI   2.0000

                   11 models checked
                    4 models found
           MODEL   1
 CALCITE             10.65234
 SiO2                 -.55902
 NaCl      +           1.12836
 K-SPAR               -.01187
 EXCHANGE            11.58414
 DOLOMITE             -.14788
 GYPSUM                .87691
 HEMATITE            -1.31037
 PYRITE               2.62063
 ALBITE                .01027
                Computed    Observed
Carbon-13       -5.0181     -5.0400
C-14 (% mod)    11.1003*       .1700
Sulfur-34      -22.4588    -18.3000
Strontium-87    .000000   Undefined
Nitrogen-15       .0000   Undefined
-------------------------------------------------------------------------
Adjusted C-14 age in years:  34546.*     * = based on Original Data
```

Model (for initial A0)	A0 (initial)	Computed (no decay)	Observed	age (final)
Original Data	73.33	11.10	.17	34546.
Mass Balance	67.33	10.19	.17	33840.
Vogel	85.00	12.87	.17	35767.
Tamers	56.12	8.49	.17	32334.
Ingerson and Pearson	55.88	8.46	.17	32299.
Mook	42.38	6.42	.17	30013.
Fontes and Garnier	55.87	8.46	.17	32298.
Eichinger	53.18	8.05	.17	31889.
User-defined	100.00	15.14	.17	37110.

Data used for Carbon-13

Initial Value: -13.9690 Modeled Final Value: -5.0181

1 dissolving phases:

Phase	Delta C	Isotopic composition (o/oo)
CALCITE	10.65234	-3.4000

1 precipitating phases:

Phase	Delta C	Fractionation factor	Average Isotopic composition (o/oo)
DOLOMITE	-.29576	.7726	-6.2362

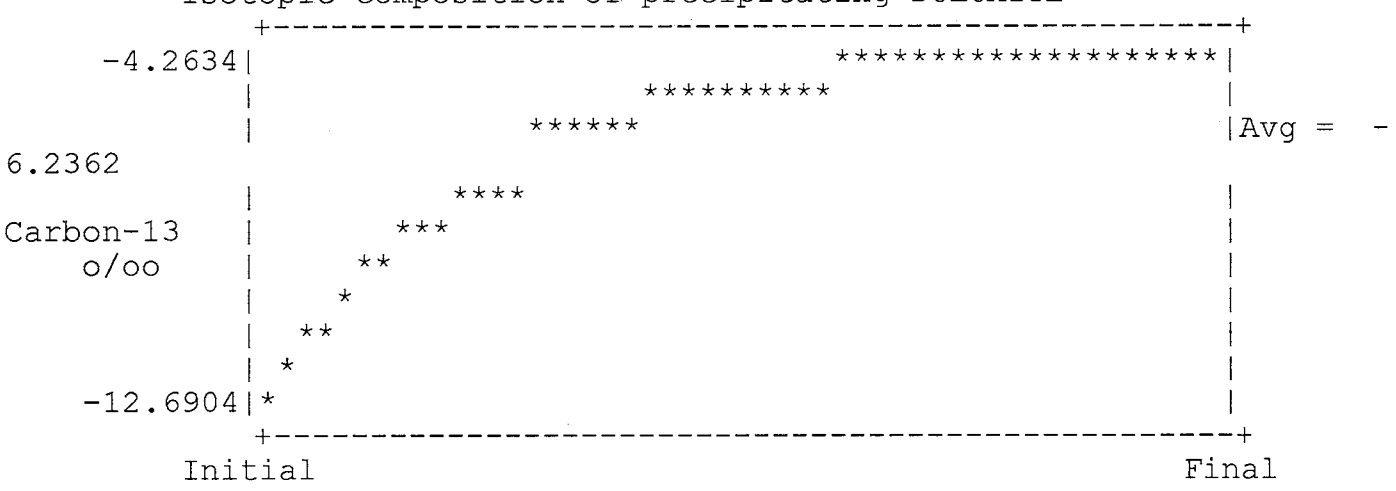

Data used for C-14 (% mod)

Initial Value: 73.3300 Modeled Final Value: 11.1003

1 dissolving phases:

Phase	Delta C	Isotopic composition (% modern)
CALCITE	10.65234	.0000

1 precipitating phases:

Phase	Delta C	Fractionation factor	Average Isotopic composition (% mod
DOLOMITE	-.29576	1.5453	24.9411

Isotopic composition of precipitating DOLOMITE

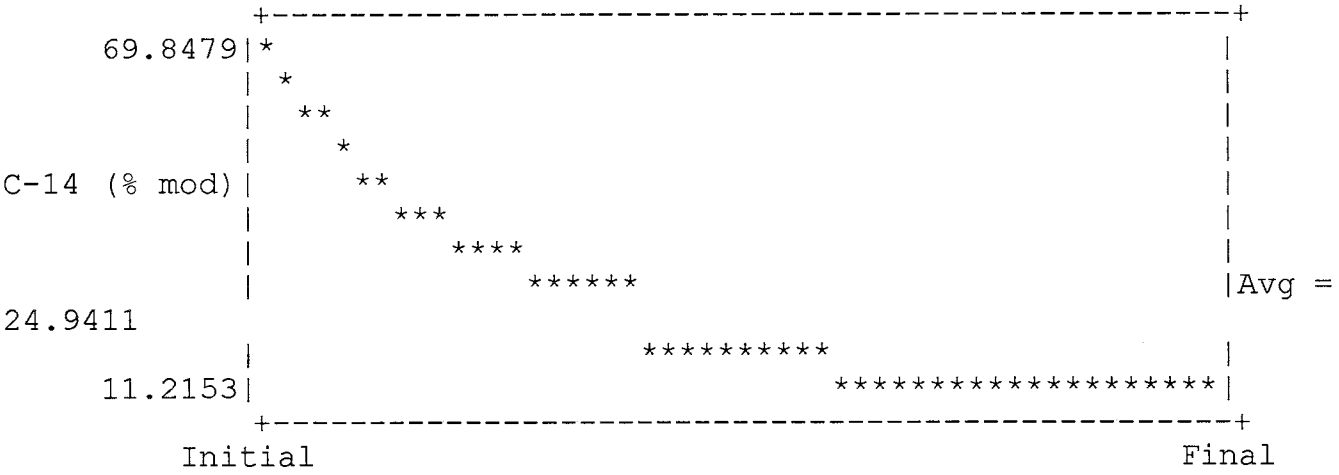

Data used for Sulfur-34

Initial Value: .0000 Modeled Final Value: -22.4588

2 dissolving phases:

Phase	Delta S	Isotopic composition (o/oo)
GYPSUM	.87691	22.0000
PYRITE	5.24126	-30.0000

Data used for Strontium-87
Initial Value: .0000 Modeled Final Value: .0000
No incoming or outgoing phases

```
Initial Well : Presbyterian
Final Well   : MW-68
          Final      Initial
C       10.1260       1.9659
NA      31.5861        .4632
CA        .0000        .4022
K         .1103        .0980
AL        .0000        .0016
SI        .3619        .8344
MG        .1845        .2641
S       11.8113        .0240
CL       1.7375        .0770
FE        .0130        .0001

CALCITE  CA    1.0000 C    1.0000 RS   4.0000 I1  -2.5000 I2    .0000
SiO2     SI    1.0000
NaCl     NA    1.0000 CL   1.0000
K-SPAR   K     1.0000 AL   1.0000 SI   3.0000
EXCHANGE CA   -1.0000 NA   2.0000 MG    .0000
DOLOMITE CA    1.0000 MG   1.0000 C    2.0000 RS   8.0000 I1    .0000
         I2     .0000
GYPSUM   CA    1.0000 S    1.0000 RS   6.0000 I3  22.0000
HEMATITE FE    2.0000 RS   6.0000
PYRITE   FE    1.0000 S    2.0000 RS    .0000 I3 -60.0000
ALBITE   NA    1.0000 AL   1.0000 SI   3.0000
ANORTH   CA    1.0000 AL   2.0000 SI   2.0000

                   11 models checked
                    4 models found
           MODEL   1
 CALCITE              8.31942
 SiO2                 -.46763
 NaCl      +          1.66043
 K-SPAR                .01224
 EXCHANGE             14.73814
 DOLOMITE              -.07964
 GYPSUM                6.09619
 HEMATITE             -1.41632
 PYRITE                2.84556
 ALBITE                -.01384
                Computed    Observed
Carbon-13       -4.6683     -4.6700
C-14 (% mod)    13.7873*       .1100
Sulfur-34       -3.1002    -19.1800
Strontium-87    .000000    Undefined
Nitrogen-15       .0000    Undefined
-------------------------------------------------------------------------
Adjusted C-14 age in years:  39936.*     * = based on Original Data
```

Model (for initial A0)	A0 (initial)	Computed (no decay)	Observed	age (final)
Original Data	73.33	13.79	.11	39936.
Mass Balance	67.33	12.66	.11	39230.
Vogel	85.00	15.98	.11	41157.
Tamers	56.12	10.55	.11	37725.
Ingerson and Pearson	55.88	10.51	.11	37689.
Mook	42.38	7.97	.11	35404.
Fontes and Garnier	55.87	10.51	.11	37689.
Eichinger	53.18	10.00	.11	37280.
User-defined	100.00	18.80	.11	42501.

Data used for Carbon-13

Initial Value: -13.9690 Modeled Final Value: -4.6683

1 dissolving phases:

Phase	Delta C	Isotopic composition (o/oo)
CALCITE	8.31942	-2.5000

1 precipitating phases:

Phase	Delta C	Fractionation factor	Average Isotopic composition (o/oo)
DOLOMITE	-.15928	.7690	-6.2042

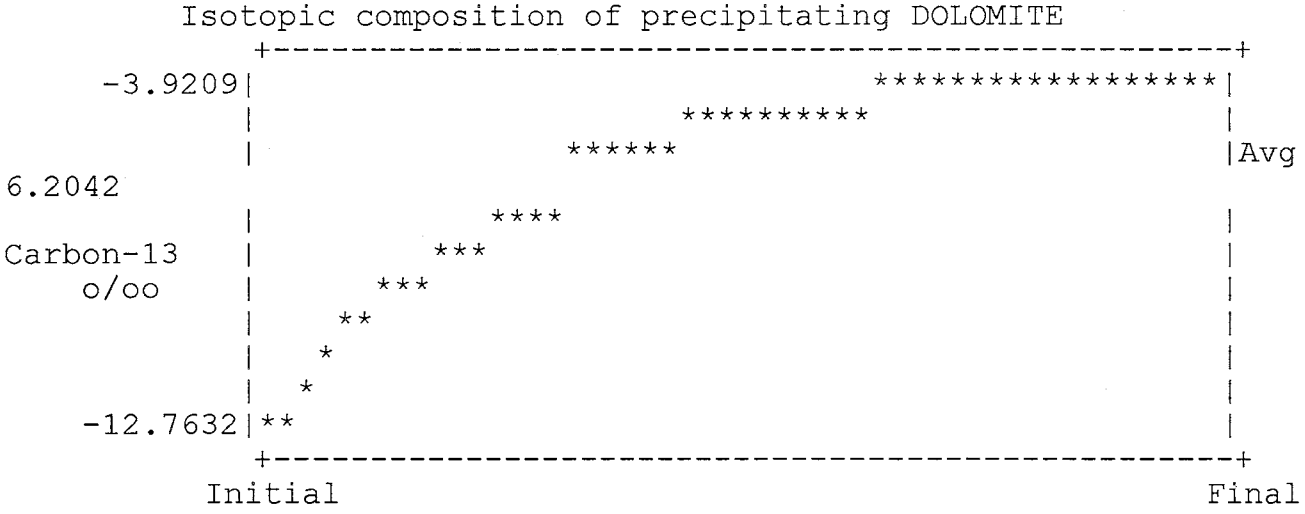

Data used for C-14 (% mod)

Initial Value: 73.3300 Modeled Final Value: 13.7873

1 dissolving phases:

Phase	Delta C	Isotopic composition (% modern)
CALCITE	8.31942	.0000

1 precipitating phases:

Phase	Delta C	Fractionation factor	Average Isotopic composition (% mod
DOLOMITE	-.15928	1.5380	28.5523

Isotopic composition of precipitating DOLOMITE

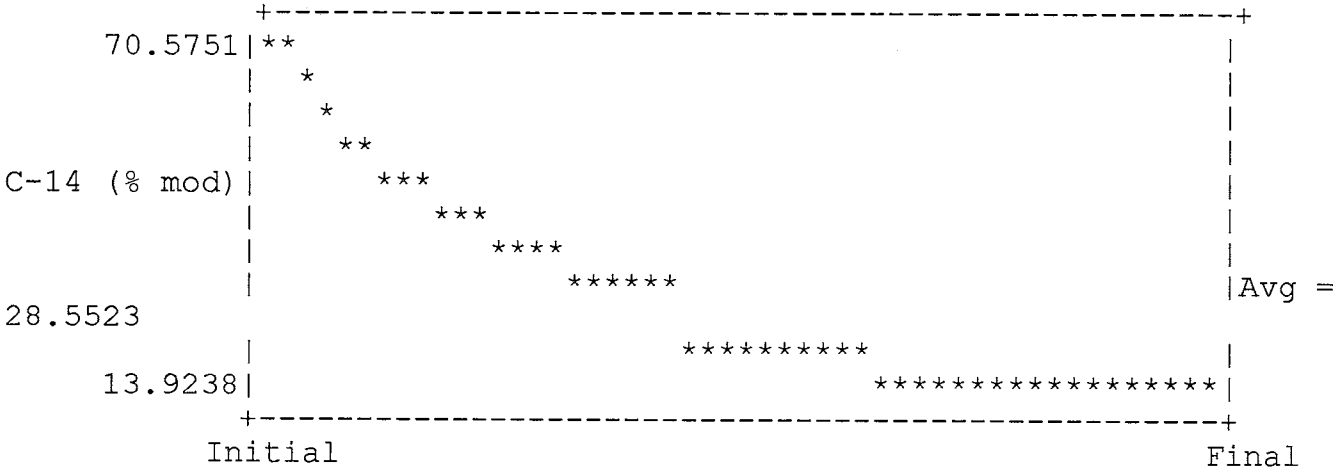

Data used for Sulfur-34

Initial Value: .0000 Modeled Final Value: -3.1002

2 dissolving phases:

Phase	Delta S	Isotopic composition (o/oo)
GYPSUM	6.09619	22.0000
PYRITE	5.69112	-30.0000

Data used for Strontium-87

Initial Value: .0000 Modeled Final Value: .0000

No incoming or outgoing phases

Data used for Nitrogen-15

Initial Value: .0000 Modeled Final Value: .0000

No incoming or outgoing phases

```
Initial Well : Presbyterian
Final Well   : L-Bar
          Final      Initial
C        7.9770       1.9659
NA      12.5951        .4632
CA        .0901        .4022
K         .0441        .0980
AL        .0007        .0016
SI        .1682        .8344
MG        .0541        .2641
S        2.4618        .0240
CL        .4275        .0770
FE        .0006        .0001

CALCITE   CA    1.0000 C    1.0000 RS   4.0000 I1  -3.6000 I2    .0000
SiO2      SI    1.0000
NaCl      NA    1.0000 CL   1.0000
K-SPAR    K     1.0000 AL   1.0000 SI   3.0000
EXCHANGE  CA   -1.0000 NA   2.0000 MG    .0000
DOLOMITE  CA    1.0000 MG   1.0000 C    2.0000 RS   8.0000 I1    .0000
          I2     .0000
GYPSUM    CA    1.0000 S    1.0000 RS   6.0000 I3  22.0000
HEMATITE  FE    2.0000 RS   6.0000
PYRITE    FE    1.0000 S    2.0000 RS    .0000 I3 -60.0000
ALBITE    NA    1.0000 AL   1.0000 SI   3.0000
ANORTH    CA    1.0000 AL   2.0000 SI   2.0000

                  11 models checked
                   4 models found
            MODEL   1
 CALCITE               6.43121
 SiO2                  -.66347
 NaCl       +           .35045
 K-SPAR                -.05399
 EXCHANGE              5.86420
 DOLOMITE              -.21005
 GYPSUM                -.66903
 HEMATITE              -.77645
 PYRITE                1.55339
 ALBITE                 .05309
                 Computed    Observed
Carbon-13         -5.9525     -5.9860
C-14 (% mod)      16.3841*      .1600
Sulfur-34        -29.9179     -8.8900
Strontium-87      .000000   Undefined
Nitrogen-15         .0000   Undefined
-------------------------------------------------------------------------
Adjusted C-14 age in years:  38265.*     * = based on Original Data
```

Model (for initial A0)	A0 (initial)	Computed (no decay)	Observed	age (final)
Original Data	73.33	16.38	.16	38265.
Mass Balance	67.33	15.04	.16	37560.
Vogel	85.00	18.99	.16	39486.
Tamers	56.12	12.54	.16	36054.
Ingerson and Pearson	55.88	12.48	.16	36018.
Mook	42.38	9.47	.16	33733.
Fontes and Garnier	55.87	12.48	.16	36018.
Eichinger	53.18	11.88	.16	35609.
User-defined	100.00	22.34	.16	40830.

Data used for Carbon-13

Initial Value: -13.9690 Modeled Final Value: -5.9525

1 dissolving phases:

Phase	Delta C	Isotopic composition (o/oo)
CALCITE	6.43121	-3.6000

1 precipitating phases:

Phase	Delta C	Fractionation factor	Average Isotopic composition (o/oo)
DOLOMITE	-.42010	.7039	-7.4531

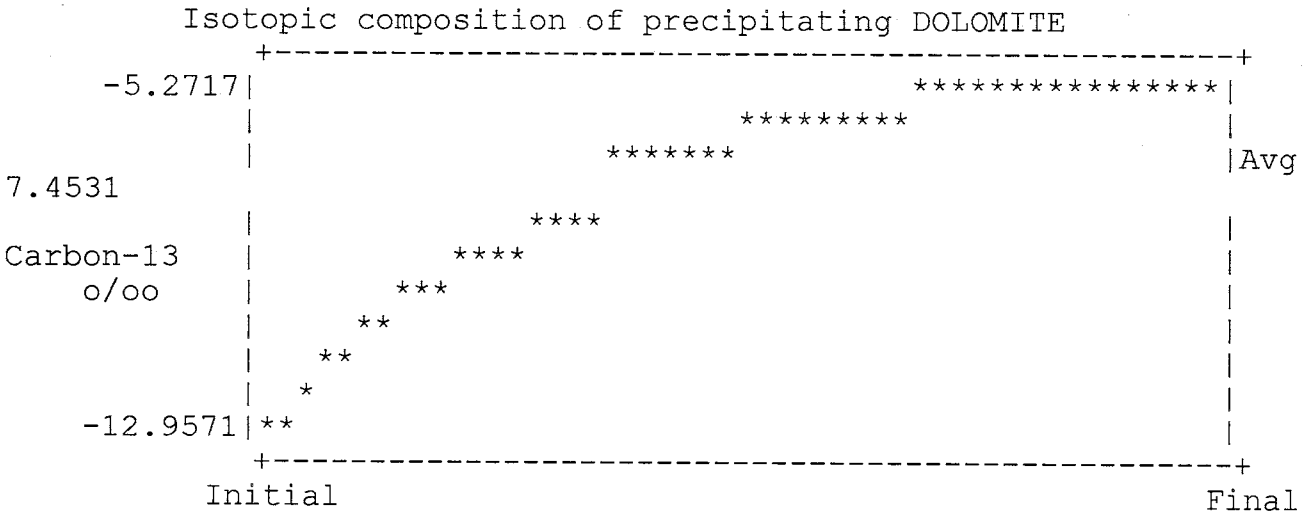

Data used for C-14 (% mod)

Initial Value: 73.3300 Modeled Final Value: 16.3841

1 dissolving phases:

Phase	Delta C	Isotopic composition (% modern)
CALCITE	6.43121	.0000

1 precipitating phases:

Phase	Delta C	Fractionation factor	Average Isotopic composition (% mod
DOLOMITE	-.42010	1.4077	32.0482

Isotopic composition of precipitating DOLOMITE

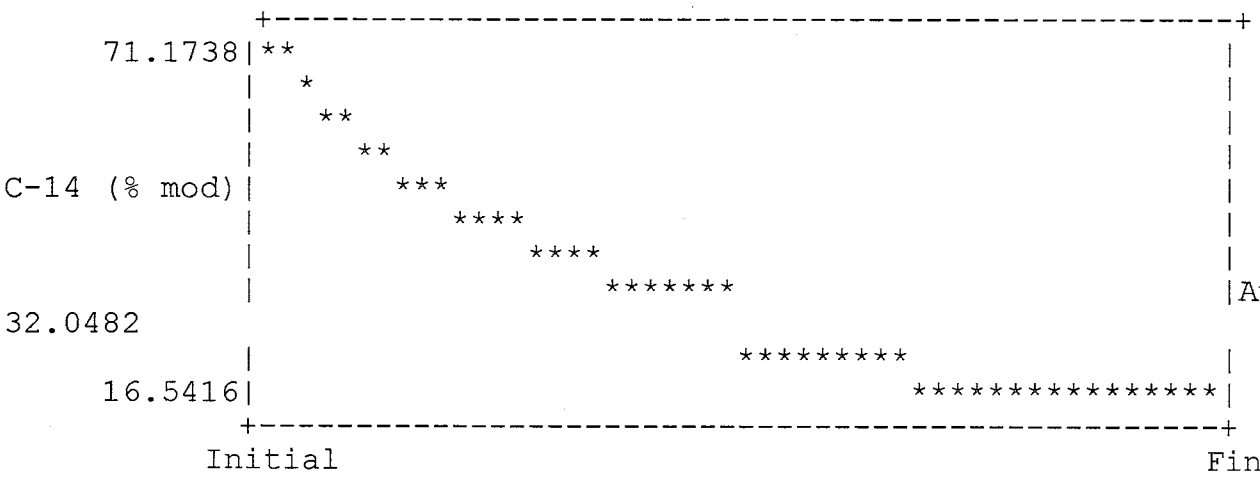

Data used for Sulfur-34

Initial Value: .0000 Modeled Final Value: -29.9179

1 dissolving phases:

Phase	Delta S	Isotopic composition (o/oo)
PYRITE	3.10678	-30.0000

1 precipitating phases:

Phase	Delta S	Fractionation factor	Average Isotopic composition (o/oo)
GYPSUM	-.66903	.0000	-29.1250

Isotopic composition of precipitating GYPSUM

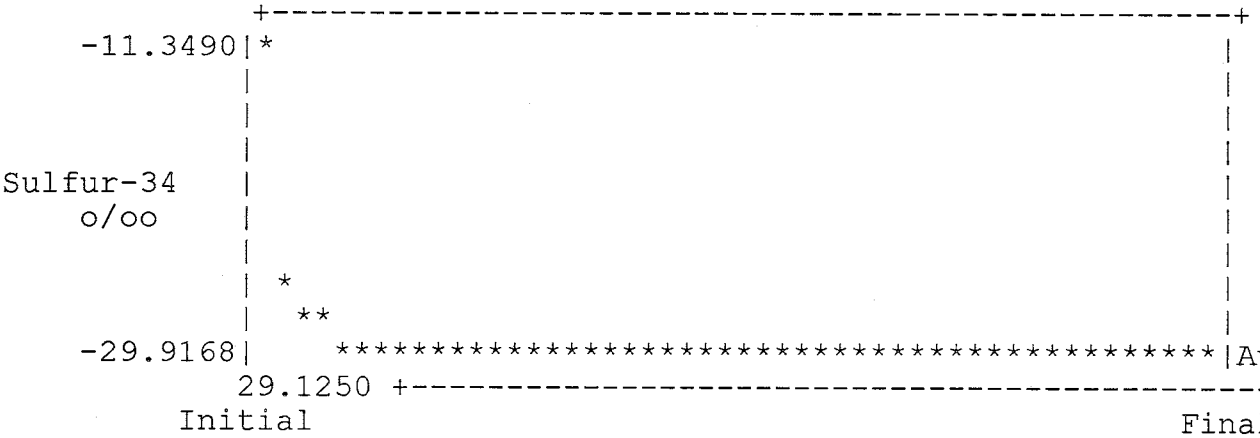

Data used for Strontium-87

Initial Value: .0000 Modeled Final Value: .0000

No incoming or outgoing phases

1MW-68 Corrected 1/20/1998 by Michelle Walvoord

INITIAL SOLUTION

TEMPERATURE = 19.00 DEGREES C PH = 8.100
ANALYTICAL EPMCAT = 32.813 ANALYTICAL EPMAN = 35.617

***** OXIDATION - REDUCTION *****

DISSOLVED OXYGEN = 0.000 MMOLES/KG H2O
EH MEASURED WITH CALOMEL = 9.9000 VOLTS
MEASURED EH OF ZOBELL SOLUTION = 9.9000 VOLTS
CORRECTED EH = 0.0000 VOLTS
PE COMPUTED FROM CORRECTED EH = 0.000

FLAG	CORALK	PECALC	IDAVES
2	1	1	0

*** TOTAL CONCENTRATIONS OF INPUT SPECIES ***

SPECIES		TOTAL MOLALITY	LOG TOTAL MOLALITY	TOTAL MG/LITRE
Ca+2	2.0	3.25060E-04	-3.4880	1.29950E+01
Mg+2	2.0	1.84333E-04	-3.7344	4.47000E+00
Na+	1.0	3.15863E-02	-1.5005	7.24300E+02
K+	1.0	1.10252E-04	-3.9576	4.30000E+00
Fe+2	2.0	6.46276E-06	-5.1896	3.60000E-01
Mn+2	2.0	1.82491E-07	-6.7388	1.00000E-02
H4SiO4	0.0	1.69279E-04	-3.7714	1.01450E+01
Cl-	-1.0	1.73689E-03	-2.7602	6.14200E+01
HCO3-	-1.0	1.00667E-02	-1.9971	6.12670E+02
SO4-2	-2.0	1.18124E-02	-1.9277	1.13181E+03
NO3-	-1.0	2.86312E-06	-5.5432	4.00000E-02
F-	-1.0	9.02390E-05	-4.0446	1.71000E+00
Br-	-1.0	2.50944E-06	-5.6004	2.00000E-01

MW-68

****DESCRIPTION OF SOLUTION ****

	ANALYT.	COMP.	PH	ACTIVITY H2O = 0.9991
EPMCAT	32.81	31.38	8.100	PCO2= 3.914931E-03
EPMAN	35.62	34.17		LOG PCO2 = -2.4073
			TEMPERATURE	PO2 = 1.586488E-53
EH = 0.0000	PE = 0.000		19.00 DEG C	PCH4 = 4.134447E-44
PE CALC S =	0.000			CO2 TOT = 1.010965E-02
PE CALC DOX=	0.000		IONIC STRENGTH	DENSITY = 1.0000
PE SATO DOX=	0.000		4.414060E-02	TDS = 2564.4MG/L
TOT ALK =	1.007E+01 MEQ			CARB ALK = 1.007E+01 MEQ
ELECT	= -2.800E+00 MEQ			CHARGE IMBALANCE = -4.3%

IN COMPUTING THE DISTRIBUTION OF SPECIES,
PE = 0.000 EQUIVALENT EH = 0.000VOLTS

DISTRIBUTION OF SPECIES

I	SPECIES		MOLALITY	ACTIVITY	LOG ACT	GAMMA
1	H+	1.	9.2388E-09	7.9433E-09	-8.100	8.5977E-01
2	E-	-1.	1.0000E+00	1.0000E+00	0.000	1.0000E+00
4	Ca+2	2.	2.0774E-04	1.0199E-04	-3.991	4.9095E-01
5	Mg+2	2.	1.1542E-04	5.7913E-05	-4.237	5.0174E-01
6	Na+	1.	3.0678E-02	2.5516E-02	-1.593	8.3173E-01
7	K+	1.	1.0676E-04	8.7785E-05	-4.057	8.2228E-01
8	Fe+2	2.	2.6664E-06	1.3338E-06	-5.875	5.0022E-01
9	Mn+2	2.	5.2103E-08	2.6063E-08	-7.584	5.0022E-01
13	H4SiO4	0.	1.6625E-04	1.6795E-04	-3.775	1.0102E+00
14	Cl-	-1.	1.7369E-03	1.4282E-03	-2.845	8.2228E-01
15	CO3-2	-2.	8.5868E-05	4.2066E-05	-4.376	4.8989E-01
16	SO4-2	-2.	1.0873E-02	5.2281E-03	-2.282	4.8082E-01
17	NO3-	-1.	2.6771E-19	2.1856E-19	-18.660	8.1642E-01
20	F-	-1.	8.8809E-05	7.2914E-05	-4.137	8.2103E-01
22	Br-	-1.	2.5094E-06	2.0488E-06	-5.689	8.1642E-01
31	OH-	-1.	9.5992E-07	7.8812E-07	-6.103	8.2103E-01
33	H2 AQ	0.	4.6996E-20	4.7477E-20	-19.324	1.0102E+00
34	HCO3-	-1.	9.7060E-03	8.1202E-03	-2.090	8.3661E-01
35	H2CO3	0.	1.5640E-04	1.5800E-04	-3.801	1.0102E+00
40	HSO4-	-1.	4.2836E-09	3.5537E-09	-8.449	8.2960E-01
48	NO2-	-1.	2.8631E-06	2.3375E-06	-5.631	8.1642E-01
69	HF AQ	0.	7.7285E-10	7.8074E-10	-9.107	1.0102E+00

70	HF2-	-1.	2.5018E-13	2.0755E-13	-12.683	8.2960E-01
75	CaOH+	1.	2.5661E-09	2.1289E-09	-8.672	8.2960E-01
76	CaCO3	0.	6.4116E-06	6.4771E-06	-5.189	1.0102E+00
77	CaHCO3+	1.	1.1381E-05	9.5212E-06	-5.021	8.3661E-01
78	CaSO4	0.	9.9458E-05	1.0047E-04	-3.998	1.0102E+00
79	CaHSO4	1.	5.9707E-12	4.9533E-12	-11.305	8.2960E-01
83	CaF+	1.	6.7682E-08	5.6149E-08	-7.251	8.2960E-01
85	MgOH+	1.	1.8568E-08	1.5404E-08	-7.812	8.2960E-01
86	MgCO3	0.	2.0986E-06	2.1201E-06	-5.674	1.0102E+00
87	MgHCO3+	1.	6.4826E-06	5.3780E-06	-5.269	8.2960E-01
88	MgSO4	0.	6.0007E-05	6.0620E-05	-4.217	1.0102E+00
92	MgF+	1.	3.0098E-07	2.4970E-07	-6.603	8.2960E-01
93	NaOH	0.	2.0989E-08	2.1203E-08	-7.674	1.0102E+00
94	NaCO3-	-1.	1.7690E-05	1.4676E-05	-4.833	8.2960E-01
95	NaHCO3	0.	1.1453E-04	1.1570E-04	-3.937	1.0102E+00
96	NaSO4-	-1.	7.7520E-04	6.4311E-04	-3.192	8.2960E-01
98	NaF aq	0.	1.0598E-06	1.0706E-06	-5.970	1.0102E+00
99	KOH	0.	3.7897E-11	3.8284E-11	-10.417	1.0102E+00
100	KSO4-	-1.	3.4932E-06	2.8980E-06	-5.538	8.2960E-01
102	FeOH+	1.	4.0467E-08	3.3571E-08	-7.474	8.2960E-01
105	FeCl+	1.	3.1697E-09	2.6296E-09	-8.580	8.2960E-01
106	FeCO3	0.	1.3323E-06	1.3459E-06	-5.871	1.0102E+00
107	FeHCO3+	1.	1.2965E-06	1.0756E-06	-5.968	8.2960E-01
108	FeSO4	0.	1.0975E-06	1.1087E-06	-5.955	1.0102E+00
109	FeHSO4+	1.	7.8084E-14	6.4779E-14	-13.189	8.2960E-01
114	FeF+	1.	1.1723E-09	9.7253E-10	-9.012	8.2960E-01
115	Fe+3	3.	3.5476E-19	9.1068E-20	-19.041	2.5671E-01
117	FeOH+2	2.	1.0887E-13	5.1570E-14	-13.288	4.7368E-01
118	FeOH2+	1.	2.0524E-09	1.7027E-09	-8.769	8.2960E-01
119	FeOH3	0.	2.0912E-08	2.1125E-08	-7.675	1.0102E+00
120	FeOH4-	-1.	2.2837E-09	1.8946E-09	-8.722	8.2960E-01
121	Fe2OH2+4	4.	1.8313E-24	9.2192E-26	-25.035	5.0342E-02
122	Fe3OH4+5	5.	6.1579E-30	5.7704E-32	-31.239	9.3707E-03
123	FeCl+2	2.	6.8292E-21	3.2349E-21	-20.490	4.7368E-01
124	FeCl2+	1.	3.0205E-23	2.5058E-23	-22.601	8.2960E-01
125	FeCl3	0.	3.5426E-27	3.5788E-27	-26.446	1.0102E+00
126	FeSO4+	1.	5.4951E-18	4.5588E-18	-17.341	8.2960E-01
127	FeHSO4+2	2.	3.2806E-25	1.5539E-25	-24.809	4.7368E-01
128	FeSO42-	-1.	6.1366E-19	5.0910E-19	-18.293	8.2960E-01
131	FeF+2	2.	2.0233E-17	9.5837E-18	-17.018	4.7368E-01
132	FeF2+	1.	3.1179E-17	2.5866E-17	-16.587	8.2960E-01
133	FeF3	0.	2.8980E-18	2.9276E-18	-17.533	1.0102E+00
134	MnOH+	1.	6.1655E-11	5.1149E-11	-10.291	8.2960E-01
136	MnCl+	1.	1.8279E-10	1.5164E-10	-9.819	8.2960E-01
137	MnCl2	0.	9.3583E-14	9.4539E-14	-13.024	1.0102E+00
138	MnCl3-	-1.	4.4826E-17	3.7188E-17	-16.430	8.2960E-01
139	MnCO3	0.	8.6208E-08	8.7088E-08	-7.060	1.0102E+00
140	MnHCO3+	1.	2.2579E-08	1.8731E-08	-7.727	8.2960E-01
141	MnSO4	0.	2.1341E-08	2.1559E-08	-7.666	1.0102E+00
143	MnF+	1.	1.5848E-11	1.3147E-11	-10.881	8.2960E-01
144	Mn+3	3.	1.7693E-33	3.2933E-34	-33.482	1.8614E-01
164	H3SiO4-	-1.	3.0248E-06	2.5093E-06	-5.600	8.2960E-01
165	H2SiO4-2	-2.	3.0260E-11	1.4334E-11	-10.844	4.7368E-01
166	SiF6-2	-2.	5.6622E-31	2.6821E-31	-30.572	4.7368E-01

	PHASE	IAP	KT	LOG IAP	LOG KT	IAP/KT	LOG IAP/KT
1	Calcite	4.290E-09	3.561E-09	-8.368	-8.448	1.205E+00	0.081
2	Aragonit	4.290E-09	5.009E-09	-8.368	-8.300	8.565E-01	-0.067
3	Dolomite	1.045E-17	1.127E-17	-16.981	-16.948	9.271E-01	-0.033
4	Siderite	5.611E-11	1.404E-11	-10.251	-10.853	3.997E+00	0.602
5	Rhodochr	1.096E-12	7.790E-12	-11.960	-11.108	1.407E-01	-0.852
8	Gypsum	5.322E-07	2.621E-05	-6.274	-4.582	2.031E-02	-1.692
9	Anhydrit	5.332E-07	4.556E-05	-6.273	-4.341	1.170E-02	-1.932
13	Fluorite	5.422E-13	2.125E-11	-12.266	-10.673	2.552E-02	-1.593
14	SiO2 (a)	1.683E-04	1.729E-03	-3.774	-2.762	9.731E-02	-1.012
15	Chalcedy	1.683E-04	2.385E-04	-3.774	-3.622	7.054E-01	-0.152
16	Quartz	1.683E-04	8.500E-05	-3.774	-4.071	1.980E+00	0.297
26	Talc	6.176E+20	1.250E+22	20.791	22.097	4.942E-02	-1.306
28	Chrysotl	2.179E+28	9.109E+32	28.338	32.959	2.392E-05	-4.621
29	Sepiol c	3.993E+12	8.338E+15	12.601	15.921	4.789E-04	-3.320
30	Sepiol d	3.993E+12	4.571E+18	12.601	18.660	8.736E-07	-6.059
31	Hematite	3.292E+10	2.860E-04	10.518	-3.544	1.151E+14	14.061
32	Goethite	1.814E+05	6.054E-02	5.259	-1.218	2.996E+06	6.477
33	Fe(OH)3a	1.812E+05	7.780E+04	5.258	4.891	2.329E+00	0.367
38	Pyrolusi	6.535E+24	2.292E+42	24.815	42.360	2.851E-18	-17.545
39	Hausmani	1.113E+42	3.508E+62	42.046	62.545	3.173E-21	-20.499
40	Manganit	5.191E+16	2.188E+25	16.715	25.340	2.373E-09	-8.625
41	Pyrochro	4.123E+08	1.585E+15	8.615	15.200	2.601E-07	-6.585
42	PCO2	1.580E-04	4.036E-02	-3.801	-1.394	3.915E-03	-2.407
44	H2 gas	4.748E-20	7.525E-04	-19.324	-3.124	6.310E-17	-16.200
49	Melanter	6.928E-09	5.192E-03	-8.159	-2.285	1.334E-06	-5.875
51	K-Jarosi	7.174E-18	1.823E-09	-17.144	-8.739	3.934E-09	-8.405